

Copyright is owned by the Author of the thesis. Permission is given for a copy to be downloaded by an individual for the purpose of research and private study only. The thesis may not be reproduced elsewhere without the permission of the Author.

**Novel particulate vaccine candidates  
recombinantly produced by pathogenic and  
nonpathogenic bacterial hosts**

A thesis presented in partial fulfillment of the requirements for the degree  
of

Doctor of Philosophy

In

Microbiology

at Massey University, Manawatu,  
New Zealand

Jason Wong Lee

2017

## Abstract

Polyhydroxyalkanoates (PHAs) are biopolyesters synthesized as small spherical cytoplasmic inclusion bodies by a range of bacteria. Recently, PHA beads have been investigated for use as a vaccine delivery platform by using engineered heterologous production hosts that allowed the efficient display of vaccine candidate antigens on the beads surface and were found to greatly improve immunogenicity of the displayed antigens. However, like other subunit vaccines, these antigen-displaying (vaccine) PHA beads only provide a limited repertoire of antigens.

In this thesis we investigate the idea of directly utilizing the disease causative pathogen or model organism to produce vaccine PHA beads with a large antigenic repertoire. These beads are hypothesized to have the potential to induce greater protective immunity compared to production of the same PHA bead in a heterologous production host.

This concept was exemplified with *Pseudomonas aeruginosa* and *Mycobacterium tuberculosis* as model human pathogens. For *P. aeruginosa* we describe the engineering of this bacterium to promote PHA and Psl (polysaccharide) production. This represents a new mode of functional display for the engineering, production, and validation of a novel OprI/F-AlgE fusion antigen-displayed on PHA beads. For the disease tuberculosis we investigated the use of nonpathogenic *M. smegmatis* as a model organism for *M. tuberculosis*. We described the bioengineering, production, and validation of Ag85A-ESAT-6 displayed on PHA beads produced in *M. smegmatis*.

Here we showed that both organisms were harnessed to produce custom-made PHA beads for use as particulate subunit vaccines that carried copurifying pathogen-derived proteins as a large antigenic repertoire and the ability of these vaccine PHA beads to generate a protective immune response.

This novel bioengineering concept of particulate subunit vaccine production could be applied to a range of pathogens naturally producing PHA inclusions for developing efficacious subunit vaccines for infectious diseases.

## **Acknowledgements**

“Success, 100% persistence and a bit of luck”

The road to completing this milestone in my life has not been easy, but thanks to my friends, family, and most importantly my partner Yifang has made this journey a lot easier.

I would like to give a big thanks to my supervisor Bernd Rehm and my cosupervisors Bryce Buddle, Axel Heiser, and Neil Wedlock for allowing me this opportunity.

I would also like to give a special mention to Natalie Parlane for her guidance and help with immunology, to all those in the Rehm lab, and those in the Infectious diseases group.

This project was made possible by the funding provided by AgResearch, Bill and Melinda Gates Foundation, and Massey University.

## **Preface**

Below lists the publication status of all chapters in this thesis.

### **Chapter 1.**

#### **General introduction.**

This chapter review was written as an introductory chapter for this thesis by Jason Lee.

### **Chapter 2.**

#### **Bioengineering *Pseudomonas aeruginosa* to assemble its own particulate vaccine capable of inducing cellular immunity.**

Published: Lee, J. W., Parlane, N. A., Wedlock, D. N., & Rehm, B. H. A. (2017). Bioengineering a bacterial pathogen to assemble its own particulate vaccine capable of inducing cellular immunity. *Scientific Reports*, 7.

This article was written by Jason Lee and reviewed by all other authors. The concept was conceived by Jason Lee and Bernd H. A. Rehm. Experimental design was performed by Jason Lee with the advice of Bernd H.A. Rehm. All experiments were performed by Jason Lee with the exception of some immunological experiments which were planned and performed with the guidance of Natalie Parlane.

### **Chapter 3.**

#### **Engineering mycobacteria for the production of self-assembling biopolyesters displaying mycobacterial antigens for use as tuberculosis vaccine.**

Published: Lee, J. W., Parlane, N. A., Rehm, B. H. A., Buddle, B. M., & Heiser, A. (2017). Engineering mycobacteria for the production of self-assembling biopolyesters displaying mycobacterial antigens for use as a tuberculosis vaccine. *Applied and Environmental Microbiology*, 85(4), 2289-2289.

This article was written by Jason Lee and reviewed by all other authors. The concept was conceived by Jason Lee, Axel Heiser, and Bernd H. A. Rehm. All experiments and planning related to molecular biology (Cloning, expression, isolation, and analysis) was performed by Jason Lee with the advice of Axel Heiser and Bernd H.A. Rehm. All experiments related to immunology were planned and performed by Axel Heiser and Natalie Parlane.

## Table of contents

<b>Abstract.....</b>	<b>I</b>
<b>Acknowledgements .....</b>	<b>II</b>
<b>Preface.....</b>	<b>III</b>
<b>Table of Contents .....</b>	<b>V</b>
<b>List of Figures.....</b>	<b>VIII</b>
<b>List of Tables .....</b>	<b>X</b>
<b>Abbreviations .....</b>	<b>XI</b>
<b>Chapter 1: General introduction.....</b>	<b>1</b>
1.1 Introduction to immunology .....	1
1.2 Innate immunity.....	1
1.2.1 Pattern recognition receptors (PRRs) .....	3
1.2.2 Complement system .....	5
1.2.3 Phagocytosis .....	6
1.3 Adaptive immunity .....	7
1.3.1 Effector T cells .....	8
1.3.2 Interplay and plasticity of effector T cells.....	9
1.3.3 Effector B cells .....	12
1.4 Introduction to vaccines .....	13
1.5 Traditional vaccines.....	14
1.5.1 Live attenuated .....	14
1.5.2 Killed inactivated.....	15
1.5.3 Toxoid.....	15
1.5.4 Subunit.....	15
1.6 Novel vaccines approaches.....	16
1.6.1 Adjuvants.....	18
1.6.2 Deoxyribonucleic acid.....	19
1.6.3 Delivery systems.....	20
1.7 Polyhydroxyalkanoate .....	25
1.7.1 Polyester synthases .....	26
1.7.2 Self-assembly of polyester particles .....	27
1.7.3 Granule-associated-proteins (GAPs) .....	30

1.8 Tuberculosis .....	31
1.9 <i>Pseudomonas aeruginosa</i> .....	35
1.9.1 Potential vaccine targets against <i>P. aeruginosa</i> .....	37
1.10 Conclusion .....	40
1.11 References.....	41
<b>Chapter 1A: Thesis scope.....</b>	<b>50</b>
1.12 Problem statement .....	50
1.13 Aim .....	50
1.14 Objectives .....	50
1.15 Scope.....	51
<b>Link to next chapter .....</b>	<b>52</b>
<b>Chapter 2: Bioengineering <i>Pseudomonas aeruginosa</i> to assemble its own particulate vaccine capable of inducing cellular immunity .....</b>	<b>53</b>
Abstract.....	53
2.1 Introduction.....	54
2.2 Results.....	58
2.2.1 Bioengineering of <i>P. aeruginosa</i> for self-assembly of antigen-displaying PHA inclusions.....	58
2.2.2 Immunological response to vaccination with antigen-displaying PHA <sub>MCL</sub> beads.....	68
2.3 Discussion.....	74
2.4 Methods .....	79
2.5 Acknowledgements.....	91
2.6 References.....	91
Supplementary material .....	95
<b>Link to next chapter .....</b>	<b>118</b>
<b>Chapter 3: Engineering mycobacteria for the production of self-assembling biopolyesters displaying mycobacterial antigens for use as tuberculosis vaccine ...</b>	<b>119</b>
Abstract.....	119
3.1 Introduction.....	120
3.2 Methods .....	123
3.3 Results.....	131
3.3.1 Production of MBB .....	131
3.3.2 Production of MBB displaying Ag85A and ESAT-6 (A:E-MBB).....	135

3.3.3 TEM analysis .....	136
3.3.4 MBB vaccination and challenge with <i>M. bovis</i> .....	136
3.4 Discussion.....	140
3.5 Conclusions.....	145
3.6 Acknowledgements.....	146
3.7 References.....	146
Supplementary material .....	149
<b>Chapter 4: Discussion and outlook .....</b>	<b>165</b>
4.1 Discussion.....	165
4.2 Outlook .....	171
4.2.1 Optimization of PHA production and antigen-display .....	171
4.2.2 Bead isolation .....	174
4.2.3 Bead purification .....	175
4.2.4 Alternative antigens .....	176
4.2.5 Adjuvants.....	177
4.2.6 Alternative mycobacterial production host.....	177
4.2.7 Characterization of <i>P. aeruginosa</i> mutant PAO1 $\Delta$ CD8 $\Delta$ F .....	178
4.2.8 Challenge trial – <i>Pseudomonas</i> vaccine beads .....	178
4.2.9 Route of administration – Mucosal immunity .....	179
4.2.10 Heterologous prime-boost strategy.....	180
4.3 References.....	181
<b>Appendix.....</b>	<b>185</b>
Statement of contribution to doctoral thesis containing publications.	
Copyright form and declaration confirming content of digital version of thesis.	

# List of Figures

## Chapter 1

<b>Figure 1.1.</b> The four classes of polyester synthases .....	26
<b>Figure 1.2.</b> Metabolic pathways of PHA production .....	28
<b>Figure 1.3.</b> Models for polyester bead self-assembly .....	29
<b>Figure 1.4.</b> Schematic representation of a PHA granule and its associated proteins ...	30

## Chapter 2

<b>Figure 2.1.</b> Engineering the pathogens intrinsic ability to produce PHA <sub>MCL</sub> beads as particulate subunit vaccines.....	56
<b>Figure 2.2.</b> A schematic of the generation of <i>P. aeruginosa</i> knockout mutant PAO1 $\Delta C\Delta 8\Delta F$ .....	58
<b>Figure 2.3.</b> Assessment of the tolerance of the class II PHA synthase (PhaC <sub>1Pa</sub> ) to C terminal fusion.....	60
<b>Figure 2.4.</b> Antigenic epitopes of OprI, OprF, and AlgE.....	61
<b>Figure 2.5.</b> Bioengineering and production of vaccine PHA <sub>MCL</sub> inclusions <i>in vivo</i> ....	63
<b>Figure 2.6.</b> Protein analysis of vaccine PHA <sub>MCL</sub> beads .....	66
<b>Figure 2.7.</b> Analysis of soluble recombinant protein His <sub>10</sub> -Ag.....	67
<b>Figure 2.8.</b> Antibody response to vaccination with vaccine PHA <sub>MCL</sub> beads .....	69
<b>Figure 2.9.</b> Antigenic response to vaccination with alum formulated vaccine PHA <sub>MCL</sub> beads .....	71
<b>Figure 2.10.</b> Cytokine response to vaccination with vaccine PHA <sub>MCL</sub> beads .....	72
<b>Supplementary Figure 2.1.</b> DNA sequencing results for the generation of <i>P. aeruginosa</i> knockout mutant PAO1 $\Delta C\Delta 8\Delta F$ .....	96
<b>Supplementary Figure 2.2.</b> Multiple alignment of primary structures from 33 known and putative PHA synthase from bacterial human pathogens .....	97

## Chapter 3

<b>Figure 3.1.</b> Two-plasmid and one-plasmid system for PHB expression in mycobacteria .....	133
<b>Figure 3.2.</b> SDS-PAGE and immunoblot analysis of proteins from whole-cell lysate and isolated mycobacterial PHA biobeads material .....	134
<b>Figure 3.3.</b> TEM analysis of isolated mycobacterial PHA biobeads material by density gradient .....	137
<b>Figure 3.4.</b> Cytokine responses from vaccinated mice .....	138
<b>Figure 3.5.</b> Bacterial counts in lungs and spleens of vaccinated mice .....	139
<b>Supplementary Figure 3.1.</b> Construction of plasmid pMycVec1_pNit- <i>phaC</i> .....	150
<b>Supplementary Figure 3.2.</b> Construction of plasmid pMycVec2_Pwmyc- <i>phaAB</i> ...	151
<b>Supplementary Figure 3.3.</b> Construction of plasmid pMIND_pTet- <i>phaC</i> .....	152
<b>Supplementary Figure 3.4.</b> Construction of plasmid pMV261_pNit- <i>phaC</i> .....	152
<b>Supplementary Figure 3.5.</b> Construction of plasmid pMV261_pNit-A:E- <i>phaC</i> .....	153
<b>Supplementary Figure 3.6.</b> Construction of plasmid pMV261_pNit- <i>phaC</i> -Pwmyc- <i>phaAB</i> .....	154
<b>Supplementary Figure 3.7.</b> Analysis of PHB in whole-cell by GC/MS .....	155
<b>Supplementary Figure 3.8.</b> Confirmation of pNit promoter activity .....	157
<b>Supplementary Figure 3.9.</b> Analysis of PHB in whole-cell by GC/MS .....	158
<b>Supplementary Figure 3.10.</b> Confirmation of ESAT-6 .....	164

## Chapter 4

<b>Figure 4.1.</b> Epitope arrangement .....	172
--	-----

## List of Tables

### Chapter 1

<b>Table 1.1</b> Current novel TB vaccines in clinical trials .....	34
<b>Table 1.2</b> Potential vaccine targets against <i>P. aeruginosa</i> .....	36
<b>Table 1.3</b> <i>P. aeruginosa</i> vaccines .....	37

### Chapter 2

<b>Supplementary Table 2.1</b> Protein identification of fusion proteins by MALDI-TOF MS .....	101
<b>Supplementary Table 2.2</b> Protein identification of dominant HCPs by peptide finger printing using MALDI-TOF MS .....	102
<b>Supplementary Table 2.3</b> Amino acid alignment of peptides identified by MALDI-TOF MS in dominant HCPs with respective PHA synthase fusion protein and mapping of anti-PhaC1 antibody epitopes .....	108
<b>Supplementary Table 2.4</b> 33 known and putative PHA synthases from bacterial human pathogens .....	111
<b>Supplementary Table 2.5</b> Percent Identity Matrix from multiple sequence alignment of 33 known and putative PHA synthases from bacterial human pathogens .....	114
<b>Supplementary Table 2.6</b> Strains, plasmids, and oligonucleotides used in this study ... ..	115

### Chapter 3

<b>Table 3.1</b> Bacterial strains and plasmids used in this study .....	124
<b>Table 3.2</b> PHB biosynthesis of <i>M. smegmatis</i> harboring various plasmids .....	135

## Abbreviations

3-HB	methyl 3-hydroxybutanoate
3-HD	methyl 3-hydroxydecanoate
3-HDD	methyl 3-hydroxydodecanoate
3-HH	methyl 3-hydroxyhexanoate
3-HHD	methyl 3-hydroxyhexadecanoate
3-HN	methyl 3-hydroxynonanoate
3-HO	methyl 3-hydroxyoctanoate
3-HTD	methyl 3-hydroxytetradecanoate
3-HUD	methyl 3-hydroxyundecanoate
A:E	Fusion antigen of Ag85A and ESAT-6 epitopes
A:E-MBB	Ag85A-ESAT-6 displaying mycobacterial biobeads
Ag	Fusion antigen of OprI/F-AlgE
Ag-PhaC1 <sub>pa</sub>	N terminal fusion of OprI/F-AlgE to the PHA synthase
Ag85A	Antigen 85A
Alum	Aluminum hydroxide
Ap	Ampicillin
APC	Antigen Presenting Cell
BCG	Bacillus Calmette–Guérin
BDW	Bead Dry Weight
Cb	Carbenicillin
CD	Cluster of Differentiation
CD40L	Cluster of Differentiation 40 ligand
CDW	Cell Dry Weight
CF	Cystic Fibrosis
CFTR	Cystic Fibrosis Transmembrane Regulator
CLR	C-type Ligand Receptor
CLSM	Confocal Laser Scanning Fluorescence Microscopy
ConA	Concanavalin A
CTL	Cytotoxic T Lymphocytes
DAMP	Damage Associated Molecular Patterns
DC	Dendritic cell
DMEM	Dulbecco's Modified Eagle's Medium
DNA	Deoxyribonucleic acid
ELISA	Enzyme-Linked Immunosorbent Assay
EPS	Exopolysaccharide

ESAT-6	6 kDa early secretory antigenic target
FM	Fluorescence microscopy
GAP	Granule Associated Protein
GC/MS	Gas Chromatography/Mass Spectrometry
GFP	Green Fluorescent Protein
Gm	Gentamicin
HCP	Host Cell Protein
HCV	Hepatitis C Virus
His <sub>10</sub> -Ag	10x His-tagged fusion antigen
HIV	Human Immunodeficiency Virus
HRP	Horseradish peroxidase
IFN	Interferon
IgG	Immunoglobulin G
IL	Interleukin
ISCOM	Immune stimulating complex
kDa	Kilodalton
LB	Luria Broth
LPS	Lipopolysaccharide
MAC	Membrane Attack Complex
MALDI-TOF MS	Matrix-Assisted Laser Desorption-Ionization Time-Of-Flight Mass Spectroscopy
MASPs	MBL-Associated Serine Proteases
MBB	Mycobacterial biobeads
MBL	Mannose Binding Lectin
MDR	Multidrug-resistance
MHC	Major Histocompatibility Complex
MOG	Myelin Oligodendrocyte Glycoprotein
MSM	Mineral Salt Medium
MVC	Mycobacterial vector control
ND	Not detected
NF-κB	Nuclear Factor-κB
NK	Natural Killer
NLR	(NOD)-Like Receptor
NLRA	NOD-Like Receptor Acidic transactivating domain
NLRB	NOD-Like Receptor Baculovirus inhibitor of apoptosis protein repeat
NLRC	NOD-Like Receptor Caspase activation and recruitment domains
NLRP	NOD-Like Receptor Pyrin domain
OD	Optical Density

OMP	Outer membrane protein
OMV	Outer Membrane Vesicle
OpdA	Organophosphorus pesticide hydrolase
OprF	Outer membrane protein F
OprI	Outer membrane lipoprotein I
OprI/F-AlgE	Fusion antigen of OprI, OprF, and AlgE (loops 5 & 6) epitopes
PAMP	Pathogen Associated Molecular Patterns
PAO1 $\Delta$ C $\Delta$ 8 $\Delta$ F	<i>P. aeruginosa</i> PAO1 triple knockout mutant
PBS	Phosphate Buffer Saline
PBST	Phosphate buffer saline + tween 20
PHA	Polyhydroxyalkanoate
PhaC <sub>1Pa</sub> -Ag	C terminal fusion of OprI/F-AlgE to the PHA synthase
PhaC <sub>Pa</sub>	PHA synthase from <i>P. aeruginosa</i>
PhaC <sub>Re</sub>	PHA synthase from <i>Ralstonia eutropha</i>
PHA <sub>LCL</sub>	Long chain length polyhydroxyalkanoate
PHA <sub>MCL</sub>	Medium chain length polyhydroxyalkanoate
PHA <sub>SCL</sub>	Short chain length polyhydroxyalkanoate
PHB	Polyhydroxybutyrate
PHBHHx	Copolymers of 3-hydroxybutyrate and 3-hydroxyhexanoate
PHBV	Copolymers of 3-hydroxybutyrate and 3-hydroxyvalerate
PHO	Poly 3-hydroxyoctanoate
PLGA	Poly(lactic-co-glycolic acid)
PMLA	Poly( $\beta$ ,L-malic acid)
RLH	(RIG-I)-Like Helicases
RNA	Ribonucleic acid
scFv	Single-chain antibody variable fragment
TB	Tuberculosis
TCR	T Cell Receptor
TEM	Transmission Electron Microscopy
Tfh	T Follicular helper cell
Th	T helper
TIR	Toll/Interleukin-1 Receptor
TLR	Toll-Like Receptor
TNF	Tumor Necrosis Factor
TRIF	TIR-domain-containing adapter-inducing interferon-beta
VLP	Virus Like Particle
WHO	World Health Organization
XDR	Extensively drug-resistant

# **Chapter 1: General introduction**

## **1.1 Introduction to immunity**

Immunity is a state of protection from microbes (bacteria, virus, fungi, and parasites) or foreign antigens and in mammals is the result of the complex interplay between the innate and adaptive (or acquired) immune systems that have specific immune functions. The ability of the immune system to differentiate self and nonself antigens is critical as dysfunction can lead to autoimmune/inflammatory diseases e.g. type 1 diabetes and inflammatory bowel disease. Innate immunity provides the first line of defense and effects are immediate. The innate immune response is nonspecific, recognizing foreign antigens by pathogen associated molecular patterns (PAMPs) and does not generate immunological memory, that is the ability to respond more rapidly to a pathogen in subsequent encounters. In contrast, the adaptive immunity is slow but highly specific requiring antigen presentation by antigen presenting cells (APCs) to specialized T cell lymphocytes and exhibits immunological memory. The innate immune response functions to prime and guide the correct adaptive immune response, which in turn regulates innate immunity.

## **1.2 Innate immunity**

Anatomical and physiological barriers are the primary barriers of the innate immune system. Anatomical barriers namely the skin and mucosal epithelia serve as the main interface between the host and the external environment functioning to physically prevent entry of microorganisms. Physiological barriers include temperature, pH, and chemical mediators that function to kill and prevent microbial growth.

If these barriers happen to be compromised, the innate immune system needs to be able to detect and respond to the pathogen appropriately. Initiation of innate immune responses induce cellular and molecular defense mechanisms which include inflammation, complement, phagocytosis, and antimicrobial enzymes (e.g. lysozyme) and peptides (e.g. defensins) [1].

Acute inflammation is the primary protective response to infection and/or tissue injury and is activated by resident innate immune cells such as dendritic cells, macrophages, and mast cells. Inflammation is triggered when germline encoded pattern recognition receptors (PRR) which include toll-like receptors (TLRs), nucleotide-binding oligomerization domain (NOD)-like receptors (NLRs), and retinoic acid-inducible gene I (RIG-I)-like helicases (RLHs), and C-type Lectin Receptors (CLRs) detect conserved microbial structures referred to as pathogen-associated molecular patterns (PAMPs) and/or alarm signals of injured host cells called damage-associated molecular patterns (DAMPs) [1-3]. PAMPs are unique to microbes and essential to their physiology or virulence and include bacterial cell wall components (such as lipopolysaccharides, peptidoglycan, and porins), flagellin, and nucleic acids (bacterial and viral RNA and DNA) [3]. DAMPs are nuclear or cytosolic components released into the extracellular environment from dead or injured cells and examples include heat-shock protein, high-mobility group box 1 protein, adenosine triphosphate, deoxyribonucleic acid (DNA), and ribonucleic acid (RNA) [4].

During acute infection, multiple PRRs are activated as a result of PAMPs and DAMPs, which generates a specific signature to tailor an appropriate host immune response [5]. For example, infection with *Pseudomonas aeruginosa* can initiate Toll-like receptor (TLR)4 (binding to flagellin), TLR5 (binding to LPS), and TLR9 (binding to unmethylated CpG), and NLRC4 (binding to flagellin) [6]. Activation of multiple PRRs tends to induce overlapping signaling pathways that can increase the sensitivity for detection and strength of the response to the invading pathogens [7]. PAMPs and DAMPs have been found to utilize similar signaling pathways [8].

Binding of ligand to specific PRR initiates a series of signaling pathways that leads to activation of one of several transcription factors. Transcription factors involved with induction of proinflammatory cytokines include nuclear factor- $\kappa$ B (NF- $\kappa$ B), activator protein 1, and cyclic AMP-responsive element-binding protein, while interferon-regulatory factors (IRFs) are involved with the induction of type I interferons (IFNs) [9, 10]. Type 1 IFNs function to induce an antiviral state by promoting the transcription of IFN-stimulated genes that interfere with viral replication [11]. However, induction of type 1 IFNs is not exclusive to viral infections as bacterial infection can also induce type 1 IFNs, for example, TLR4 activation by lipopolysaccharide (LPS) [12]. Type 1

IFN also contributes to the adaptive immune response through activation of antigen presenting cells (APC), natural killer (NK) cells, promoting T helper 1 (Th1) cytokine production, and the survival of activated T cells [11, 13].

Proinflammatory cytokines such as interleukin-1 (IL-1), IL-1 $\beta$ , IL-8, IL-6, and tumour-necrosis factor- $\alpha$  (TNF- $\alpha$ ) released by non-immune cells (epithelial and endothelial cells) and immune cells (macrophages, dendritic cells, neutrophils, NK cells, mast cells, eosinophils, and basophils) are involved in mediating an inflammatory response [3, 14]. Release of inflammatory mediators increases vasodilation and vascular permeability of blood capillaries, resulting in the characteristic accumulation of fluid (exudate) at the site of infection. The exudate contains various antimicrobial mediators, which includes complement, lysozyme, and antibodies to attack invading pathogens [15]. Leukocytes, mainly neutrophils are recruited during acute inflammation and migrate by chemotaxis (mediated by IL-8) to the site of infection where they are activated. Cytokines IL-1 and TNF- $\alpha$  function to induce endothelial adhesion molecules and promote adhesion of neutrophils to the endothelial cell wall for emigration into the tissue [16]. Activated neutrophils kill invading pathogens by phagocytosis and degranulation [16]. Macrophages and lymphocytes replace neutrophils in the later stages of inflammation and have a role in the resolution of inflammation [16, 17].

### **1.2.1 Pattern recognition receptors (PRRs)**

PRRs can be classified into three families based on function and ligand specificity [18].

1) Endocytic receptors: These are surface membrane bound receptors that mediate the recognition and internalization of pathogens and members of this family include CLRs.  
2) Signaling receptors: These are involved in cell activation and detect a range of PAMPs. Members of this family include the membrane bound receptors TLRs and the NLRs, and RLHs. 3) Soluble PRR such as collectins, ficolins, and pentraxins that function in complement activation and opsonization.

**Toll-like receptors (TLRs)** are type I transmembrane receptors that have leucine-rich repeats for the detection of PAMPs and activate downstream signaling pathways associated with proinflammatory cytokines and type I IFNs. TLRs are expressed either on the membrane or within endosomes of leukocytes and non-immune cells. Ten human and twelve mouse TLRs have been currently identified and detect a wide range of

distinct PAMPs from bacteria, viruses, fungi, and parasites [9, 19]. For example, lipoproteins and peptidoglycans (TLR2), flagellin (TLR5), bacterial and viral single stranded RNA (TLR7 and TLR8), and bacterial and viral DNA (TLR9).

Binding of ligand to specific TLR induces the receptor to form homo or heterodimers that initiates the recruitment of specific cytoplasmic adaptor proteins (Myeloid differentiation primary response gene 88, MyD88-adaptor-like, Toll/interleukin-1 receptor (TIR)-domain-containing adapter-inducing interferon- $\beta$  (TRIF), and TRIF-related adaptor molecule) via TIR domain [10]. Binding of these adaptor proteins to the TIR initiate a series of downstream signaling events involving the interactions of IL-1R-associated kinases and TNF receptor-associated factors which activate mitogen-activated protein kinases, JUN N-terminal kinase, and p38. This subsequently leads to the activation of downstream transcription factors such as NF- $\kappa$ B, IRFs, cyclic AMP-responsive element-binding protein and activator protein 1 [10]. TLR signaling results in the production of proinflammatory cytokines, type 1 IFNs, chemokines, and antimicrobial peptides.

**Nucleotide-binding oligomerization domain (NOD)-like receptors (NLRs)** are multidomain proteins expressed on a range of immune and epithelial cells that act as intracellular cytosolic sensors for PAMPs, DAMPs, and regulate inflammatory and apoptotic responses [20]. NLRs can be divided into NLRA (A for acidic transactivating domain), NLRB (B for Baculovirus inhibitor of apoptosis protein repeat), NLRP (P for pyrin domain), and NLRC (C for caspase activation and recruitment domains) subfamilies. The NLRA subfamily only has one member involved in the regulation of major histocompatibility complex (MHC)-II expression, the MHC-II transactivator. NLRB members are known to trigger inflammasome activation in response to bacterial PAMPs [20]. NLRPs are involved in the activation of caspase-1 and the assembly of inflammasomes, while NLRCs recognize PAMPs and DAMPs and activate inflammatory immune responses [21]. NOD1 and NOD2 are examples of NLRCs which recognize bacterial cell wall glycans and mediates the production of proinflammatory cytokines and antimicrobial peptides through NF- $\kappa$ B and mitogen-activated protein kinase signaling pathways [7].

**Retinoic acid-inducible gene I (RIG-I)-like helicases (RLHs)** (RIG-I, melanoma differentiation-associated gene 5, and laboratory of genetics and physiology 2) are helicases that function to sense viral RNA and induce type 1 IFNs and proinflammatory cytokines through NF- $\kappa$ B and IRF signaling pathways [22, 23].

**C-type Lectin Receptors (CLRs)** are membrane bound and soluble receptors that detect fungal PAMPs and play an important role in fungal immunity. CLRs are a large superfamily of proteins with diverse functions, which includes mannose receptor, dectin-1 ( $\beta$ -glucan receptor) and dectin-2, and collectins [24].

**Soluble PRR (or acute phase proteins).** Collectins [25] and ficolins [26] reside in the plasma and on mucosal surfaces. Collectins and ficolins have similar structures but differ in their lectin domains. They function to recognize PAMPs and activate complement by the lectin pathway [27, 28].

Pentraxins are a superfamily of multimeric proteins produced in the acute inflammatory response. Members of the family can be divided into short (C-reactive protein and serum amyloid P-component) and long pentraxins (PTX3) [28]. Effector functions of this family include activation of complement and facilitating pathogen recognition.

### **1.2.2 Complement system**

The complement system is a key component of the innate immune and adaptive immune systems, and plays a major role in immune protection. This system is made up of a large number of proteins and glycoproteins synthesized by hepatocytes, blood monocytes, macrophages, and epithelial cells [29]. The majorities of these components are produced as inactive proteins and require proteolytic cleavage from one another in a cascade for activation. Activation can be achieved through the classical, alternative, or lectin pathways [30].

The classical pathway is known as the “antibody dependent pathway” due to its strong association with antibodies produced by B cells for activation. IgM and IgG isotypes trigger the complement cascade by the formation of antibody-antigen complexes with microbial surface antigens. This subsequently leads to the binding of C1 (complex of C1q, two C1r, and C1s) mediated by C1q to the antibody-antigen complex.

Furthermore, C1q has been found to directly bind specific PRR for activation e.g. pentraxins [31]. Binding of C1q initiates protease C1r that cleaves and activates C1s. C1s then cleaves C4 into C4a and C4b. C2 binds to C4b and leads to C2 cleavage by C1s into C2a and C2b. The resulting small C2a fragment forms a complex with C4b and C1, generating the C3 convertase [29].

The alternative pathway is similar to the classical pathway but is antibody independent and is triggered by antigens on the microbial surface (i.e. bacterial cell-wall constituents), however, alternative pathway can also be triggered by antibody-antigen complexes [32]. C3 is naturally unstable and breaks down into C3a and C3b. C3b binds to the surface antigen and forms a complex with factor B. The C3b-factor B complex is cleaved by factor D to generate alternative C3 convertase [33].

The lectin pathway is also an antigen independent pathway and is initiated by the binding of mannose-binding lectin (MBL) or ficolins to carbohydrate residues on the microbial surface antigens. MBL-associated serine proteases (MASPs) are then activated by forming a complex with MBL or ficolins and this complex subsequently results in the cleavage of C4 and C2 to form C3 convertase [34].

Terminal effects of the complement cascade regardless of pathway have three outcomes: 1) Direct cell lysis by formation of membrane attack complex (MAC) from the activation of C5 to C9, 2) generation of proinflammatory mediators (C3a, C4a, and C5a), and 3) enhanced opsonization and clearance of the invading pathogen by phagocytic cells, such as macrophages and neutrophils mediated by C4b, and C3b.

### **1.2.3 Phagocytosis**

Professional phagocytes of the innate immune system (neutrophils, monocytes, macrophages, and dendritic cells) function to engulf and kill pathogens by phagocytosis [35]. Phagocytosis can be enhanced by opsonins, which attach to the pathogen such as antibodies [36] and complement [37]. Detection of PAMPs by PRRs on the surface of the phagocytes initiates internalization of the pathogen. Once inside the phagocyte, the pathogen is degraded by enzymes (e.g. lysosome) when a phagolysosome is formed and the waste is expelled by exocytosis. Certain phagocytes such as macrophages and dendritic cells also function as professional APCs, which means proteins from the

pathogen are degraded into small peptides and are combined with MHC and presented on the surface of the cell. This is known/inferred to as antigen processing and presentation [38]. This provides a crucial step in activation of the adaptive immune system.

### **1.3 Adaptive immunity**

The adaptive immune response ensues if the innate immune response fails to eliminate the threat. The adaptive immune system utilizes specialized classes of lymphocytes (T and B cells) that mediate different two different branches of the adaptive immune response. 1) The cell-mediated branch mediated by T cells and 2) the humoral (antibodies) branch mediated by B cells. In order for the activation of either branch of the immune system, the process of antigen processing and presentation by APCs and subsequent presentation to cluster of differentiation 4 (CD4)+ T helper cells (Th) called T cell priming is required.

Professional APCs (in particular the dendritic cell) form the bridge between the innate immune and adaptive immune systems [39]. During primary infection, pathogens are phagocytosed by APCs (e.g. tissue resident dendritic cells), processed, and small peptides of the degraded pathogen are displayed with major histocompatibility complex MHC I or MHC II on the cell surface [40]. MHC is a family of glycoproteins that plays a key role in recognizing foreign antigens and controlling T cell activation. MHC I is found on the surface of most nucleated cells and present peptides derived from endogenous antigens (e.g. cytosolic derived antigens) as a result of viral or intracellular bacterial infection, while MHC II is expressed primarily by lymphocytes, dendritic cells, and macrophages and present peptides derived from exogenous antigens e.g. from extracellular bacterial infection [38]. Conversely, exogenous antigens can also be presented onto MHC I via cross-presentation [41].

APCs displaying membrane bound antigen-MHC complexes on their surface then move to the nearest draining lymph node for presentation to naïve CD8+ or CD4+ T cells. Naïve CD8+ T cells recognize antigens presented with MHC I and promote activation of CD8+ cytotoxic T cells (CTL) involved in direct killing of infected cells [42]. CD4+ naïve Th cells recognize antigen presented with MHC II and are involved in the

activation of effector T cells and B cells. For full T cell activation, two signals are required. The first signal from T cell receptors (TCR) as a result of the specific binding to antigen-MHC complex which leads to IL-2 receptor expression, IL-2 secretion, and CD40 ligand (CD40L) upregulation. The second costimulatory signal is from the interaction of CD40L or CD28 on the CD4<sup>+</sup> and CD8<sup>+</sup> T cells with CD40 or CD80/86, respectively, on the APCs [43, 44].

Th cell proliferation and differentiation into effector T cells and memory T cells is dependent on the cytokines produced during the innate immune response. Activated Th cells can differentiate into several types of effector T cells with Th1, Th2, and Th17 being the major subsets [45]. Other types of effector T cells include regulatory T cells (Treg) and T follicular helper cells (Tfh). Effector T cells are classified based on the distinct cytokines they secrete which regulate specific innate immune functions.

### **1.3.1 Effector T cells**

**Th1 cell** differentiation is triggered by the production of IFN- $\gamma$  and IL-12 from APCs mediated via the transcription factor T-bet [46]. Th1 cells mediate cellular immunity by secreting cytokine IL-2 and IFN- $\gamma$  which promotes phagocytosis, upregulates microbial killing, activate iNOS against intracellular pathogens, and B cell IgG class switching to IgG2a [47, 48]. It is important to note that in certain mouse strains (e.g. C57BL/6), the IgG2c subclass is produced instead of IgG2a [49]. Effector cells of Th1 immunity include macrophages, CD8<sup>+</sup> T cells, B cells, IFN- $\gamma$  CD4<sup>+</sup> T cells, and NK cells.

**Th2 cells** mediate humoral immunity against extracellular pathogens such as parasites and extracellular bacteria. Th2 cells secrete a range of cytokines, which include IL-4, IL-5, IL-9, and IL-13. Activation of Th2 cells is regulated by the transcriptional master regulator GATA-3 [50, 51]. Effector cells include granulocytes (e.g. neutrophils and eosinophils), B cells, and IL-4/IL-5/IL-9/IL-13 CD4<sup>+</sup> T cells.

**Th9 cells** are a recently described subset that develops in the presence of cytokines IL-4 and TGF- $\beta$ . Th9 cells produce mainly cytokine IL-9 but production of IL-10 and IL-21 has been shown. Cytokine production is through transcription factors such as STAT6, PU.1, IRF4, and GATA3 [52]. Th9 cells have been implicated in a range of autoimmune disorders such as multiple sclerosis [53].

**Th17 cells** secrete IL-17 and promote immunity against extracellular bacteria and fungi. Differentiation into Th17 is triggered by transforming growth factor- $\beta$  (TGF- $\beta$ ) and IL-6 and/or IL-21 through transcription factor ROR $\gamma$ t [54, 55]. Activation of Th17 stimulates the production of proinflammatory cytokines and antimicrobials. Effector cells include neutrophils, macrophages [56].

**Regulatory T cells (Treg)** differentiation is triggered by TGF- $\beta$ . Tregs function to regulate the immune response and induce tolerance by down regulating mechanisms involved in the induction and proliferation of effector T cells. This can be achieved by multiple mechanisms such as producing suppressive cytokines e.g. IL-10. IL-10 signaling activates STAT3 transcription factor and has a key role in regulation of inflammation [57].

**T Follicular helper cells (Tfh)** are important for the formation and maintenance of germinal centers and provide help to B cells by producing IL-21 which stimulates differentiation of B cells into plasma cells [58].

### **1.3.2 Interplay and plasticity of effector T cells**

CD4<sup>+</sup> T cells and their differentiation into functionally distinct T cell subsets is critical for the protection against infections and also autoimmunity diseases [59]. The framework for understanding CD4<sup>+</sup> T cell differentiation into effector CD4<sup>+</sup> T cell subsets was set out by Mosmann and Coffman in the late 1980's, coining the classical Th1/Th2 paradigm. In this paradigm, naïve CD4<sup>+</sup> T cells were thought to polarize into either one of two lineages, Th1 or Th2 subsets, which was characterized by their distinct 'master regulator' transcription factors and expression of signature cytokines [60]. Th1 effector T cells typically function in response to intracellular pathogens such as bacteria or viruses and produce IFN- $\gamma$ . Th2 effector T cells on the other hand produced IL-4, IL-5, and IL-13, which are important for a humoral response for the elimination of extracellular pathogens and parasites [59, 61]. Commitment of CD4<sup>+</sup> T cells to one lineage would produce cytokines that inhibited the development of the other. For example, IFN- $\gamma$  produced by Th1 lineage inhibited the production of Th2 cytokines (IL-4) and vice versa [62].

It is now well known that the Th1/Th2 paradigm is overly simplistic and this dichotomous view is now out dated. CD4<sup>+</sup> T cells are found to differentiate into a diverse range of subsets in addition to the classical Th1 and Th2 subsets, which includes Th9, Th22, Tfh, Th17, and Treg [59].

Cytokine cues instruct CD4<sup>+</sup> T cell development and differentiation into specific lineages [62]. A given cytokine can be produced by more than one type of cell. For example, IL-10 is a signature cytokine produced by Tregs, however, other immune cells such as monocytes, neutrophils, and T and B lymphocytes can also produce IL-10 [63]. Further more, a given cytokine can also influence a number of immune cells. For example, IL-2 produced by activated T lymphocytes functions in Treg homeostasis, generation of Th17 cells, differentiation of effector CD4<sup>+</sup> T cells into Th1 or Th2 cells by promoting Th1 cell differentiation, CD8<sup>+</sup> T cell generation and differentiation, and inhibit the generation of Tfh cells [64].

In addition to CD4<sup>+</sup> T cell differentiation into number of T cell subsets, there is increasing evidence that suggest polarized T cell (effector T cell) subsets can change their phenotype and display characteristics typical of other effector T cells or fully convert into another effector T cell subset as a result of changing milieu, known as T cell plasticity [45, 60, 62]. Th17 cell subset have been found to display a high degree of plasticity, change their phenotype and repolarize to a different subset that includes Th1, iTreg, and Th22 [45, 65, 66]. For example, Th17 cells can convert to T regulatory type 1 (TR1) cell during immune response in the presence of cytokines TGF- $\beta$ 1, and AhR activation [67]. Additionally, Th17 cells can have phenotype of different effector T cell subsets by coexpressing different transcription regulators such as ROR $\gamma$ t (Th17 transcription factor) with Foxp3 (Treg transcription factor) [67].

Tregs characterized by transcriptional regulator FoxP3<sup>+</sup> are another subset of CD4<sup>+</sup> T cells that display a high degree of plasticity. Tregs function to maintain tolerance and to prevent autoimmune disease. However, evidence has shown Tregs can change into other effector T cells and promote rather than suppress inflammation, resulting from the down regulation of Foxp3. For example, IL-6 in conjunction with IL-1 and IL-23 leads to expression of transcriptional regulator ROR $\gamma$ t and down regulation of Foxp3 leading to a Th17 phenotype characterized by the production of IL-17 [68].

Regulation of T cell plasticity can occur by different means, which include extracellular cues, cytosolic signaling cascades, and signals in the nucleus [45].

Cytokines are the primary means of driving plasticity between T cell subsets. Cytokines alone are capable of polarizing CD4<sup>+</sup> T cells e.g. IL-12 for Th1 and IL-4 for Th2. Moreover, these polarized phenotypes can be reversed, for example Th1 polarized T cells can reverse by incubating cells with IL-4 or Th2 culture with IL-12 and IFN- $\gamma$  [45]. Another examples include Th9 cells exhibiting plasticity towards Th1 (IL-12), Th2 (IL-4 and TGF- $\beta$ ), and Th17 (TGF- $\beta$ , IL-1, and anti-IFN- $\gamma$ ) when cultured on polarizing media [69].

The affinity of TCR for antigen-MHC complex and co-stimulatory interactions during antigen presentation can generate varying signal strengths and found to alter the differentiation of CD4<sup>+</sup> T cells subsets. Strong TCR signaling drives polarization towards Th1 subset and very high signal strength supports differentiation into Th2 or Tfh subsets, while weak TCR signaling shown to favor development of Treg subset [45].

Cytosolic signaling by serine-threonine kinases and mammalian target of rapamycin (mTOR) pathways play a key role in T cell plasticity resulting from activation from extracellular cues [45, 62]. mTOR is a central regulator of cell metabolism, growth, proliferation and survival and integrates intracellular and extracellular signaling pathway [70]. mTOR activation leads to increased maturation of CD4<sup>+</sup> T cells into effector T cells, while absence of mTOR abrogates ability to produce Th1, Th2, or Th17 cells and a increase in Treg [62].

T cell plasticity can be seen as both being beneficial and detrimental. T cell plasticity may provide the flexibility required during events of changing circumstances, for example, ability of T cells to change from IL-17 to IFN- $\gamma$  producing T cells may better combat a pathogen going from extracellular to intracellular spaces [45]. Detrimental effects of T cell plasticity have also been shown, for example, functional plasticity in the FoxP3 expressing Tregs important in the control of viral infections towards Th17

proinflammatory phenotype during acute viral infection in patients with acute hepatitis A is associated with immunopathology [71].

### **1.3.3 Effector B cells**

B cells are an essential component of the humoral immune response and responsible for generating antigen specific antibodies. The production of antibodies has several outcomes, 1) neutralization of microbe or toxin, 2) opsonization, or 3) activation of complement. Activation of naïve B cells can occur through either the T cell dependent (TD) or independent (TI) pathway [72]. The naïve B cells acts as the APC by binding antigen mediated by specific surface immunoglobulin of the B cell receptor. The antigen-receptor complex enters the cell by endocytosis, degraded into small peptides and subsequently presented on the naïve B cell surface in a complex with MHC II for presentation to activated Th2 cells. Following presentation, T cells express CD40L and cytokines such as IL-4 and IL-21 that promote B cell proliferation and differentiation into antibody-secreting plasma cells (enhancing production of high affinity neutralizing antibodies) and memory cells [73].

Activation of naïve B cells by the T cell independent (TI) pathway generates low affinity antibodies, which can be induced by two different classes of antigen called TI-1 and TI-2 antigens [74]. TI-1 antigens, such as LPS or DNA activate TLRs expressed by B cells triggering B cell proliferation and differentiation. TI-2 antigens are highly repetitive epitopes (e.g. bacterial capsular polysaccharide and bacterial flagellin) that are able to cross-link B cell receptors on the surface of an antigen-specific mature B cell, triggering activation. Activated B cells can undergo a process called class switch recombination (CSR) as a result of antigen or presence or absence of T cell mediators [75]. Class switching results in the production of a single IgA, IgE or IgG subclass, for example, IFN- $\gamma$  a major cytokine produced by Th1 cells stimulates B cell class switching to IgG2a isotype [47, 75].

## 1.4 Introduction to vaccines

Vaccines are regarded as the most important and cost effective strategy for the prevention of infectious diseases in humans [76]. Vaccines have resulted in the successful eradication or reduction in the mortality and morbidity caused by many infectious diseases such as smallpox and polio [77]. Furthermore, vaccines have an indirect positive effect on the economy [78].

Since their discovery and introduction, vaccines have always received intense scrutiny and debate from the public [79]. Vaccination related severe adverse events are rare and more so with modern vaccines that abide by strict safety guidelines. Early vaccines however were crude and incidences of vaccine-associated complications were more common [80]. However, even with the safest vaccines there will always be a small population who are susceptible to being infected by a pathogen. Susceptible individuals are typically those that have impaired immunity, such as that caused by disease (e.g. HIV) or because of age (infants and elderly) [79, 81].

There is a major push for more effective and safer vaccines. Important advances have been made in various fields that have contributed to the improvement of existing vaccines and the development of novel vaccines that were impossible before. With the development of new technologies, new avenues for vaccine design can be explored. These fields include genomics and bioinformatics, leading to the identification of various epitopes which can be targeted; and immunology, which contributes to the understanding of the underlying mechanisms of how vaccines work [81, 82].

New vaccine technologies open new avenues for vaccine designs that minimize risks and can produce vaccines that are highly immunogenic and induce long-lasting immune responses [80].

There is a need for the development of novel vaccines as traditional approaches may not be completely effective at preventing all infectious diseases such as tuberculosis caused by intracellular bacterium *M. tuberculosis* and chronic infection caused by *P. aeruginosa*. Furthermore, new vaccine strategies are required to prevent an endemic or pandemic from new and re-emerging diseases.

## 1.5 Traditional vaccines

Traditional vaccines are typically classified into 4 types: 1) live attenuated, 2) killed inactivated, 3) toxoid, and 4) subunit. Success of these traditional vaccines is typically associated with long-lived Th2 type antibody response for the neutralization and promotion of opsonization by phagocytes.

### 1.5.1 Live attenuated

Traditionally live attenuated bacterial vaccines are produced by a series of subculturing on selective media and then selecting for attenuated mutants that have a reduced or absence of ability to cause disease. Live attenuated vaccines are the most similar to a natural infection and can confer strong, long-lived cellular and antibody responses compared to subunit vaccines [83]. For example, live attenuated *Bordetella pertussis* vaccine BPZE1 was found to protect infant mice against challenge with virulent *B. pertussis* and was fully protected for 1 year, compared to mice vaccinated with acellular *B. pertussis* vaccine was only able to confer partial protection and protection waned after 6 months [84].

However, there are significant safety concerns associated with live attenuated vaccines, as live vaccines have the potential to mutate and revert back to the virulent disease-causing form [85, 86]. Furthermore, cases of attenuated strains causing disease in people with weakened or impaired immune systems have been shown. For example, BCG (Bacille Calmette-Guérin) a commonly administered vaccine against tuberculosis can cause mild to severe BCG related infections (BCGitis and the less common BCGosis) in immune-compromised patients [87].

Modern approaches to attenuation by molecular means allow for more control during the attenuation process compared to traditional methods (e.g. subculturing on different media). This is made easier with advances in genomics whereby whole bacterial genome sequencing is possible. Genome data allows for the identification of specific virulent genes that can be targeted for removal [81]. For example, *M. tuberculosis* vaccine candidate MTBVAC, a genetically attenuated strain where two virulence genes *phoP* and *fadD26* encoding transcription factor regulator and synthesis of cell-wall lipid PDIM were deleted [88].

### **1.5.2 Killed inactivated**

Killed inactivated vaccines are typically produced by several methods that include chemical, heat, and radiation treatment. In comparison to live attenuated vaccines, killed inactivated vaccines cannot replicate and consequently provoke a weaker immune response [89]. For example, vaccination with the live attenuated influenza vaccine but not the trivalent inactivated vaccine significantly increased the influenza virus-specific IFN- $\gamma$  CD4+ and CD8+ T cells in children [90]. Therefore to maintain immunity much like subunit vaccines, boosters or adjuvants are required [86]. Furthermore, killed inactivated vaccines preferentially induce CD4+ Th2 type (humoral) immune responses and do not trigger activation of CD4+ Th1 type immune responses and CD8+ cytotoxic T cells (CTLs) which are important to control certain diseases [91]. The advantage of killed inactivated vaccines compared to live attenuated is that they are considered safer, as they cannot cause disease and tend to be more stable.

### **1.5.3 Toxoid**

Toxoid vaccines are vaccines that contain altered or inactivated toxins (e.g. formaldehyde or heat) called toxoids from certain bacterial strains that excrete disease-causing exotoxins. Examples include *Clostridium tetani*, *Corynebacterium diphtheria*, *Clostridium botulinum* and *Vibrio cholerae* which cause the diseases tetanus, diphtheria, botulism, and cholera, respectively [91]. Toxoid vaccines work by inducing antibodies to the original toxin. For example, tetanus toxoid vaccine protects against *C. tetani* by inducing antitoxin antibodies that bind and neutralize the tetanus toxin, this prevents the toxin from binding receptor sites on nerve cells [91]. An advantage of toxoid vaccines is that they do not have virulence.

### **1.5.4 Subunit**

Unlike live attenuated or killed vaccines, subunit vaccines contain defined antigens and/or epitopes known to stimulate immunity to certain diseases. Since antigens are defined, this makes subunit vaccines inherently safe and also results in the reduction of adverse reactions [86]. Antigens can be either protein or polysaccharide and tend to trigger the adaptive immune response required for generating memory. Protein antigens are able to directly interact with T cells via MHC, while polysaccharide antigens are T cell independent can bind directly to B cell receptors [91].

Both protein and polysaccharide can be conjugated together by formation of covalent bonds, resulting in protein-polysaccharide conjugate vaccines [92]. Effects of conjugation can direct the immune response towards a T cell dependent response for both protein and polysaccharide. This is beneficial particularly for the polysaccharide component as this T cell dependent response leads to the generation of B and T memory cells [91]. For example, pneumococcal conjugate vaccines (PCV) have been successfully employed to protect against invasive pneumococcal disease caused by the bacterium *Streptococcus pneumoniae*, resulting in a substantial reduction of the vaccinated serotypes [93]. Consequently, this has resulted in an unoccupied niche that was rapidly filled with an increase in the non-vaccinated serotypes [93].

A disadvantage for subunit vaccines is that a lot of time and effort is required for the identification of protective antigens. New techniques such as reverse vaccinology utilize a bioinformatic approach that can speed up the development of vaccines by identifying genes which may code for antigenic determinants and have the potential to become vaccine candidates [94].

Subunit vaccines also tend to suffer from poor immunogenicity as compared to live attenuated vaccines and require the use of adjuvants [86]. Most modern subunit vaccines are recombinant subunit vaccines, whereby antigens or epitopes identified by bioinformatics can be manufactured using recombinant DNA technologies. These vaccines tend to use highly purified recombinant proteins or synthetic peptides in combination with adjuvants [95]. Recombinant DNA technologies allow for the generation of multicomponent subunit vaccines that makes them more cost effective and simple [96].

## **1.6 Novel vaccine approaches**

Novel vaccines are required to control and eradicate infectious diseases where traditional vaccines approaches fall short. These novel vaccines are necessary to protect against current diseases where no highly effective vaccine is available (e.g. tuberculosis) and to new or re-emerging diseases (e.g. influenza) [97]. Success of most traditional vaccines tend to focus on the induction of long-lived T cell dependent IgG responses through antigen presentation by MHC II to T cells or direct activation of B

cells [98]. In addition, traditional vaccines typically do not have defined components and many of the components in these vaccines can have a negative effect, or even cause unwanted side effects such as fever. This problem can be solved by novel vaccine approaches, whereby defined components (antigens) are used in conjunction with novel adjuvants and/or delivery systems resulting in safer vaccines with enhanced potency [99].

New vaccines are subunit based and therefore, rely on the identification of appropriate antigens and epitopes to stimulate the appropriate immune response. Correct presentation of these antigens to the immune systems is important to obtain an optimal immune response [99]. Subunit based vaccines tend to suffer from poor immunogenicity, as a result of suboptimal recruitment and activation of APCs [100]. Immunogenicity and consequently protection can be improved by designing multicomponent vaccines that can contain a number of epitopes and TLR-ligands. Identification and careful selection of immunodominant epitopes is important to obtain an appropriate immune response, for example, selection of immunodominant B cell epitopes are important for promoting a humoral response against extracellular pathogens. However, care needs to be taken as certain combinations of epitopes can result in an antagonistic effect. For example, a specific combination of influenza virus epitopes (HA<sub>332-340</sub>, M1<sub>128-135</sub>, or PA<sub>224-233</sub>) resulted in delayed viral clearance [101]. The authors speculated this might have been due to the result of excessive T cell production for epitopes not present on infected lung epithelial cells, inhibition of T cell migration, or detrimental effect of either of the epitopes.

Activation of specific TLRs or multiple TLRs has been shown to influence the type of immune response and differentially regulate the appropriate cellular and humoral responses [102, 103]. A critical function of adjuvants is the activation of PRR (e.g. TLRs) to enhance immune response to subunit-based vaccines [99]. Therefore, novel vaccines that incorporate multiple TLR-ligands (PAMPs) capable of activating multiple TLRs could lead to a stronger, longer lasting, and more specific immune response than with a single ligand alone.

Novel vaccine approaches utilize different adjuvants and delivery systems to improve vaccine performance and potency. Peptides alone are poorly immunogenic and require adjuvants and next generation delivery systems such as delivery systems offer a

solution, leading to stronger and better immune responses, which may also eliminate the need for boosters.

### **1.6.1 Adjuvants**

Adjuvants are typically compounds formulated and administered with low immunogenic vaccines to enhance or direct the immune response, but have no antigenic effect by themselves. The field of adjuvant development is becoming increasingly important as new modern vaccines are based around recombinant proteins and DNA. Small particulate delivery systems such as PHA beads and virus like particles (VLPs) can also be classified as adjuvants, as they modify the immune response by mimicking properties of pathogens such its size, charge, and hydrophobicity for enhanced uptake and stimulation of APCs [95]. Delivery systems will be discussed in Chapter 1.6.3.

Aluminum compounds such as aluminum hydroxide (i.e. alum), aluminum phosphate, MF59 and AS04 are the only approved adjuvants by the US Food & Drug Administration for use in humans, of which alum is the most widely used [104]. However, alum has several limitations: the development of local reaction; it is not effective for all antigens; and mainly activates a Th2 type antibody response which is not favorable for protection against intracellular pathogens. In addition, alum is not effective at inducing an IgA antibody response, which is important for pathogens that enter through the mucosal route e.g. *M. tuberculosis* [105]. MF59 is an oil-in-water emulsion that uses squalene, which is a natural component of cell membranes [106]. MF59 has been shown to be a more potent adjuvant at inducing antibody and T cell response compared to alum [95, 107]. AS04 is a 2<sup>nd</sup> generation combinational adjuvant composed of both alum + monophosphoryl lipid A (MPL) and is currently licensed for use in hepatitis B and human papillomavirus vaccines [108].

Use of adjuvants is highly dependent on formulation and individual application. Besides alum, MF59, and A04, a number of other experimental adjuvants are available such as bacteria-derived adjuvants, carbohydrate adjuvants, and cytokine adjuvants. However, most have been shown to be too toxic to be used routinely in humans [109]. Toxicity is a key issue that needs to be addressed in the development of new adjuvants. Other factors that influence adjuvant development include, biodegradability, stability, and applicability [109].

### 1.6.2 Deoxyribonucleic acid

DNA vaccines provide an alternative to protein or carbohydrate based vaccines. DNA vaccines were designed specifically to induce a CD4<sup>+</sup> T cell response via MHC II presentation and a CTL response via MHC I. To achieve this, DNA vaccines contain bacterial plasmids that encode antigens regulated under a eukaryotic promoter and are delivered directly into a cell [110]. This enables *in vivo* expression of antigenic proteins within the cell and subsequent processing in the proteasomes and display of peptides on their surface with MHC I or MHC II. Presentation via MHC I can stimulate CD8<sup>+</sup> CTLs via antigen cross-presentation, while presentation on MHC II via APCs stimulate CD4<sup>+</sup> Th1 T cells (promotes CTL activation) [110, 111]. DNA vaccines are currently seen to only induce Th1 immune responses but weak Th2 responses [112]. A Th1 type response is particularly important for protection against intracellular pathogens such as *M. tuberculosis*.

DNA vaccines can offer several other advantages over traditional vaccines such as convenient development, production, and safety. Since DNA vaccines contain only genetic material, new vaccines can be made fast and easily by manipulation of coding sequences to counter fast drifting virus strains. Antigen production is achieved by the host and therefore, reduces the need for downstream purification and risk of LPS contamination. Moreover, expressed proteins resemble their normal structure, as recombinantly produced antigen in bacteria may not possess the correct posttranscriptional modifications and consequentially, resulting in poor immunogenicity [111, 112].

Despite their advantages, DNA vaccines currently suffer from poor immunogenicity compared to protein-based vaccines. Expression levels induced by DNA vaccines tend to be low (low picogram to nanogram range) and may contribute to this problem [111]. Therefore, improving levels of antigen expression and immunogenicity has become the primary focus of DNA vaccine development [112].

DNA vaccines offer a promising approach to vaccine design in terms of robustness and ease of development, though significant work is required to improve immunogenicity with this approach.

### 1.6.3 Delivery systems

Subunit vaccines tend to be poorly immunogenic and require the need for adjuvants and/or booster vaccinations [86]. A single dose of a subunit vaccine is typically not enough to produce an effective immune response. However, multiple vaccinations can be given over a set period of time known as boosters to circumvent this problem to produce an effective immune response through increase clonal proliferation of antigen-specific lymphocytes [113].

Antigen delivery systems are of particular interest as they can enhance the uptake of antigens by APCs, which leads to an improved immune response compared to antigen alone and therefore, may circumvent the need for booster vaccinations [114, 115].

Antigen uptake by APCs can be influenced by many factors such as size, shape, and surface charge [98]. Size has been found to be a major contributing factor influencing antigen uptake by APCs, and particulates that are similar in size to virus and bacteria are considered to be more efficiently taken up [116]. In general, particulates with a size range of between 60 – 1000 nm are defined as nanoparticles and share a similar size range to viruses, while particulates greater than 1000 nm are defined as microparticles and have a similar size range to bacteria [116]. There is currently little agreement on an effective size range for optimal uptake by APC, however, a size range of less than 200 nm has been suggested and particles in this range induce strong CD8<sup>+</sup> T cell responses [117]. Uptake by macrophages of sizes greater than 2 μm have been documented using polystyrene particles, however, they tend to be poorly phagocytosed [118].

Evidence for enhanced cellular immune responses have been shown when small particles displaying antigens are used as a vaccine compared to soluble antigen alone [119-121]. VLPs, liposomes, immune stimulating complexes (ISCOMs), chitosan, and biological polyesters such as PHAs are all examples of particulate delivery systems for antigens. Particulate delivery systems are useful as they mimic various properties of pathogens [98]. Particulate delivery systems offer several advantages such as ability to target APCs, controlled antigen release, antigen-display, and co-incorporation of immunostimulants. Furthermore, particulate antigen delivery systems are self-adjuncting and therefore, formulation with adjuvants such as alum may not be required.

**Poly lactide co-glycolide (PLG)** is a biodegradable and biocompatible polymer which has been demonstrated to be well tolerated in biological systems and has been used for many years as a surgical suture material. PLG has been extensively studied and PLG particles are used as a delivery system for both the controlled release of drugs and as an antigen delivery system. A study demonstrated the adjuvanting properties of PLG particles by co-encapsulating poorly immunogenic antigen ovalbumin (OVA) and poly(I:C) immunostimulant, which facilitated significantly better (~2 time higher) priming of Ag-specific CD8<sup>+</sup> T cells compared to soluble OVA + poly(I:C) with incomplete Freund's adjuvant in a mouse model [121].

As a vaccine delivery system PLG particles can be charged to adsorb vaccine antigens such as plasmid DNA, recombinant proteins, and immunostimulatory oligonucleotides [109, 122]. PLG particles with adsorbed antigens were successfully presented to APCs and shown to significantly enhance immune responses compared to alum alone.

PLG is produced chemically by solvent evaporation and can be engineered to have different polymeric composition and molecular weights, which affect its degradation kinetics. Controlled release of antigen has advantages for reducing the need for booster injections as a result of the depot effect e.g. subunit vaccines [109, 123].

**Chitosan** is a linear cationic polysaccharide composed of randomly distributed glucosamine and N-acetyl glucosamine co-monomer units. Chitosan possesses certain inherent properties that make them favorable as vaccine delivery agents, such as being nontoxic, having low immunogenicity, biocompatible, and biodegradable [124]. Chitosan particles have a wide size distribution (100 nm – 600 nm) and preparation allows the incorporation of protein and DNA antigens during the encapsulation process [125]. The release of encapsulated macromolecules is limited, but it can be controlled by altering matrix density such as the degree of crosslinking [126].

There has been increasing interest in the use of chitosan particles via the mucosal delivery route, as chitosan possess mucoadhesive properties that make them favorable [124]. For example, chitosan microparticles have been successfully employed as a vaccine delivery system against diphtheria [127]. Diphtheria toxoid loaded chitosan

particles were associated with significant humoral immune responses after nasal vaccination.

**Liposomes** are synthetically produced spherical particulates composed of lipid bilayers. They can be employed to encapsulate antigens or couple antigens to enhance and elicit a desired immune response [128]. However, problems related to stability, manufacturing and quality assurance have prevented their use as adjuvants [109].

**Immune stimulating complex (ISCOM)** are large, typically 40 nm diameter spherical particles made of quillaia saponins, phospholipids, cholesterol, and antigens. These particles are formed when the first three components are mixed in a specific stoichiometry and held together by hydrophobic interactions. Vaccine antigens with hydrophobic or amphipathic properties can be incorporated to these particles. Vaccination with ISCOM antigen particles have been shown to induced a mix Th1/Th2 type immune response [109, 129].

**Virus-like particles (VLPs)** are nonreplicating, inert, and empty capsids of viruses that don't contain any genetic material and have been found to stimulate both the innate and adaptive immune responses. VLPs can be genetically engineered to display antigens and have been shown to be effectively taken up by APCs [89, 130]. Best-known VLP vaccines are Gardasil (Merck) and Cervarix (manufactured by GSK) [131].

**Outer membrane vesicles (OMVs)** are 50 – 250 nm spherical shaped proteoliposomes released from the surface of, but not exclusive to, Gram-negative bacteria [132, 133]. OMVs are 'blebs' of the outer membrane and therefore, composed of outer membrane lipids (LPS, phospholipids), outer membrane proteins (e.g. bacterial antigens), and soluble periplasmic content (e.g. DNA/RNA) [133, 134]. OMVs have a number of functions, which include secretion of virulence factors, stress response, gene transfer, biofilm formation, communication, and host immune modulation [135].

Interest in OMVs as a platform for vaccine development is increasing due to their immunogenicity, self-adjuvanticity, and ability to be taken up by mammalian cells [134-137]. There are already several successful OMV based vaccines available on the market, namely meningococcal vaccines VA-MENGOC-BC, MenBvac, MeNZB, and

BexSero [138]. A number of OMV vaccine have been explored for a range of pathogenic bacteria such as *Acinetobacter baumannii* [139], *Bordetella pertussis* [140, 141], *Burkholderia pseudomallei* [142], *Mycobacterium tuberculosis* [143], and *Vibrio cholerae* [144].

OMVs are strong inducers of the immune system and elicit diverse antibody responses and cell mediated responses as a result of their bacterial-derived composition. For example LPS a major component of OMVs activate an inflammatory response through TLR4 receptor, a potent activator of immune cells such as macrophages [134]. Moreover, OMVs contain lipoproteins that activate the innate immune response through TLR2 receptor recognition [134].

OMVs can be used in their native wild-type form or produced by detergent extraction e.g. deoxycholate. The latter method has the benefits of detoxifying and reducing LPS to safe levels, as native OMVs are found to contain high amounts of endotoxin (LPS) that can cause adverse effects [138]. Detergent based methods can however can result in the lost of important protective antigens such as Factor H binding protein from OMV derived from *N. meningitidis*, therefore, detergent free methods are being evaluated [138].

OMVs can be engineered as a delivery system for the delivery of heterologous antigens for increased immunogenicity. Chen et al. [145] describes the genetic fusion of GFP with OMV protein cytolysin A. Results showed immunogenicity to GFP was enhanced compared to fusion protein alone and when protein was absorbed to adjuvant aluminum hydroxide. Another group engineered OMV (geOMV) from *E. coli* to produce OMVs with modified glycan from unrelated bacterial pathogens *streptococcus pneumoniae* and *Campylobacter jejuni* [136]. Here geOMV was able to generate high levels of antigen specific serum IgG and were effect in an opsonophagocytosis assay. Furthermore, geOMV was able to demonstrate a 10<sup>4</sup>-fold reduction in *C. jejuni* colonization compared to controls.

Although the use of OMVs as a vaccine platform have many attractive properties such as the ability to elicit a strong humoral immune response, a number of challenges exist, which includes high levels of LPS, low expression of relevant protective antigens, lower

strain coverage (narrow protection), and antigens or molecules that interfere with a protective immune response [134].

**Polyhydroxyalkanoate (PHA) beads.** Biocompatibility, low immunogenicity, biodegradability, and the small particulate size of PHA beads make them attractive as vaccine delivery agents. In comparison to other particulate systems, PHA beads offers two distinct advantages: 1) a one step production process and 2) the display of vaccine candidates that are covalently attached to the beads surface in a uniform orientation [146, 147]. This removes the need for added steps involving crosslinking or encapsulation of macromolecules.

Although the use of PHAs as functionalized beads has been extensively shown, it has only recently been demonstrated as a safe and efficient vaccine delivery agent [147]. The PHA beads were produced in a heterologous *E. coli* production host and were engineered to display *M. tuberculosis* vaccine candidate antigens 85A (Ag85A) and 6-kDa early secreted antigenic target (ESAT-6).

Gram-negative bacteria such as *E. coli* contain lipopolysaccharides (endotoxins) that are known to copurify with PHA beads and can cause a wide variety of undesired pathophysiological effects [148]. Therefore other bacterial production hosts such as Gram-positive *L. lactis* have been explored [119, 148]. Alternatively, genetically engineered endotoxin free *E. coli* strain could be used [115]. PHA beads derived from *E. coli* or *L. lactis* were found to induce significant cell-mediated immune responses and protect against aerosol *M. bovis* challenge [149].

Interestingly, the production of these PHA beads was found to carry copurifying host cell proteins (HCPs) of their production host (*E. coli* or *L. lactis*) in addition to the display of the fusion antigen. Therefore, PHA bead based vaccines produced in the disease microorganism offer additional benefits, display of known and unknown HCPs as antigens which has the potential to induce protective immunity.

PHA vaccines can suffer from low protein expression and PHA yields if produced in recombinant hosts other than *E. coli*. Expression levels can be improved by use of various vectors and promoters to drive expression, while metabolic engineering can be

used to direct metabolic carbon flux towards production of PHA and increase yield. Significant downstream processing may also contribute as a significant problem depending on production host and intended application. For example, Gram-positive bacteria like *L. lactis* are considerably difficult to efficiently lyse due to the inherent properties of their cell wall, size and shape, resulting in additional cost for extraction.

PHA based vaccines offer an exciting and new avenue for vaccine design with the ability to induce Th1 type and CTL immune responses important for the control of infectious disease.

## 1.7 Polyhydroxyalkanoate

Polyhydroxyalkanoates (PHAs) are naturally occurring biopolyesters composed of (*R*)-3-hydroxy fatty acids naturally synthesized by range of bacteria and some archaea species as insoluble cytoplasmic inclusion bodies. These inclusion bodies function as carbon and energy reserves, synthesized under conditions of growth-limitation (e.g. nitrogen) and excess carbon [150].

Poly(3-hydroxybutyric acid) (PHB) is the most commonly found form of PHA isolated from bacteria. The type of PHA produced by bacteria is primarily dependent on the bacteria and carbon source. Thioester precursors are generated from intermediates of primary metabolism and there are greater than 150 different hydroxyalkanoic acids found to be incorporated in these polyesters and of which results in PHAs with varying material properties [151, 152].

Bacteria are capable of accumulating greater than 80% of their cellular dry weight in PHA [146, 153]. Both size and diameter of these inclusions vary depending on the bacteria, typically range in size between 50 – 500 nm in diameter with 5 – 10 inclusions on average per cell [146].

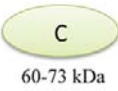



The simplest pathway for PHA formation is the PHB pathway, requiring only three key enzymes, namely  $\beta$ -ketothiolase (PhaA), acetoacetyl-CoA reductase (PhaB), and PHA synthase (PhaC) and arrange into the *phaCAB* operon. The first two enzymes PhaA and PhaB work sequentially to form precursor (*R*)-3-hydroxybutyryl-CoA, while PhaC is

involved in the final stereo-selective conversion of this precursor into PHA with the concurrent release of CoA [151, 154].

PHA are known to have a range of attractive properties making them potentially useful for a large range of applications in the industrial and medical fields. These properties include biocompatibility, biodegradability, modifiable physical and thermal properties, and production from renewable resources [155]. Only recently has PHA been used in their natural particulate form and functionalized by incorporating various proteins or chemicals for use in specialized applications such as drug and gene delivery, vaccines, diagnostics, fluorescent labeling, and affinity purification [146, 156]. However, none are commercially available.

### 1.7.1 Polyester synthases

PHA synthases are involved in the final stereo-selective conversion of different (*R*)-hydroxyacyl-CoA thioester monomers into PHA, with the concurrent release of CoA. PHA synthases can be divided into four major classes predominantly based on subunit composition and sequence similarity [157] (Fig. 1.1).

Class	Subunits	Key Species	Primary Substrate
I	 C 60-73 kDa	<i>Ralstonia eutropha</i>	SCL
II	 C 60-65 kDa	<i>Pseudomonas aeruginosa</i>	MCL
III	 C E 40 kDa 40 kDa	<i>Allochromatium vinosum</i>	SCL, MCL
IV	 C R 40 kDa 22 kDa	<i>Bacillus megaterium</i>	MCL

**Figure 1.1. The four classes of polyester synthases** (reproduced from Draper et al, 2013 [156]).

**Class I** PHA synthases belonging to this class (e.g. *Cupriavidus necator*) are comprised of a singular PhaC subunit with a molecular mass of around 61 - 73 kDa. Class I PHA synthase primarily utilize short chain length (*R*)-3-hydroxy fatty acids (3HA<sub>SCL</sub>)

comprising of 3 - 5 carbon atoms [157]. Class I PHA synthase however also demonstrate broad substrate specificity such as the incorporation of medium chain length (R)-3-hydroxy fatty acids ( $3HA_{MCL}$ ) comprising of 6 to 14 carbon atoms from *R. eutropha* [158].

**Class II** synthases show similarity to the class I PHA synthases, the class II PHA synthases (e.g. *Pseudomonas aeruginosa*) are also composed of a single PhaC subunit, which has a slightly smaller molecular weight of 60 – 65 kDa. Synthases belonging to this class however primarily utilizes  $3HA_{MCL}$  compared to class I PHA synthases [157].

**Class III** PHA synthases (e.g. *Allochromatium vinosum*) are composed of a two subunits, PhaC and a PhaE and each subunit has an approximant molecular weight of 40 kDa. PhaC has been found to show only 21 – 28% amino acid sequence similarity to the class I and II PhaC, while PhaE shows no amino acid sequence similarity to PhaC. PHA synthases of this class primarily utilizes both  $3HA_{SCL}$  and  $3HA_{MCL}$  [157].

**Class IV** synthases (e.g. *Bacillus megaterium*) have a similar subunit composition to the class III PHA synthases. Here PhaE subunit is replaced with a small 20 kDa PhaR subunit. Class IV synthases primarily utilize  $3HA_{MCL}$  [157].

### 1.7.2 Self-assembly of polyester particles

Three metabolic pathways provide precursors for PHA production (**Fig. 1.2**). Bacteria utilizing pathway I (*phaCAB*) produces PHA of short-chain-length ( $PHA_{SCL}$ ), such as *C. necator*, while Pathways II (fatty acid  $\beta$ -oxidation) and III (fatty acid *de novo* synthesis) produce medium chain length PHAs ( $PHA_{MCL}$ ) from fatty acid metabolism, such as *P. aeruginosa*.

Pathway I encode the formation of PHB and require three key enzymes,  $\beta$ -ketothiolase (PhaA), acetoacetyl-CoA reductase (PhaB), and PHA synthase (PhaC). The first two enzymes PhaA and PhaB work sequentially to form substrate (R)-3-hydroxybutyryl-CoA. Firstly, PhaA condenses two acetyl-CoA monomers into acetoacetyl-CoA, which is subsequently reduced by PhaB. Next, the substrate is polymerized by the PhaC in the final stereo-selective conversion into PHA with the concurrent release of CoA [146].

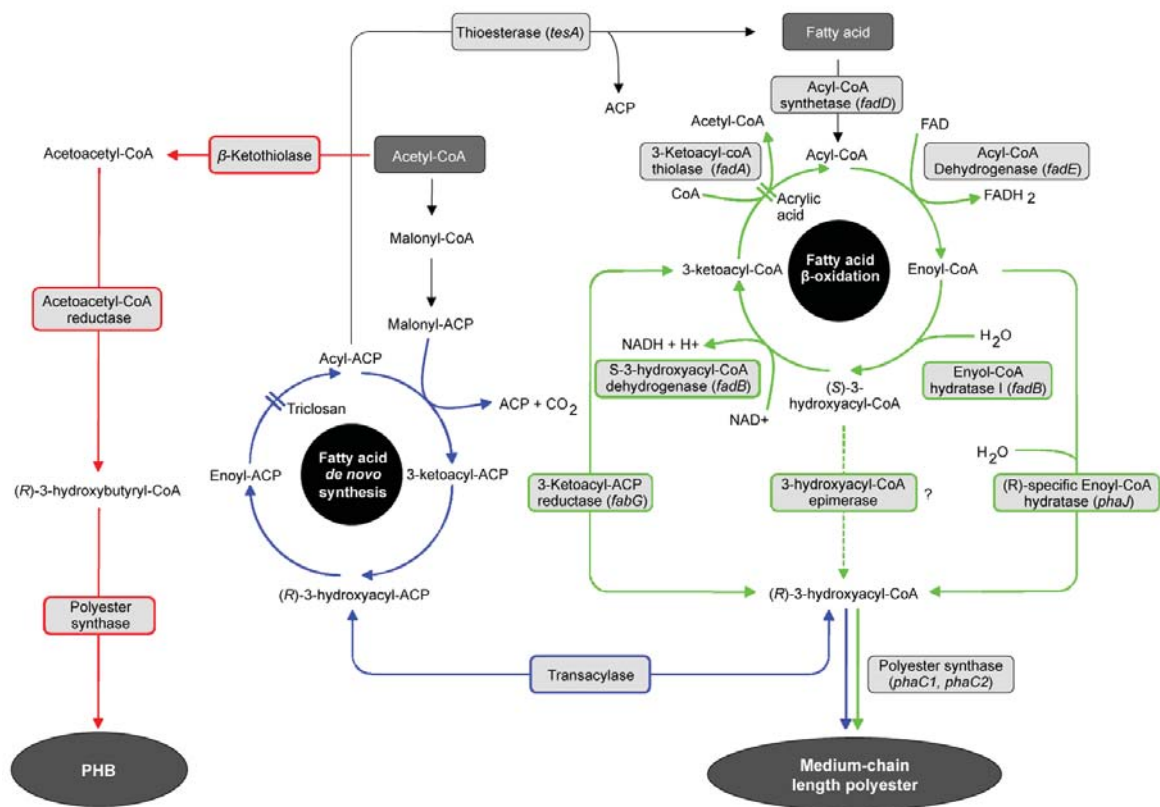


**Figure 1.2. Metabolic pathways of PHA production** (adapted from Draper et al, 2013 [156]). There are 3 well known metabolic pathways towards PHB biogenesis depending on carbon source and type of organism. Pathway I (red lines), Pathway II (green lines) and Pathway III (blue lines)

Pathway II bacteria, such as *P. aeruginosa* are known to utilize intermediates generated from the fatty acid  $\beta$ -oxidation pathway and from related carbon sources. Here various  $\beta$ -oxidation pathway intermediates (alkanes, alkenes, and alkanoates) are converted into (R)-3-hydroxyacyl-CoA thioesters. Non-related sources like sucrose, glucose, or gluconate are metabolized to acetyl-CoA, which enter Pathway III, the fatty acid *de novo* biosynthesis pathway [157, 159].

In all pathways, the PHA synthase (PhaC) is the only required for the conversion of (R)-3-hydroxyacyl-CoA thioesters into PHA [146].

*In vivo* or *in vitro* PHA inclusion formation is initiated by the presence of substrate (*R*)-3-hydroxyacyl-CoA thioesters. During the polymerization process the PHA synthase remains covalently attached to the growing polyester chain while more substrate is being constantly incorporated until metabolic or spatial constraints terminate polymerization [156].

The exact mechanism of PHA inclusion biosynthesis is still currently undetermined. Two models have been described for PHA formation *in vivo*: (1) the micelle model and (2) the budding model (**Fig. 1.3**).

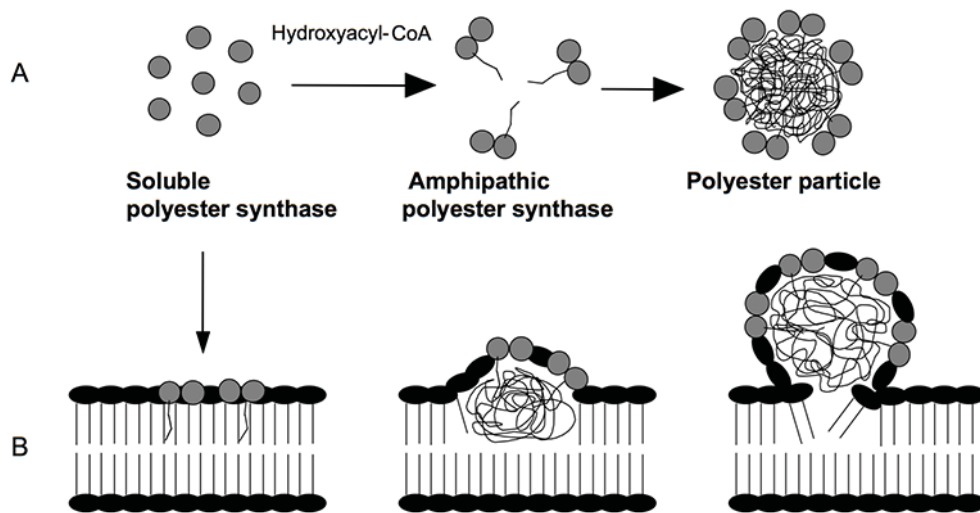


**Figure 1.3. Models for polyester bead self-assembly.** (a) Micelle model and (b) Budding model (reproduced from Rehm, 2007 [157]).

In the micelle model of PHA formation, soluble enzyme in the presence of (*R*)-3-hydroxyacyl-CoA thioesters dimerizes and becomes amphipathic. The amphipathic property of the dimerized PHA synthase causes it to undergo self-assembly, forming a micelle-like structure where the growing nascent PHA chain aggregates in the center. Phospholipids and other granule-associated-proteins (GAPs) are then incorporated to the growing structure. The micelle model is only supported by the formation of PHA granules *in vitro* using only purified PHA synthase and substrate [160, 161]

In the budding model the dimerized enzyme instead localizes to the cytoplasmic membrane where the growing polyester chain is synthesized into the inner membrane

space. The inclusion is consequently surrounded with a monophospholipid layer, where GAPs are also incorporated into the growing PHA inclusion. The growing inclusion will eventually bud off into the cytoplasm [157, 162].

The existence of a phospholipid layer on the surface of PHA beads is still currently being debated. Evidence for its existence *in vivo* is lacking and maybe an artifact of bead isolation during cell lysis [156]. A recent study using several different natural produces such as *Ralstonia eutropha* and *Pseudomonas putida* suggests PHA granules *in vivo* don't have a phospholipid layer and consist of only GAP proteins [163].

### 1.7.3 Granule-associated-proteins (GAPs)

GAPs are proteins that are typically associated and embedded on to the surface of the granule (Fig. 1.4). These proteins play various roles in bead synthesis (PHA synthase), formation (phasins and regulatory proteins), and degradation (depolymerases). PHA synthases are discussed in section 1.7.1.

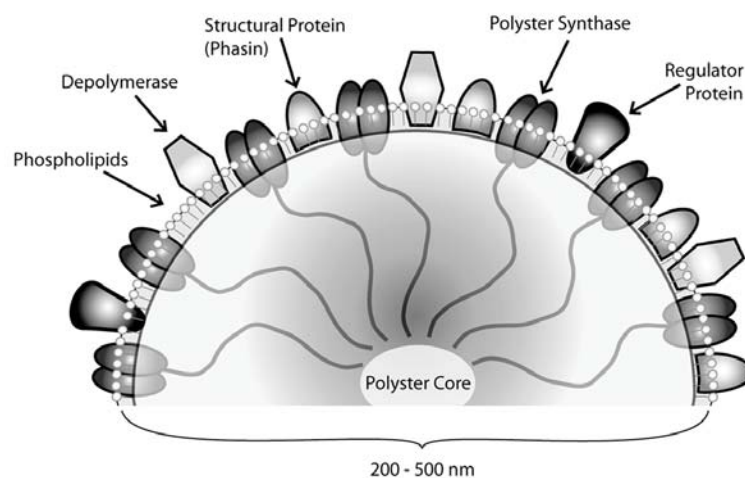


**Figure 1.4. Schematic representation of a PHA granule and its associated proteins** (reproduced from Draper et al, 2013 [156]).

**Phasins** are non-covalently attached low-molecular-weight proteins of 11 – 25 kDa and account for as much as 5% of the total GAPs [156]. A number of phasins have been described, and are encoded by *phaP* gene [154, 164]. Phasins are nonessential for PHA accumulation, but have been shown to play a structural role influencing both bead size and number by preventing coalesce and interacting with other GAPs [163]. Cells

defective in phasin production lead to the formation of a small number of large beads compared to many small beads seen when phasin are produced [165]. Phasins have been implicated in mediating distribution of granules among daughter cells [166, 167].

**Regulatory proteins.** Transcriptional regulator protein PhaR binds non-covalently to the PHA granules and functions in regulating PHA bead formation and phasin production. An autoregulation model involving PhaR and phasin has been described [167, 168]. Under non-permissive PHA accumulating conditions, PhaR binds the *phaP* promoter and therefore, inhibits its transcription. During permissive (PHA accumulating) conditions, PhaR is able to interact and bind with nascent PHA beads and therefore, depressed repression of *phaP* and thus transcription. Phasins will keep binding to the growing bead until bead surface has been completely covered, this in turn prevents additional binding of PhaR. Consequently, levels of cytoplasmic PhaR will increase, again result in the repression of PhaP transcription [167, 168].

**PHA depolymerases** (encoded by *phaZ*) are important for the degradation and mobilization of PHA by thiolysis. Depolymerases can be either intracellular or extracellular. Intracellular depolymerases are associated on the surface of PHA beads only in the native host and function to mobilize intracellular PHAs [168]. Extracellular PHA depolymerases however can be encoded by many bacteria including non-PHA producers and are secreted into the environment and function to degrade PHA released by dead bacteria [146].

## 1.8 Tuberculosis

Tuberculosis (TB) in humans is caused by the pathogen *Mycobacterium tuberculosis*. This pathogen is a member of the *M. tuberculosis* complex that contains 5 other closely related *Mycobacterium species* (*M. tuberculosis*, *M. africanum*, *M. canettii*, *M. microti*, and *M. bovis*), which are all causative agents of TB in either human and/or animals [169]. *M. tuberculosis* is an intracellular pathogen that infects macrophages after being phagocytosed. *M. tuberculosis* has several mechanisms which allow it to successfully evade destruction from the phagolysosome, such as changing endosomal pH, inhibiting apoptosis, and destroying toxic superoxides, making *M. tuberculosis* highly virulent [96].

TB is a major cause of morbidity and mortality worldwide. A quarter of the world's population is infected with TB and causes more deaths (1.4 million people per year in 2015) than any other infectious disease by a single organism [170, 171]. TB is highly infectious with 10% of those individuals who are infected will develop progressive TB and the remaining 90% of individuals developing a latent form of TB, which has the possibility of reactivating in the future. Immunocompromised individuals such as those with HIV or those who have a disrupted immune system (diabetes and nutritional deficiencies) have a significantly higher risk of reactivation [172].

TB is mainly prevalent in developing countries in Africa and Asia. The control and prevention of TB is currently by the use of multiple anti-tuberculosis drugs and a partially effective live attenuated vaccine called Bacillus Calmette–Guérin (BCG) [173]. BCG still remains the only available TB vaccine on the market to date. The exact nature of how BCG confers protection after administration has not been fully elucidated [174]. It is believed that protection against *M. tuberculosis* is mediated by the generation of CD4<sup>+</sup> and CD8<sup>+</sup> T cells [175, 176]. Activation of CD4<sup>+</sup> T cells involved in the Th1 type response leads to the production of macrophage activating cytokines IFN- $\gamma$  and TNF- $\alpha$ , which has been found to be critical in the control of *M. tuberculosis* [177]. The cytokine IFN- $\gamma$  was proposed to be an important vaccine induced marker for protection against TB, however evidence has suggested levels of IFN- $\gamma$  may not correlate with protection [176]. CD8<sup>+</sup> T cells are considered to be important in the killing infected cells and to mediate direct killing of *M. tuberculosis* [176]. Th17 cells that produce cytokine IL-17 have also been proposed to be important for protection and of which mediates the recruitment of Th1 cells and neutrophils to control the pathogen [175].

BCG however only protects against severe forms of childhood TB (e.g. tuberculosis meningitis and miliary tuberculosis) and confers variable protection in adults from pulmonary TB [178, 179]. Several reasons have been suggested as to why BCG offers such variable protection in adults, such as interference from previous exposure to environmental mycobacteria; variation of vaccine strain or phenotypic changes during passage and manufacturing; variations in dose and route of administration; and genetic variations among individuals who are vaccinated [96].

Furthermore, incidences of multidrug-resistant (MDR) and extensively drug-resistant (XDR-TB) strains of *M. tuberculosis* have been increasing worldwide during the past decade. Figures from the 2016 Global Tuberculosis report [170] has estimated 480 000 new cases of MDR-TB and accounts for an estimated 250 000 deaths annually. XDR-TB is estimated to account for 9.5% of MDR-TB patients. Additional complications include the increasing incidence and burden of HIV-associated TB (HIV-TB) of which accounted an additional 0.4 million deaths in 2015.

Hence, there is a significant need for new vaccines that can offer better protection for the prevention of TB. Currently there are significant effort to develop new and improved vaccines against TB, with 13 candidate vaccines in clinical trials and a number in early development [170, 180, 181]. These new vaccines in development include improvements to the current BCG vaccine by employing recombinant methods; subunit vaccines displaying primarily immunodominant-secreted antigens; and DNA, and viral-vectored vaccines.

New recombinant strains of BCG (rBCG) offer the ability to reintroduce lost protective genes during the attenuation process while selectively knocking out unwanted virulent genes [175]. Additionally, important protective genes can also be overexpressed along with other genes that may increase the generation of protective T cells. For examples, a group demonstrated that an rBCG vaccine made to secrete *Listeria monocytogenes* Hly (listeriolysin) and deficient in urease C resulted in the rBCG leaking from the phagosome. This allowed rBCG to be presented to MHC I molecules and activate CD8+ CTLs [182]. This rBCG strain is referred to as VPM1002 and is currently in phase IIa clinical trials (<http://www.clinicaltrials.gov: NCT02391415>).

Subunit vaccines tend to primarily utilize secreted proteins that are found to be the most abundant proteins (ESAT-6, Ag85 complex, TB10.4, and Mtb72f) [179]. Subunit vaccines tend to have low immunogenicity and typically administered in conjunction with adjuvants for activation of Th1 type response [86]. Immunogenicity can be increased also by the generation of recombinant fusion proteins that contain several components e.g. Ag85B and ESAT-6 [183]. Prime-boost strategies are also attractive options.

Prime-boost vaccine strategies expand on existing TB specific preexisting CD4+ memory T cells for antigens. These antigens are shared between the prime, typically BCG and the booster vaccine. Experiments have shown that individuals who were primed with BCG and boosted with a vaccine containing Ag85 protein showed better protection than those individuals that did not receive the booster [184].

Although significant progress has been made towards a novel vaccine to combat tuberculosis, with many being in clinical trials (**Table 1.1**), limited understanding of the immunity to *M. tuberculosis* has significantly hindered vaccine development [173]. To date BCG still remains the only available TB vaccine on the market.

**Table 1.1** Current novel TB vaccines in clinical trials (adapted from Evans et al, 2011 [180] and Tang et al, 2016 [181]).

Candidate name/identifier	Type	Stage of development
Ad5 Ag85A	Human adenovirus 5 1 antigen	Phase I
AERAS-402 and MVA85A	AERAS-402 prime followed by MVA85A boost	Phase I
TB/Flu-04L	Attenuated influenza	Phase I
DAR-901	Heat-killed non-tuberculous-mycobacteria	Phase I
ChAdOx1.85A/MVA85A	Chimp adenovirus/modified vaccinia	Phase I
MTBVAC (rMtbΔPhoPΔFadD26)	Live attenuated TB	Phase I
H1:CAF01	Fusion protein Ag85B-ESAT-6 in CAF01 adjuvant	Phase I
AERAS-402	Recombinant human adenovirus type 5 expressing Ag85A, Ag85B and TB10.4	Phase II
ID93 + GLA-SE	4 Ag adjuvanted fusion protein	Phase II
VPM 1002 (rBCGΔureC:Hly)	rBCG expressing listeriolysin and lacking urease gene	Phase II
H1 + IC31	Fusion protein Ag85B-ESAT-6 in IC31 adjuvant	Phase II
RUTI	Lysate of <i>M. tb</i>	Phase II
H4/Aeras-404 + IC31	Fusion protein Ag85B-TB10.4 in IC31 adjuvant	Phase II
H56/Aeras-456 + IC31	<i>M. tb</i> fusion proteins Ag85B-ESAT-6-Rv2660c in IC31 adjuvant	Phase II
M72 + AS01E	Fusion protein Mtb32a-Mtb39a in AS01 adjuvant	Phase IIb
MVA85A/AERAS-485	Modified vaccinia virus Ankara expressing Ag85A	Phase IIb
<i>M. Vaccae</i>	Lysate of non-tuberculous-mycobacteria	Phase III

## **1.9 *Pseudomonas aeruginosa***

*P. aeruginosa* is a motile Gram-negative opportunistic pathogen which is a commonly occurring microorganism found in a range of environments e.g. reservoirs and soil. *P. aeruginosa* can tolerate and adapt to extreme environments such as in hospitals e.g. on mechanical ventilators, endoscopes, and sinks [185]. This has resulted in *P. aeruginosa* becoming the leading cause of hospital-acquired infections from a Gram-negative bacterium worldwide [186]. *P. aeruginosa* can cause infections of the body such as the urinary tract, skin, eye, and ear. Infection with *P. aeruginosa* is a major concern for burns, HIV, and for cystic fibrosis (CF) patients whereby these individuals have an impaired or compromised immune systems. Infection with *P. aeruginosa* can be life threatening and difficult to treat. *P. aeruginosa* is the primary reason for chronic infections in CF patients and is the major cause of mortality of these individuals [186, 187].

CF is an inherited autosomal recessive disorder that leads to abnormalities in the production and function of cystic fibrosis transmembrane conductance regulator (CFTR) [188]. Chronic obstructive lung disease is the most common cause of morbidity and mortality in CF patients. CFTR protein functions as a chloride channel which regulates the transport of chloride, sodium, and bicarbonate across the airway epithelium [188]. Dysfunction of the CFTR results in the production of a thick mucus that is favorable for colonization with *P. aeruginosa*. Infection with *P. aeruginosa* is commonly with the nonmucoid form, which subsequently reverts to a mucoid form, characterized by the overproduction (production of more/excess compared to wild-type strain) of alginate when under stress caused by the immune system and in combination with antibiotics [189, 190]. This mucoid form results in the establishment of biofilms containing extracellular polysaccharides (alginate, Psl, and Pel), extracellular DNA, and proteins [191]. The biofilm offers protection from the host immune system (phagocytosis) and reduces susceptibility to antibiotics by preventing effective diffusion [191]. Furthermore, *P. aeruginosa* is intrinsically resistant to many antibiotics and chemotherapeutic agents due to inherent low membrane permeability, multidrug efflux pumps,  $\beta$ -lactamases, and chromosomally encoded antibiotic resistance genes [192]. Colonization of CF lungs happen early in life and conversion to mucoid phenotype can be anywhere between months to years [193]. The inability of the immune system to

clear the infection consequences results in the infection becoming chronic, and leads to a decline in pulmonary function [194].

It has been suggested that a Th1 type cell-mediated response is more protective, as high levels of antibodies associated with a Th2 type immune response have been found to be associated with more severe lung disease [195].

The need to vaccinate against *P. aeruginosa* is becoming increasingly important due to its increasing presence and antibiotic resistance, making development of an effective vaccine key to its control. Various research groups have targeted virulence associated and cellular factors as immunogens for vaccine development (see **Table 1.2**).

**Table 1.2** Potential vaccine targets against *P. aeruginosa* (adapted from Sharma et al, 2011 [195]).

Antigens	Advantages	Limitations
LPS and O-polysaccharides	Generation of high levels of opsonic antibodies	High heterogeneity, low immunogenicity, Pyrogenic and toxic
Outer Membrane proteins	Highly conserved and immunogenic (OprF, OprI)	No significant drawback
Flagella	Moderate heterogeneity, Adjuvant effect through TLR5	Loss of flagella in CF variants
Pili	High immunogenicity	High heterogeneity, Hidden receptor binding site
PcrV, Exotoxin A, and proteases	Neutralizes toxic effects and pathology	Less effective in bacterial clearance

Currently there is no commercially available prophylactic vaccine against *P. aeruginosa* and treatment is still solely reliant on the use of specific antibiotic combinations and enzymes. However, there is substantial progress being made towards a vaccine, with many being in clinical trials (**Table 1.3**) [196].

**Table 1.3** *P. aeruginosa* vaccines (modified from Sharma et al, 2011 [195]).

Candidate name/identifier	Type	Stage of development
IC43 (VLA43)	Fusion protein OprF/I vaccine	Phase II/III [197]
Attenuated <i>Salmonella enterica</i> delivered O-antigen or OprF-Opri	Efficient activation of mucosal immunity	Phase I/II
AdZ.Epi8	High immunogenicity and adjuvant properties	Preclinical
AdZ.F(FG)Epi8 or AdZ.F(HI)Epi8	High immunogenicity and adjuvant properties	Preclinical [198]
Live attenuated ( <i>P. aeruginosa</i> $\Delta$ aroA)	Presentation of multiple antigens to immune system	Preclinical
Inactivated whole-cell <i>P. aeruginosa</i>	Presentation of multiple antigens to immune system	Phase I

### 1.9.1 Potential vaccine targets against *P. aeruginosa*

A brief overview of potential vaccine targets against *P. aeruginosa* is described in **Table 1.2**.

**Lipopolysaccharides (LPS).** Many of the earlier vaccines were directed against cell wall components such as LPS, which are potent immune stimulator. Although positive results with multivalent vaccines have been demonstrated in animal and human testing, LPS based vaccines were never clinically accepted due to their inherent pyrogenic and toxic properties [199].

**Flagella.** *P. aeruginosa* has only a single polar flagellum of which is made up of highly conserved protein filaments (flagellin), with only two serotypes A and B. A double-blind randomized placebo-controlled phase III study in cystic fibrosis patients demonstrated that flagella based vaccine resulted in a strong humoral immune response and induced mucosal immunity in the respiratory tract [199]. Results indicated 37 of 189 vaccinated patients compared to 59 of 192 in the placebo group had infection episodes. Antibodies directed against flagella as a whole were demonstrated to be more protective than flagellin alone [200]. A vaccine developed against the flagella may be promising due to its high immunogenicity and cross-reactivity, however conversion to mucoid phenotype consequently results in a loss of flagella production and therefore the effectiveness of a flagella only vaccine, which would be limited against the mucoid

phenotype. Loss of the flagella is thought to be an adaptive response to avoid detection by host defenses [201].

**Pili.** The Type IV pili of *P. aeruginosa* are a known virulence-associated factor and a possible vaccine target. The pilus is a cell surface structure that is used by bacteria for mediating interactions between other bacteria, the host, and environment [202]. Mutant nonpiliated strains have been found to lose their ability to adhere to epidermal cells and are associated with lower virulence [202, 203]. A recent study demonstrated robust Th1 cellular (IFN- $\gamma$ , IL-17, and IgG1) and Th2 humoral (IL-4 and IgG2a) responses which conferred protection in a mouse model of acute infection when Type IV pilus protein PilA was formulated with alum and naloxone adjuvant [204].

**Exopolysaccharides (EPS).** The mucoid phenotype of *P. aeruginosa* is produced following the overproduction of EPS alginate. Alginate is a high molecular weight polysaccharide composed of nonrepeating monomers of D-mannuronic acid and its C5' epimer L-guluronic acid [205]. D-mannuronic acid hydroxyl residue can also be modified by O-acetylation. Alginate is found only with mucoid forms of *P. aeruginosa* and is an important component in biofilm architecture, but has been shown to be dispensable [206]. The mucoid phenotype of *P. aeruginosa* is more susceptible to antibiotics than the nonmucoid form [207].

The structure of alginate is highly conserved and has been targeted as a vaccine candidate. Pure alginate however has been found to be a poor inducer of protective antibodies. Immunogenicity can be improved by conjugate vaccine strategies [208]. Due to alginates poor immunogenicity, vaccine development based on alginate has stalled.

EPS Psl is a major virulence factor of *P. aeruginosa* and offers an alternative target to alginate. Psl can be found in both nonmucoid and mucoid forms conferring protection from host defenses such as reactive oxidative species, complement, and phagocytic immune cells [209, 210]. Psl is composed of repeating pentasaccharide units of D-mannose, D-glucose and L-rhamnose. Psl is found to surround the bacterium's surface in a helical fashion as demonstrated by Psl staining [205].

*P. aeruginosa* strain lacking Psl have been demonstrated to be more efficiently phagocytosed by neutrophils and macrophages in comparison to wild-type and Psl overexpression strains [193]. This indicates Psl provides a fitness advantage to nonmucoid *P. aeruginosa* prior to mucoid conversion and subsequent biofilm formation. Psl also plays a critical role in initial reversible surface attachment during biofilm formation of nonmucoid forms of *P. aeruginosa* [211].

**Outer membrane proteins (OMPs).** There is substantial interest around the use of OMPs as vaccine candidates, namely major OMP F (OprF) and outer membrane lipoprotein I (OprI). Both OprF and OprI are highly conserved and immunization with these antigens induces broad protection against all *P. aeruginosa* serotypes [208, 212, 213]. There are a large number of studies in animal models that demonstrate encouraging results, in particular long-lived antibody titers [203]. The use of immunogenic epitopes of OprF fused with or without OprI has been the main candidate for use in recent vaccine developments in combination with different delivery vectors such as adenoviral vectors, pulsed dendritic cells, and mannose-modified chitosan microspheres [214-216]. Evidence has suggested C3b component of complement binds OprF and promote complement mediated killing and interaction with neutrophils [209]. OprI is a natural adjuvant that has been shown to induce long-lived Th1 type immune responses resulting in activation and maturation of APCs [217]. It has been suggested that OprI can modulate the immune response from a Th2 type antibody response towards a Th1 type cell-mediated response, which is important for protection against intracellular pathogens [217, 218]. In addition, OprI has been found to promote adherence to mucosal surfaces and may be important for the use in vaccine design for immunization via the mucosal route.

OMP AlgE is another important protein found of the cell surface that possesses potential as a target for vaccine development [219]. AlgE is required for alginate transport in *P. aeruginosa* and found on mucoid forms of *P. aeruginosa*, correlating to the infection status of CF patients [219, 220]. Although alginate itself is a poor inducer of antibodies, AlgE may provide an alternative target and has been suggested to have a strong antigenic potential based on results seen with high anti-AlgE antibody titer from experiments involving injecting denatured or native AlgE in rabbits and by analyzing sera antibody levels in CF patients [219]. The 54 kDa OMP is not found on nonmucoid

strains of *P. aeruginosa*. Based on membrane topology prediction, AlgE has been suggested to form an 18 stranded  $\beta$ -barrel with extended extracellular loops [221]. Recently, the crystal structure of AlgE has been resolved and the structure correlates well with the predicted topology models [222]. B cell epitope prediction of AlgE has indicated that the extended extracellular loops provide possible antigenic epitopes that can be used as part of a multicomponent subunit vaccine.

**Type III secretion system.** *P. aeruginosa* uses a type III secretion system as a virulence factor to deliver bacterial toxins and effector proteins during infection. Components of the type III secretion system have been targeted, in particular the translocation protein PcrV located on the bacterial surface. Protection in murine lung infection models [223] and burn mouse models [224] have been demonstrated with PcrV based vaccines.

## 1.10 Conclusion

Immunity against pathogenic microbes is a result of the complicated interplay between cells and mechanisms of the innate and adaptive immune systems. This requires the ability of the host to detect foreign pathogens and induce appropriate immune responses that result in the elimination of the pathogen and the generation of protective immunity (immunological memory). Generation of immunological memory is the basis of vaccination. Novel vaccines and strategies are required to control and prevent infectious disease for which traditional vaccines fail. The prevention of infectious disease caused by *M. tuberculosis* or *P. aeruginosa* is becoming increasingly important particularly with increasing incidences of multidrug resistance. The use of a PHA bead based delivery system offers a new and exciting approach to tailor made vaccines.

## 1.11 References

1. Turvey, S.E. and D.H. Broide, *Innate immunity*. Journal of Allergy and Clinical Immunology, 2010. **125**(2): p. S24-S32.
2. Janeway, C.A. *Approaching the asymptote? Evolution and revolution in immunology*. in *Cold Spring Harbor symposia on quantitative biology*. 1989. Cold Spring Harbor Laboratory Press.
3. Iwasaki, A. and R. Medzhitov, *Control of adaptive immunity by the innate immune system*. Nature Immunology, 2015. **16**(4): p. 343-353.
4. Krysko, D.V., et al., *Emerging role of damage-associated molecular patterns derived from mitochondria in inflammation*. Trends in Immunology, 2011. **32**(4): p. 157-164.
5. Takeuchi, O. and S. Akira, *Pattern recognition receptors and inflammation*. Cell, 2010. **140**(6): p. 805-820.
6. Lavoie, E.G., T. Wangdi, and B.I. Kazmierczak, *Innate immune responses to Pseudomonas aeruginosa infection*. Microbes and Infection, 2011. **13**(14): p. 1133-1145.
7. Franchi, L., et al., *Function of Nod - like receptors in microbial recognition and host defense*. Immunological Reviews, 2009. **227**(1): p. 106-128.
8. Zhang, Q., et al., *Circulating mitochondrial DAMPs cause inflammatory responses to injury*. Nature, 2010. **464**(7285): p. 104-107.
9. Broz, P. and D.M. Monack, *Newly described pattern recognition receptors team up against intracellular pathogens*. Nature Reviews Immunology, 2013. **13**(8): p. 551-565.
10. O'Neill, L.A.J., D. Golenbock, and A.G. Bowie, *The history of Toll-like receptors [mdash] redefining innate immunity*. Nature Reviews Immunology, 2013. **13**(6): p. 453-460.
11. Ivashkiv, L.B. and L.T. Donlin, *Regulation of type I interferon responses*. Nature reviews Immunology, 2014. **14**(1): p. 36-49.
12. Thompson, M.R., et al., *Pattern recognition receptors and the innate immune response to viral infection*. Viruses, 2011. **3**(6): p. 920-940.
13. Kolumam, G.A., et al., *Type I interferons act directly on CD8 T cells to allow clonal expansion and memory formation in response to viral infection*. The Journal of Experimental Medicine, 2005. **202**(5): p. 637-650.
14. Zhang, J.M. and J. An, *Cytokines, inflammation and pain*. International Anesthesiology Clinics, 2007. **45**(2): p. 27-37.
15. Rock, K.L. and H. Kono, *The inflammatory response to cell death*. Annual Review of Pathology, 2008. **3**: p. 99-126.
16. Kolaczowska, E. and P. Kubes, *Neutrophil recruitment and function in health and inflammation*. Nature Reviews Immunology, 2013. **13**(3): p. 159-175.
17. Medzhitov, R., *Origin and physiological roles of inflammation*. Nature, 2008. **454**(7203): p. 428-435.
18. Litvack, M.L. and N. Palaniyar, *Review: Soluble innate immune pattern-recognition proteins for clearing dying cells and cellular components: implications on exacerbating or resolving inflammation*. Innate Immunity, 2010. **16**(3): p. 191-200.
19. De Nardo, D., *Toll-like receptors: Activation, signalling and transcriptional modulation*. Cytokine, 2015. **74**(2): p. 181-189.
20. Motta, V., et al., *NOD-like receptors: versatile cytosolic sentinels*. Physiological Reviews, 2015. **95**(1): p. 149-178.
21. Moreira, L. and D.S. Zamboni, *NOD1 and NOD2 signaling in infection and inflammation*. Frontiers in Immunology, 2012. **3**.
22. Matsumiya, T. and D.M. Stafforini, *Function and regulation of retinoic acid-inducible gene-I*. Critical Reviews in Immunology, 2010. **30**(6): p. 489-513.
23. Gack, M.U., *Mechanisms of RIG-I-like receptor activation and manipulation by viral pathogens*. Journal of Virology, 2014. **88**(10): p. 5213-5216.
24. Kanazawa, N., *C-Type Lectin Receptors*, in *Immunology of the skin*. 2016, Springer. p. 255-274.
25. Hansen, S., et al., *Collectin 11 (CL-11, CL-K1) Is a MASP-1/3-Associated plasma collectin with microbial-Binding activity*. The Journal of Immunology, 2010. **185**(10): p. 6096-6104.
26. Runza, V.L., W. Schwaeble, and D.N. Männel, *Ficolins: novel pattern recognition molecules of the innate immune response*. Immunobiology, 2008. **213**(3): p. 297-306.
27. Holmskov, U., S. Thiel, and J.C. Jensenius, *Collectins and ficolins: humoral lectins of the innate immune defense*. Annual Review of Immunology, 2003. **21**(1): p. 547-578.
28. Foo, S.-S., et al., *Pentraxins and collectins: friend or foe during pathogen invasion?* Trends in microbiology, 2015. **23**(12): p. 799-811.

29. Dunkelberger, J.R. and W.-C. Song, *Complement and its role in innate and adaptive immune responses*. Cell Research, 2010. **20**(1): p. 34-50.
30. Mathern, D.R. and P.S. Heeger, *Molecules great and small: the complement system*. Clinical Journal of the American Society of Nephrology, 2015. **10**(9): p. 1636-1650.
31. Ricklin, D., et al., *Complement: a key system for immune surveillance and homeostasis*. Nature Immunology, 2010. **11**(9): p. 785-797.
32. Kouser, L., et al., *A recombinant two-module form of human properdin is an inhibitor of the complement alternative pathway*. Molecular immunology, 2016. **73**: p. 76-87.
33. Maibaum, J., et al., *Small-molecule factor D inhibitors targeting the alternative complement pathway*. Nature Chemical Biology, 2016. **12**(12): p. 1105-1110.
34. Garred, P., et al., *A journey through the lectin pathway of complement—MBL and beyond*. Immunological Reviews, 2016. **274**(1): p. 74-97.
35. Flannagan, R.S., V. Jaumouillé, and S. Grinstein, *The cell biology of phagocytosis*. Annual Review of Pathology: Mechanisms of Disease, 2012. **7**: p. 61-98.
36. Lindow, J.C., et al., *Antibodies in action: role of human opsonins in killing Salmonella enterica serovar Typhi*. Infection and Immunity, 2011. **79**(8): p. 3188-3194.
37. Bajic, G., et al., *Structural insight on the recognition of surface-bound opsonins by the integrin I domain of complement receptor 3*. Proceedings of the National Academy of Sciences, 2013. **110**(41): p. 16426-16431.
38. Blum, J.S., P.A. Wearsch, and P. Cresswell, *Pathways of antigen processing*. Annual Review of Immunology, 2013. **31**: p. 443-473.
39. den Haan, J.M.M., R. Arens, and M.C. van Zelm, *The activation of the adaptive immune system: cross-talk between antigen-presenting cells, T cells and B cells*. Immunology Letters, 2014. **162**(2): p. 103-112.
40. Adams, J.J., et al., *T cell receptor signaling is limited by docking geometry to peptide-major histocompatibility complex*. Immunity, 2011. **35**(5): p. 681-693.
41. Joffe, O.P., et al., *Cross-presentation by dendritic cells*. Nature Reviews Immunology, 2012. **12**(8): p. 557-569.
42. Dolan, B.P., K.D. Gibbs, and S. Ostrand-Rosenberg, *Dendritic cells cross-dressed with peptide MHC class I complexes prime CD8+ T cells*. The Journal of Immunology, 2006. **177**(9): p. 6018-6024.
43. Smith-Garvin, J.E., G.A. Koretzky, and M.S. Jordan, *T cell activation*. Annual Review of Immunology, 2009. **27**: p. 591-619.
44. Edelmann, K.H. and C.B. Wilson, *Role of CD28/CD80-86 and CD40/CD154 costimulatory interactions in host defense to primary herpes simplex virus infection*. Journal of Virology, 2001. **75**(2): p. 612-621.
45. DuPage, M. and J.A. Bluestone, *Harnessing the plasticity of CD4(+) T cells to treat immune-mediated disease*. Nature Reviews Immunology, 2016. **16**(3): p. 149-163.
46. Lazarevic, V. and L.H. Glimcher, *T-bet in disease*. Nature Immunology, 2011. **12**(7): p. 597-606.
47. Peng, S.L., S.J. Szabo, and L.H. Glimcher, *T-bet regulates IgG class switching and pathogenic autoantibody production*. Proceedings of the National Academy of Sciences, 2002. **99**(8): p. 5545-5550.
48. Hu, X. and L.B. Ivashkiv, *Cross-regulation of signaling pathways by interferon- $\gamma$ : implications for immune responses and autoimmune diseases*. Immunity, 2009. **31**(4): p. 539-550.
49. Martin, R.M. and A.M. Lew, *Is IgG2a a good Th1 marker in mice?* Immunology Today, 1998. **19**(1): p. 49.
50. Zhu, J., et al., *GATA-3 promotes Th2 responses through three different mechanisms: induction of Th2 cytokine production, selective growth of Th2 cells and inhibition of Th1 cell-specific factors*. Cell Research, 2006. **16**(1): p. 3-10.
51. Wynn, T.A., *Type 2 cytokines: mechanisms and therapeutic strategies*. Nature Review Immunology, 2015. **15**(5): p. 271-282.
52. Kaplan, M.H., *Th9 cells: differentiation and disease*. Immunological Reviews, 2013. **252**(1): p. 104-115.
53. Deng, Y., et al., *Th9 cells and IL-9 in autoimmune disorders: Pathogenesis and therapeutic potentials*. Human immunology, 2017. **78**(2): p. 120-128.
54. Ivanov, I.I., et al., *The orphan nuclear receptor ROR $\gamma$ t directs the differentiation program of proinflammatory IL-17+ T helper cells*. Cell, 2006. **126**(6): p. 1121-1133.
55. Yang, L., et al., *IL-21 and TGF- $\beta$  are required for differentiation of human TH17 cells*. Nature, 2008. **454**(7202): p. 350-352.

56. Crome, S.Q., A.Y. Wang, and M.K. Levings, *Translational mini - review series on Th17 cells: Function and regulation of human T helper 17 cells in health and disease*. Clinical & Experimental Immunology, 2010. **159**(2): p. 109-119.
57. Stewart, C.A. and G. Trinchieri, *At 17, in-10's passion need not inflame*. Immunity, 2011. **34**(4): p. 460-462.
58. Crotty, S., *Follicular helper CD4 T cells (Tfh)*. Annual Review of Immunology, 2011. **29**: p. 621-663.
59. Bonelli, M., et al., *Helper T cell plasticity: Impact of extrinsic and intrinsic signals on transcriptomes and epigenomes*, in *Transcriptional control of lineage differentiation in immune cells*, W. Ellmeier and I. Taniuchi, Editors. 2014. p. 279-326.
60. Nakayamada, S., et al., *Helper T cell diversity and plasticity*. Current Opinion in Immunology, 2012. **24**(3): p. 297-302.
61. Murphy, K.M. and B. Stockinger, *Effector T cell plasticity: flexibility in the face of changing circumstances*. Nature Immunology, 2010. **11**(8): p. 674-680.
62. Caza, T. and S. Landas, *Functional and phenotypic plasticity of CD4(+) T cell subsets*. BioMed Research International, 2015. **2015**: p. 521957-521957.
63. Arce-Sillas, A., et al., *Regulatory T cells: Molecular actions on effector cells in immune regulation*. Journal of Immunology Research, 2016.
64. Boyman, O. and J. Sprent, *The role of interleukin-2 during homeostasis and activation of the immune system*. Nature Reviews Immunology, 2012. **12**(3): p. 180-190.
65. Basu, R. and S. Bhaumik, *Cellular and molecular dynamics of Th17 differentiation and its developmental plasticity in the intestinal immune response*. Frontiers in Immunology, 2017. **8**: p. 254.
66. Harbour, S.N., et al., *Th17 cells give rise to Th1 cells that are required for the pathogenesis of colitis*. Proceedings of the National Academy of Sciences, 2015. **112**(22): p. 7061-7066.
67. Gagliani, N., et al., *Th17 cells transdifferentiate into regulatory T cells during resolution of inflammation*. Nature, 2015. **523**(7559): p. 221-225.
68. Sawant, D.V. and D.A.A. Vignali, *Once a Treg, always a Treg?* Immunological Reviews, 2014. **259**(1): p. 173-191.
69. Tan, C.Y., et al., *Antigen-specific Th9 cells exhibit uniqueness in their kinetics of cytokine production and short retention at the inflammatory site*. Journal of Immunology, 2010. **185**(11): p. 6795-6801.
70. Laplante, M. and D.M. Sabatini, *mTOR signaling at a glance*. Journal of Cell Science, 2009. **122**(20): p. 3589-3594.
71. Choi, Y.S., et al., *Lineage-plasticity and inflammatory change of human FoxP3(+) regulatory T cells in acute viral infection: Implication in immune-mediated tissue injury*. Blood, 2014. **124**(21).
72. Harwood, N.E. and F.D. Batista, *Early events in B cell activation*. Annual Review of Immunology, 2009. **28**: p. 185-210.
73. Kuchen, S., et al., *Essential role of IL-21 in B cell activation, expansion, and plasma cell generation during CD4+ T cell-B cell collaboration*. The Journal of Immunology, 2007. **179**(9): p. 5886-5896.
74. Obukhanych, T.V. and M.C. Nussenzweig, *T-independent type II immune responses generate memory B cells*. The Journal of Experimental Medicine, 2006. **203**(2): p. 305-310.
75. Xu, Z., et al., *Immunoglobulin class-switch DNA recombination: induction, targeting and beyond*. Nature Reviews Immunology, 2012. **12**(7): p. 517-531.
76. Delany, I., R. Rappuoli, and E. De Gregorio, *Vaccines for the 21st century*. EMBO Molecular Medicine, 2014. **6**(6): p. 708-720.
77. Greenwood, B., *The contribution of vaccination to global health: past, present and future*. Philosophical Transactions of the Royal Society B-Biological Sciences, 2014. **369**(1645).
78. Bärnighausen, T., et al., *Valuing vaccination*. Proceedings of the National Academy of Sciences, 2014. **111**(34): p. 12313-12319.
79. O'Hagan, D.T. and R. Rappuoli, *The safety of vaccines*. Drug discovery today, 2004. **9**(19): p. 846-854.
80. Rappuoli, R., *Twenty-first century vaccines*. Philosophical Transactions of the Royal Society B-Biological Sciences, 2011. **366**(1579): p. 2756-2758.
81. Rappuoli, R., et al., *Vaccines for the twenty-first century society*. Nature Reviews Immunology, 2012. **12**(3): p. 225-225.
82. Rappuoli, R., et al., *Vaccines, new opportunities for a new society*. Proceedings of the National Academy of Sciences, 2014. **111**(34): p. 12288-12293.

83. Pulendran, B. and R. Ahmed, *Immunological mechanisms of vaccination*. Nature Immunology, 2011. **12**(6): p. 509-517.
84. Locht, C. and N. Mielcarek, *Live attenuated vaccines against pertussis*. Expert Review of Vaccines, 2014. **13**(9): p. 1147-1158.
85. Zepp, F., *Principles of vaccine design-Lessons from nature*. Vaccine, 2010. **28**: p. C14-C24.
86. Moyle, P.M. and I. Toth, *Modern subunit vaccines: development, components, and research opportunities*. ChemMedChem, 2013. **8**(3): p. 360-376.
87. Shrot, S., et al., *BCGitis and BCGosis in children with primary immunodeficiency - imaging characteristics*. Pediatric Radiology, 2016. **46**(2): p. 237-245.
88. Spertini, F., et al., *Safety of human immunisation with a live-attenuated Mycobacterium tuberculosis vaccine: a randomised, double-blind, controlled phase I trial*. The Lancet Respiratory Medicine, 2015. **3**(12): p. 953-962.
89. Roy, P. and R. Noad, *Virus-like particles as a vaccine delivery system: myths and facts*, in *Pharmaceutical Biotechnology*. 2009, Springer. p. 145-158.
90. He, X.-S., et al., *Cellular immune responses in children and adults receiving inactivated or live attenuated influenza vaccines*. Journal of virology, 2006. **80**(23): p. 11756-11766.
91. Baxter, D., *Active and passive immunity, vaccine types, excipients and licensing*. Occupational Medicine, 2007. **57**(8): p. 552-556.
92. Pollard, A.J., K.P. Perrett, and P.C. Beverley, *Maintaining protection against invasive bacteria with protein-polysaccharide conjugate vaccines*. Nature Reviews Immunology, 2009. **9**(3): p. 212-220.
93. Straume, D., G.A. Stamsås, and L.S. Håvarstein, *Natural transformation and genome evolution in Streptococcus pneumoniae*. Infection, Genetics and Evolution, 2015. **33**: p. 371-380.
94. Delany, I., R. Rappuoli, and K.L. Seib, *Vaccines, reverse vaccinology, and bacterial pathogenesis*. Cold Spring Harbor Perspectives in Medicine, 2013. **3**(5).
95. Milacic, V., et al., *Injectable PLGA systems for delivery of vaccine antigens*. Long Acting Injections and Implants, 2012: p. 429-458.
96. Skeiky, Y.A.W. and J.C. Sadoff, *Advances in tuberculosis vaccine strategies*. Nature Reviews Microbiology, 2006. **4**(6): p. 469-476.
97. O'Hagan, D.T. and R. Rappuoli, *Novel approaches to pediatric vaccine delivery*. Advanced Drug Delivery Reviews, 2006. **58**(1): p. 29-51.
98. Bachmann, M.F. and G.T. Jennings, *Vaccine delivery: a matter of size, geometry, kinetics and molecular patterns*. Nature Reviews Immunology, 2010. **10**(11): p. 787-796.
99. Awate, S., L. Babiuk, and G. Mutwiri, *Mechanisms of Action of Adjuvants*. Frontiers in Immunology, 2013. **4**(114): p. 1-10.
100. Leroux-Roels, G., *Unmet needs in modern vaccinology Adjuvants to improve the immune response*. Vaccine, 2010. **28**: p. C25-C36.
101. Crowe, S.R., S.C. Miller, and D.L. Woodland, *Identification of protective and non-protective T cell epitopes in influenza*. Vaccine, 2006. **24**(4): p. 452-456.
102. Dadley-Moore, D., *Learning from our successes*. Nature Reviews Immunology, 2006. **6**(4): p. 256-257.
103. Querec, T., et al., *Yellow fever vaccine YF-17D activates multiple dendritic cell subsets via TLR2, 7, 8, and 9 to stimulate polyvalent immunity*. Journal of Experimental Medicine, 2006. **203**(2): p. 413-424.
104. Brito, L.A. and D.T. O'Hagan, *Designing and building the next generation of improved vaccine adjuvants*. Journal of Controlled Release, 2014. **190**: p. 563-579.
105. Singh, M. and D.T. O'Hagan, *Recent advances in vaccine adjuvants*. Pharmaceutical Research, 2002. **19**(6): p. 715-728.
106. Schultze, V., et al., *Safety of MF59 adjuvant*. Vaccine, 2008. **26**(26): p. 3209-3222.
107. Calabro, S., et al., *Vaccine adjuvants alum and MF59 induce rapid recruitment of neutrophils and monocytes that participate in antigen transport to draining lymph nodes*. Vaccine, 2011. **29**(9): p. 1812-1823.
108. Mbow, M.L., et al., *New adjuvants for human vaccines*. Current opinion in immunology, 2010. **22**(3): p. 411-416.
109. Aguilar, J. and E. Rodriguez, *Vaccine adjuvants revisited*. Vaccine, 2007. **25**(19): p. 3752-3762.
110. Liu, M.A., *DNA vaccines: an historical perspective and view to the future*. Immunological Reviews, 2011. **239**(1): p. 62-84.
111. Li, L., F. Saade, and N. Petrovsky, *The future of human DNA vaccines*. Journal of Biotechnology, 2012. **162**(2-3): p. 171-182.

112. Okuda, K., Y. Wada, and M. Shimada, *Recent developments in preclinical DNA vaccination*. *Vaccines*, 2014. **2**(1): p. 89-106.
113. Schiller, J.T. and D.R. Lowy, *Raising expectations for subunit vaccine*. *Journal of Infectious Diseases*, 2015. **211**(9): p. 1373-1375.
114. Sahdev, P., L.J. Ochyl, and J.J. Moon, *Biomaterials for nanoparticle vaccine delivery systems*. *Pharmaceutical Research*, 2014. **31**(10): p. 2563-2582.
115. Martínez-Donato, G., et al., *Protective T cell and antibody immune response against Hepatitis C Virus using the biopolyester beads based vaccine delivery system*. *Clinical and Vaccine Immunology*, 2016: p. 370-378.
116. Slutter, B. and W. Jiskoot, *Sizing the optimal dimensions of a vaccine delivery system: a particulate matter*. *Expert Opinion on Drug Delivery*, 2016. **13**(2): p. 167-170.
117. Mottram, P.L., et al., *Type 1 and 2 immunity following vaccination is influenced by nanoparticle size: formulation of a model vaccine for respiratory syncytial virus*. *Molecular Pharmaceutics*, 2007. **4**(1): p. 73-84.
118. Pacheco, P., D. White, and T. Sulchek, *Effects of microparticle size and Fc density on macrophage phagocytosis*. *Plos One*, 2013. **8**(4).
119. Parlane, N.A., et al., *Production of a particulate hepatitis C vaccine candidate by an engineered Lactococcus lactis strain*. *Applied and Environmental Microbiology*, 2011. **77**(24): p. 8516-8522.
120. Parlane, N.A., et al., *Novel particulate vaccines utilizing polyester nanoparticles (bio-beads) for protection against Mycobacterium bovis infection—A review*. *Veterinary Immunology and Immunopathology*, 2014. **158**(1): p. 8-13.
121. Silva, A.L., et al., *Poly-(lactic-co-glycolic-acid)-based particulate vaccines: Particle uptake by dendritic cells is a key parameter for immune activation*. *Vaccine*, 2015. **33**(7): p. 847-854.
122. Singh, M., et al., *Polylactide-co-glycolide microparticles with surface adsorbed antigens as vaccine delivery systems*. *Current Drug Delivery*, 2006. **3**(1): p. 115-20.
123. O'hagan, D.T., et al., *Biodegradable microparticles as controlled release antigen delivery systems*. *Immunology*, 1991. **73**(2): p. 239-242.
124. Li, X., et al., *Preparation of alginate coated chitosan microparticles for vaccine delivery*. *BMC biotechnology*, 2008. **8**(1): p. 89.
125. Gan, Q., et al., *Modulation of surface charge, particle size and morphological properties of chitosan-TPP nanoparticles intended for gene delivery*. *Colloids and Surfaces B: Biointerfaces*, 2005. **44**(2): p. 65-73.
126. Ko, J., et al., *Chitosan microparticle preparation for controlled drug release by response surface methodology*. *Journal of microencapsulation*, 2003. **20**(6): p. 791-797.
127. van der Lubben, I.M., et al., *Chitosan microparticles for mucosal vaccination against diphtheria: oral and nasal efficacy studies in mice*. *Vaccine*, 2003. **21**(13): p. 1400-1408.
128. Schwendener, R.A., *Liposomes as vaccine delivery systems: a review of the recent advances*. *Therapeutic Advances in Vaccines*, 2014. **2**(6): p. 159-182.
129. Smith, R.E., A.M. Donachie, and A.M. Mowat, *Immune stimulating complexes as mucosal vaccines*. *Immunology and Cell Biology*, 1998. **76**(3): p. 263-269.
130. Keller, S.A., et al., *Cutting edge: limited specialization of dendritic cell subsets for MHC class II-associated presentation of viral particles*. *The journal of immunology*, 2010. **184**(1): p. 26-29.
131. Lua, L.H.L., et al., *Bioengineering virus - like particles as vaccines*. *Biotechnology and Bioengineering*, 2014. **111**(3): p. 425-440.
132. Brown, L., et al., *Through the wall: extracellular vesicles in Gram-positive bacteria, mycobacteria and fungi*. *Nature Reviews Microbiology*, 2015. **13**(10): p. 620-630.
133. Schwechheimer, C. and M.J. Kuehn, *Outer-membrane vesicles from Gram-negative bacteria: biogenesis and functions*. *Nature Reviews Microbiology*, 2015. **13**(10): p. 605-619.
134. van der Pol, L., M. Stork, and P. van der Ley, *Outer membrane vesicles as platform vaccine technology*. *Biotechnology Journal*, 2015. **10**(11): p. 1689-1706.
135. McCaig, W.D., et al., *Characterization and vaccine potential of outer membrane vesicles produced by haemophilus parasuis*. *Plos One*, 2016. **11**(3).
136. Price, N.L., et al., *Glycoengineered outer membrane vesicles: A novel platform for bacterial vaccines*. *Scientific Reports*, 2016. **6**.
137. Collins, B.S., *Gram-negative outer membrane vesicles in vaccine development*. *Discovery medicine*, 2011. **12**(62): p. 7-15.
138. Acevedo, R., et al., *Bacterial outer membrane vesicles and vaccine applications*. *Frontiers in Immunology*, 2014. **5**.

139. McConnell, M.J., et al., *Outer membrane vesicles as an acellular vaccine against Acinetobacter baumannii*. *Vaccine*, 2011. **29**(34): p. 5705-5710.
140. Bottero, D., et al., *Outer membrane vesicles derived from Bordetella parapertussis as an acellular vaccine against Bordetella parapertussis and Bordetella pertussis infection*. *Vaccine*, 2013. **31**(45): p. 5262-5268.
141. Roberts, R., et al., *Outer membrane vesicles as acellular vaccine against pertussis*. *Vaccine*, 2008. **26**(36): p. 4639-4646.
142. Nieves, W., et al., *A naturally derived outer-membrane vesicle vaccine protects against lethal pulmonary Burkholderia pseudomallei infection*. *Vaccine*, 2011. **29**(46): p. 8381-8389.
143. Reyes, F., et al., *Immunogenicity and cross-reactivity against Mycobacterium tuberculosis of proteoliposomes derived from Mycobacterium bovis BCG*. *BMC Immunology*, 2013. **14**(Suppl 1).
144. Wang, Z., D.W. Lazinski, and A. Camilli, *Immunity provided by an outer membrane vesicle cholera vaccine is due to O-antigen-specific antibodies inhibiting bacterial motility*. *Infection and Immunity*, 2017. **85**(1).
145. Chen, D.J., et al., *Delivery of foreign antigens by engineered outer membrane vesicle vaccines*. *Proceedings of the National Academy of Sciences* 2010. **107**(7): p. 3099-3104.
146. Grage, K., et al., *Bacterial polyhydroxyalkanoate granules: biogenesis, structure, and potential use as nano-/micro-beads in biotechnological and biomedical applications*. *Biomacromolecules*, 2009. **10**(4): p. 660-669.
147. Parlane, N.A., et al., *Bacterial polyester inclusions engineered to display vaccine candidate antigens for use as a novel class of safe and efficient vaccine delivery agents*. *Applied and Environmental Microbiology*, 2009. **75**(24): p. 7739-7744.
148. Mifune, J., K. Grage, and B.H.A. Rehm, *Production of functionalized biopolyester granules by recombinant Lactococcus lactis*. *Applied and Environmental Microbiology*, 2009. **75**(14): p. 4668-4675.
149. Parlane, N.A., et al., *Vaccines displaying mycobacterial proteins on biopolyester beads stimulate cellular immunity and induce protection against tuberculosis*. *Clinical and Vaccine Immunology*, 2012. **19**(1): p. 37-44.
150. Chen, S., et al., *New skin test for detection of bovine tuberculosis on the basis of antigen-displaying polyester inclusions produced by recombinant Escherichia coli*. *Applied and Environmental Microbiology*, 2014. **80**(8): p. 2526-2535.
151. Rehm, B.H.A., *Bacterial polymers: biosynthesis, modifications and applications*. *Nature Reviews Microbiology*, 2010. **8**(8): p. 578-592.
152. Urtuvia, V., et al., *Bacterial production of the biodegradable plastics polyhydroxyalkanoates*. *International Journal of Biological Macromolecules*, 2014. **70**: p. 208-213.
153. Sakai, K., et al., *Polyhydroxyalkanoate (PHA) accumulation potential and PHA - accumulating microbial communities in various activated sludge processes of municipal wastewater treatment plants*. *Journal of Applied Microbiology*, 2015. **118**(1): p. 255-266.
154. Eggers, J. and A. Steinbuechel, *Impact of Ralstonia eutropha's poly(3-Hydroxybutyrate) (PHB) depolymerases and phasins on PHB storage in recombinant Escherichia coli*. *Applied and Environmental Microbiology*, 2014. **80**(24): p. 7702-7709.
155. Reyes, P.R., et al., *Immunogenicity of antigens from Mycobacterium tuberculosis self-assembled as particulate vaccines*. *International Journal of Medical Microbiology*, 2016. **306**(8): p. 624-632.
156. Draper, J., et al., eds. *Polyhydroxyalkanoate inclusions: polymer synthesis, self-assembly and display technology*. *Bionanotechnology: biological self assembly and its applications*, ed. B.H.A. Rehm. 2013, Caister Academic Press: Norfolk 8045-8053.
157. Rehm, B.H.A., *Biogenesis of microbial polyhydroxyalkanoate granules: a platform technology for the production of tailor-made bioparticles*. *Current Issues in Molecular Biology*, 2007. **9**(1): p. 41-62.
158. Kozhevnikov, I.V., et al., *Cloning and molecular organization of the polyhydroxyalkanoic acid synthase gene (phaC) of Ralstonia eutropha strain B5786*. *Applied Biochemistry and Microbiology*, 2010. **46**(2): p. 140-147.
159. Lu, J., R.C. Tappel, and C.T. Nomura, *Mini-review: biosynthesis of poly (hydroxyalkanoates)*. *Polymer Reviews*, 2009. **49**(3): p. 226-248.
160. Rehm, B.H.A., *Genetics and biochemistry of polyhydroxyalkanoate granule self-assembly: The key role of polyester synthases*. *Biotechnology Letters*, 2006. **28**(4): p. 207-213.

161. Gerngross, T.U. and D.P. Martin, *Enzyme-catalyzed synthesis of poly (R)-(-)-3-hydroxybutyrate - formation of macroscopic granules in-vitro*. Proceedings of the National Academy of Sciences, 1995. **92**(14): p. 6279-6283.
162. Thomson, N. and E. Sivaniah, *Synthesis , properties and uses of bacterial storage lipid granules as naturally occurring nanoparticles*. Soft Matter, 2010: p. 4045-4057.
163. Bresan, S., et al., *Polyhydroxyalkanoate (PHA) granules have no phospholipids*. Scientific Reports, 2016. **6**.
164. Mezzina, M.P., et al., *A phasin with many faces: structural insights on PhaP from Azotobacter sp FA8*. Plos One, 2014. **9**(7).
165. Hanley, S.Z., et al., *Re-evaluation of the primary structure of Ralstonia eutropha phasin and implications for polyhydroxyalkanoic acid granule binding*. FEBS letters, 1999. **447**: p. 99-105.
166. Galán, B., et al., *Nucleoid-associated PhaF phasin drives intracellular location and segregation of polyhydroxyalkanoate granules in Pseudomonas putida KT2442*. Molecular microbiology, 2011. **79**: p. 402-18.
167. Cai, S., et al., *A novel DNA-binding protein, PhaR, plays a central role in the regulation of polyhydroxyalkanoate accumulation and granule formation in the Haloarchaeon Haloferax mediterranei*. Applied and Environmental Microbiology, 2015. **81**(1): p. 373-385.
168. Potter, M. and A. Steinbuchel, *Poly(3-hydroxybutyrate) granule-associated proteins: Impacts on poly(3-hydroxybutyrate) synthesis and degradation*. Biomacromolecules, 2005. **6**(2): p. 552-560.
169. Forrellad, M.A., et al., *Virulence factors of the Mycobacterium tuberculosis complex*. Virulence, 2013. **4**(1): p. 3-66.
170. WHO, *World Health Organisation. Global tuberculosis report 2016*. 2016.
171. Houben, R.M.G.J. and P.J. Dodd, *The global burden of latent tuberculosis infection: A re-estimation using mathematical modelling*. Plos Medicine, 2016. **13**(10).
172. Rook, G.A., K. Dheda, and A. Zumla, *Immune responses to tuberculosis in developing countries: implications for new vaccines*. Nature Reviews Immunology, 2005. **5**(8): p. 661-667.
173. Ernst, J.D., *The immunological life cycle of tuberculosis*. Nature Reviews Immunology, 2012. **12**(8): p. 581-591.
174. Nuttall, J.J.C. and B.S. Eley, *BCG vaccination in HIV-infected children*. Tuberculosis Research and Treatment, 2011. **2011**.
175. Kaufmann, S.H.E. *Tuberculosis vaccines: time to think about the next generation*. in *Seminars in Immunology*. 2013. Elsevier.
176. Mittrücker, H.-W., et al., *Poor correlation between BCG vaccination-induced T cell responses and protection against tuberculosis*. Proceedings of the National Academy of Sciences, 2007. **104**(30): p. 12434-12439.
177. Quesniaux, V.F.J., et al., *TNF in host resistance to tuberculosis infection*. 2010.
178. Kaufmann, S.H.E., *Essay - Envisioning future strategies for vaccination against tuberculosis*. Nature Reviews Immunology, 2006. **6**(9): p. 699-704.
179. Nossal, G.J.V., *Vaccines of the future*. Vaccine, 2011. **29**: p. D111-D115.
180. Evans, T.G., L. Schragar, and J. Thole, *Status of vaccine research and development of vaccines for tuberculosis*. Vaccine, 2016. **34**(26): p. 2911-2914.
181. Tang, J., W.-C. Yam, and Z. Chen, *Mycobacterium tuberculosis infection and vaccine development*. Tuberculosis, 2016. **98**: p. 30-41.
182. Grode, L., et al., *Increased vaccine efficacy against tuberculosis of recombinant Mycobacterium bovis bacille Calmette-Guerin mutants that secrete listeriolysin*. The Journal of clinical investigation, 2005. **115**(9): p. 2472-2479.
183. Langermans, J.A., et al., *Protection of macaques against Mycobacterium tuberculosis infection by a subunit vaccine based on a fusion protein of antigen 85B and ESAT-6*. Vaccine, 2005. **23**(21): p. 2740-2750.
184. Brooks, J.V., et al., *Boosting vaccine for tuberculosis*. Infection and Immunity, 2001. **69**(4): p. 2714-2717.
185. Zaheer, A., et al., *Multi-drug resistant Pseudomonas aeruginosa: a threat of nosocomial infections in tertiary care hospitals*. JPMA, Journal of the Pakistan Medical Association, 2015. **65**(1): p. 12-16.
186. Chatterjee, M., et al., *Antibiotic resistance in Pseudomonas aeruginosa and alternative therapeutic options*. International Journal of Medical Microbiology, 2016. **306**(1): p. 48-58.
187. Doering, G., *Prevention of Pseudomonas aeruginosa infection in cystic fibrosis patients*. International Journal of Medical Microbiology, 2010. **300**(8): p. 573-577.
188. Mall, M.A. and D. Hartl, *CFTR: cystic fibrosis and beyond*. European Respiratory Journal, 2014. **44**(4): p. 1042-1054.

189. Ma, L., et al., *Synthesis of multiple Pseudomonas aeruginosa biofilm matrix exopolysaccharides is post-transcriptionally regulated*. Environmental Microbiology, 2012. **14**(8): p. 1995-2005.
190. Priebe, G.P. and J.B. Goldberg, *Vaccines for Pseudomonas aeruginosa: a long and winding road*. Expert review of Vaccines, 2014. **13**(4): p. 507-519.
191. Wilkins, M., et al., *New approaches to the treatment of biofilm-related infections*. Journal of Infection, 2014. **69**: p. S47-S52.
192. Remans, K., et al., *Genome-wide analysis and literature-based survey of lipoproteins in Pseudomonas aeruginosa*. Microbiology, 2010. **156**: p. 2597-2607.
193. Mishra, M., et al., *Pseudomonas aeruginosa Psl polysaccharide reduces neutrophil phagocytosis and the oxidative response by limiting complement-mediated opsonization*. Cellular Microbiology, 2012. **14**(1): p. 95-106.
194. Mayer-Hamblett, N., et al., *Impact of sustained eradication of new Pseudomonas aeruginosa infection on long-term outcomes in cystic fibrosis*. Clinical Infectious Diseases, 2015. **61**(5): p. 707-715.
195. Sharma, A., A. Krause, and S. Worgall, *Recent developments for Pseudomonas vaccines*. Human Vaccines, 2011. **7**(10): p. 999-1011.
196. Grimwood, K., et al., *Vaccination against respiratory Pseudomonas aeruginosa infection*. Human Vaccines & Immunotherapeutics, 2015. **11**(1): p. 14-20.
197. Rello, J., et al., *A randomized placebo-controlled phase II study of a Pseudomonas vaccine in ventilated ICU patients*. Critical Care, 2017. **21**(1): p. 22.
198. Sharma, A., et al., *Adenovirus-based vaccine with epitopes incorporated in novel fiber sites to induce protective immunity against Pseudomonas aeruginosa*. Plos One, 2013. **8**(2).
199. Döring, G., C. Meisner, and M. Stern, *A double-blind randomized placebo-controlled phase III study of a Pseudomonas aeruginosa flagella vaccine in cystic fibrosis patients*. Proceedings of the National Academy of Sciences, 2007. **104**(26): p. 11020-11025.
200. Campodonico, V.L., et al., *Evaluation of flagella and flagellin of Pseudomonas aeruginosa as vaccines*. Infection and Immunity, 2010. **78**(2): p. 746-755.
201. Wolfgang, M.C., et al., *Pseudomonas aeruginosa regulates flagellin expression as part of a global response to airway fluid from cystic fibrosis patients*. Proceedings of the National Academy of Sciences, 2004. **101**(17): p. 6664-6668.
202. Leighton, T.L., et al., *Biogenesis of Pseudomonas aeruginosa type IV pili and regulation of their function*. Environmental microbiology, 2015. **17**(11): p. 4148-4163.
203. Holder, I.A., *Pseudomonas immunotherapy: a historical overview*. Vaccine, 2004. **22**(7): p. 831-839.
204. Banadkoki, A.Z., et al., *Protective effect of pilin protein with alum plus naloxone adjuvant against acute pulmonary Pseudomonas aeruginosa infection*. Biologicals, 2016. **44**(5): p. 367-373.
205. Franklin, M.J., et al., *Biosynthesis of the Pseudomonas aeruginosa extracellular polysaccharides, alginate, Pel, and Psl*. Frontiers in Microbiology, 2011. **2**.
206. Ramsey, D.M. and D.J. Wozniak, *Understanding the control of Pseudomonas aeruginosa alginate synthesis and the prospects for management of chronic infections in cystic fibrosis*. Molecular Microbiology, 2005. **56**(2): p. 309-322.
207. Ciofu, O., et al., *Characterization of paired mucoid/non-mucoid Pseudomonas aeruginosa isolates from Danish cystic fibrosis patients: antibiotic resistance,  $\beta$ -lactamase activity and RiboPrinting*. Journal of Antimicrobial Chemotherapy, 2001. **48**(3): p. 391-396.
208. Doring, G. and G.B. Pier, *Vaccines and immunotherapy against Pseudomonas aeruginosa*. Vaccine, 2008. **26**(8): p. 1011-1024.
209. Byrd, M.S., et al., *Genetic and biochemical analyses of the Pseudomonas aeruginosa Psl exopolysaccharide reveal overlapping roles for polysaccharide synthesis enzymes in Psl and LPS production*. Molecular Microbiology, 2009. **73**(4): p. 622-638.
210. Mishra, M., et al., *Identification of OprF as a complement component C3 binding acceptor molecule on the surface of Pseudomonas aeruginosa*. Infection and Immunity, 2015. **83**(8): p. 3006-3014.
211. Ma, L., et al., *Assembly and development of the Pseudomonas aeruginosa biofilm matrix*. Plos Pathogens, 2009. **5**(3).
212. Martin, N.L., et al., *Conservation of surface epitopes in Pseudomonas aeruginosa outer membrane porin protein OprF*. Fems Microbiology Letters, 1993. **113**(3): p. 261-266.
213. Westritschnig, K., et al., *A randomized, placebo-controlled phase I study assessing the safety and immunogenicity of a Pseudomonas aeruginosa hybrid outer membrane protein OprF/I*

- vaccine (IC43) in healthy volunteers*. Human Vaccines & Immunotherapeutics, 2014. **10**(1): p. 170-183.
214. Matthews, Q.L., *Capsid-incorporation of antigens into adenovirus capsid proteins for a vaccine approach*. Molecular Pharmaceutics, 2011. **8**(1): p. 3-11.
  215. Peluso, L., et al., *Protection against Pseudomonas aeruginosa lung infection in mice by recombinant OprF-pulsed dendritic cell immunization*. BMC Microbiology, 2010. **10**.
  216. Cui, Z., et al., *Mannose-modified chitosan microspheres enhance OprF-OprI-mediated protection of mice against Pseudomonas aeruginosa infection via induction of mucosal immunity*. Applied Microbiology and Biotechnology, 2015. **99**(2): p. 667-680.
  217. Revets, H., et al., *Lipoprotein I, a TLR2/4 ligand modulates Th2-driven allergic immune responses*. The Journal of Immunology, 2005. **174**(2): p. 1097-1103.
  218. Gartner, T., et al., *Mucosal prime-boost vaccination for tuberculosis based on TLR triggering OprI lipoprotein from Pseudomonas aeruginosa fused to mycolyl-transferase Ag85A*. Immunology Letters, 2007. **111**(1): p. 26-35.
  219. Rehm, B.H.A., et al., *Antibody-response of rabbits and cystic-fibrosis patients to an alginate-specific outer-membrane protein of a mucoid strain of Pseudomonas aeruginosa*. Microbial Pathogenesis, 1994. **16**(1): p. 43-51.
  220. Rehm, B.H.A., et al., *Overexpression of algE in Escherichia coli: subcellular-localization, purification, and ion-channel properties*. Journal of Bacteriology, 1994. **176**(18): p. 5639-5647.
  221. Hay, I.D., Z.U. Rehman, and B.H.A. Rehm, *Membrane topology of outer membrane protein AlgE, which is required for alginate production in Pseudomonas aeruginosa*. Applied and Environmental Microbiology, 2010. **76**(6): p. 1806-1812.
  222. Whitney, J.C., et al., *Structural basis for alginate secretion across the bacterial outer membrane*. Proceedings of the National Academy of Sciences, 2011. **108**(32): p. 13083-13088.
  223. Sawa, T., et al., *Active and passive immunization with the Pseudomonas V antigen protects against type III intoxication and lung injury*. Nature Medicine, 1999. **5**(4): p. 392-398.
  224. Golpasha, I.D., et al., *Recombinant Pcrv induced poly-isotypic humoral immune responses against Pseudomonas aeruginosa in balb/c mice*. Iranian Journal of Public Health, 2014. **43**(2): p. 294-294.

## Chapter 1A: Thesis scope

### 1.12 Problem statement

The success of traditional prophylactic vaccines has contributed significantly to the prevention and eradication of many infectious diseases. However, despite their success, traditional vaccines are not effective in the prevention of all infectious diseases. Therefore, new and novel vaccines are required for the control and prevention of diseases for which cannot be achieved by traditional means, namely TB caused by the bacterium *M. tuberculosis* and chronic pulmonary infection caused by the bacterium *P. aeruginosa*. These two bacteria cause high levels of mortality and morbidity worldwide. Currently, a licensed vaccine is available for the prevention of TB but demonstrates little to no protection in adults against pulmonary TB, while there is no commercially available vaccine against *P. aeruginosa*.

### 1.13 Aim

To develop antigen-displaying PHA bead based prophylactic vaccines for the prevention of tuberculosis caused by pathogenic *M. tuberculosis* or chronic infection associated with opportunistic *P. aeruginosa*.

### 1.14 Objectives

My research will be divided into two main projects.

<i>P. aeruginosa</i> vaccine PHA beads	Mycobacterial vaccine PHA beads
<p><b>Identification of protective antigens</b></p> <ul style="list-style-type: none"><li>• Identification of protective antigens of <i>P. aeruginosa</i> that are found to be immunodominant and shown to confer protective immunity.</li></ul> <p><b>PHA synthase (PhaC1) N-terminal protein fusion functionalized beads</b></p> <ul style="list-style-type: none"><li>• Design and cloning of PhaC1 N terminal antigen fusion plasmids</li></ul>	<p><b>Establishment of PHA pathway</b></p> <ul style="list-style-type: none"><li>• Design and cloning of plasmids required to establish poly-3-hydroxybutarate (PHB) pathway and subsequently antigen-displaying PHA beads</li><li>• Production of PHB beads in nonpathogenic host <i>M. smegmatis</i> as a model organism for <i>M. tuberculosis</i>.</li><li>• Functional assessment of vaccine PHA beads</li></ul>

<ul style="list-style-type: none"> <li>• Production of vaccine PHA beads in host <i>P. aeruginosa</i></li> <li>• Functional assessment of vaccine PHA beads for surface antigen-display</li> <li>• Immunology studies in a mouse model</li> </ul> <p><b>Assessment of class II PHA synthase (PhaC1) to tolerate C terminal fusion</b></p> <ul style="list-style-type: none"> <li>• Design and cloning of PhaC1 C terminal GFP fusion</li> <li>• Assessment of vaccine PHA bead production in host <i>P. aeruginosa</i></li> <li>• Functional assessment of vaccine PHA beads</li> </ul>	<ul style="list-style-type: none"> <li>• Immunology and challenge studies in a mouse model</li> </ul>
---	---

### 1.15 Scope

Antigen-displaying (vaccine) PHA beads produced in heterologous *E. coli* and *L. lactis* host have been shown to protect against challenge with *M. tuberculosis*. These vaccine PHA beads were found to carry copurifying HCPs of their production host (*E. coli* or *L. lactis*) in addition to the display of the fusion antigen. Therefore, using the disease causing or model organism as a host for the production of vaccine PHA beads will result in these beads coated with known and unknown HCPs. These additional known and unknown proteins may have the potential to induce protective immunity. If successful, the concept of producing vaccine beads in the pathogen or model organism could be applied to other infectious diseases and to accelerate vaccine development.

## Link to next chapter

Antigen-displaying (vaccine) PHA beads produced in heterologous host have been shown to be an efficacious vaccine delivery system. However, these vaccine PHA beads tend to carry unwanted copurifying HCPs of the production host.

Therefore, the production of antigen-displaying (vaccine) PHA beads in the disease causative host will result in these beads coated with known and unknown HCPs of the pathogen. These additional known and unknown proteins may have the potential to induce protective immunity.

To exemplify this concept, chapter 2 describes the development of antigen-displaying PHA bead based prophylactic vaccine for the prevention of infection associated with opportunistic pathogen *P. aeruginosa*. *P. aeruginosa* is a major cause of hospital-acquired infections of immune-compromised individuals and currently, there is no commercially available prophylactic vaccine against this organism.

This chapter describes the bioengineering of *P. aeruginosa* to promote the production of PHA and vaccine candidate exopolysaccharide (EPS) Psl production; a new mode of functional display using the class II PHA synthase (C terminus); and the engineering, production, and immunological validation of OprI/F-AlgE fusion antigen-displayed on PHA beads.

## Chapter 2: Bioengineering *Pseudomonas aeruginosa* to assemble its own particulate vaccine capable of inducing cellular immunity

Jason W. Lee<sup>1,2</sup>, Natalie A. Parlane<sup>2</sup>, D. Neil Wedlock<sup>2</sup>, and Bernd H. A. Rehm<sup>1,3,4,\*</sup>

*Institute of Fundamental Sciences, Massey University, Palmerston North, New Zealand<sup>1</sup>, AgResearch, Hopkirk Research Institute, Palmerston North, New Zealand<sup>2</sup>, The MacDiarmid Institute for Advanced Materials and Nanotechnology, Wellington, New Zealand<sup>3</sup>, and PolyBatics, Palmerston North, New Zealand<sup>4</sup>*

\*Corresponding author: Bernd H. A. Rehm, e-mail: b.rehm@massey.ac.nz,  
phone: +64 6 350 5515, fax: +64 6 350 5688

### Abstract

Many bacterial pathogens naturally form cellular inclusions. Here the immunogenicity of polyhydroxyalkanoate (PHA) inclusions and their use as particulate vaccines delivering a range of host derived antigens to serve as safe and efficient agent to prevent infection by the pathogen was assessed. Our study showed that PHA inclusions of opportunistic pathogenic *Pseudomonas aeruginosa* are immunogenic mediating a specific cell-mediated immune response. Protein engineering of the PHA inclusion forming enzyme by translational fusion of epitopes from vaccine candidates outer membrane proteins OprI, OprF, and AlgE mediated self-assembly of PHA inclusions coated by these selected antigens. Mice vaccinated with isolated OprI/F-AlgE displaying PHA inclusions produced a Th1 type immune response characterized by antigen-specific production of IFN- $\gamma$  and IgG2c isotype antibodies. This study showed that cellular inclusions of pathogenic bacteria are immunogenic and can be engineered to display selected antigens suitable to serve as particulate subunit vaccines against infectious diseases.

## 2.1 Introduction

Many bacteria including various human pathogens form polymeric intracellular inclusions such as e.g. polyhydroxyalkanoate (PHA) inclusions that serve as energy and carbon storage material [1, 2]. While cell surface structures of pathogens had been the focus of studies towards identifying vaccine candidate antigens, the immunogenicity of intracellular structures had not been studied. However nano-/micro-sized intracellular structures such as polymer inclusions might serve as particulate vaccines suitable for efficient antigen delivery. Particulate antigen delivery systems are being increasingly considered for vaccine formulations evidenced by recent successful application and commercialization of particle-based vaccines [3, 4]. PHA beads had been previously shown to enable delivery of antigens inducing protective immunity in animal models against tuberculosis [5, 6] and hepatitis C [7, 8]. PHAs are deposited as spherical cytoplasmic inclusions surrounded by proteins [1, 9]. Protein engineering of one of these coating proteins, the PHA synthase (PhaC<sub>Re</sub>), which catalyzes polyhydroxybutyrate (PHB) formation [10-13] enabled antigen-display on PHB beads inducing a specific and protective immune response [5, 8, 14, 15]. Vaccine candidate antigens formulated as particles (< 1  $\mu\text{m}$ ) showed enhanced immunogenicity due to an efficient cellular uptake by professional antigen presenting cells [16].

Here we selected opportunistic pathogen *Pseudomonas aeruginosa* as a model human pathogen because it naturally forms PHA inclusions and traditional vaccine development approaches were unsuccessful [17]. Its PHA is composed of medium chain length 3-hydroxy fatty acids (MCL) which polymerization is catalyzed by the MCL-PHA synthase (e.g. PhaC<sub>1Pa</sub>) [1, 2].

Opportunistic pathogen *P. aeruginosa* is one of the leading causes of nosocomial infections and causes serious life-threatening infections due to intrinsic and acquired antibiotic resistances [17]. Immunocompromised individuals are most at risk, such as those with severe burns and wounds, infected by human immunodeficiency virus (HIV) as well as cystic fibrosis (CF) patients [18]. Vaccines provide a strategy for prevention of the disease caused by *P. aeruginosa* [19].

Vaccine candidates include outer membrane proteins (OMPs), flagellin and pilin, toxins as well as killed or live attenuated whole-cells [17, 20]. The most promising immunogens are the major OMP F (OprF) and outer membrane lipoprotein I (OprI), which are highly conserved, serotype independent and well tolerated [21, 22]. Vaccination studies in animals have shown long-lived antibody titers and broad protection against all *P. aeruginosa* serotypes [23]. However high levels of antibodies were associated with more severe lung disease [24]. It has been suggested that a CD4+ Th1 type cell mediated response maybe more protective [24-26], and that OprI vaccination can modulate the immune response from a CD4+ Th2 towards a CD4+ Th1 cell mediated response [27]. OprI vaccination induced protection in mice [28]. OMP AlgE, the alginate pore, may provide an alternative target for vaccine development. AlgE is overproduced in the mucoid alginate overproducing form found in the lung of CF patients and has been suggested to be immunogenic [29, 30]. The crystal structure of AlgE revealed a 18-stranded  $\beta$ -barrel with extended extracellular loops representing possible cell surface exposed antigenic epitopes [31, 32]. The use of immunogenic epitopes of OprF fused with OprI has been the main candidates for use in *P. aeruginosa* vaccine studies [21, 22, 33], and have shown synergistic effects [34].

In this study we investigated the immunogenicity of cellular inclusions formed by *P. aeruginosa* (**Fig. 2.1**). Immunological properties of PHA inclusions encouraged to engineer *P. aeruginosa* for the production of antigen-displaying PHA inclusions by harnessing its inherent PHA production system. These PHA inclusions were engineered to display selected vaccine antigens of the same host at high density while associated host cell components might serve as additional antigens enhancing the induction of broadly protective immunity and/or having adjuvant properties. This is the first study investigating the immunological properties of cellular polymer inclusions of pathogenic bacteria and to utilize the pathogens own inclusions as carrier of its own antigens to be used as a particulate vaccine.

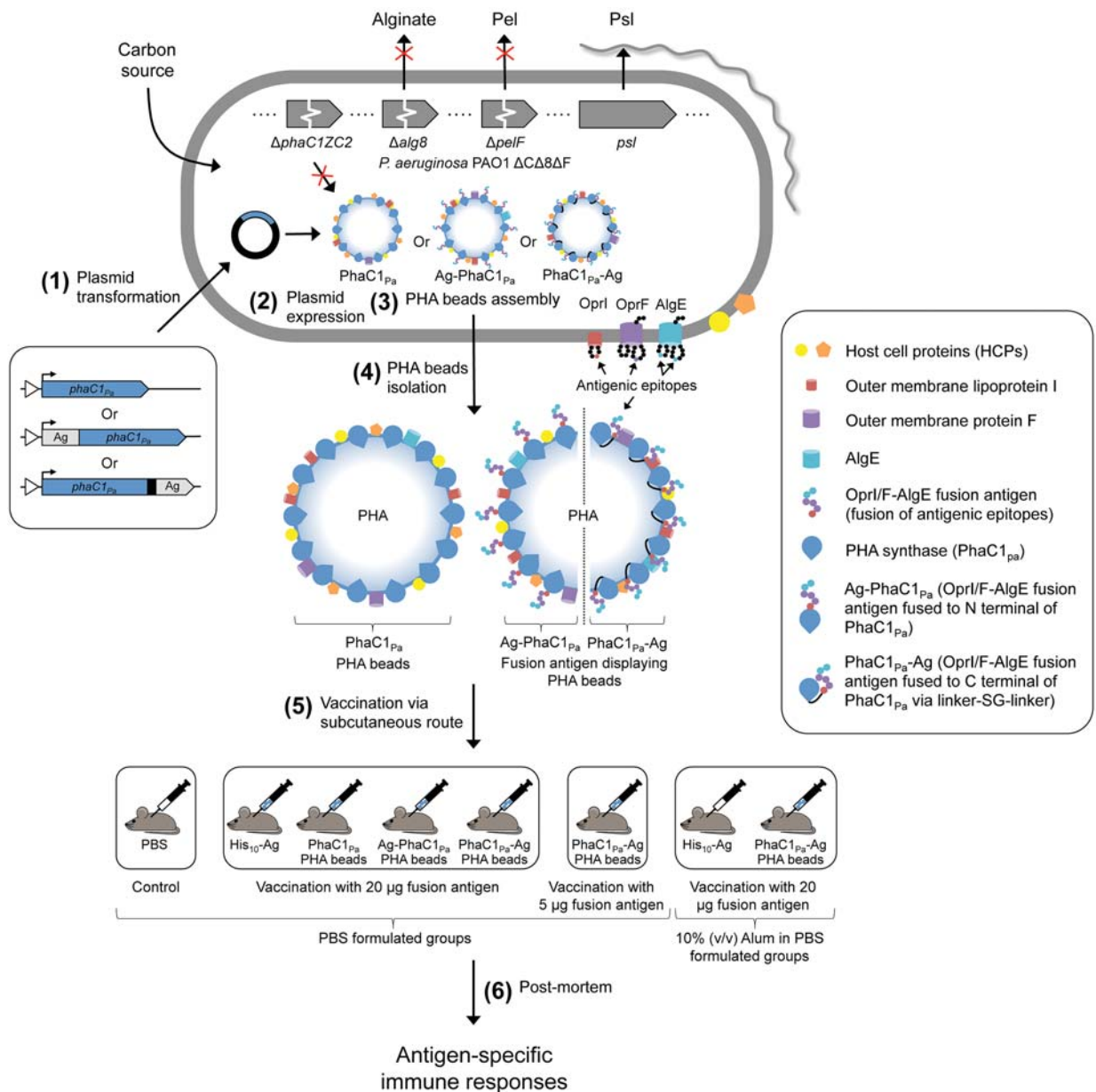


**Figure 2.1. Engineering the pathogens intrinsic ability to produce PHA<sub>MCL</sub> beads as particulate subunit vaccines.** A schematic overview of the production and immunological evaluation of custom-made PHA<sub>MCL</sub> beads displaying both engineered vaccine candidate antigens and antigens derived from the host expression cells. (1) Plasmid encoding wild-type PHA synthase (*phaC1<sub>Pa</sub>*) or OprI/F-AlgE fusion antigen fused to the N terminal of PhaC1<sub>Pa</sub> or OprI/F-AlgE fusion antigen fused to the C terminal of PhaC1<sub>Pa</sub> via linker-SG-linker were transformed in to *P. aeruginosa* PAO1  $\Delta C\Delta 8\Delta F$  mutant strain. This strain is defective in production of native PHA<sub>MCL</sub> and of EPS alginate and Pel (see Fig. 2.2). (2) Plasmid harboring strains are then grown under PHA<sub>MCL</sub> accumulating conditions to mediate overproduction of the fusion protein and subsequent PHA<sub>MCL</sub> bead assembly (See Fig. 2.5a-c). (3) Formation of PHA<sub>MCL</sub> beads results in the display of fusion antigens covalently linked to the PHA synthase and the incorporation of granule associated and HCPs (See Fig. 2.6). (4) PHA<sub>MCL</sub> beads are isolated from the host by mechanical disruption and subsequently purified. (5) C57BL/6 mice

were vaccinated with sterilized PHA<sub>MCL</sub> beads, recombinant His-tagged Oprl/F-AlgE, and PBS via subcutaneous route three times at biweekly intervals. (6) Blood and splenocytes were collected from mice euthanized three-weeks after the last vaccination for analysis. Antigen-specific serum antibodies (ELISA) (see **Fig. 2.8a**) and cytokines (Cytometric bead array, mouse Th1/Th2/Th17 cytokine kit) (see **Fig. 2.10**) were measured.

## 2.2 Results

### 2.2.1 Bioengineering of *P. aeruginosa* for self-assembly of antigen-displaying PHA inclusions

To enable the production of antigen-associated PHA<sub>MCL</sub> inclusions mediated solely by the introduced PHA synthase (PhaC1<sub>Pa</sub> = non-engineered wild-type) and its fusion protein derivatives (engineered to incorporate vaccine candidate antigens), an isogenic PHA<sub>MCL</sub> deficient strain PAO1  $\Delta$ *phaC1ZC2* was employed. To promote production of PHA<sub>MCL</sub> and the vaccine candidate exopolysaccharide (EPS) Psl, essential genes for competing biosynthesis pathways towards the production of alginate and the glucose-rich Pel polysaccharide, respectively, were deleted (**Fig. 2.2**) [35].

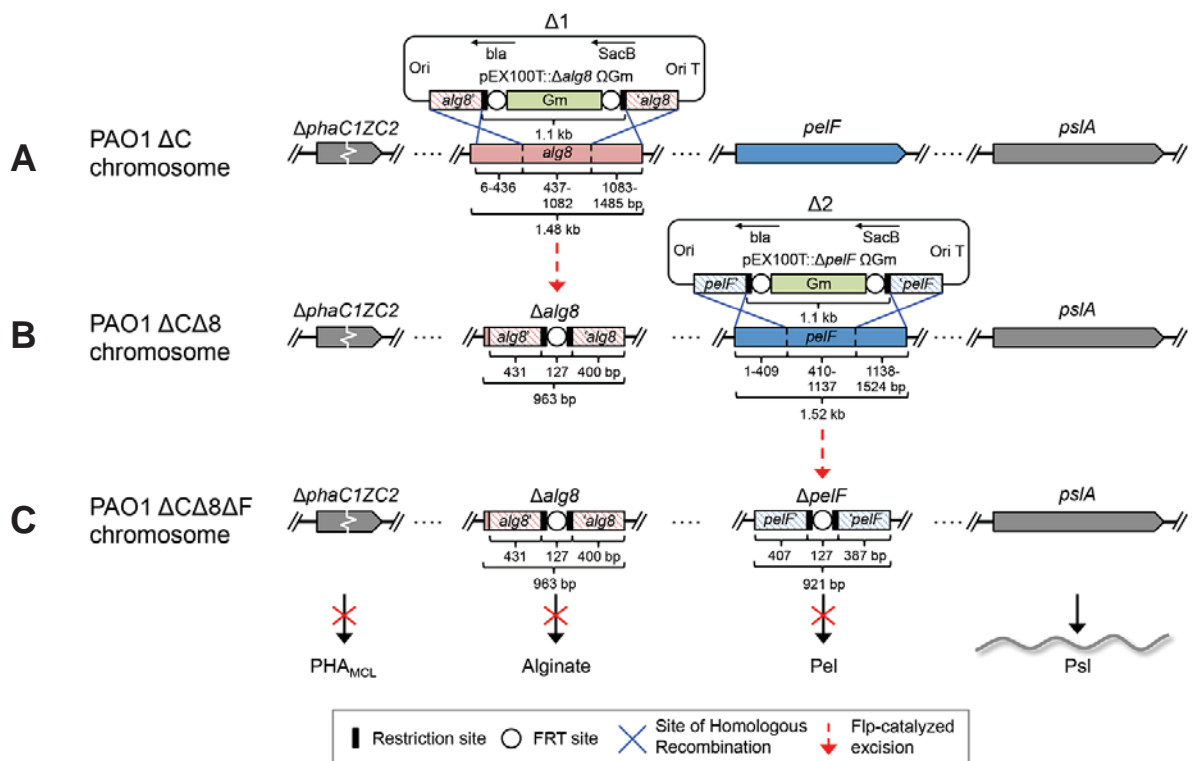


**Figure 2.2.** A schematic of the generation of *P. aeruginosa* knockout mutant PAO1  $\Delta$ *C* $\Delta$ *8* $\Delta$ *F*. In order to promote the production of PHA<sub>MCL</sub> inclusions and vaccine candidate EPS Psl, site-directed homologous recombination was used to delete major parts of (a) *alg8* and (b) *pelF* genes encoding a glycosyltransferase in the PHA negative mutant PAO1  $\Delta$ *phaC1ZC2*. (c) Resultant triple mutant strain is defective in PHA/alginate/pel polysaccharide was verified by DNA sequencing (see **Supplementary Fig. 2.1**).

Formation of PHA<sub>MCL</sub> inclusions mediated by recombinant PhaC1<sub>Pa</sub> (natural wild-type inclusions) or PhaC1<sub>Pa</sub>-GFP was assessed by fluorescence microscopy, GC/MS, and immunoblot analysis (**Fig. 2.3**). In order to assess whether PhaC1<sub>Pa</sub> tolerates C terminal translational fusions, GFP was fused to its C terminus. A designed linker [10] was inserted in order to retain functionality of PhaC1<sub>Pa</sub> and to display the fusion partner GFP on the surface of PHA<sub>MCL</sub> beads (**Fig. 2.3a**). Colocalization of fluorescent foci for GFP and PHA<sub>MCL</sub> visualized within PAO1  $\Delta C\Delta 8\Delta F$  cells producing PhaC1<sub>Pa</sub>-GFP indicated that the GFP fusion to C terminus of PhaC1<sub>Pa</sub> did not abolish PhaC1<sub>Pa</sub> activity and implies that GFP fused to the C terminus of this class II PHA synthase was functionally displayed on the surface of the PHA<sub>MCL</sub> inclusion *in vivo* (**Fig. 2.3b**).

Display of GFP on PHA inclusions anchored via fusion to the C terminus of PhaC1<sub>Pa</sub> was observed by fluorescence microscopy expanding the scope of PhaC1<sub>Pa</sub> engineering to C terminally fusible antigens. Selected epitopes of the OMPs OprF, OprI (lipoprotein), and AlgE (alginate secretion porin) from *P. aeruginosa* were used as vaccine candidates to be immobilized to the surface of PHA inclusions. Selection of antigenic epitopes of OprF and OprI was based on previous studies that demonstrated protective immunity in animal models (**Fig. 2.4a**). Antigenic epitopes of AlgE were selected based on its structure using B-cell antigenic epitope prediction method EPCES (**Fig. 2.4b**).

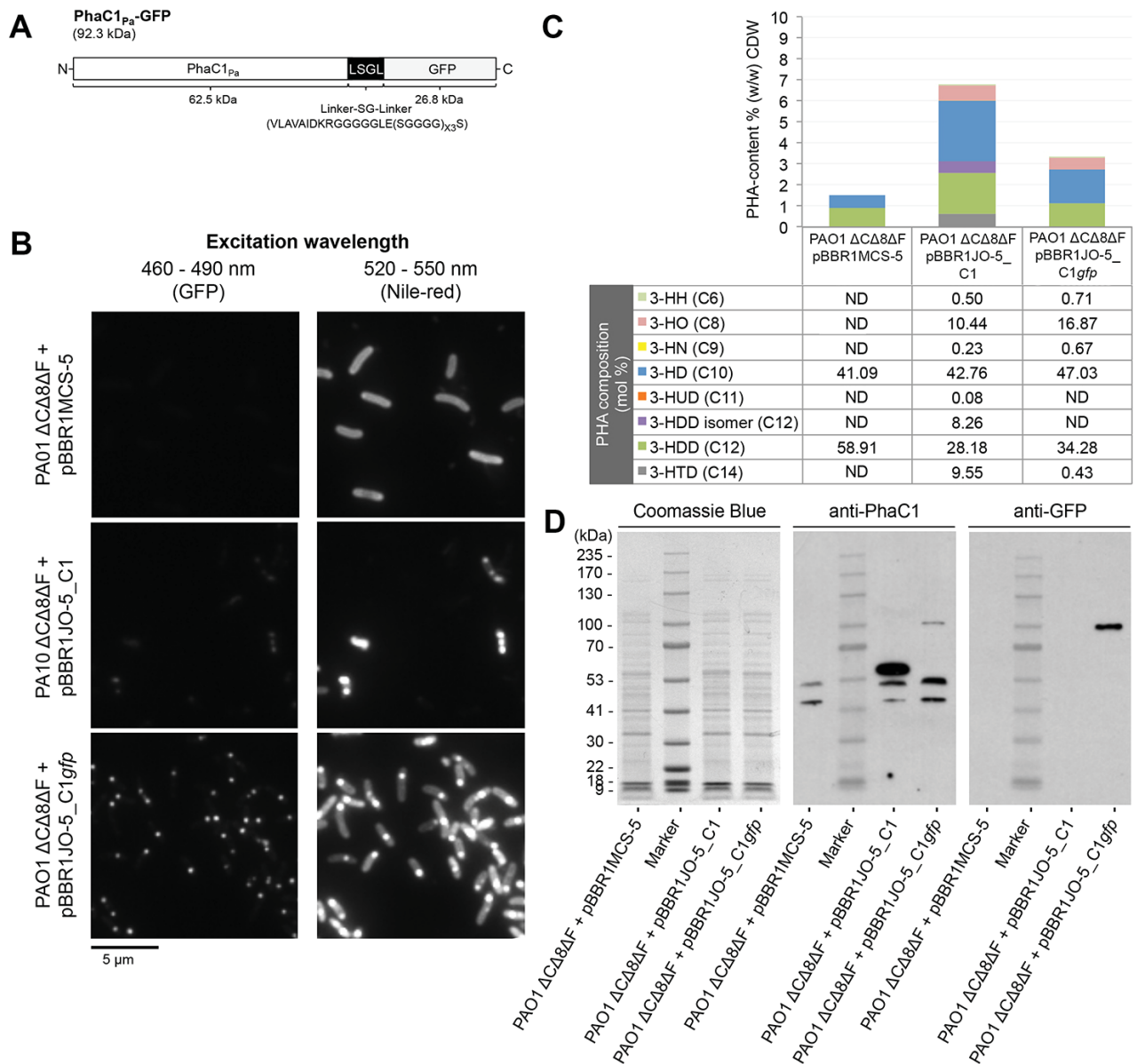
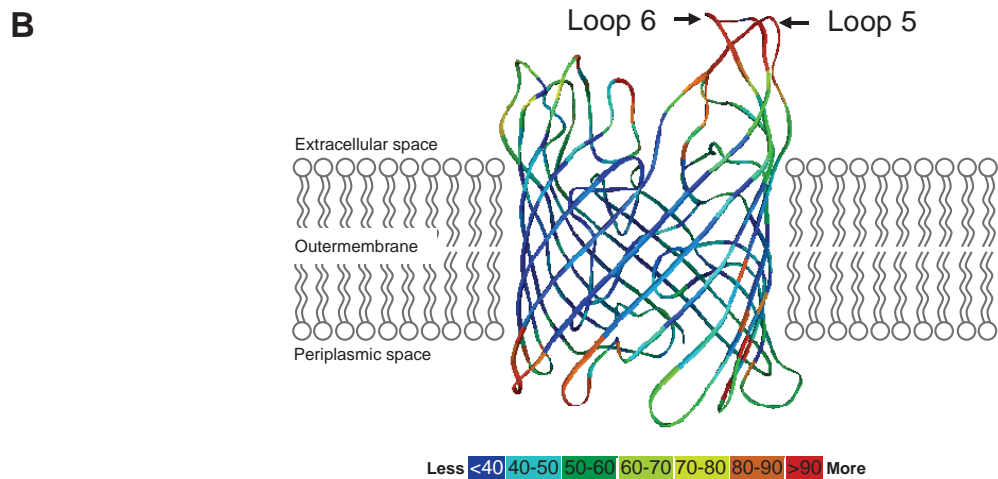


**Figure 2.3. Assessment of the tolerance of the class II PHA synthase (PhaC1<sub>Pa</sub>) to C terminal fusion.** (a) Schematic representation of fusion protein PhaC1<sub>Pa</sub>-GFP for assessment of class II PHA synthase tolerance to C terminal fusion. (b) Fluorescence microscopy analysis of Nile-red stained *P. aeruginosa* PAO1 ΔCΔ8ΔF cultures harboring various plasmids grown under PHA<sub>MCL</sub> accumulating conditions for 24 h and visualized for GFP and *in vivo* PHA<sub>MCL</sub> inclusions (white arrow). (c) Quantification and compositional analysis of PHA<sub>MCL</sub> in whole-cell by Gas chromatography-mass spectrometry (GC/MS). (d) SDS-PAGE and immunoblot analysis of cell lysates to confirm the production of fusion protein. ND, not detected; 3-HH (C6), methyl 3-hydroxyhexanoate; 3-HO (C8), methyl 3-hydroxyoctanoate; 3-HN (C9), methyl 3-hydroxynonanoate; 3-HD (C10), methyl 3-hydroxydecanoate; 3-HUD (C11), methyl 3-hydroxyundecanoate; 3-HDD isomer (C12), methyl 3-hydroxydodecanoate isomer; 3-HDD (C12), methyl 3-hydroxydodecanoate; 3-HTD (C14), methyl 3-hydroxytetradecanoate.

**A**

OprI { Amino acid sequence:  
MNNVLKFSALALAAVLATGCSSSHKETEARLTATEDAAARAQARADEAYRKADEALGAAQKAQQTAD  
EANERALRMLEKASRK

OprF { Amino acid sequence:  
MKLKNTLGVVIGSLVAASAMNAFAQQQNSVEIEAFGKRYFTDSVRNMKNADLYGGSIGYFLTDDVELA  
LSYGEYHDVVRGTYETGNKKVHGNTSLDAIYHFGTPGVGLRPYVSAGLAHQNITNINSDSQGRQQMT  
MANIGAGLKYYFTENFFAKASLDGQYGLEKRDNGHQGEWMAGLGVGFNFGGSKAAPAPEPVADVCS  
DSDNDGVCDNVDKCPDTPANVTVDANGCPAVAEVVRVQLDVKFDKSKVKENSYADIKNLADFMK  
QYPSTSTTVEGHTDSVGTDAYNQKLSERRANAVRVNEYGVEGGRVNAVGYGESRPVADNATAEGRA  
INRRVEAEVEAEAK



AlgE { Amino acid sequence:  
KNFGLDVKITGESENRDLGTAPGGTLNDIGIDLRPWAFGQWGDWSAYFGQAVAATDIETDTPDKSY  
LAAREFWVDYAGLTAYPGEHLRFGRQRLREDSGQWQDTNIEALNWSFETLLNAHAGVAQRFSEYRT  
DLDELAPEDKDRTHVFGDISTQWAPHHRIGVRIHHADDSG<L5>HLRRPGEEV<L5>DNLDKTYTGQLT  
WLGIEATGDAYNYRSSLNLYWASATWLTGDRD<L6>NLTTTTRIAATGKQ<L6>SGDVNAFGVDLGLRWNI  
DEQWKAGVGYARGSGGGKDGEEQFQQTGLESNRSNFTGTRSRVHRFGEAFRGELSNLQAATLFGS  
WQLREDYDASLVYHKFWRVDDSDIGTSGINAALQPGEKDIGQELDLVVTKYFKQGLLPASSQYVDEP  
SALIRFRGGLFKPGDAYGPGTDSTHRAFVDFIWRP

**Figure 2.4. Antigenic epitopes of OprI, OprF, and AlgE.** (a) The amino acid sequences of OprI and OprF. Selected antigenic epitopes are indicated in red. (b) EPCES B-cell epitope prediction of AlgE epitopes. Analysis of chain B in AlgE RCSB Protein Data Bank (3RBH) entry identified extracellular loop 5 (L5) and loop 6 (L6) out of the 9 extracellular loops of AlgE to have high probability of being immunogenic. L5 and L6 correspond to amino acids 233 – 241 (HLRRPGEEV) and amino acids 287 – 303 (NLTTTTRIAATGKQ) when compared to the AlgE reference sequence (Refseq: NP\_252234.1). Predicted antigenic epitopes are illustrated by color, ranging from low (blue) to high (red) probability of being antigenic. The amino acid sequences of selected antigenic epitopes in loops 5 and 6 of AlgE identified by EPCES with >80% probability is indicated in red.

Antigenic epitopes of AlgE, OprF, and OprI were combined as a single fusion antigen (OprI/F-AlgE) and translationally fused to either the N or C terminus of PhaC1<sub>Pa</sub> and the impact on the production of PHA<sub>MCL</sub> inclusions as well as the functionality of the fusion partners was analyzed (**Fig. 2.5a-c**).

Recombinant *P. aeruginosa* expressing the various genes, PhaC1<sub>Pa</sub> (wild-type control) or Ag-PhaC1<sub>Pa</sub> (antigens fused to N terminus) or PhaC1<sub>Pa</sub>-Ag (antigens fused to C terminus) accumulated PHA<sub>MCL</sub> inclusions, enabling subsequent isolation as PHA<sub>MCL</sub> bead material as observed by TEM (**Fig. 2.5b**). Interestingly, PhaC1<sub>Pa</sub>-Ag mediated production of significantly smaller inclusion (15 to 186 nm, average 48 nm  $\pm$  1.16 s.e.m) compared to Ag-PhaC1<sub>Pa</sub> fusion protein (46 to 316 nm, average 130 nm  $\pm$  1.98 s.e.m) and PhaC1<sub>Pa</sub> protein (45 to 377 nm, average 172 nm  $\pm$  2.61 s.e.m).

Quantification and composition of intracellular PHA<sub>MCL</sub> and purity of the isolated PHA<sub>MCL</sub> bead material was assessed by GC/MS analysis (**Fig. 2.5c**). Low levels of 3-hydroxyalkanoic acids mainly composed of 3-hydroxydecanoate (C10) and 3-hydroxydodecanoate (C12) likely derived from rhamolipid synthesis [36] contributing to about 1.8% (w/w) of CDW were detected in PHA<sub>MCL</sub> negative control i.e. means in cells harboring only vector pHERD20T. PAO1  $\Delta$ C $\Delta$ 8 $\Delta$ F cells harboring the plasmid encoding PhaC1<sub>Pa</sub> accumulated PHA<sub>MCL</sub> contributing to about 17% (w/w) of cellular dry weight (CDW), while strain PAO1  $\Delta$ C $\Delta$ 8 $\Delta$ F harboring the plasmid encoding Ag-PhaC1<sub>Pa</sub> or PhaC1<sub>Pa</sub>-Ag accumulated PHA<sub>MCL</sub> contributing to about 13% and 12.5% (w/w) of CDW, respectively. The composition of the PHA<sub>MCL</sub>, i.e. the molar fractions of comonomers, between the different PHA<sub>MCL</sub> beads showed only slight variation. The beads were composed mainly of 3-hydroxyoctanoate (C8), 3-hydroxydecanoate (C10) and 3-hydroxydodecanoate (C12) and reflected the composition of PHA<sub>MCL</sub> in whole-cells. PHA<sub>MCL</sub> purity of the isolated bead material is displayed as percentage of the bead dry weight (BDW). Both PhaC1<sub>Pa</sub> and Ag-PhaC1<sub>Pa</sub> beads were purified to approximately 87% of PHA<sub>MCL</sub> content, while PhaC1<sub>Pa</sub>-Ag beads contained only 48.5% of PHA<sub>MCL</sub>.

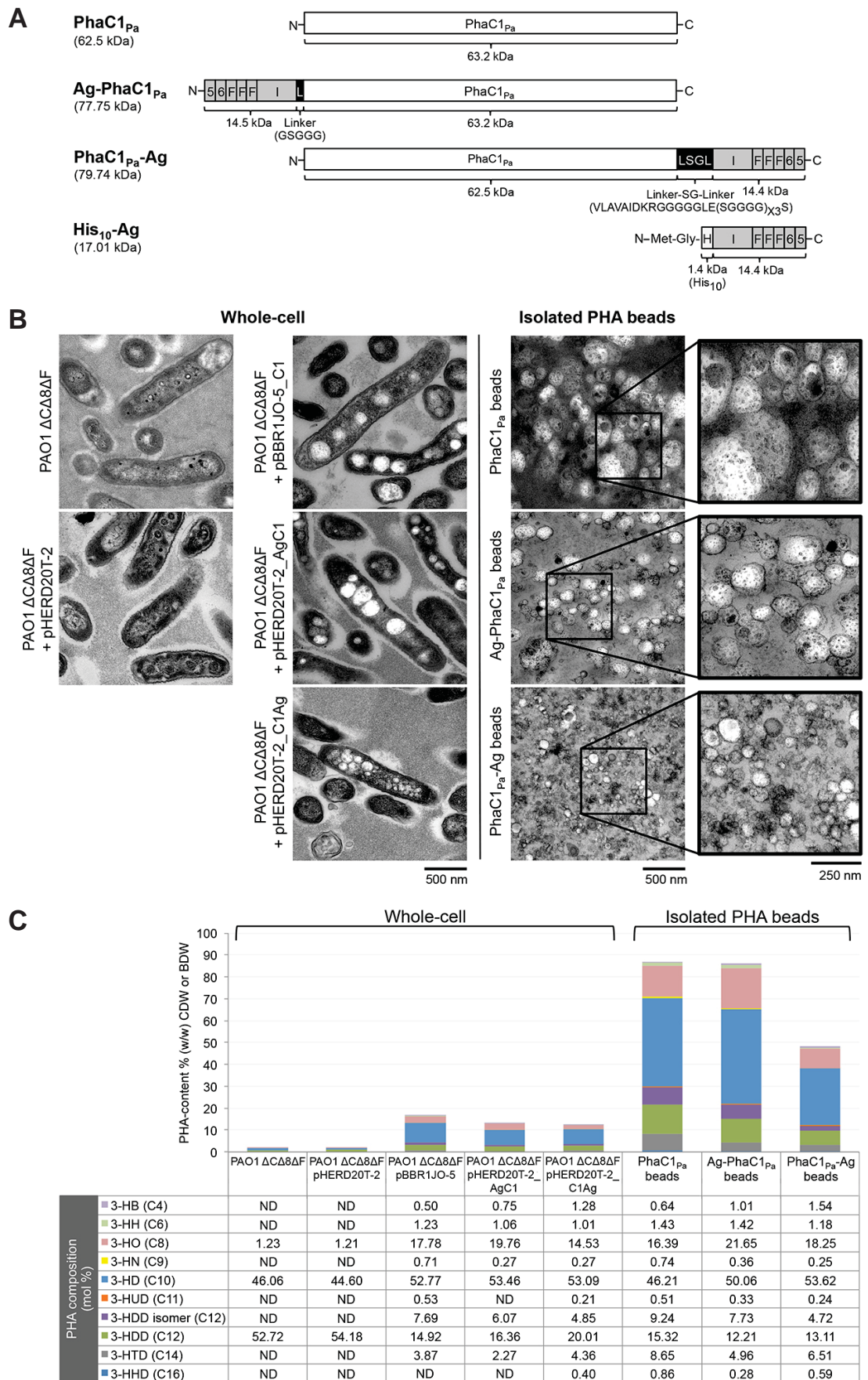


**Figure 2.5. Bioengineering and production of vaccine PHA<sub>MCL</sub> inclusions *in vivo*.** PAO1  $\Delta$ C $\Delta$ 8 $\Delta$ F cells harboring various plasmids cultivated under PHA<sub>MCL</sub> accumulating condition for

48 h and their respective isolated PHA<sub>MCL</sub> beads. **(a)** A schematic representation of various fusion proteins which mediate PHA<sub>MCL</sub> bead production in strain PAO1  $\Delta C\Delta 8\Delta F$  or recombinant protein production in *E. coli* (see **Fig. 2.7**). **(b)** Accumulation and size of PHA<sub>MCL</sub> inclusions were analyzed by Transmission Electron Microscopy (TEM) in whole-cells and of the isolated PHA<sub>MCL</sub> bead material. **(c)** Quantification and compositional analysis of PHA<sub>MCL</sub> using GC/MS. BDW, percentage of the bead dry weight; ND, not detected; 3-HH (C4), methyl 3-hydroxybutanoate; 3-HH (C6), methyl 3-hydroxyhexanoate; 3-HO (C8), methyl 3-hydroxyoctanoate; 3-HN (C9), methyl 3-hydroxynonanoate; 3-HD (C10), methyl 3-hydroxydecanoate; 3-HUD (C11), methyl 3-hydroxyundecanoate; 3-HDD isomer (C12), methyl 3-hydroxydodecanoate isomer; 3-HDD (C12), methyl 3-hydroxydodecanoate; 3-HTD (C14), methyl 3-hydroxytetradecanoate; 3-HHD (C16), methyl 3-hydroxyhexadecanoate.

Whole-cell lysates and isolated PHA<sub>MCL</sub> beads contained dominant proteins with an apparent molecular weight of 62.5 kDa (PhaC1<sub>Pa</sub>), 77.75 kDa (Ag-PhaC1<sub>Pa</sub>) and 79.74 kDa (PhaC1<sub>Pa</sub>-Ag) (**Fig. 2.6a**), and their identity was confirmed (**Fig. 2.6b,c** and **Supplementary Table 2.1**). Densitometry analysis indicated that PhaC1<sub>Pa</sub>, Ag-PhaC1<sub>Pa</sub>, and PhaC1<sub>Pa</sub>-Ag fusion proteins accounted for 8.8%, 12.3%, and 9.9% of total PHA<sub>MCL</sub> bead associated protein, respectively (data not shown). Several additional copurifying host cell proteins (HCPs) were detected within the bead material (**Fig. 2.6b,c**). The major copurifying eleven proteins (**Fig. 2.6a**) were selected (labeled I – XI) for identification and peptides belonging to *P. aeruginosa* proteins for each protein band (**Fig. 2.6d** and **Supplementary Table 2.2**) were ranked based on combined score i.e. –log(*P*) value. Database hits included the PHA synthase, OMPs (i.e. OprI and OprF), ribosomal proteins, naturally bead associated proteins (i.e. PhaI and PhaF), and heat-shock proteins. Some of these OprI, OprF, and AlgE related protein bands were additionally confirmed by immunoblot analysis (**Fig. 2.6c**). Interestingly, tryptic peptides of the PhaC<sub>Pa</sub> were identified in the majority of protein bands as the best hit (**Fig. 2.6d**, bands I – IV and VII – XI) and second best hits (**Fig. 2.6d**, bands V – VI). Identified PhaC1<sub>Pa</sub> peptides suggested some degradation from the C terminus. Immunoblot analysis using the antibody anti-PhaC1\_1 detected copurifying protein bands I, II, VII, and VIII, while anti-PhaC1\_67 detected protein bands I, VII, and VIII indicating some degradation of the fusion protein.

Antibody detected epitopes were aligned with peptides identified by MALDI-TOF MS for each band and showed that anti-PhaC1\_1 recognized epitopes exhibited a coverage of 22% for bands I, II and VII and 71% coverage for band VIII, while anti-PhaC1\_67 showed full epitope coverage for bands I and VIII and partial coverage of 17% for band VII (**Supplementary Table 2.3**). Alignment of the anti-PhaC1\_529 recognized epitope with peptides identified by MALDI-TOF MS in the eleven bands showed that the respective epitope was absent.

The recombinant soluble fusion antigen was produced and purified as shown in **Fig. 2.7**.

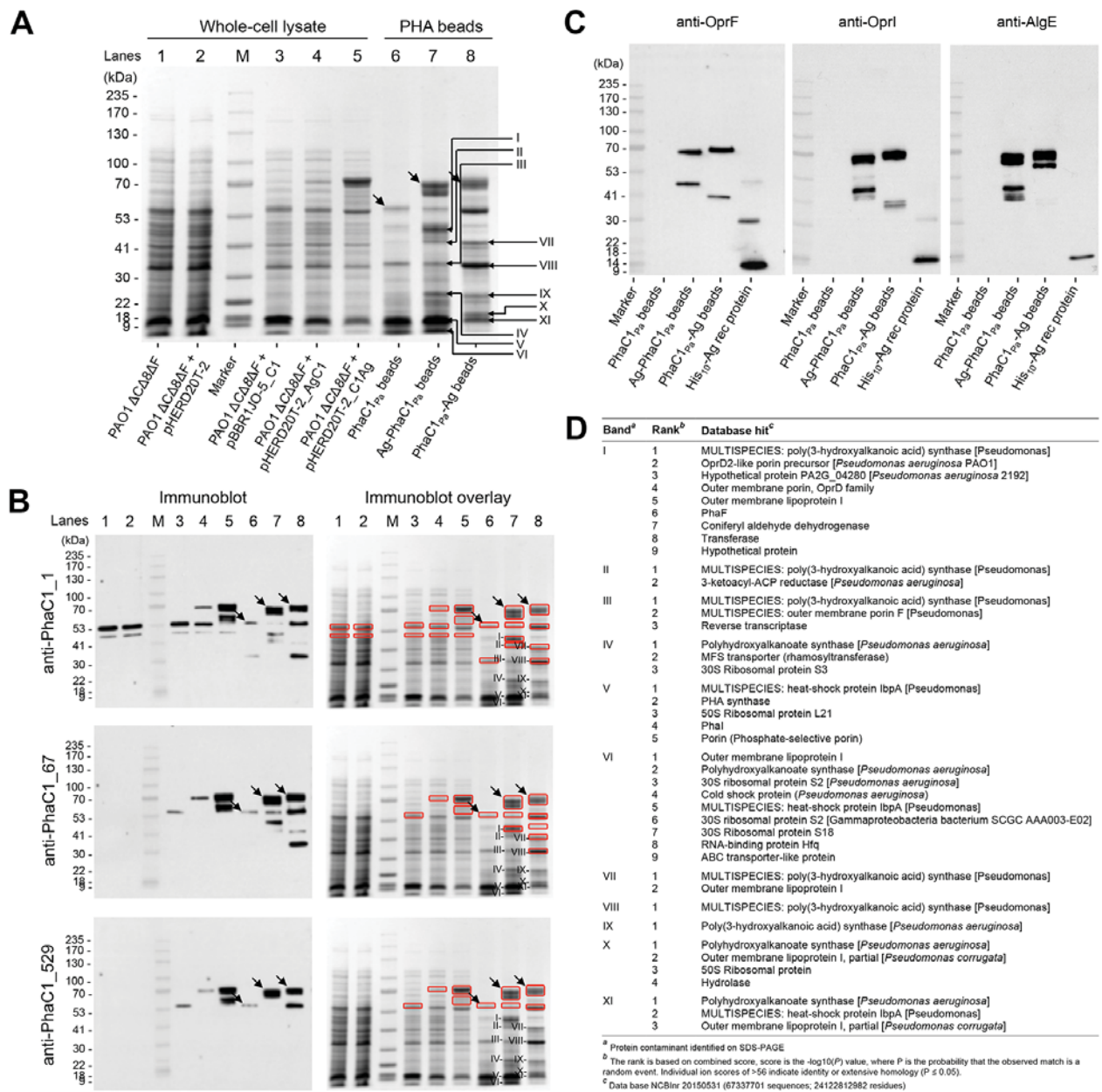
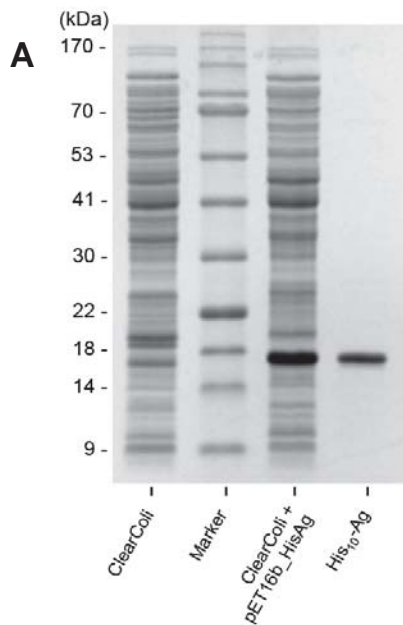


**Figure 2.6. Protein analysis of vaccine PHA<sub>MCL</sub> beads.** (a) SDS-PAGE analysis of whole-cell lysate and PHA<sub>MCL</sub> beads stained with Coomassie Blue or (b) probed using anti-PhaC1 polyclonal antibodies raised against various epitopes of PhaC1<sub>Pa</sub> (see Materials). Fusion proteins of interest in PHA<sub>MCL</sub> bead samples are indicated by black arrows and the eleven HCP bands identified of interest are indicated in roman numerals. These indicated proteins were isolated for protein identification by MALDI-TOF MS (see **Supplementary Table 2.1** and **2.2**). Detected bands from **b** immunoblotting were overlaid and matched to specific bands on the Coomassie Blue stained gel (red square). Antibody detected epitopes were aligned with peptides identified by MALDI-TOF MS (see **Supplementary Table 2.3**). Major copurified protein bands from PHA<sub>MCL</sub> beads formed by PHA synthase antigen fusions were identified on SDS-PAGE (see Materials for criteria). (c) Immunoblot analysis of isolated PHA<sub>MCL</sub> beads using polyclonal antibodies raised against epitopes of OprF or OprI or AlgE. (d) Table summarizing the identification of the eleven PHA<sub>MCL</sub> bead associated HCPs by MALDI-TOF MS (see also **Supplementary Table 2.2**).



**B**

**His<sub>10</sub>-Ag**

Peptide no.	$M_r$			Miss <sup>a</sup>	Score <sup>b</sup>	Expected <sup>c</sup>	Peptide <sup>d</sup>
	Observed	Exptl	Calculated				
1	724.3178	723.3105	723.3187	0	37	0.00019	R.ADEAYR.K
4	829.361	828.3537	828.3548	0	34	3.70E-04	R.HMSSHSEK.E + Oxidation (M)
8	946.4615	945.4542	945.4516	0	73	7.40E-08	R.VENATAEGR.A
9	973.4897	972.4825	972.4876	0	53	4.80E-06	K.ADEALGAAQK.A
10	1018.5169	1017.5096	1017.5091	0	91	8.00E-10	R.LTATEDAAAR.A
13	1102.5703	1101.563	1101.5527	1	69	1.10E-07	R.RVENATAEGR.A
17	1232.5596	1231.5523	1231.5429	0	102	6.00E-11	K.AQQTAEANER.A
28	1519.7744	1518.7671	1518.7638	1	77	6.40E-08	R.RVENLTTTTVDDR.R
31	1675.866	1674.8587	1674.8649	2	74	3.60E-08	R.RVENLTTTTVDDRR.I

<sup>a</sup> The number of missed cleavage sites

<sup>b</sup> The score is the  $-\log_{10}(P)$  value, where P is the probability that the observed match is a random event. Individual ion scores of >56 indicate identity or extensive homology ( $P \leq 0.05$ );

<sup>c</sup> Expected score based on BLAST search;

<sup>d</sup> The sequence between the peptides was identified by MS. The amino acid before the period at the N terminal and that after the period at the C terminal indicate the cleavage sites.

**Figure 2.7. Analysis of soluble recombinant protein His<sub>10</sub>-Ag.** His<sub>10</sub>-tagged fusion protein was produced by recombinant ClearColi and subjected to Ni<sup>2+</sup>-NTA based His-affinity purification. Soluble His<sub>10</sub>-Ag was recovered as 95% pure protein as assessed by (a) SDS-PAGE and densitometry (data not shown). (b) Protein identification of His<sub>10</sub>-Ag fusion proteins by peptide finger printing using MALDI-TOF MS. (For confirmation by immunoblot analysis see Fig. 2.6c).

### 2.2.2 Immunological response to vaccination with antigen-displaying PHA<sub>MCL</sub> beads

Mice were vaccinated with 20 µg of PhaC1<sub>Pa</sub> attached to beads or 20 µg OprI/F-AlgE antigen immobilized to beads (Ag-PhaC1<sub>Pa</sub> or PhaC1<sub>Pa</sub>-Ag) formulated in saline without alum adjuvant. Following vaccination, no obvious adverse effects were observed in any of the animals, with mice gaining weight in all groups. PHA<sub>MCL</sub> beads stimulated the generation of OprI/F-AlgE antigen specific IgG2c antibodies, indicating a Th1 dominant response (**Fig. 2.8a**).

The greatest response was obtained in groups vaccinated with 20 µg of OprI/F-AlgE antigen immobilized to PhaC1<sub>Pa</sub> beads or 20 µg PhaC1<sub>Pa</sub> immobilized to Ag-PhaC1<sub>Pa</sub> beads. No significant difference, but a positive trend was seen between vaccinated groups receiving vaccine formulated with alum compared to their respective groups formulated without alum (**Fig. 2.9a**). All beads induced sera antibodies specific for epitopes in bead-associated proteins (HCPs, PhaC<sub>Pa</sub> and PhaC<sub>Pa</sub> antigen fusions) while this was not observed in the PBS or soluble antigen His<sub>10</sub>-Ag group (**Fig. 2.8b**). Reactivity of sera antibodies to whole organisms of different *P. aeruginosa* strains was tested (**Fig. 2.8c**). Results suggest strong reactivity of sera antibodies in the bead vaccinated groups to both nonmucoid and mucoid strains of *P. aeruginosa*. The PhaC1<sub>Pa</sub> vaccinated group showed the strongest overall responses compared to Ag-PhaC1<sub>Pa</sub> or PhaC1<sub>Pa</sub>-Ag bead vaccinated groups. Minimal responses were seen with PBS and recombinant protein vaccinated groups.

An opsonophagocytic killing assay testing serum antibodies from the vaccinated mice was also conducted (**Fig. 2.8d**). Serum antibodies from both PhaC1<sub>Pa</sub> and PhaC1<sub>Pa</sub>-Ag biobead vaccinated groups showed significantly higher killing against strain PA01 than serum antibodies from the PBS and soluble antigen His<sub>10</sub>-Ag groups ( $p < 0.05$ ).

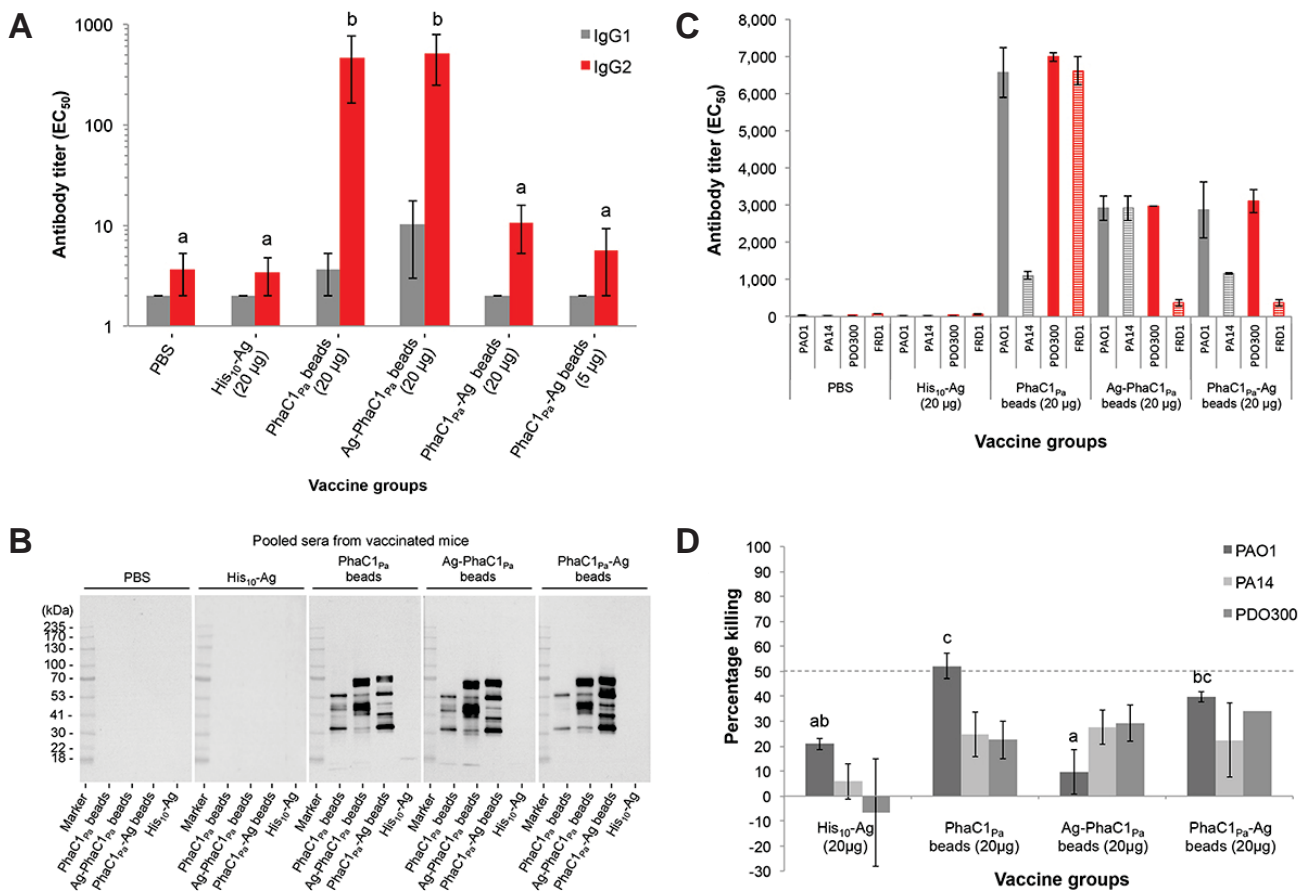


**Figure 2.8. Antibody response to vaccination with vaccine PHA<sub>MCL</sub> beads.** (a) Antigen-specific IgG1 or IgG2c isotype antibody responses measured by ELISA using a pool of OprI, OprF, and AlgE antigen specific peptides from sera. Results are expressed in reciprocal antibody titers, representing the dilution required to obtain half of the maximal amount of the OD signal (EC<sub>50</sub>). (b) To identify antigenic proteins on PHA<sub>MCL</sub> beads, sera obtained was pooled in to their respective groups and used as a primary antibody for detection of epitopes on PHA<sub>MCL</sub> beads separated by SDS-PAGE. (c) Reactivity of pooled immune sera to different *P. aeruginosa* strains using a whole-cell ELISA was used. Nonmucoid (grey bars) and mucoid (red bars) strains of *P. aeruginosa* were tested. (d) Opsonic killing of *P. aeruginosa* nonmucoid strains by serum from mice immunized with vaccine PHA<sub>MCL</sub> beads. Bar represents the mean percent killing of three replicates for PAO1 and PA14 or duplicates for PDO300 relative to sera of the PBS vaccinated control group, and error bars represents the s.e.m. Data of graph for IgG are reported as means ± s.e.m (6 mice per group). Statistical significance ( $p < 0.05$ ) of IgG2c is indicated by 'letter based' representation of pairwise comparisons between groups using Tukey's post-hoc test. IgG1 were not statistically significant. Data of graph for whole-cell ELISA represent means of two replicates of pooled sera ± the s.e.m of the replicates. There are insufficient replicates to undertake a statistical analysis. Statistical significance ( $p < 0.05$ ) for opsonic killing assay is indicated by 'letter based' representation of pairwise comparisons between groups using Tukey's post-hoc test. PA14 were not statistically significant. There are insufficient replicates to undertake a statistical analysis for PDO300.

Cytokine responses of splenocytes to soluble recombinant protein His<sub>10</sub>-Ag (**Fig. 2.10a,b**) showed that Ag-PhaC1<sub>Pa</sub> beads induced production of significantly more IFN- $\gamma$ , IL-10, IL-17a, and IL-6 than found in the PBS group, while the PhaC1<sub>Pa</sub>-Ag beads induced significantly more IFN- $\gamma$  and IL-2 (**Fig. 2.10a,b**). Vaccination with 20  $\mu$ g of PhaC1<sub>Pa</sub> on beads induced significantly more IFN- $\gamma$ , IL-4, and IL-6 compared to the PBS group. While the His<sub>10</sub>-Ag group produced significantly more IFN- $\gamma$ , IL-10, IL-17a, IL-2, and IL-4 compared to the PBS group (**Fig. 2.10a,b**). Minimal cytokine responses were observed when splenocytes were re-stimulated with AlgE or OprI or OprF peptides or a combined pool of all peptides (data not shown). Antigens presented on PHA<sub>MCL</sub> beads did not induce cytokine responses significantly greater than the His<sub>10</sub>-Ag (**Fig. 2.10a**). Only the group vaccinated with 20  $\mu$ g of OprI/F-AlgE antigen on Ag-PhaC1<sub>Pa</sub> beads produced significantly more IL-6 than the His<sub>10</sub>-Ag group. Notably, a positive trend was observed for cytokines IFN- $\gamma$  and TNF- $\alpha$  for this Ag-PhaC1<sub>Pa</sub> beads group and TNF- $\alpha$  for the 20  $\mu$ g PhaC1<sub>Pa</sub> beads group when compared with His<sub>10</sub>-Ag group.

Attachment of antigenic proteins to the surface of the beads mediated an enhanced immune response. Significantly more IFN- $\gamma$  was produced by mice vaccinated with 20  $\mu$ g OprI/F-AlgE antigen on Ag-PhaC1<sub>Pa</sub> beads compared with the 20  $\mu$ g PhaC1<sub>Pa</sub> beads group (**Fig. 2.10a,b**). Although not significant, a positive trend was observed for IFN- $\gamma$  with the group receiving 20  $\mu$ g OprI/F-AlgE antigen on PhaC1<sub>Pa</sub>-Ag beads compared to the PhaC1<sub>Pa</sub> beads group. Comparatively, the N terminal fusion of OprI/F-AlgE antigen to PhaC1<sub>Pa</sub> on Ag-PhaC1<sub>Pa</sub> beads induced a greater cytokine response with significantly more IFN- $\gamma$ , IL-10, IL-6 and TNF- $\alpha$  than its C terminal fusion counterpart, the PhaC1<sub>Pa</sub>-Ag beads. No significant dose response difference was observed in mice receiving either 20  $\mu$ g or 5  $\mu$ g of OprI/F-AlgE antigen immobilized on PhaC1<sub>Pa</sub>-Ag beads (**Fig. 2.10a**). The addition of adjuvant, alum, generally enhanced the immune response (**Fig. 2.9b**).

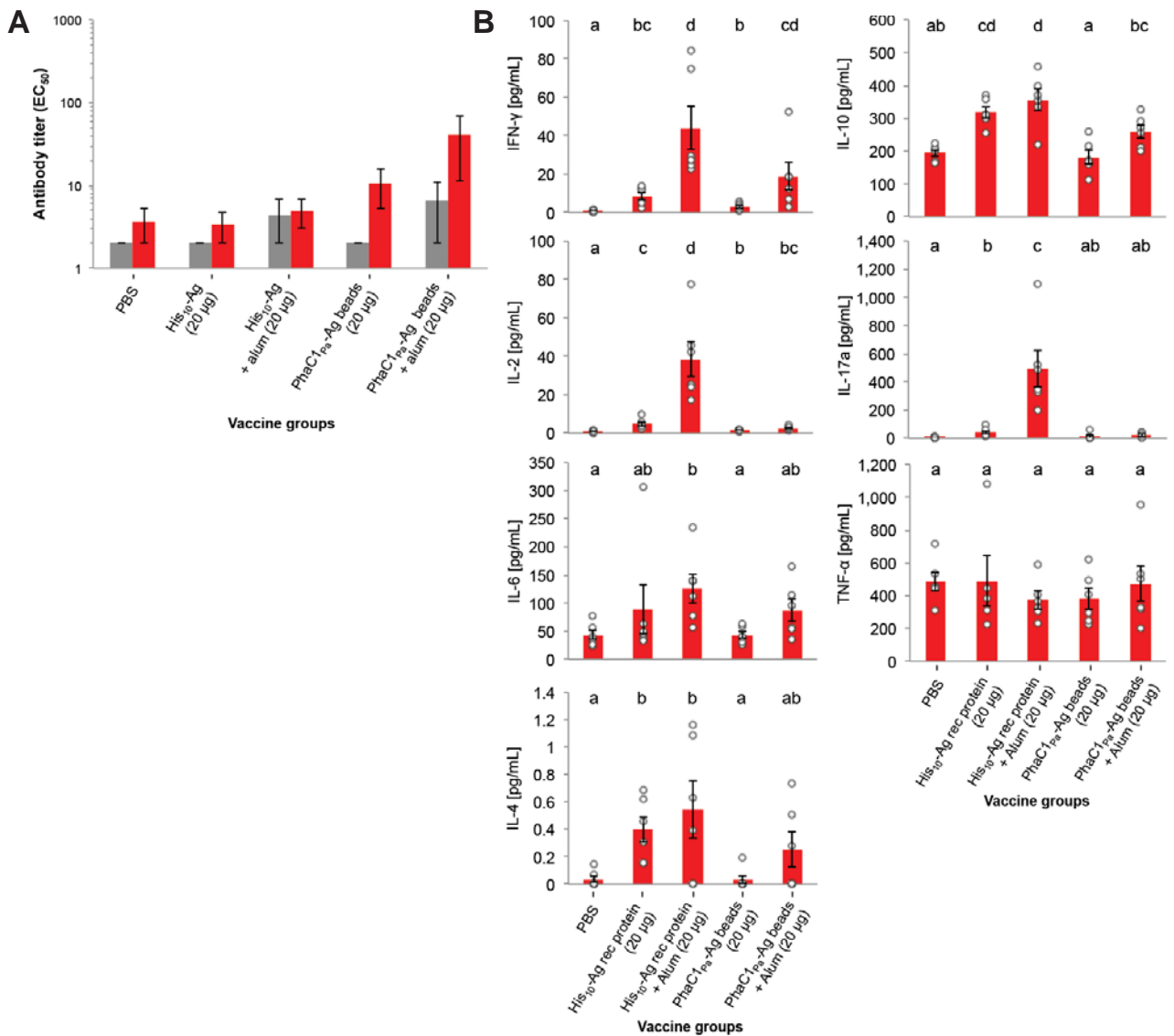


**Figure 2.9. Antigenic response to vaccination with alum formulated vaccine PHA<sub>MCL</sub> beads.** Analysis of antigen-specific antibody and cytokine responses in mice, a comparison of alum and their respective non-alum vaccinated groups. **(a)** Antigen-specific IgG1 or IgG2c isotype antibody responses measured by ELISA using a pool of OprI, OprF, and AlgE antigen specific peptides from sera. Data are reported as means  $\pm$  s.e.m (6 mice per group). No significance was found. **(b)** Release of cytokines from splenocyte cultures restimulated with soluble recombinant His<sub>10</sub>-Ag was measured by cytometric bead array. Results are calculated by subtracting cytokine values of the media-stimulated samples from the cytokine values of the recombinant protein stimulated samples. Data of graphs are reported as means  $\pm$  s.e.m and each individual mouse are reported as a dot (6 mice per group). Statistical significance ( $p < 0.05$ ) is indicated by 'letter-based' representation of pairwise comparisons between groups.

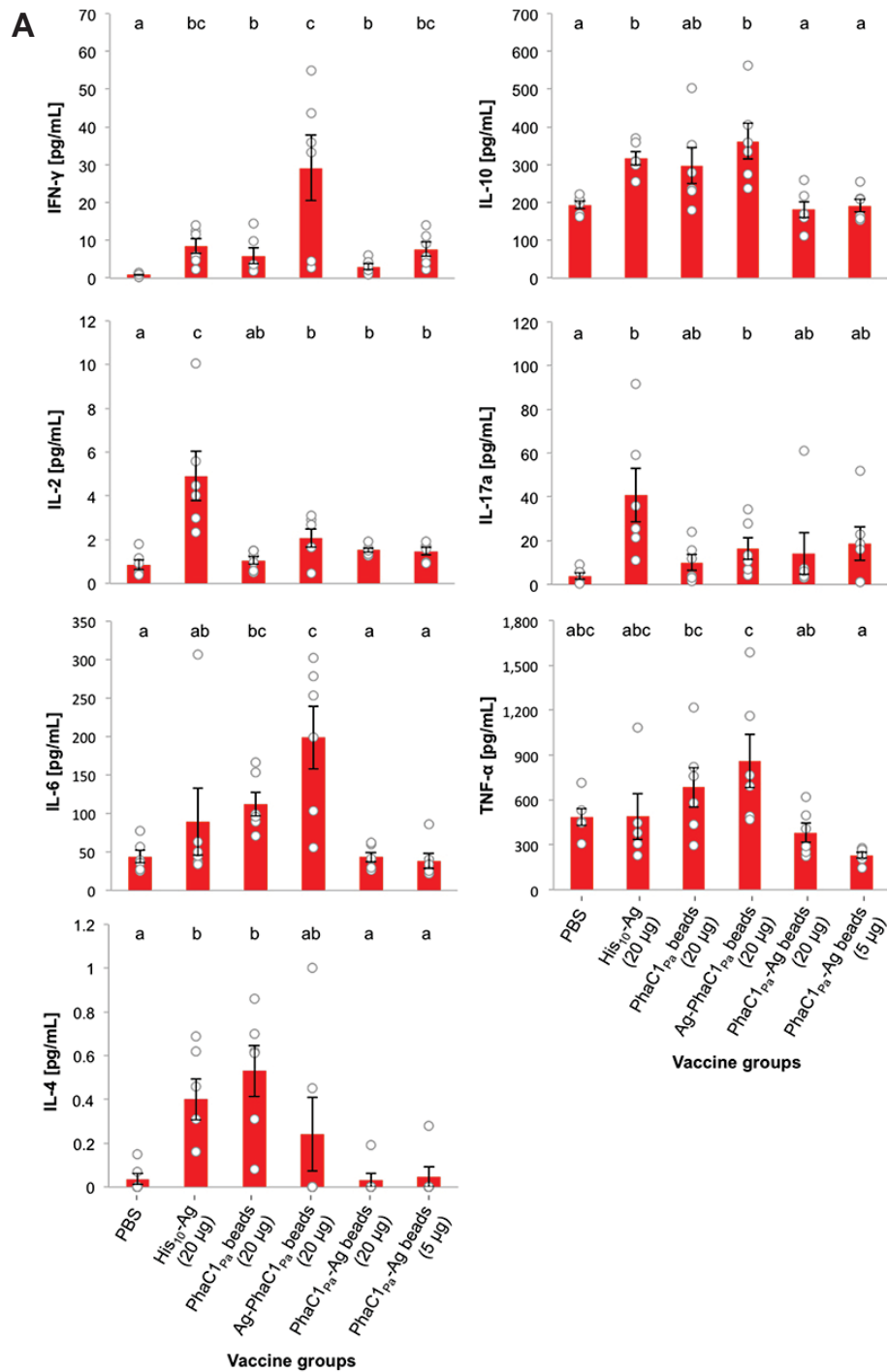


**Figure 2.10. Cytokine response to vaccination with vaccine PHA<sub>MCL</sub> beads.** (a) Release of cytokines from splenocyte cultures restimulated with soluble recombinant His<sub>10</sub>-Ag was measured by cytometric bead array. Results are calculated by subtracting cytokine values of the

media-stimulated samples from the cytokine values of the recombinant protein stimulated samples. **(b)** Summary of the cytokine response as a comparison to PBS negative control group. Data of graphs are reported as means  $\pm$  s.e.m and each individual mouse are reported as a dot (n = 6 per group). Statistical significance ( $p < 0.05$ ) is indicated by 'letter-based' representation of pairwise comparisons between groups.

## 2.3 Discussion

Many bacteria, including animal and human pathogens, are capable of producing spherical discrete PHA inclusions for carbon and energy storage [37]. Here we utilized the intrinsic PHA<sub>MCL</sub> synthesis capacity of the disease causing opportunistic pathogen *P. aeruginosa* towards production of antigen-displaying PHA<sub>MCL</sub> beads. The aim was to display selected repeated epitopes of vaccine candidate antigens of *P. aeruginosa* at high copy number on the surface of the PHA storage granules [5, 8, 14]. Design and production of PHA beads in the respective pathogen potentially avoids the need for extensive downstream processing in order to remove host cell derived impurities such as HCPs. Impurities originating from the pathogen could be beneficial, by providing additional epitopes, i.e. a large antigen repertoire, and acting as an adjuvant towards enhanced protective immunity to infections caused by *P. aeruginosa*.

*P. aeruginosa* strain PAO1 was genetically engineered (**Fig. 2.2a,b**) by deleting key genes required for the synthesis of PHA, alginate, and pel polysaccharide to enable enhanced recombinant production of its own PHA<sub>MCL</sub> beads additionally coated with surface epitopes of outer membrane vaccine candidates AlgE, OprF, and OprI as an OprI/F-AlgE fusion antigen [28, 30, 38]. This was achieved by protein engineering of the *P. aeruginosa* PhaC1<sub>Pa</sub> that catalyzes PHA<sub>MCL</sub> synthesis mediating PHA<sub>MCL</sub> bead assembly while remaining covalently attached to the surface of PHA<sub>MCL</sub> inclusions [39]. Various studies have shown great promise for epitopes of OprF and OprI to be used in vaccine formulations [21, 22, 34, 40, 41].

The successful recognition and uptake of the vaccine PHA beads by professional antigen presenting cells (APCs) may differ due to the mode of display of the OprI/F-AlgE antigen being presented to immune cells. The tolerance of C terminal fusion was assessed by translational fusion with GFP (**Fig. 2.3a-d**), while translational fusion to the N terminus of the PhaC<sub>Pa</sub> had been previously shown [42]. Hence the OprI/F-AlgE vaccine candidate antigen was fused to either the N or C terminus of PhaC1<sub>Pa</sub> (**Fig. 2.5a**). Translational fusion of the OprI/F-AlgE antigen to the different termini of PhaC1<sub>Pa</sub> impacted on PHA<sub>MCL</sub> bead size suggesting an impact of the fusion partner and fusion site on PHA bead assembly (**Fig. 2.5b**). Data also showed fusion to the N terminus or C terminus of PhaC1<sub>Pa</sub> did not influence PHA composition e.g. substrate

specificity of PhaC1<sub>Pa</sub>, but reduced PHA<sub>MCL</sub> accumulation compared to the wild-type (PhaC1<sub>Pa</sub>) implying an impact of the fusion on *in vivo* activity (**Fig. 2.5c**). This impact had been found for PhaC<sub>Re</sub> and was dependent on the fusion partner [10, 12, 13].

Significantly more fusion protein was produced if the OprI/F-AlgE antigen was fused to the C terminus (PhaC1<sub>Pa</sub>-Ag) compared to N terminal fusion (Ag-PhaC1<sub>Pa</sub>) (**Fig. 2.6a**). However, the amount of fusion protein did not correlate with the amount of PHA accumulated e.g. PhaC1<sub>Pa</sub>-Ag did not mediate greater levels of PHA<sub>MCL</sub> accumulation (**Fig. 2.5c**).

Successful control of disease caused by many extracellular pathogens typically requires an antibody response characterized by the production of IgG1 isotype and production of cytokines IL-4 and IL-5. However, this might not be the case for chronically *P. aeruginosa* infected CF patients who predominantly show a bias towards a Th2 type immune response when compared to noninfected CF patients or healthy controls [24, 43]. Elevated levels of antibodies in CF patients tend to be associated with a poor prognosis. There is increasing evidence that a Th1 type immune response characterized by increased cytokine IFN- $\gamma$  leads to better pulmonary outcomes and may be the preferred response for the successful control of acute and chronically infected CF patients [24, 26, 43].

Here we showed that vaccination of mice with *P. aeruginosa* derived PHA<sub>MCL</sub> beads displaying the OprI/F-AlgE antigen fused to the N terminus of PhaC1<sub>Pa</sub> (Ag-PhaC1<sub>Pa</sub>) without adjuvants induced a robust T cell immune response with a Th1 pattern. The immune response was characterized by enhanced production of IgG2c isotype titers and antigen-specific cytokine IFN- $\gamma$  in association with low levels of IL-4 and IgG1 isotype that are both elevated in the Th2 type response. This suggested induction of a Th1 type response through enhanced CD4<sup>+</sup> type 1 [6] T cell and Toll-like receptor (TLR) activation [44].

Vaccination with Ag-PhaC1<sub>Pa</sub> beads induced significant levels of antigen-specific serum antibodies (**Fig. 2.8a**). These antibodies may have resulted from B cell class-switching to IgG2c isotype associated with the activation of Th1 antigen-specific T cells [45],

which conceivably playing a critical role in clearance of acute infection with *P. aeruginosa* [46].

Vaccination with plain PhaC1<sub>Pa</sub> beads without OprI/F-AlgE antigen also generated an antigen-specific antibody response to epitopes of the OprI/F-AlgE antigen at levels similar to the Ag-PhaC1<sub>Pa</sub> bead group (**Fig. 2.8a**). This indicated an immune response to the copurified HCPs associated with plain PhaC1<sub>Pa</sub> beads. For example, the full-length OMP OprF was identified in band III of the separated copurified proteins (**Supplementary Table 2**). OprI and OprF are present in high copy numbers in the OM of *P. aeruginosa* [47] and therefore, more likely to be found as part of the HCP impurities compared to the low copy number AlgE [29]. The detection of antibodies against a wide range of copurifying HCPs supported the concept of the immunogenic delivery of a large antigen repertoire using isolated PHA beads produced by the pathogen (**Fig. 2.8b**). Moreover, these serum antibodies in the bead vaccinated groups showed strong reactivity across different *P. aeruginosa* strains, which include nonmucoid and mucoid forms (**Fig. 2.8c**). Opsonic killing activity of serum antibodies as an indication of protective immunity was also tested (**Fig. 2.8d**). Interestingly, only sera antibodies from PhaC1<sub>Pa</sub> vaccinated group mediated biologically significant opsonic killing ( $\geq 50\%$  killing) against the nonmucoid PAO1 strain, possibly correlating with the strong reactivity of the sera antibodies to PAO1 (**Fig. 2.8c**). The relatively low killing shown for all vaccine groups may have been due to high MOI of 100:1 in the assay and greater antibody-mediated enhancement of killing may have been seen at a lower MOI. However, sera antibodies from all bead vaccinated groups could mediate around 20% - 30% killing to nonmucoid and mucoid forms, with lower killing typically for His<sub>10</sub>-Ag.

Alum added to PhaC1<sub>Pa</sub>-Ag beads induced an increase in levels of antigen-specific antibodies (**Fig. 2.9a**) and a significant increase in some cytokines (**Fig. 2.9b**) suggesting further scope to enhance immunogenicity of PHA<sub>MCL</sub> beads.

Attachment of OprI/F-AlgE antigen to the PHA<sub>MCL</sub> beads enhanced the immune response with a bias towards a Th1 response when compared to vaccination with only antigen. Soluble peptides/proteins require addition of a suitable adjuvant and/or delivery system to generate an optimal immune response [48]. Our results showed that

vaccination with His<sub>10</sub>-Ag formulated with alum adjuvant induced mainly a humoral Th2 type response (**Fig. 2.9a,b**). Conversely, vaccination with OprI/F-AlgE antigen fused to the C terminus of PhaC1<sub>Pa</sub> and displayed on PHA<sub>MCL</sub> beads induced a response similar to plain PHA<sub>MCL</sub> beads (PhaC1<sub>Pa</sub>), but a weaker response than observed when vaccinating with Ag-PhaC1<sub>Pa</sub> beads (**Fig. 2.8a** and **Fig. 2.10a**). This suggests the OprI/F-AlgE antigen fused to the C terminus of PhaC1<sub>Pa</sub> may not be fully displayed on the surface of the PHA<sub>MCL</sub> beads. Due to the inherent orientation of the PHA synthase on the bead surface, the hydrophobic C terminus of PhaC1<sub>Pa</sub> is proposed to be attached to the hydrophobic PHA core and hence, required a designed linker to enable surface exposure of the fusion partner [10]. The length of the linker may have not been adequate for the full display of the OprI/F-AlgE antigen on the PHA<sub>MCL</sub> beads surface compared to the N terminal fusion to the PhaC1<sub>Pa</sub>, possibly resulting in reduced OprI/F-AlgE antigen processing by APCs and therefore, leading to a poor antigen-specific immune response [49].

The reduced immune response seen with PhaC1<sub>Pa</sub>-Ag beads compared to Ag-PhaC1<sub>Pa</sub> beads could be due to the smaller bead size, resulting in suboptimal antigen uptake compared to the larger Ag-PhaC1<sub>Pa</sub> beads. Bead size is a major contributing factor influencing particulate antigen uptake by APCs [16]. The mechanism of antigen uptake can influence the type of immune response, inducing humoral and/or cell-mediated immunity. However, the actual size for the most efficient uptake of particulates by APCs is still controversial as efficiency can be affected by a range of other factors including shape, surface charge, hydrophobicity/hydrophilicity and mode of administration [16]. Therefore, it remains unclear if size was a contributing factor for the reduced response to the PhaC1<sub>Pa</sub>-Ag beads. PHA<sub>MCL</sub> beads produced in this study were all within the generally accepted effective range (< 0.5 µm) for uptake by professional APCs and induced an antigen-specific immune response [50].

Vaccination with Ag-PhaC1<sub>Pa</sub> beads resulted in significantly increased levels of cytokines IFN-γ, IL-6 and IL-10 with low but significant levels of IL-17a and IL-2 compared to the PBS group suggesting a Th1 and Th17 type immune response (**Fig. 2.10a,b**). IL-17a plays a critical role in maintaining control of host defense against extracellular pathogens [51]. Significant level of IL-6 was induced with vaccination using Ag-PhaC1<sub>Pa</sub> beads, but this did not correlate with high levels of IL-17a. IL-6

together with cytokines IL-1 $\beta$  or TNF- $\alpha$  during acute inflammation can also result in the recruitment of neutrophils [52]. TNF- $\alpha$  levels were elevated but not significantly in mice vaccinated with Ag-PhaC1<sub>Pa</sub> beads. IL-6 and IL-10 may limit damage in the lungs of CF patients caused by hyper inflammation associated with exacerbated recruitment of neutrophils that lead to pulmonary decline.

In conclusion, this study showed that cellular inclusions of bacterial pathogens are immunogenic capable of inducing cell-mediated immune responses. Hence, it is proposed that vaccine research should consider nano-/micro-sized cellular inclusions as antigen reservoir and delivery system towards the development of safe and efficient particulate vaccines. We proofed the concept of hijacking the capacity of the opportunistic pathogen *P. aeruginosa* to naturally produce PHA<sub>MCL</sub> inclusions for the design and production of PHA<sub>MCL</sub> beads displaying selected antigens of the same host as particulate vaccine candidates. PHA<sub>MCL</sub> beads with associated HCPs represented as a large antigenic repertoire. PHA<sub>MCL</sub> beads displaying vaccine candidates AlgE, OprF and OprI without adjuvant induced a dominant Th1 type response required for the control of *P. aeruginosa* infection [26, 43]. Since, a range of pathogens such as e.g. *Mycobacterium tuberculosis*, *Legionella pneumophila*, and *Bacillus anthracis* (**Supplementary Fig. 2.2** and **Supplementary Tables 2.4** and **2.5**), are able to inherently produce PHA inclusions, the demonstrated concept of producing particulate subunit vaccines within the disease causing pathogen represents a novel approach to subunit vaccine development applicable to a range of infectious diseases.

## 2.4 Methods

### Bacterial strains and growth conditions

All bacterial strains and plasmids used are listed in **Supplementary Table 2.6**. *E. coli* strains were grown in Luria broth (LB) medium (Difco, Detroit, MI) at 37°C unless stated. LB medium was supplemented with 1% NaCl for growth of osmosensitive *E. coli* strain ClearColi (Lucigen, Middleton, WI). When required, antibiotics were used at the following concentrations: ampicillin, 100 µg/mL; and gentamycin 10 µg/mL.

*P. aeruginosa* strains were grown in LB medium (Difco, Detroit, MI) or mineral salt medium (MSM) [53] at 37°C and when required, antibiotics were added at the following concentrations: carbenicillin, 300 µg/mL; and gentamycin, 100 to 300 µg/mL.

### Isolation and manipulation of DNA

General cloning procedures were performed as described previously [54]. Electroporation was used for the transfer of plasmid into *P. aeruginosa* strains as described elsewhere [55]. All plasmid isolations were performed using High Pure Plasmid Isolation Kit (Roche, BASEL, Switzerland). DNA primers were purchased from Integrated DNA Technologies (Coralville, IA). *Taq* and platinum *pfx* polymerases were purchased from Invitrogen (Carlsbad, CA). Synthesized peptides and antibodies were purchased from GenScript (Piscataway, NJ). All newly amplified DNA fragments and final plasmid constructs were confirmed by DNA sequencing.

### Construction of alginate- pel- deletion mutant in a PHA negative background

Generation of the isogenic triple mutant (PAO1  $\Delta C\Delta 8\Delta F$ ) incapable of PHA/alginate/Pel production is outlined in **Fig. 2.2**.

The alginate biosynthesis gene *alg8* was disrupted by using the previously described gene-knockout plasmid pEX100T:: $\Delta alg8$   $\Omega$  Gm [56]. The plasmid was transferred via electroporation into PHA<sub>MCL</sub> negative *P. aeruginosa* strain PAO1  $\Delta phaC1ZC2$  [36] and transformants having undergone the first homologous recombination event were selected on LB medium containing 100 µg/mL of gentamicin. Subsequently, a second homologous recombination event was selected for by plating single cell colonies on LB medium containing 300 µg/mL of gentamicin and 5% (w/v) sucrose. Insertion of FRT-Gm-FRT cassette was confirmed by PCR with primers Alg8\_XUP and Alg8\_XDN.

Gentamicin cassette was removed by the introduction of Flp recombinase-encoding plasmid pFLP2 [57] by electroporation and plated on to LB medium containing carbenicillin (300 µg/mL). Resistant colonies were then screened on LB medium containing 5% (w/v) sucrose. CFU were subsequently screened for gentamicin (300 µg/mL) and carbenicillin (300 µg/mL) sensitivity. PCR with primers Alg8\_XUP and Alg8\_XDN were used to confirm loss of gentamicin cassette and therefore, *P. aeruginosa* PAO1  $\Delta phaC1ZC2 \Delta alg8$  double mutant was generated.

Disruption of *pelF* in newly generated strain PAO1  $\Delta phaC1ZC2 \Delta alg8$  was achieved similarly as described above with the introduction of previously described gene-knockout plasmid pEX100T:: $\Delta pelF \Omega$  Gm [58]. PCR with primers PelF\_XUP and PelF\_XDN was used to confirm the insertion and subsequent removal of the gentamicin cassette. Consequently, *P. aeruginosa* PAO1  $\Delta phaC1ZC2 \Delta alg8 \Delta pelF$  triple mutant was generated, and from now will be referred to as PAO1  $\Delta C\Delta 8\Delta F$ . PCR products amplified with primers flanking  $\Delta alg8$  (Alg8\_XUP and Alg8\_XDN) and  $\Delta pelF$  (PelF\_XUP and PelF\_XDN) were subsequently used to confirm deletion by DNA sequencing (**Supplementary Fig. 2.1**).

### **Analysis of the tolerance of translational fusions to the C terminus of the class II PHA synthase.**

A DNA fragment comprising the Shine-Dalgarno (SD) sequence and gene encoding the class II PHA synthase (*phaC1<sub>Pa</sub>*) was excised from pBHR71 with XbaI and BamHI [59]. The fragment was subsequently ligated into the corresponding sites in pBBR1JO-5. The Resultant plasmid pBBR1JO-5\_C1 constitutively expressed *phaC1<sub>Pa</sub>* in *P. aeruginosa*.

To assess the ability of the class II PHA synthase to tolerate C terminal fusions, a flexible linker extension fusion with the GFP reporter (Linker-SG-linker-*gfp*) used previously to assess C terminal fusion to class I PHA synthase from *Ralstonia eutropha* (PhaC<sub>Re</sub>) [10] was adapted for use in this study.

The stop codon of *phaC1<sub>Pa</sub>* was removed by PCR amplification using primers F\_phaC1 and R\_phaC1\_(-)stop\_BamHI with pBHR71 as template. The amplified PCR fragment

encoding SD sequence and *phaC1<sub>Pa</sub>* flanked by sites XbaI and BamHI were ligated into vector pGEM-T easy. The resultant plasmid pGEM-T\_C1(-) was hydrolyzed with XbaI and BamHI. The excised DNA fragment was ligated into the corresponding sites in vector pBBR1JO-5 giving intermediate plasmid pBBR1JO-5\_C1(-). To generate the corresponding insert, primers F\_BgIII\_LSGLgfp and R\_LSGLgfp\_BamHI were used to amplify the DNA sequence encoding the Linker-SG-Linker-*gfp* (LSGL*gfp*) region of pET-14b PhaC-linker-SG-Linker-*gfp*. The resultant fragment flanked with newly introduced BgIII and BamHI sites was ligated into vector pGEM-T easy. Following confirmation, LSGL*gfp* fragment was excised from pGEM-T\_LSGL*gfp* with introduced sites and subsequently ligated into the BamHI site in plasmid pBBR1JO-5\_C1(-) downstream and in frame of *phaC1<sub>Pa</sub>*, resulting in plasmid pBBR1JO-5\_C1*gfp*. Ligation resulted in the destruction of the BgIII and BamHI site between *phaC1<sub>Pa</sub>* and linker. Orientation was confirmed by directional PCR.

### **Construction of plasmids for the production of OprI/F-AlgE antigen-displaying PHA inclusions**

Antigenic epitopes from the outer membrane protein F (OprF<sub>329 – 342</sub>), mature outer membrane lipoprotein I (OprI<sub>21 – 83</sub>), and outer membrane porin AlgE (AlgE<sub>233 – 241–287 – 303</sub>) were combined in a single chain fusion antigen (OprI/F-AlgE) and covalently displayed on the surface of the PHA<sub>MCL</sub> inclusions. Epitopes of OprF and OprI (**Fig. 2.4a**) were selected as previously described [22, 34, 38, 41, 60, 61]. Analysis of chain B in AlgE RCSB Protein Data Bank (3RBH) entry identified two epitopes, HLRRPGEEV (L5) and NLTTTTRIATGKQ (L6) by B-cell epitope prediction method EPCES [62] (**Fig. 2.4b**). When mapped to an AlgE reference sequence (Refseq: NP\_252234.1), L5 corresponded to amino acids 233 – 241, however the amino acid sequence of L6 identified from entry 3RBH was incomplete. The complete amino acid sequence of L6 from the AlgE reference sequence was used, which corresponded to amino acids 287 – 303 (NLTTTTVDDRRIATGKQ). The OprI/F-AlgE antigen was designed with one copy of AlgE (L5 and L6) and OprI epitopes while including three repeats of the OprF epitope (**Fig. 2.5a**). Epitopes in the fusion antigen fragment were arranged as follows: L5-L6-OprF(x3)-OprI for N terminal PhaC1<sub>Pa</sub> fusion and OprI-OprF(x3)-L6-L5 for C terminal PhaC1<sub>Pa</sub> fusion. All epitope encoding DNA fragments were synthesized with codon usage bias for *P. aeruginosa* by GenScript (Piscataway, NJ).

An arabinose inducible system (pHERD20T) [63] was chosen for the expression of genes required for the production of antigen-displaying PHA<sub>MCL</sub> inclusions in *P. aeruginosa*. Modification of pHERD20T vector was required to remove an alternative start site encoded by *LacZ*. The vector was linearized with NcoI and EcoRI. Resulting cohesive ends of the vector fragment were blunted using T4 DNA polymerase to allow religation, resulting in vector pHERD20T-2.

Generation of the plasmid encoding the N terminal fusion of OprI/F-AlgE antigen to PhaC1<sub>Pa</sub> was achieved in two steps. Firstly, the DNA fragment encoding *phaC1<sub>Pa</sub>* was excised from plasmid pBBR1JO5\_C1 by hydrolysis with XbaI and HindIII and subsequently ligated into the corresponding sites in vector pHERD20T-2. Secondly, resultant plasmid pHERD20T-2\_C1 was linearized by hydrolysis with XbaI and NdeI and OprI/F-AlgE antigen fragment excised from pUC57\_Ag(N) was successively ligated upstream of *phaC1<sub>Pa</sub>* with corresponding sites, generating the final plasmid pHERD20T-2\_AgC1 which encodes for fusion protein Ag-PhaC1<sub>Pa</sub>.

Generation of plasmid encoding C terminal fusion to PhaC1<sub>Pa</sub> was achieved in a similar fashion to the above. OprI/F-AlgE antigen fragment from pUC57\_Ag(C) was excised with SmaI and EcoRI and linear fragment ligated into corresponding sites of plasmid pBBR1JO-5\_C1*gfp*, replacing GFP reporter. Newly generated plasmid pBBR1JO-5\_C1Ag was hydrolyzed with XbaI and HindIII and resultant linear fragment encoding *phaC1Ag* was ligated into corresponding sites of vector pHERD20T-2, generating final plasmid pHERD20T-2\_C1Ag that encodes for fusion protein PhaC1<sub>Pa</sub>-Ag.

### **Construction of plasmid pET16b-HisAg for soluble recombinant antigen production**

Plasmid pUC57\_Ag containing the DNA fragment encoding OprI/F-AlgE antigen fragment with the following arrangement of epitopes OprI-OprF(x3)-L6-L5 synthesized by GenScript with codon usage bias for *E. coli* was hydrolyzed with NdeI and BamHI. The resulting linear OprI/F-AlgE antigen encoding DNA fragment was ligated into the corresponding sites of vector pET16b located downstream and in frame with His<sub>10</sub>-tag resulting in plasmid pET16b-HisAg which encodes for fusion protein Met-Gly-His<sub>10</sub>-OprI<sub>21-83</sub>-(OprF<sub>329-342</sub>)<sub>x3</sub>-AlgE<sub>233-241-287-303</sub> (His<sub>10</sub>-Ag) (**Fig. 2.5a**).

### **Production of PHA inclusions and isolation (beads)**

To promote PHA inclusion formation, *P. aeruginosa* strain PAO1  $\Delta C\Delta 8\Delta F$  was grown under nitrogen limitation utilizing sodium gluconate as a carbon source [64]. MSM was modified with the following: 0.05% (w/v)  $NH_4Cl$ ; and supplemented with 1% (w/v) sodium gluconate [42]. Antibiotics were added at the following concentrations: carbenicillin, 300  $\mu g/mL$  for strains harboring pHERD20T-2 derivatives; and gentamycin, 300  $\mu g/mL$  for strains harboring pBBR1MCS-5 derivatives.

A preculture was inoculated from frozen stock and incubated at 37°C for 10 – 12 h with agitation. The preculture was then used to inoculate MSM using 5% (v/v) inoculum and grown for further 10 – 12 h. Main cultures were inoculated with overnight culture giving a starting with  $OD_{600}$  of 0.5 and were cultivated at 37°C with agitation. Induction of main cultures with a final concentration of 0.5% (w/v) arabinose was required when  $OD_{600}$  reached 0.4 for PAO1  $\Delta C\Delta 8\Delta F$  strains harboring pHERD20T-2 derivatives. PAO1  $\Delta C\Delta 8\Delta F$  strains harboring pBBR1MCS-5 derivatives were constitutively expressed in *P. aeruginosa* and did not require induction. All cultures were cultivated for a further 48 h.

Cells were harvested at 4°C by centrifugation for 10 min at 9,000 x g. The pellet was washed with 100 mL of 50 mM Tris-buffer (pH 8) and then again with 50 mL for a total of two washes. Washed cells were then centrifuged at 9,500 x g for 40 min at 4°C. The pellet was suspended as a 10% slurry (w/v) in lysis buffer (50 mM Tris-buffer [pH 8], 50 mM EDTA, 62.5  $\mu g/mL$  lysozyme) and incubated at 37°C for 35 min with agitation to digest the cell walls. Cells were then sonicated for 30 sec with a power output of 15 W to shear DNA prior to mechanical lysis by passing the cell suspension through a French press four times at 6,000 Psi. The crude cell lysate was then sonicated for 30 sec with a power output of 15 W, diluted five times in TE buffer (50 mM Tris-buffer [pH 8], 50 mM EDTA) and collected by centrifugation at 9,500 x g for 1 h and 4°C. The pellet containing crude PHA<sub>MCL</sub> beads and cell debris was washed with 50 mM Tris-buffer (pH 8) and pelleted at 9,500 x g for 30 min and 4°C and then re-suspended in 20 mL of 50 mM Tris-buffer (pH 8) and treated with 0.05 mg/mL DNase + 5 mM  $MgCl_2$  for 20 min at 4°C with mixing. Following DNase treatment, the crude PHA<sub>MCL</sub> bead suspension was sonicated for 30 sec with a power output of 9 W and subsequently washed two times with 50 mM Tris-buffer (pH 8), centrifuging for 30 min at 9,500 x g

and 4°C. The PHA<sub>MCL</sub> bead material was then suspended as 20% slurry (w/v) in 50 mM Tris-buffer (pH 8) with 25% glycerol as a cryoprotectant for storage at -80°C.

### **Production and isolation of recombinant protein**

*E. coli* strain ClearColi (Lucigen, Middleton, WI) was transformed with pET16b-HisAg and grown in LB miller medium containing 100 µg/mL ampicillin. The main culture was inoculated with overnight culture to give a starting OD<sub>600</sub> of 0.1 and cultivated at 37°C. Induction of main culture was achieved with 1 mM IPTG when cultures had reached OD<sub>600</sub> of 0.3 and further cultivated at a reduced temperature of 30°C for 15 h with agitation. Cells were harvested at 4°C by centrifugation for 10 min at 9,000 x g and washed once with 1x PBS (pH 7.4). The pellet was then suspended as 20% slurry (w/v) in binding buffer (50 mM Tris-buffer [pH 7.7], 300 mM NaCl, 10 mM Imidazole). To achieve lysis, cell slurry was sonicated for 10 sec 'on' and 10 sec 'off' for a total of 10 min 'on' at a power setting of 21 W. Crude cell lysate was centrifuged at 9,500 x g for 5 min and supernatant fraction containing soluble protein was filtered through a 0.45 µM pore size filter. Zymo (Irvine, CA) His-Spin Protein Miniprep was used for affinity purification of recombinant His-tagged proteins with the following modifications to the manufacturer's instructions: 400 µL of filtered cell lysate was mixed with 300 µL of dried His-Affinity Gel per P1 column, and with mixing on a tilting platform left to bind for 5 min. The column was centrifuged at 17,000 x g and sample binding step was repeated several times. Each column was washed twice with 250 µL of wash buffer (50 mM Tris-buffer [pH 7.7], 300 mM NaCl, 50 mM Imidazole) and subsequently eluted with 150 µL of elution buffer (50 mM Tris-buffer [pH 7.7], 300 mM NaCl, 500 mM Imidazole). The eluted protein was dialyzed against 1x PBS (pH 7.4) at 4°C overnight using dialysis tubing with 10K MWCO. Insoluble material was removed by centrifugation at 17,000 x g for 10 min. Recombinant protein His<sub>10</sub>-Ag was sterilized by filtration through a 0.22 µM pore size syringe filter.

### **Sterilization of PHA beads**

PHA<sub>MCL</sub> beads were thawed and washed two times using 1x PBS (pH 7.4), centrifuging for 1 h at 14,500 x g and 4°C. PHA<sub>MCL</sub> beads were suspended to a 20% slurry (w/v) in 1x PBS (pH 7.4). For sterilization, 1 mg/mL carbenicillin was added to PhaC1<sub>Pa</sub> PHA beads and 1 mg/mL gentamycin was added to both Ag-PhaC1<sub>Pa</sub> and PhaC1<sub>Pa</sub>-Ag PHA<sub>MCL</sub> beads. PHA<sub>MCL</sub> beads were then distributed into 2 mL screw cap vials and placed in a sonication water bath for 1 h while maintaining a water temperature below 50°C. Respective PHA<sub>MCL</sub> bead samples were pooled and washed two times with 1x PBS (pH 7.4), centrifuged at 14,500 x g for 40 min at 4°C. Beads were suspended as a 10% slurry (w/v) in 1x PBS (pH 7.4) and a representative sample of 200 µl was plated for each group onto LB agar and incubated at 37°C to check for CFU.

### **Nile Red staining and fluorescence microscopy**

The presence of PHA<sub>MCL</sub> inclusions were observed with fluorescent microscopy by staining cells with lipophilic dye Nile Red [65]. MagnaFire imaging software was used to digitally capture images.

### **TEM**

Transmission electron microscopy (TEM) analysis was used to confirm the accumulation, shape and size of PHA<sub>MCL</sub> inclusions inside PHA<sub>MCL</sub> producing recombinant *P. aeruginosa* and respective PHA<sub>MCL</sub> bead material. Samples were processed for TEM analysis as previously described [66]. Diameters of PHA<sub>MCL</sub> inclusions in whole-cells was quantified using ImageJ imaging and analysis software (Wayne Rasband) giving approximately 500 data points for each fusion protein.

### **Analysis of proteins attached to PHA<sub>MCL</sub> beads**

Sodium dodecyl sulfate-polyacrylamide gel electrophoresis (SDS-PAGE) was used as previously described [67] to assess the protein profiles of PHA<sub>MCL</sub> beads and recombinant protein. The gels were stained with Coomassie Brilliant Blue G250. The amount of fusion protein was determined by densitometry against known bovine serum albumin (BSA) standards using Gel Doc XR for detection and Image lab software (version 5.2.1) (Bio-Rad, CA) for analysis. Protein bands of interest were excised from the gels and identified by tryptic peptide fingerprint analysis using Matrix-Assisted Laser Desorption-Ionisation Time-Of-Flight Mass Spectrometry (MALDI-TOF MS).

The major copurified protein bands from PHA<sub>MCL</sub> beads formed by PHA synthase antigen fusions were identified on SDS-PAGE using the following criteria: Image lab software (BioRad, USA) was used for the identification of dominant bands which had a volume threshold of > 1,000,000 as analyzed by Image lab software (BioRad, USA) and which were not detected using the specific anti-PhaC1\_529 antibody. The anti-PhaC1\_529 antibody as opposed to anti-PhaC1\_1 and anti-PhaC\_67 was specifically detecting the proteins PhaC1<sub>pa</sub> (62.5 kDa), Ag-PhaC1<sub>pa</sub> (77.8 kDa), and PhaC1<sub>pa</sub>-Ag (79.7 kDa).

For immunoblot analysis, proteins were separated by SDS-PAGE and transferred to nitrocellulose membranes using an i-BLOT system (Invitrogen, Carlsbad, CA). Membranes were blocked with 2% skim milk in 1x PBS with 0.05% Tween 20 (PBS-T) for 1 h. Following washing with PBS-T, primary antibodies were diluted in 2% BSA and used as follows: For detection of PhaC1<sub>pa</sub> (the epitope used for generating anti-PhaC1<sub>pa</sub> antibodies: anti-PhaC1\_1, MSQKNNNELPKQAA; anti-PhaC1\_67, QSELRPGDDRRFS; and anti-PhaC1\_529, RSGKTRKAPASLGN), 0.15 - 0.2 µg/mL rabbit polyclonal; AlgE (anti-AlgE, and left at room temperature for phase separation. The bottom phase containing HLRRPGEEVC), OprF (anti-OprF, NATAEGRAINRRVEC) and OprI (anti-OprI, SHSKETEARLTATC), 0.1 µg/mL rabbit polyclonal; GFP, 1:4000 dilution rabbit polyclonal (A01388, GenScript, NJ); and specificity of mouse sera antibodies for epitopes in the bead-associated proteins, 1:1500 dilution of pooled mouse serum. After incubation for 1 h, the membrane was washed three times using PBS-T for each 5 min. Secondary antibodies were diluted in 2% BSA and used as follows: anti-mouse HRP at 1:20,000 dilution, and anti-Rabbit HRP at 1:25,000 (Ab6721, Abcam, UK) and incubated for 1 h. After three washes with PBS-T, development was carried out using SuperSignal West Pico chemiluminescent substrate (ThermoFisher, Waltham, MA).

### **Quantification and analysis of PHA**

Typically 10 – 20 mg of lyophilized cells was subjected to methanolysis as described previously [68]. Methyl esters of the corresponding fatty acid constituents was recovered and analyzed by Gas chromatography-mass spectrometry (GC/MS) for 3-hydroxyalkanoate methyl esters.

### **Vaccination of mice**

All animal experiments had the approval of the AgResearch Animal Ethics Committee. Female C57BL/6 mice aged 6 to 8 weeks (obtained from the animal breeding facility of AgResearch, Ruakura, Hamilton, New Zealand) were vaccinated three times subcutaneously with 200 µl/injection at 2 week intervals (n = 6 per group) with 20 µg of PHA synthase on PhaC1<sub>Pa</sub> PHA<sub>MCL</sub> beads or 20 µg of OprI/F-AlgE fusion antigen on Ag-PhaC1<sub>Pa</sub> or PhaC1<sub>Pa</sub>-Ag PHA<sub>MCL</sub> beads or 5 µg OprI/F-AlgE fusion antigen on PhaC1<sub>Pa</sub>-Ag PHA<sub>MCL</sub> beads (low dose). Additional adjuvant formulated groups were included, 20 µg OprI/F-AlgE fusion antigen on PhaC1<sub>Pa</sub>-Ag PHA<sub>MCL</sub> beads were mixed with 10% (v/v) alum (A8222, Sigma, MO) or 20 µg soluble recombinant antigen His<sub>10</sub>-Ag protein either alone or mixed with alum to a final concentration of 10% (v/v). PBS-vaccinated control animals were included. Protein concentration was calculated using densitometry and BSA standards.

### **Immunological assay**

Immunological assays were performed as previously described [14]. Briefly, all mice were anesthetized using a mix of ketamine and xylazine hydrochloride three weeks after last vaccinated. Blood was collected by cardiac puncture, allowed to clot and centrifuged before serum was collected. Spleens were removed and single-cell suspensions were prepared by pushing the samples through a sieve and then repeatedly drawn through a 23g needle. Suspensions were washed with TAC buffer (17 mM Tris-HCl and 140 mM NH<sub>4</sub>Cl), followed by subsequent washes with PBS. Cells were then cultured at 37°C and 10% CO<sub>2</sub> in Dulbecco's modified Eagle medium supplemented with 2 mM glutamine, 100 U/mL penicillin, 100 µg/mL streptomycin, 5 x 10<sup>-5</sup> M 2-mercaptoethanol, and 5% (w/v) FCS in 7 well of a flat-bottomed 46-well plate at a concentration of 2 x 10<sup>6</sup> cells/well in a 1 mL volume. Cells were incubated in medium alone or medium containing 5 µg/mL recombinant protein His<sub>10</sub>-Ag (calculated based on OprI/F-AlgE fusion protein) or 5 µg/mL synthesized peptide (AlgE<sub>233-241-287-303</sub> or OprF<sub>329-342</sub> or overlapping peptides OprI<sub>21-48, 39-66, 57-83</sub>) or a peptide pool containing a combination of all peptides. 5 µg/mL of Concanavalin A (ConA, Sigma) was used as a positive control.

### Measurement of cytokines

A cytometric bead array (CBA; mouse Th1/Th2/Th17 cytokine kit, BD) was used according to the manufacturer's instructions to measure interleukin-2 (IL-2), interleukin-4 (IL-4), Interleukin-6 (IL-6), interferon- $\gamma$  (IFN- $\gamma$ ), tumor Necrosis Factor- $\alpha$  (TNF- $\alpha$ ), interleukin-17 (IL-17A), and interleukin-10 (IL-10). Fluorescence was measured using a FACSverse<sup>TM</sup> flow cytometer (BD) and analyzed using FCAP array software (BD).

### Measurement of serum antibody

Serum antibodies were measured using ELISA. For measuring serum antibodies against recombinant protein, MICROLON 600 (Greiner Bio-One) 96 well flat bottom high binding plates were coated overnight with 5  $\mu\text{g/mL}$  soluble recombinant protein His<sub>10</sub>-Ag or a pool of peptides containing 5  $\mu\text{g/mL}$  of each peptide (AlgE<sub>233-241-287-303</sub>, OprF<sub>329-342</sub>, OprI<sub>21-48, 39-66, 57-83</sub>) in carbonate-bicarbonate buffer (Sigma). Following washing with PBST, plates were blocked for 1 h using PBS-B (1x PBS with 1% (w/v) BSA). After washing with PBS-T, sera was diluted 1:10 and then serially diluted 1:5 in 1x PBS (pH 7.4) were added and incubated for 1 h. After PBS-T wash, secondary IgG1-HRP or IgG2c-HRP (ICL, Newberg, OR) was added at a concentration of 1:5000 and 1:7500, respectively, and incubated for 1 h. Plates were washed and tetramethylbenzidine substrate (BD) was added, color allowed to develop and the reaction was stopped by the addition of 0.5 M H<sub>2</sub>SO<sub>4</sub> and absorbance read at 450 nm on a VersaMax microplate reader.

Whole-cell EILSA was used to measure reactivity of serum antibodies to different *P. aeruginosa* strains and were conducted as previously described [69, 70]. Briefly, *P. aeruginosa* strains were cultivated overnight, cells were washed and diluted to OD<sub>600</sub> of 0.5 in 1x PBS. Subsequently, resuspended cells were diluted 1:2 and used to coat MICROLON 600 (Greiner Bio-One) 96 well flat bottom high binding plates overnight. Plates were washed with PBS-T and blocked for 1 h using PBS-B. Following washing with PBS-T, plates were blocked for 1 h with serum 1:3 serially diluted in PBS-B starting with a dilution of 1:40. Plates were washed with PBS-T and treated with HRP-conjugated anti-mouse secondary antibodies at a dilution of 1:5000 for 1 h. Plates were washed, OPD substrate (Sigma) added and the reaction was stopped by the addition of 3 M H<sub>2</sub>SO<sub>4</sub>. Absorbance was then read at 490 nm.

### **Measurement of opsonic killing activity of serum antibody**

Opsonic assay was performed as previously described [71] with some modifications. In brief, assays were performed in 96-well plates using 25 µl of the following assay components: mouse serum diluted 1:2.5 (final concentration 1:10), mouse macrophage RAW 264.7 cells at  $2 \times 10^6$ /ml, *P. aeruginosa* from log-phase culture at  $2 \times 10^8$ /ml, and 4% guinea pig complement as complement (1% final concentration). DMEM medium with 10% heat-inactivated fetal calf serum was used as the diluent. Control reactions, wherein antibody was omitted and substituted with DMEM-10%FCS. Assay was performed at 37°C with mixing on a plate mixer for 90 mins. Following incubation 25 µl was removed and diluted in deionized water and the serially in saline as described previously [72], and plated on LB agar for bacteria counts. Plates were incubated overnight at 37°C. The percent killing was calculated as follows:  $[1 - (\text{CFU surviving in immune serum at 90 min} / \text{CFU surviving in PBS vaccinated serum at 90 min})] \times 100$ .

### **Identification of PHA synthases in bacterial human pathogens**

eggNOG 4.5 [73], a hierarchical orthology framework with annotations was used for the identification of PHA synthases in bacteria. A sequence search of the database with the amino acid reference sequence of PhaC<sub>1pa</sub> from *P. aeruginosa* (X66592.1) identified greater than 359 species of bacteria (e-value ranging from 6.56e-185 to 1.6e-07). 33 human pathogens of interest were identified (**Supplementary Table 2.4**). Homology between the PHA synthases from the selected 33 human pathogens was inferred by multiple alignment of the primary amino acid sequence using T-Coffee [74] with BLOSUM (**Supplementary Fig. 2.2** and **Supplementary Table 2.5**).

### **Statistical analysis**

ELISA data were analyzed using SoftMax pro 7 and expressed in titers representing the reciprocal of the serum dilution that gave half the maximal optical density (OD) (EC<sub>50</sub>).

For IgG analysis, data of graph are reported as means ± s.e.m (6 mice per group). Statistical analyses were undertaken on log(e)-transformed IgG1 and IgG2c values.

IgG1 was analyzed by Kruskal-Wallis nonparametric test, no significant differences found between the groups. IgG2 was analyzed by one-way ANOVA with statistical significance ( $p < 0.05$ ) indicated by 'letter based' representation of pairwise comparisons between groups using Tukey's post-hoc test. Groups that share a common

letter are not statistically significant to each other, while groups that don't share a common letters are statistically significant to each other ( $p < 0.05$ ). Alphabetical order donates significance, with a higher letter being more significant to a lower letter e.g. a < b < c. Statistical analysis was performed with R software version 3.3.1 [75]

Analysis of the mean percent kill from triplicate samples of serum were compared by one-way ANOVA with pairwise comparison between groups using Tukey's post-hoc test ( $p < 0.05$ ). Statistical analysis was performed with GraphPad Prism version 6.00.

For analysis of cytokines, results are calculated by subtracting cytokine values of the media-stimulated samples from the cytokine values of the recombinant protein stimulated samples. Data of graphs are reported as means  $\pm$  s.e.m and each individual mouse are reported as a dot (6 mice per group). Statistical analyses were undertaken on log(e)-transformed IFN- $\gamma$ , IL-17a and IL-2 values and square root-transformed IL-4, IL-6 and TNF- $\alpha$  values, while the raw data was analyzed for IL-10. Comparison of multiple groups for statistical significance ( $p < 0.05$ ) is indicated by 'letter-based' representation of pairwise comparisons between groups, with  $p$ -value adjusted by 'Benjamini-Hochberg' method. Statistical analysis was performed with R software version 3.3.1 [75]

## 2.5 Acknowledgements

The authors wish to acknowledge Dongwen Luo for his help with statistical analyses and Joanna Roberts for her assistance with flow cytometry. We would also like to acknowledge the Manawatu Microscopy and Imaging Centre for preparation of electron microscopy sections and use of their facility. This research was funded by Massey University and The MacDiarmid Institute for Advanced Materials and Nanotechnology.

## 2.6 References

1. Draper, J., et al., eds. *Polyhydroxyalkanoate inclusions: polymer synthesis, self-assembly and display technology*. Bionanotechnology: biological self assembly and its applications, ed. B.H.A. Rehm. 2013, Caister Academic Press: Norfolk 8045-8053.
2. Rehm, B.H.A., *Polyester synthases: natural catalysts for plastics*. *Biochemical Journal*, 2003. **376**: p. 15-33.
3. Foged, C., *Subunit vaccines of the future: the need for safe, customized and optimized particulate delivery systems*. *Therapeutic Delivery*, 2011. **2**(8): p. 1057-1077.
4. Leleux, J. and K. Roy, *Micro and nanoparticle - based delivery systems for vaccine immunotherapy: an immunological and materials perspective*. *Advanced Healthcare Materials*, 2013. **2**(1): p. 72-94.
5. Parlane, N.A., et al., *Vaccines displaying mycobacterial proteins on biopolyester beads stimulate cellular immunity and induce protection against tuberculosis*. *Clinical and Vaccine Immunology*, 2012. **19**(1): p. 37-44.
6. Parlane, N.A., et al., *Novel particulate vaccines utilizing polyester nanoparticles (bio-beads) for protection against Mycobacterium bovis infection—A review*. *Veterinary Immunology and Immunopathology*, 2014. **158**(1): p. 8-13.
7. Martínez-Donato, G., et al., *Protective T cell and antibody immune response against Hepatitis C Virus using the biopolyester beads based vaccine delivery system*. *Clinical and Vaccine Immunology*, 2016: p. 370-378.
8. Parlane, N.A., et al., *Production of a particulate hepatitis C vaccine candidate by an engineered Lactococcus lactis strain*. *Applied and Environmental Microbiology*, 2011. **77**(24): p. 8516-8522.
9. Grage, K., et al., *Bacterial polyhydroxyalkanoate granules: biogenesis, structure, and potential use as nano-/micro-beads in biotechnological and biomedical applications*. *Biomacromolecules*, 2009. **10**(4): p. 660-669.
10. Jahns, A.C. and B.H.A. Rehm, *Tolerance of the Ralstonia eutropha Class I Polyhydroxyalkanoate Synthase for Translational Fusions to Its C Terminus Reveals a New Mode of Functional Display*. *Applied and Environmental Microbiology*, 2009. **75**(17): p. 5461-5466.
11. Peters, V. and B.H.A. Rehm, *In vivo monitoring of PHA granule formation using GFP-labeled PHA synthases*. *FEMS Microbiology Letters*, 2005. **248**(1): p. 93-100.
12. Chen, S., et al., *New skin test for detection of bovine tuberculosis on the basis of antigen-displaying polyester inclusions produced by recombinant Escherichia coli*. *Applied and Environmental Microbiology*, 2014. **80**(8): p. 2526-2535.
13. Hooks, D.O., P.A. Blatchford, and B.H.A. Rehm, *Bioengineering of bacterial polymer inclusions catalyzing the synthesis of N-acetylneuraminic acid*. *Applied and Environmental Microbiology*, 2013. **79**(9): p. 3116-3121.
14. Parlane, N.A., et al., *Bacterial polyester inclusions engineered to display vaccine candidate antigens for use as a novel class of safe and efficient vaccine delivery agents*. *Applied and Environmental Microbiology*, 2009. **75**(24): p. 7739-7744.
15. Reyes, P.R., et al., *Immunogenicity of antigens from Mycobacterium tuberculosis self-assembled as particulate vaccines*. *International Journal of Medical Microbiology*, 2016.
16. Bachmann, M.F. and G.T. Jennings, *Vaccine delivery: a matter of size, geometry, kinetics and molecular patterns*. *Nature Reviews Immunology*, 2010. **10**(11): p. 787-796.

17. Priebe, G.P. and J.B. Goldberg, *Vaccines for Pseudomonas aeruginosa: a long and winding road*. Expert review of Vaccines, 2014. **13**(4): p. 507-519.
18. Center for Disease Control and Prevention. *Antibiotic resistance threats in the United States, 2013*. 2013; Available from: <http://www.cdc.gov/drugresistance/threat-report-2013/>.
19. Finco, O. and R. Rappuoli, *Designing vaccines for the twenty-first century society*. Frontiers in Immunology, 2014. **5**.
20. Sharma, A., A. Krause, and S. Worgall, *Recent developments for Pseudomonas vaccines*. Human Vaccines, 2011. **7**(10): p. 999-1011.
21. Westritschnig, K., et al., *A randomized, placebo-controlled phase I study assessing the safety and immunogenicity of a Pseudomonas aeruginosa hybrid outer membrane protein OprF/I vaccine (IC43) in healthy volunteers*. Human Vaccines & Immunotherapeutics, 2014. **10**(1): p. 170-183.
22. Baumann, U., E. Mansouri, and B.U. von Specht, *Recombinant OprF-OprI as a vaccine against Pseudomonas aeruginosa infections*. Vaccine, 2004. **22**(7): p. 840-847.
23. Holder, I.A., *Pseudomonas immunotherapy: a historical overview*. Vaccine, 2004. **22**(7): p. 831-839.
24. Moser, C., et al., *The immune response to chronic Pseudomonas aeruginosa lung infection in cystic fibrosis patients is predominantly of the Th2 type*. Apmis, 2000. **108**(5): p. 329-335.
25. Jensen, P.Ø., et al., *The immune system vs. Pseudomonas aeruginosa biofilms*. FEMS Immunology & Medical Microbiology, 2010. **59**(3): p. 292-305.
26. Moser, C., et al., *Improved outcome of chronic Pseudomonas aeruginosa lung infection is associated with induction of a Th1 - dominated cytokine response*. Clinical & Experimental Immunology, 2002. **127**(2): p. 206-213.
27. Revets, H., et al., *Lipoprotein I, a TLR2/4 ligand modulates Th2-driven allergic immune responses*. The Journal of Immunology, 2005. **174**(2): p. 1097-1103.
28. Finke, M., et al., *Protection against experimental Pseudomonas aeruginosa infection by recombinant P. aeruginosa lipoprotein I expressed in Escherichia coli*. Infection and Immunity, 1990. **58**(7): p. 2241-2244.
29. Rehm, B.H.A., et al., *Overexpression of algE in Escherichia coli: subcellular-localization, purification, and ion-channel properties*. Journal of Bacteriology, 1994. **176**(18): p. 5639-5647.
30. Rehm, B.H.A., et al., *Antibody-response of rabbits and cystic-fibrosis patients to an alginate-specific outer-membrane protein of a mucoid strain of Pseudomonas aeruginosa*. Microbial Pathogenesis, 1994. **16**(1): p. 43-51.
31. Rehman, Z.U. and B.H.A. Rehm, *Dual roles of Pseudomonas aeruginosa AlgE in secretion of the virulence factor alginate and formation of the secretion complex*. Applied and Environmental Microbiology, 2013. **79**(6): p. 2002-2011.
32. Whitney, J.C., et al., *Structural basis for alginate secretion across the bacterial outer membrane*. Proceedings of the National Academy of Sciences, 2011. **108**(32): p. 13083-13088.
33. Weimer, E.T., et al., *Immunization of young African green monkeys with OprF epitope 8-OprI-type A- and B-flagellin fusion proteins promotes the production of protective antibodies against nonmucoid Pseudomonas aeruginosa*. Vaccine, 2009. **27**(48): p. 6762-6769.
34. Von Specht, B.U., et al., *Immunogenic efficacy of differently produced recombinant vaccines candidates against Pseudomonas aeruginosa infections*. Journal of Biotechnology, 2000. **83**(1): p. 3-12.
35. Rehm, B., *Microbial production of biopolymers and polymer precursors: applications and perspectives*. 2009: Horizon Scientific Press.
36. Pham, T.H., J.S. Webb, and B.H.A. Rehm, *The role of polyhydroxyalkanoate biosynthesis by Pseudomonas aeruginosa in rhamnolipid and alginate production as well as stress tolerance and biofilm formation*. Microbiology, 2004. **150**(10): p. 3405-3413.
37. Rehm, B.H.A., *Bacterial polymers: biosynthesis, modifications and applications*. Nature Reviews Microbiology, 2010. **8**(8): p. 578-592.
38. Gilleland, L.B. and H.E. Gilleland, *Synthetic peptides representing 2 protective, linear B-cell epitopes of outer-membrane protein-F of Pseudomonas aeruginosa elicit whole-cell-reactive antibodies that are functionally pseudomonad specific*. Infection and Immunity, 1995. **63**(6): p. 2347-2351.
39. Amara, A. and B. Rehm, *Replacement of the catalytic nucleophile cysteine-296 by serine in class II polyhydroxyalkanoate synthase from Pseudomonas aeruginosa-mediated synthesis of a new polyester: identification of catalytic residues*. Biochemical Journal, 2003. **374**: p. 413-421.

40. Weimer, E.T., et al., *A fusion protein vaccine containing OprF epitope 8, OprI, and type A and B flagellins promotes enhanced clearance of nonmucoid Pseudomonas aeruginosa*. Infection and Immunity, 2009. **77**(6): p. 2356-2366.
41. Cui, Z., et al., *Mannose-modified chitosan microspheres enhance OprF-OprI-mediated protection of mice against Pseudomonas aeruginosa infection via induction of mucosal immunity*. Applied Microbiology and Biotechnology, 2015. **99**(2): p. 667-680.
42. Peters, V. and B.H.A. Rehm, *In vivo enzyme immobilization by use of engineered polyhydroxyalkanoate synthase*. Applied and Environmental Microbiology, 2006. **72**(3): p. 1777-1783.
43. Hartl, D., et al., *Pulmonary TH2 response in Pseudomonas aeruginosa-infected patients with cystic fibrosis*. Journal of allergy and clinical immunology, 2006. **117**(1): p. 204-211.
44. Van Duin, D., R. Medzhitov, and A.C. Shaw, *Triggering TLR signaling in vaccination*. Trends in Immunology, 2006. **27**(1): p. 49-55.
45. Braun, M., et al., *Virus - like particles induce robust human T - helper cell responses*. European journal of immunology, 2012. **42**(2): p. 330-340.
46. Brennan, F.R., et al., *Pseudomonas aeruginosa outer-membrane protein F epitopes are highly immunogenic in mice when expressed on a plant virus*. Microbiology, 1999. **145**(1): p. 211-220.
47. Mizuno, T. and M. Kageyama, *Separation and characterization of the outer membrane of Pseudomonas aeruginosa*. Journal of Biochemistry, 1978. **84**(1): p. 179-191.
48. Rosalia, R.A., et al., *Efficient ex vivo induction of T cells with potent anti-tumor activity by protein antigen encapsulated in nanoparticles*. Cancer Immunology, Immunotherapy, 2013. **62**(7): p. 1161-1173.
49. Vyas, J.M., A.G. Van der Veen, and H.L. Ploegh, *The known unknowns of antigen processing and presentation*. Nature Reviews Immunology, 2008. **8**(8): p. 607-618.
50. Xiang, S.D., et al., *Pathogen recognition and development of particulate vaccines: does size matter?* Methods, 2006. **40**(1): p. 1-9.
51. Wu, W., et al., *Th17-stimulating protein vaccines confer protection against Pseudomonas aeruginosa pneumonia*. American Journal of Respiratory and Critical Care Medicine, 2012. **186**(5): p. 420-427.
52. Scheller, J., et al., *The pro-and anti-inflammatory properties of the cytokine interleukin-6*. Biochimica et Biophysica Acta (BBA)-Molecular Cell Research, 2011. **1813**(5): p. 878-888.
53. Schlegel, H.G., H. Kaltwasser, and G. Gottschalk, *A submersion method for culture of hydrogen-oxidizing bacteria: growth physiological studies*. Archiv fur Mikrobiologie, 1961. **38**: p. 209-222.
54. Sambrook, J., E.F. Fritsch, and T. Maniatis, *Molecular cloning: a laboratory manual*. Vol. 2. 1989: Cold spring harbor laboratory press New York.
55. Choi, K.H., A. Kumar, and H.P. Schweizer, *A 10-min method for preparation of highly electrocompetent Pseudomonas aeruginosa cells: Application for DNA fragment transfer between chromosomes and plasmid transformation*. Journal of Microbiological Methods, 2006. **64**(3): p. 391-397.
56. Remminghorst, U. and B.H.A. Rehm, *In vitro alginate polymerization and the functional role of Alg8 in alginate production by Pseudomonas aeruginosa*. Applied and Environmental Microbiology, 2006. **72**(1): p. 298-305.
57. Hoang, T.T., et al., *A broad-host-range Flp-FRT recombination system for site-specific excision of chromosomally-located DNA sequences: application for isolation of unmarked Pseudomonas aeruginosa mutants*. Gene, 1998. **212**(1): p. 77-86.
58. Ghafoor, A., I.D. Hay, and B.H.A. Rehm, *Role of exopolysaccharides in Pseudomonas aeruginosa biofilm formation and architecture*. Applied and Environmental Microbiology, 2011. **77**(15): p. 5238-5246.
59. Langenbach, S., B.H.A. Rehm, and A. Steinbüchel, *Functional expression of the PHA synthase gene phaC1 from Pseudomonas aeruginosa in Escherichia coli results in poly (3-hydroxyalkanoate) synthesis*. FEMS Microbiology Letters, 1997. **150**(2): p. 303-309.
60. Hughes, E.E., L.B. Gilleland, and H.E. Gilleland, *Synthetic peptides representing epitopes of outer-membrane protein-F of Pseudomonas aeruginosa that elicit antibodies reactive with whole cells of heterologous immunotype strains of P. aeruginosa*. Infection and Immunity, 1992. **60**(9): p. 3497-3503.
61. Rawling, E.G., N.L. Martin, and R. Hancock, *Epitope mapping of the Pseudomonas aeruginosa major outer membrane porin protein OprF*. Infection and Immunity, 1995. **63**(1): p. 38-42.
62. Liang, S.D., et al., *Prediction of antigenic epitopes on protein surfaces by consensus scoring*. BMC Bioinformatics, 2009. **10**.

63. Qiu, D., et al., *PBAD-based shuttle vectors for functional analysis of toxic and highly regulated genes in Pseudomonas and Burkholderia spp. and other bacteria*. Applied and Environmental Microbiology, 2008. **74**(23): p. 7422-7426.
64. Hoffmann, N. and B.H.A. Rehm, *Regulation of polyhydroxyalkanoate biosynthesis in Pseudomonas putida and Pseudomonas aeruginosa*. Fems Microbiology Letters, 2004. **237**(1): p. 1-7.
65. Spiekermann, P., et al., *A sensitive, viable-colony staining method using Nile red for direct screening of bacteria that accumulate polyhydroxyalkanoic acids and other lipid storage compounds*. Archives of Microbiology, 1999. **171**(2): p. 73-80.
66. Grage, K. and B.H.A. Rehm, *In vivo production of scFv-displaying biopolymer beads using a self-assembly-promoting fusion partner*. Bioconjugate Chemistry, 2007. **19**(1): p. 254-262.
67. Mifune, J., K. Grage, and B.H.A. Rehm, *Production of functionalized biopolyester granules by recombinant Lactococcus lactis*. Applied and Environmental Microbiology, 2009. **75**(14): p. 4668-4675.
68. Brandl, H., et al., *Pseudomonas oleovorans as a source of poly ( $\beta$ -hydroxyalkanoates) for potential applications as biodegradable polyesters*. Applied and Environmental Microbiology, 1988. **54**(8): p. 1977-1982.
69. DiGiandomenico, A., et al., *Identification of broadly protective human antibodies to Pseudomonas aeruginosa exopolysaccharide Psl by phenotypic screening*. The Journal of Experimental Medicine, 2012. **209**(7): p. 1273-1287.
70. DiGiandomenico, A., J. Rao, and J.B. Goldberg, *Oral vaccination of BALB/c mice with Salmonella enterica serovar Typhimurium expressing Pseudomonas aeruginosa O antigen promotes increased survival in an acute fatal pneumonia model*. Infection and Immunity, 2004. **72**(12): p. 7012-7021.
71. Garner, C.V., D. DesJardins, and G.B. Pier, *Immunogenic properties of Pseudomonas aeruginosa mucoid exopolysaccharide*. Infection and Immunity, 1990. **58**(6): p. 1835-1842.
72. Ames, P., D. DesJardins, and G.B. Pier, *Opsonophagocytic killing activity of rabbit antibody to Pseudomonas aeruginosa mucoid exopolysaccharide*. Infection and Immunity, 1985. **49**(2): p. 281-285.
73. Huerta-Cepas, J., et al., *eggNOG 4.5: a hierarchical orthology framework with improved functional annotations for eukaryotic, prokaryotic and viral sequences*. Nucleic Acids Research, 2015: p. 1248.
74. Li, W., et al., *The EMBL-EBI bioinformatics web and programmatic tools framework*. Nucleic Acids Research, 2015: p. 279.
75. R\_Core\_Team, *R: A language and environment for statistical computing*. 2016, R Foundation for Statistical Computing.

# **Supplementary material for: Bioengineering *Pseudomonas aeruginosa* to assemble its own particulate vaccine capable of inducing cellular immunity**

Jason W. Lee<sup>1,2</sup>, Natalie A. Parlane<sup>2</sup>, D. Neil Wedlock<sup>2</sup>, and Bernd H. A. Rehm<sup>1,3,4,\*</sup>

*Institute of Fundamental Sciences, Massey University, Palmerston North, New Zealand<sup>1</sup>, AgResearch, Hopkirk Research Institute, Palmerston North, New Zealand<sup>2</sup>, The MacDiarmid Institute for Advanced Materials and Nanotechnology, Wellington, New Zealand<sup>3</sup>, and PolyBatics, Palmerston North, New Zealand<sup>4</sup>*

\*Corresponding author: Bernd H. A. Rehm, e-mail: [b.rehm@massey.ac.nz](mailto:b.rehm@massey.ac.nz),  
phone: +64 6 350 5515, fax: +64 6 350 5688

$\Delta alg8$  Nucleotide sequence:  
 ATGATGGAAACTTACAAACGTGGCCTCGCCGAAGCCACCGGCTGGCTGGTGTTCCTCAGCCTGC  
 TGATGGTGTCTCGCGCTGGCAGTGCCGAAGACCGTGTTCGACGCCGACTCCAAGGATTTATCCT  
 GCTTATCGGGCGCCGTGGCATCTGGCGCTACTCCATGGGCGGCGTGCACCTCCTGCGCGGCAT  
 GCAGTTCCTCCACGTGGTCTACCCGTACTACCTCCGGCGCGTGCGCCAGTTGGGCAGCGCGGC  
 CGACCCGTGCGACGTGTTCTGATGGTACCAGTTTCCGCATCGACGCCCTGACCACTGCCATG  
 GTCTATCGCTCGGTGATCCGCGAAGCCATCGACAGCGGCTACCCGACCACCGTGGTCTGCTCCA  
 TCGTCGAGATGTCCGACGAGGTCTGGTCCGTTCTCTGTGGGAGAAGATGAACC<>GGATCCCC  
GGGTACCGAGCTCGAATTAGCTTCAAAGCGCTCTGAAGTTCCTATACTTTCTAGAGAATAGGAA  
CTTCGGAATAGGTACTCAAGATCCCCAATTCGAGCTCGGTACCCGGGGATCCG<>TCACCATGC  
 TGGTGTGTTTCGACCAGCGCTCTCGATGTGGACCAGCTGCTCGGCCCTGGTGGTGGCGATCCT  
 CGCCAGCCTCAAGTACAGCATCGCCTTCTGCTGGTGTACCTGCTCTGGATCGGCCTCACCCGC  
 CTGGTGTGACCCCTGCTCCTCTCGCTCTCCGGGCACCGCATCGGCCCGGCCTATCCGCTGATCC  
 TCTATTACAACCAGATCGTCGGCGCGCTGGTGAAGATCTACGTGTTCTCCGCTCGACCCGGCAG  
 TCCTGGACCCGCCAGCCGACCAAGCTGGAGCGCGGCCTGGCCAGCTTCCAGCGCTGGTTCAAC  
 GCCTGGTGTGTCGCGGGCCATGACCTTCTCTGCCGCCAGCATCTCGTCGCCGTGCTCTATTACAA  
 CCAGATCGTCGGCGCGCTGGTGAAGATCTACGTGTTCTTCCGCTCGACCCGGCAGTCTGGACC  
 CGCCAGCCGACCAAGCTGGAGCGCGGCCTGGCCAGCTTCCAGCGCTGGTTCAACGCCTGGTCTG  
 TCGGGGCCATGACCTTCTCTGCCGCCAGCATCTTCTCGCCGTGCTGCTGACCATCGTATGA

$\Delta pelF$  Nucleotide sequence:  
 ATGACCGAACACACCGCTCCGACGGCGCCCGTCCGCGATGTCTGCCTGCTGCTGGAGGGCACC  
 TGGCCCTATGTCCGCGGGCGCGTCTCCAGCTGGGTCAACCAGTTGATCCTCGGTCTCCCCGACC  
 TGACCTTCTCGGTGTTCTTTCATCGGCGGCCAGAAGGATGCCTACGGCAAGCGCCACTACCCGAT  
 CCCGGACAATGTGCTGCACATCGAGGAACACTTCTGGAAACCGCCTGGAGTTCGCCGAACCCG  
 CAGACGCGACAGGGCAGTAGCGAGACCGAAAAGGCGTTGCGCGATCTGCACCGTTTCTTCCACT  
 ACCCGGAGACGCGGACGTGGAGGAGGGCGACGCGCTGCTCGACCTGCTCGCCGAGGGCCGC  
 ATCGGCCGCGAGGACTTTCTCCACAGCA<>GGATCCCCGGGTACCGAGCTCGAATTGGGGATCT  
TGAAGTACCTATTCCGAAGTTCCTATTCTCTAGAAAGTATAGGAACTTCAGAGCGCTTTTGAAGC  
TAATTCGAGCTCGGTACCCGGGGATCC<>GTGAAGTTCCTCGGTTTCCGTCGGATCGGCGAGGT  
 CCTGCCGAACTCGGCCTGATGGTCTCACCTCGATCAGCGAAGCGCAGCCGCTGGTGTATCCTC  
 GAAGCCTGGGCTGCCGGCGCCCCGGTGGTGAAGCAGCGACGTCCGCTCCTGCCGCGAACTGATC  
 GAAGGCGCCGACGCCGAAGATCGCGCCCTGGGTGCGCGCCGGGAGGTGGTGGCGATCGCCGA  
 CCCGCAGGCCACTTCGCGGGCGATCCTCGCCCTGCTGCGCAATCCGCAGCGCTGGCAGGGCGGC  
 CCAGGGGTGCGCCTGCAACGGGTGCAACGCTACTACCCGAGGCCTGATGCTCGGACGTTA  
 CCGCGGGCTGTACCGCGAAGCCACGGAGATTGCATGACCATGGCCGGCATCGGCTCCGGGGAG  
 GTGGTGGCGATCGCCGACCCGCAAGGCCACTTCGCGGGCGATCCTCGCCCTGCTGCGCAATCCG  
 CAGCGCTGGCAGGGCGGCCAGGGCGTCCGGCTGCAACGGGTGCAACGCTACTACCCGAGGC  
 GCTGATGCTCGGACGTTACCGCGGGCTGTACCGCGAAGCCACGGAGATTGCATGA

**Supplementary Figure 2.1. DNA sequencing results for the generation of *P. aeruginosa* knockout mutant PAO1  $\Delta C\Delta 8\Delta F$ .** Nucleotide sequences of the truncated genes are displayed and annotated as follows: gene unrelated nucleotides (red), BamHI restriction sites (underlined), and FRT site (Bold).



NSMAGI...  
 1: A. baumannii (HMPREF0010\_00690)  
 2: A. cactobacillus (BDGL\_001038)  
 3: A. radoniosis (HMPREF0018\_01802)  
 4: B. anthracis (PHAC)  
 5: B. pertussis (PHBC)  
 6: B. cenocepacia (PHBC)  
 7: B. mallei (PHAC)  
 8: B. multivorans (BMUL\_1483)  
 10: B. multivorans (BMUL\_01759)  
 11: B. pseudomallei (PHBC)  
 12: B. pseudomallei (BPSS1954)  
 13: L. pneumophila (lpg1059)  
 14: L. pneumophila (lpg1089)  
 15: L. pneumophila (lpg2860)  
 16: L. pneumophila (lpg2860)  
 17: L. borgpetersenii (LBI\_2632)  
 18: L. borgpetersenii (LBI\_2632)  
 19: M. abscessus (MAB\_2034)  
 19: M. abscessus (MAB\_2348)  
 20: M. avium (MAP1389)  
 21: M. kansasii (MIKAN1\_010100013815)  
 21: M. kansasii (MIKAN1\_010100013815)  
 22: M. leprea (ML1348)  
 23: M. tuberculosis (MT1723)  
 24: N. farcinica (NFA\_45720)  
 25: P. aeruginosa (PhaC1)  
 26: P. aeruginosa (PhaC2)  
 27: R. equi (REQ\_24810)  
 28: R. prowazekii (ERP280)  
 28: R. prowazekii (ERP280)  
 29: R. typhi (PHBC)  
 30: S. rugosus (HMPREF0336\_01483)  
 31: S. maltophilia (SMAL\_2415)  
 32: V. cholera (VC\_A0688)  
 33: V. vulnificus (VV2\_0739)

CONSENSUS  
 1: A. baumannii (HMPREF0010\_00690)  
 2: A. cactobacillus (BDGL\_001038)  
 3: A. radoniosis (HMPREF0018\_01802)  
 4: B. anthracis (PHAC)  
 5: B. pertussis (PHBC)  
 6: B. cenocepacia (PHBC)  
 7: B. mallei (PHAC)  
 8: B. multivorans (BMUL\_1483)  
 10: B. multivorans (BMUL\_01759)  
 11: B. pseudomallei (PHBC)  
 12: B. pseudomallei (BPSS1954)  
 13: L. pneumophila (lpg1059)  
 14: L. pneumophila (lpg1089)  
 15: L. pneumophila (lpg2860)  
 16: L. pneumophila (lpg2860)  
 17: L. borgpetersenii (LBI\_2632)  
 18: L. borgpetersenii (LBI\_2632)  
 19: M. abscessus (MAB\_2034)  
 19: M. abscessus (MAB\_2348)  
 20: M. avium (MAP1389)  
 21: M. kansasii (MIKAN1\_010100013815)  
 21: M. kansasii (MIKAN1\_010100013815)  
 22: M. leprea (ML1348)  
 23: M. tuberculosis (MT1723)  
 24: N. farcinica (NFA\_45720)  
 25: P. aeruginosa (PhaC1)  
 26: P. aeruginosa (PhaC2)  
 27: R. equi (REQ\_24810)  
 28: R. prowazekii (ERP280)  
 28: R. prowazekii (ERP280)  
 29: R. typhi (PHBC)  
 30: S. rugosus (HMPREF0336\_01483)  
 31: S. maltophilia (SMAL\_2415)  
 32: V. cholera (VC\_A0688)  
 33: V. vulnificus (VV2\_0739)

CONSENSUS  
 1: A. baumannii (HMPREF0010\_00690)  
 2: A. cactobacillus (BDGL\_001038)  
 3: A. radoniosis (HMPREF0018\_01802)  
 4: B. anthracis (PHAC)  
 5: B. pertussis (PHBC)  
 6: B. cenocepacia (PHBC)  
 7: B. mallei (PHAC)  
 8: B. multivorans (BMUL\_1483)  
 10: B. multivorans (BMUL\_01759)  
 11: B. pseudomallei (PHBC)  
 12: B. pseudomallei (BPSS1954)  
 13: L. pneumophila (lpg1059)  
 14: L. pneumophila (lpg1089)  
 15: L. pneumophila (lpg2860)  
 16: L. pneumophila (lpg2860)  
 17: L. borgpetersenii (LBI\_2632)  
 18: L. borgpetersenii (LBI\_2632)  
 19: M. abscessus (MAB\_2034)  
 19: M. abscessus (MAB\_2348)  
 20: M. avium (MAP1389)  
 21: M. kansasii (MIKAN1\_010100013815)  
 21: M. kansasii (MIKAN1\_010100013815)  
 22: M. leprea (ML1348)  
 23: M. tuberculosis (MT1723)  
 24: N. farcinica (NFA\_45720)  
 25: P. aeruginosa (PhaC1)  
 26: P. aeruginosa (PhaC2)  
 27: R. equi (REQ\_24810)  
 28: R. prowazekii (ERP280)  
 28: R. prowazekii (ERP280)  
 29: R. typhi (PHBC)  
 30: S. rugosus (HMPREF0336\_01483)  
 31: S. maltophilia (SMAL\_2415)  
 32: V. cholera (VC\_A0688)  
 33: V. vulnificus (VV2\_0739)

CONSENSUS  
 1: A. baumannii (HMPREF0010\_00690)  
 2: A. cactobacillus (BDGL\_001038)  
 3: A. radoniosis (HMPREF0018\_01802)  
 4: B. anthracis (PHAC)  
 5: B. pertussis (PHBC)  
 6: B. cenocepacia (PHBC)  
 7: B. mallei (PHAC)  
 8: B. multivorans (BMUL\_1483)  
 10: B. multivorans (BMUL\_01759)  
 11: B. pseudomallei (PHBC)  
 12: B. pseudomallei (BPSS1954)  
 13: L. pneumophila (lpg1059)  
 14: L. pneumophila (lpg1089)  
 15: L. pneumophila (lpg2860)  
 16: L. pneumophila (lpg2860)  
 17: L. borgpetersenii (LBI\_2632)  
 18: L. borgpetersenii (LBI\_2632)  
 19: M. abscessus (MAB\_2034)  
 19: M. abscessus (MAB\_2348)  
 20: M. avium (MAP1389)  
 21: M. kansasii (MIKAN1\_010100013815)  
 21: M. kansasii (MIKAN1\_010100013815)  
 22: M. leprea (ML1348)  
 23: M. tuberculosis (MT1723)  
 24: N. farcinica (NFA\_45720)  
 25: P. aeruginosa (PhaC1)  
 26: P. aeruginosa (PhaC2)  
 27: R. equi (REQ\_24810)  
 28: R. prowazekii (ERP280)  
 28: R. prowazekii (ERP280)  
 29: R. typhi (PHBC)  
 30: S. rugosus (HMPREF0336\_01483)  
 31: S. maltophilia (SMAL\_2415)  
 32: V. cholera (VC\_A0688)  
 33: V. vulnificus (VV2\_0739)

CONSENSUS  
 1: A. baumannii (HMPREF0010\_00690)  
 2: A. cactobacillus (BDGL\_001038)  
 3: A. radoniosis (HMPREF0018\_01802)  
 4: B. anthracis (PHAC)  
 5: B. pertussis (PHBC)  
 6: B. cenocepacia (PHBC)  
 7: B. mallei (PHAC)  
 8: B. multivorans (BMUL\_1483)  
 10: B. multivorans (BMUL\_01759)  
 11: B. pseudomallei (PHBC)  
 12: B. pseudomallei (BPSS1954)  
 13: L. pneumophila (lpg1059)  
 14: L. pneumophila (lpg1089)  
 15: L. pneumophila (lpg2860)  
 16: L. pneumophila (lpg2860)  
 17: L. borgpetersenii (LBI\_2632)  
 18: L. borgpetersenii (LBI\_2632)  
 19: M. abscessus (MAB\_2034)  
 19: M. abscessus (MAB\_2348)  
 20: M. avium (MAP1389)  
 21: M. kansasii (MIKAN1\_010100013815)  
 21: M. kansasii (MIKAN1\_010100013815)  
 22: M. leprea (ML1348)  
 23: M. tuberculosis (MT1723)  
 24: N. farcinica (NFA\_45720)  
 25: P. aeruginosa (PhaC1)  
 26: P. aeruginosa (PhaC2)  
 27: R. equi (REQ\_24810)  
 28: R. prowazekii (ERP280)  
 28: R. prowazekii (ERP280)  
 29: R. typhi (PHBC)  
 30: S. rugosus (HMPREF0336\_01483)  
 31: S. maltophilia (SMAL\_2415)  
 32: V. cholera (VC\_A0688)  
 33: V. vulnificus (VV2\_0739)

CONSENSUS  
 1: A. baumannii (HMPREF0010\_00690)  
 2: A. cactobacillus (BDGL\_001038)  
 3: A. radoniosis (HMPREF0018\_01802)  
 4: B. anthracis (PHAC)  
 5: B. pertussis (PHBC)  
 6: B. cenocepacia (PHBC)  
 7: B. mallei (PHAC)  
 8: B. multivorans (BMUL\_1483)  
 10: B. multivorans (BMUL\_01759)  
 11: B. pseudomallei (PHBC)  
 12: B. pseudomallei (BPSS1954)  
 13: L. pneumophila (lpg1059)  
 14: L. pneumophila (lpg1089)  
 15: L. pneumophila (lpg2860)  
 16: L. pneumophila (lpg2860)  
 17: L. borgpetersenii (LBI\_2632)  
 18: L. borgpetersenii (LBI\_2632)  
 19: M. abscessus (MAB\_2034)  
 19: M. abscessus (MAB\_2348)  
 20: M. avium (MAP1389)  
 21: M. kansasii (MIKAN1\_010100013815)  
 21: M. kansasii (MIKAN1\_010100013815)  
 22: M. leprea (ML1348)  
 23: M. tuberculosis (MT1723)  
 24: N. farcinica (NFA\_45720)  
 25: P. aeruginosa (PhaC1)  
 26: P. aeruginosa (PhaC2)  
 27: R. equi (REQ\_24810)  
 28: R. prowazekii (ERP280)  
 28: R. prowazekii (ERP280)  
 29: R. typhi (PHBC)  
 30: S. rugosus (HMPREF0336\_01483)  
 31: S. maltophilia (SMAL\_2415)  
 32: V. cholera (VC\_A0688)  
 33: V. vulnificus (VV2\_0739)

Supplementary Figure 2.2. (Continued).





**Supplementary Table 2.1. Protein identification of fusion proteins by MALDI-TOF MS.**

<b>PhaC1<sub>Pa</sub></b>								
Peptide no.	<i>M<sub>r</sub></i>				Miss <sup>a)</sup>	Score <sup>b)</sup>	Expected <sup>c)</sup>	Peptide <sup>d)</sup>
		Observed	Exptl	Calculated				
4	960.5614	959.5541	959.54	1	20	0.0094	R.GKDLLTSAR.M	
6	1123.6532	1122.6459	1122.6397	0	45	3.30E-05	K.SLLDGLGHLAK.D	
7	1180.6414	1179.6341	1179.64	0	55	2.90E-06	R.HVAHFSLLELK.N	
8	1230.6066	1229.5993	1229.5968	0	51	8.00E-06	K.FYVFDLSPDK.S	
11	1277.6785	1276.6712	1276.6776	0	58	1.60E-06	K.NLATTEGAVVFR.N	
12	1306.6865	1305.6792	1305.683	0	71	7.90E-08	R.NGVQTFIVSWR.N	
15	1375.6666	1374.6593	1374.6754	1	23	0.0055	R.YMQTYLAWRK.E + Oxidation (M)	
17	1552.7399	1551.7326	1551.7358	0	54	3.60E-06	R.FSDPAWSQNPLYK.R	
18	1570.84	1569.8327	1569.8555	0	114	3.80E-12	R.LPAALHGEFVELFK.S	
21	1657.8287	1656.8214	1656.8512	1	77	2.00E-08	K.FYVFDLSPDKSLAR.F	
22	1708.8257	1707.8184	1707.8369	1	54	3.80E-06	R.FSDPAWSQNPLYKR.Y	
23	1722.9229	1721.9156	1721.9424	0	81	2.50E-08	K.QAAENTLNLNPVIGIR.G	
25	1746.9027	1745.8954	1745.9213	1	51	7.70E-06	R.NGVQTFIVSWRNPTK.S	
26	2078.094	2077.0867	2077.1167	0	128	1.50E-13	K.SNPLNRPGALEVSGTPIDLK.Q	
28	2106.988	2105.9807	2106.013	0	137	2.00E-14	K.ELHSWISHSDLSPQDISR.G	
29	2148.9773	2147.97	2148.0078	0	95	2.90E-10	K.HADSWWLHWQQLAER.S	
32	2254.9692	2253.9619	2253.9882	0	27	0.0021	K.DLVNNGMPSQVDMDAFEVVGK.N + 2 Oxidation (M)	
34	2618.2908	2617.2835	2617.3421	0	134	4.00E-14	R.GQFVINLLTEAMSPNTLSNPAAVK.R + Oxidation (M)	
35	2618.293	2617.2857	2617.3421	0	136	2.30E-14	R.GQFVINLLTEAMSPNTLSNPAAVK.R + Oxidation (M)	
36	2945.4719	2944.4646	2944.5155	1	26	0.0028	R.HVAHFSLLELKNVLLGQSELRPGDDDR.R	

<b>Ag-PhaC1<sub>Pa</sub></b>								
Peptide no.	<i>M<sub>r</sub></i>				Miss <sup>a)</sup>	Score <sup>b)</sup>	Expected <sup>c)</sup>	Peptide <sup>d)</sup>
		Observed	Exptl	Calculated				
1	808.4259	807.4186	807.4351	0	48	1.50E-05	R.QPLHSAR.H	
2	808.4373	807.43	807.4351	0	40	9.70E-05	R.QPLHSAR.H	
6	902.4549	901.4476	901.4657	0	35	0.00034	K.AWLEQAGK.H	
7	945.5485	944.5412	944.5477	0	16	2.70E-02	R.MVLLQAVR.Q + Oxidation (M)	
8	960.5267	959.5194	959.54	1	33	5.20E-04	R.GKDLLTSAR.M	
9	1018.5068	1017.4995	1017.5091	0	36	2.30E-04	R.LTATEDAAAAR.A	
10	1102.5591	1101.5518	1101.5527	1	62	5.60E-07	R.RVENATAEGR.A	
11	1123.6243	1122.617	1122.6397	0	65	3.30E-07	K.SLLDGLGHLAK.D	
12	1123.6356	1122.6283	1122.6397	0	54	4.00E-06	K.SLLDGLGHLAK.D	
13	1180.6248	1179.6175	1179.64	0	64	4.10E-07	R.HVAHFSLLELK.N	
14	1230.5981	1229.5908	1229.5968	0	47	2.10E-05	K.FYVFDLSPDK.S	
16	1277.6775	1276.6702	1276.6776	0	52	6.70E-06	K.NLATTEGAVVFR.N	
17	1306.6832	1305.6759	1305.683	0	82	6.90E-09	R.NGVQTFIVSWR.N	
18	1316.6763	1315.669	1315.6844	1	30	9.30E-04	R.IATGKQNATAEGR.A	
20	1389.6586	1388.6513	1388.6646	0	44	4.20E-05	R.FMTNPELPAEPK.A + Oxidation (M)	
21	1552.7253	1551.718	1551.7358	0	50	1.10E-05	R.FSDPAWSQNPLYK.R	
22	1552.7335	1551.7262	1551.7358	0	29	0.0013	R.FSDPAWSQNPLYK.R	
23	1570.8461	1569.8388	1569.8555	0	121	8.00E-13	R.LPAALHGEFVELFK.S	
25	1657.8307	1656.8234	1656.8512	1	24	3.60E-03	K.FYVFDLSPDKSLAR.F	
26	1657.8418	1656.8345	1656.8512	1	32	6.80E-04	K.FYVFDLSPDKSLAR.F	
27	1722.9312	1721.9239	1721.9424	0	66	7.80E-07	K.QAAENTLNLNPVIGIR.G	
28	1806.8674	1805.8601	1805.8907	2	48	1.50E-05	R.ADEAYRKADEALGAAQK.A	
30	1939.9419	1938.9346	1938.9871	1	46	2.40E-05	K.NVLLGQSELRPGDDDRR.F	
31	1939.965	1938.9577	1938.9871	1	35	2.90E-04	K.NVLLGQSELRPGDDDRR.F	
32	1958.9553	1957.948	1957.9817	1	32	0.0027	R.RPGEENVLNTTTTVDVDRR.I	
33	2078.0969	2077.0896	2077.1167	0	96	2.40E-10	K.SNPLNRPGALEVSGTPIDLK.Q	
34	2106.9761	2105.9688	2106.013	0	110	1.00E-11	K.ELHSWISHSDLSPQDISR.G	
35	2106.9861	2105.9788	2106.013	0	50	1.00E-05	K.ELHSWISHSDLSPQDISR.G	

<b>PhaC1<sub>Pa</sub>-Ag</b>								
Peptide no.	<i>M<sub>r</sub></i>				Miss <sup>a)</sup>	Score <sup>b)</sup>	Expected <sup>c)</sup>	Peptide <sup>d)</sup>
		Observed	Exptl	Calculated				
1	945.5907	944.5834	944.5477	0	19	0.012	R.MVLLQAVR.Q + Oxidation (M)	
3	1018.5368	1017.5295	1017.5091	0	76	2.30E-08	R.LTATEDAAAAR.A	
4	1018.5511	1017.5438	1017.5091	0	70	9.40E-08	R.LTATEDAAAAR.A	
6	1102.5912	1101.5839	1101.5527	1	76	2.60E-08	R.RVENATAEGR.A	
8	1128.7003	1127.693	1127.6662	1	39	0.00013	R.GSVLVAIDKRG	
9	1180.6682	1179.6609	1179.64	0	71	7.90E-08	R.HVAHFSLLELK.N	
10	1232.594	1231.5867	1231.5429	0	62	7.00E-07	K.AQQTADAEANER.A	
11	1247.6101	1246.6028	1246.5805	0	21	8.50E-03	R.YMQTYLAWRK.K + Oxidation (M)	
13	1277.7007	1276.6934	1276.6776	0	88	1.50E-09	K.NLATTEGAVVFR.N	
14	1306.7054	1305.6981	1305.683	0	79	1.30E-08	R.NGVQTFIVSWR.N	
17	1389.688	1388.6807	1388.6646	0	66	2.80E-07	R.FMTNPELPAEPK.A + Oxidation (M)	
20	1552.7488	1551.7415	1551.7358	0	94	4.40E-10	R.FSDPAWSQNPLYK.R	
21	1570.871	1569.8637	1569.8555	0	110	9.20E-12	R.LPAALHGEFVELFK.S	
22	1657.8372	1656.8299	1656.8512	1	42	6.20E-05	K.FYVFDLSPDKSLAR.F	
23	1675.8689	1674.8616	1674.8649	2	33	0.0005	R.RVENLTTTVDVDRR.I	
26	1718.818	1717.8107	1717.806	0	88	1.60E-09	K.TYPAGEAAPTGYVHER.G	
27	1783.8763	1782.869	1782.886	0	35	3.30E-04	K.NVLLGQSELRPGDDDRR.R	
28	1939.9861	1938.9788	1938.9871	1	60	1.10E-06	K.NVLLGQSELRPGDDDRR.F	
29	2078.1182	2077.1109	2077.1167	0	136	2.30E-14	K.SNPLNRPGALEVSGTPIDLK.Q	
31	2107.0269	2106.0196	2106.013	0	139	1.30E-14	K.ELHSWISHSDLSPQDISR.G	
32	2148.9878	2147.9805	2148.0078	0	39	1.20E-04	K.HADSWWLHWQQLAER.S	
33	2254.9812	2253.9739	2253.9882	0	60	1.10E-06	K.DLVNNGMPSQVDMDAFEVVGK.N + 2 Oxidation (M)	
34	2618.3159	2617.3086	2617.3421	0	96	2.70E-10	R.GQFVINLLTEAMSPNTLSNPAAVK.R + Oxidation (M)	
35	2618.3567	2617.3494	2617.3421	0	170	9.10E-18	R.GQFVINLLTEAMSPNTLSNPAAVK.R + Oxidation (M)	
36	3509.9448	3508.9375	3508.9406	0	74	4.00E-08	R.NDVLELIQYRPITESVHERPLLVPQINK.F	

a) The number of missed cleavage sites.

b) The score is the  $-\log_{10}(P)$  value, where P is the probability that the observed match is a random event. Individual ion scores of  $>56$  indicate identity or extensive homology ( $P \leq 0.05$ ).

c) Expected score based on BLAST search.

d) The sequence between the peptides was identified by MS. The amino acid before the period at the N terminal and that after the period at the C terminal indicate the cleavage sites.

**Supplementary Table 2.2.** Protein identification of dominant HCPs by peptide finger printing using MALDI-TOF MS.

<b>Band I</b>								
Peptide no.	$M_r$				Miss <sup>a)</sup>	Score <sup>b)</sup>	Expected <sup>c)</sup>	Peptide <sup>d)</sup>
		Observed	Exptl	Calculated				
1	808.4307	807.4235	807.4715	0	55	0.24	KPLHSAR	
2	828.4216	827.4143	827.4137	0	35	24	QNAAQAPK + Deamidated (NQ)	
3	853.4464	852.4391	852.4276	0	3.20E+01	63	EMALHPR	
4	860.3954	859.3881	859.3824	0	2.90E+01	1.70E+02	NFSSYSR	
5	906.4799	905.4726	905.4429	0	3.10E+01	1.70E+02	CGFPDVIR	
6	945.5456	944.5383	944.5113	1	41	20	NMPLKGR + Deamidated (NQ); Oxidation (M)	
7	1018.5084	1017.5011	1017.509	0	6.30E+01	0.13	LTATENAAAR + Deamidated (NQ)	
8	1078.5586	1077.5513	1077.5607	0	47	5.2	EVVQGFPPR	
9	1089.5977	1088.5904	1088.5462	1	33	1.30E+02	LRQTPPTSDA	
10	1102.5491	1101.5418	1101.5778	0	5.80E+01	0.35	AGVSSPAGTTVR	
11	1123.6383	1122.631	1122.6397	0	58	2.10E-01	K.SLLDGLGHLAK.D	
12	1180.6326	1179.6253	1179.64	0	65	0.054	R.HVAHFSLELK.N	
13	1230.5875	1229.5802	1229.509	0	54	0.84	MNMMDLSALR + Deamidated (NQ); 3 Oxidation (M)	
14	1247.5771	1246.5698	1246.6517	1	38	33	ANSSALSAIEKR + Deamidated (NQ)	
15	1262.6642	1261.6569	1261.6666	0	73	0.013	R.NDVLELIQYR.A	
16	1277.6748	1276.6675	1276.6776	0	98	4.20E-05	K.NLATTEGAVVFR.N	
17	1289.6681	1288.6608	1288.7139	0	3.50E+01	87	NLALTEGAVVFR	
18	1306.6881	1305.6808	1305.683	0	68	0.04	R.NGVQTFIVSWR.N	
19	1318.6893	1317.682	1317.6347	0	2.60E+01	6.40E+02	AAITAMPSQASDR	
20	1338.6746	1337.6673	1337.6762	1	3.20E+01	1.50E+02	VAACDLAGKSTFR	
21	1409.6619	1408.6546	1408.6623	1	60	0.21	WSELEEFDKR	
22	1421.6638	1420.6565	1420.6946	1	4.50E+01	6.4	ERELEELGYQR	
23	1552.7418	1551.7345	1551.7358	0	77	0.0046	R.FSDPAWSQNPLYK.R	
24	1620.7782	1619.7709	1619.7791	0	91	0.00024	R.LSDNPDYTAIINER.Q	
25	1687.8799	1686.8726	1686.8835	1	37	54	NGRMGVAELASSLGVAR	
26	1705.915	1704.9077	1704.9887	1	34	1.00E+02	DVPANTLVAGVPAVVKR	
27	1722.9327	1721.9254	1721.9424	0	125	7.30E-08	K.QAAENTLNLNPFVIGIR.G	
28	1792.9099	1791.9026	1791.9057	0	2.90E+01	3.50E+02	GGFAYGPHQVLLSYQR	
29	1792.9309	1791.9236	1791.9057	0	47	6.1	GGFAYGPHQVLLSYQR	
30	1877.9371	1876.9298	1876.9319	0	109	4.30E-06	R.VGDVPFETPVVIQGNRSR.L	
31	1939.9679	1938.9606	1938.9871	1	75	9.20E-03	K.NVLLGQSELRPDQDDRR.F	
32	2106.9988	2105.9915	2106.013	0	144	1.30E-09	K.ELHSWISHSDLSPODISR.G	
33	2107.0269	2106.0196	2106.013	0	-143	1.40E-09	K.ELHSWISHSDLSPODISR.G	
34	2254.9941	2253.9868	2253.9882	0	123	1.10E-07	K.DLVNNGGMPQVMDAFEVVGK.N+ 2Oxidation (M)	
35	2618.3281	2617.3208	2617.3421	0	116	7.40E-07	R.GQFVINLLTEAMSPNTLSNPAAVK.R+Oxidation(M)	
36	3509.9463	3508.939	3508.9406	0	72	1.20E-02	R.NDVLELIQYRPITESVHERPLLVPPQINK.F	

<b>Band II</b>								
Peptide no.	$M_r$				Miss <sup>a)</sup>	Score <sup>b)</sup>	Expected <sup>c)</sup>	Peptide <sup>d)</sup>
		Observed	Exptl	Calculated				
1	828.4369	827.4296	827.4137	0	43	4.1	NEIQAPR + Deamidated (NQ)	
2	888.4688	887.4615	887.4461	0	29	2.90E+02	NANINSVR + Deamidated (NQ)	
3	929.4977	928.4905	928.5342	0	51	1.5	AELVGTLAR	
4	945.5476	944.5403	944.4749	0	38	34	LPTNGLACR + Deamidated (NQ)	
5	960.5375	959.5302	959.5036	0	52	1.3	AQVGVATSAR + Deamidated (NQ)	
6	975.5542	974.5469	974.5549	0	54	0.8	FEQLVALR	
7	986.5489	985.5416	985.4968	0	33	1.10E+02	EPSLAEIDL	
8	993.5276	992.5203	992.508	0	41	16	DFFKPSPR	
9	1079.5712	1078.5639	1078.5771	0	47	4.6	SAYVSGVIR	
10	1123.6278	1122.6205	1122.6397	0	52	0.97	SLLDGLGHLAK	
11	1142.6404	1141.6331	1141.6455	0	50	1.9	GIGAAIAQTLAR + Deamidated (NQ)	
12	1142.6411	1141.6338	1141.6455	0	74	0.008	R.GIGAAIAETLAR.D	
13	1149.6171	1148.6098	1148.619	0	57	0.42	K.AVLFDAAGLTR.F	
14	1158.5688	1157.5615	1157.5676	0	49	2.5	GAEDQLEGALR	
15	1180.6403	1179.633	1179.64	0	55	0.62	HVAHFSLELK	
16	1194.6215	1193.6142	1193.6193	0	46	4.8	YIAFANSPVGR	
17	1230.5911	1229.5838	1229.5968	0	47	4.6	FVYFDLSPDK	
18	1247.5825	1246.5752	1246.5805	0	33	1.00E+02	YMQTYLAWR + Oxidation (M)	
19	1262.6631	1261.6558	1261.6666	0	56	0.73	NDVLELIQYR	
20	1277.6764	1276.6691	1276.6776	0	95	7.80E-05	K.NLATTEGAVVFR.N	
21	1289.6682	1288.6609	1288.7139	0	41	23	NLALTEGAVVFR	
22	1306.686	1305.6787	1305.683	0	103	1.40E-05	R.NGVQTFIVSWR.N	
23	1318.6794	1317.6721	1317.616	0	28	4.00E+02	AAIAANQTQADSR + 2 Deamidated (NQ)	
24	1450.782	1449.7747	1449.7827	0	78	0.0038	R.DGAEVVLVDVPPAR.E	
25	1559.8	1558.7927	1558.8719	0	33	1.60E+02	LLNSLFATSEVPIR	
26	1705.9141	1704.9068	1704.8869	1	32	1.70E+02	AEKATQVPLMGEIYR	
27	1705.9148	1704.9075	1705.0111	2	37	57	RTAIDKRPVAGVAVR	
28	1722.9375	1721.9302	1721.9424	0	128	3.30E-08	K.QAAENTLNLNPFVIGIR.G	
29	1783.8733	1782.866	1782.886	0	43	13	NVLLGQSELRPDQDDRR	
30	1848.9384	1847.9311	1847.9418	0	150	3.20E-10	K.LTDVAVFAVDGQFELPR.W	
31	1939.973	1938.9657	1938.9871	1	56	0.67	K.NVLLGQSELRPDQDDRR.F	
32	2247.2532	2246.2459	2246.2747	1	48	3.2	VVVLGRPPSELKDPVTASVQR	
33	2490.3936	2489.3863	2489.4006	0	102	1.40E-05	R.VRPVDGPLVIGGSGALAEAVLPFAGK.L	
34	2618.3447	2617.3374	2617.3421	0	118	5.00E-07	R.GQFVINLLTEAMSPNTLSNPAAVK.R+Oxidation(M)	
35	3509.926	3508.9187	3508.9406	0	78	0.0036	R.NDVLELIQYRPITESVHERPLLVPPQINK.F	
36	3509.9485	3508.9412	3508.9406	0	-66	0.055	R.NDVLELIQYRPITESVHERPLLVPPQINK.F	

a) The number of missed cleavage sites.

b) The score is the  $-\log_{10}(P)$  value, where P is the probability that the observed match is a random event. Individual ion scores of  $>56$  indicate identity or extensive homology ( $P \leq 0.05$ ).

c) Expected score based on BLAST search.

d) The sequence between the peptides was identified by MS. The amino acid before the period at the N terminal and that after the period at the C terminal indicate the cleavage sites.

Supplementary Table 2.2. (Continued).

Band III							
Peptide no.	$M_r$			Miss <sup>a)</sup>	Score <sup>b)</sup>	Expected <sup>c)</sup>	Peptide <sup>d)</sup>
	Observed	Exptl	Calculated				
1	808.4261	807.4188	807.4351	0	50	0.81	R.QPLHSAR.H
2	887.4237	886.4164	886.4185	0	33	62	YFTNSVR + Deamidated (NQ)
3	945.5349	944.5276	944.5841	1	45	8.30E+00	MVLLKAVR + Oxidation (M)
4	960.5441	959.5369	959.5036	0	54	0.95	AGDGLTITGR
5	1024.5002	1023.4929	1023.4985	0	44	6.7	TLQSEFSGR
6	1089.5287	1088.5214	1088.576	1	35	67	RPGMKTNLR + Deamidated (NQ); Oxidation (M)
7	1102.5559	1101.5486	1101.603	0	50	2.10E+00	VTLAGQSLGK
8	1102.5585	1101.5512	1101.5526	1	49	3.2	AERAATAAAGR
9	1123.641	1122.6337	1122.6397	0	65	4.00E-02	K.SLLDGLGHLAK.D
10	1180.6158	1179.6085	1179.64	0	66	0.053	R.HVAHFSELEK.N
11	1192.6191	1191.6118	1191.6573	0	44	8.90E+00	VPMLFLESELK + Oxidation (M)
12	1230.588	1229.5807	1229.5968	0	50	2.20E+00	FYVFDLSPDK
13	1247.5695	1246.5622	1246.5805	0	39	21	YMQTYLAWR + Oxidation (M)
14	1262.6544	1261.6471	1261.6666	0	69	0.035	R.NDVLELIQYR.A
15	1277.6613	1276.654	1276.6776	0	98	4.30E-05	K.NLATTEGAVVFR.N
16	1289.6799	1288.6726	1288.7139	0	42	1.50E+01	NLALTEGAVVFR
17	1306.6748	1305.6675	1305.683	0	99	3.30E-05	R.NGVQTFIVSWR.N
18	1329.5942	1328.5869	1328.6077	0	51	1.1	K.YYFTENFFAK.A
19	1338.6759	1337.6686	1337.7667	0	30	2.10E+02	TTQLPAVVGSPR
20	1406.6688	1405.6615	1405.6838	0	101	2.10E-05	R.DVLVNEYGVEGGR.V
21	1552.7375	1551.7302	1551.7358	0	67	0.053	R.FSDPAWSQNPLYK.R
22	1562.781	1561.7737	1561.7525	0	34	1.10E+02	LVQGFDEAVWNGAR + Deamidated (NQ)
23	1562.788	1561.7807	1561.7848	1	35	8.70E+01	QSQLQRLQAFQGR + 3 Deamidated (NQ)
24	1705.924	1704.9167	1704.9649	2	38	3.60E+01	GVGFRHGGGLRGPGLLR
25	1722.9219	1721.9146	1721.9424	0	127	5.30E-08	K.QAAENTLNLNPVIGIR.G
26	1783.8738	1782.8665	1782.886	0	53	1.3	K.NVLLGQSELRPQDDRR.R
27	1921.9922	1920.9849	1921.0268	2	32	1.80E+02	VQPSLEPNKKAPKPGSR + 2 Deamidated (NQ)
28	1939.959	1938.9517	1938.9871	1	63	0.15	K.NVLLGQSELRPQDDRR.F
29	2107.0146	2106.0073	2106.013	0	130	2.90E-08	K.ELHSWISHSDLSPQDISR.G
30	2132.9958	2131.9885	2132.0246	0	115	9.20E-07	R.VNAVGYGESRPVADNATAEGR.A
31	2278.2817	2277.2744	2277.1531	1	23	1.00E+03	MVKALGADCVGMSTVPEVIVAR + 2 Oxidation (M)
32	2311.2021	2310.1948	2310.2114	1	37	55	AGIVTLQARCSVIAAANPVGGR + Carbamidomethyl (C); 2 Deamidated (NQ)
33	2431.1848	2430.1775	2430.3006	2	24	1.20E+03	VEAVVADDGKIVFVGKEEQALK
34	2586.1782	2585.1709	2585.1518	0	162	1.70E-11	K.QYPSTSTTVEGHTDSVGTDAYNQK.L
35	2618.3262	2617.3189	2617.3421	0	155	9.70E-11	R.GQFVINLLTEAMSPNTLSLNPAAVK.R + Oxidation (M)
36	3509.9482	3508.9409	3508.9406	0	98	2.90E-05	R.NDVLELIQYRPITESVHERPLLVVPPQINK.F

Band IV							
1	828.3899	827.3826	827.429	1	42	3	AGKYAYR
2	849.4656	848.4584	848.4062	0	32	1.10E+02	NQACTIAK + Deamidated (NQ)
3	907.4406	906.4333	906.4229	0	22	1.10E+03	SGAGAEMLR + Oxidation (M)
4	914.4651	913.4578	913.5233	0	28	2.00E+02	VGLLENLR + Deamidated (NQ)
5	934.4504	933.4431	933.4767	1	34	8.20E+01	SSNELKAGK + Deamidated (NQ)
6	973.4255	972.4182	972.4512	0	21	5.60E+02	LDNAPQASR + 2 Deamidated (NQ)
7	973.4382	972.431	972.4876	0	29	1.20E+02	NAAPSPSEAK
8	1064.5614	1063.5541	1063.5298	0	39	2.80E+01	LSNFGQLR + Deamidated (NQ)
9	1180.6057	1179.5984	1179.64	0	42	13	HVAHFSELEK
10	1211.605	1210.5977	1210.5805	0	32	1.10E+02	LVAMSFQWQR + Deamidated (NQ); Oxidation (M)
11	1223.6154	1222.6081	1222.6743	1	34	9.50E+01	KMEYLLSALR
12	1223.6355	1222.6282	1222.5829	1	31	1.80E+02	KEYDQLSPSR + Deamidated (NQ)
13	1232.5498	1231.5425	1231.623	1	31	1.20E+02	RGVVMNLSNPK + 2 Deamidated (NQ); Oxidation (M)
14	1232.5765	1231.5692	1231.6482	1	30	2.20E+02	KGILMNLNPK + 2 Deamidated (NQ); Oxidation (M)
15	1247.5802	1246.5729	1246.634	1	27	4.00E+02	VVEMNLDAKGR + Oxidation (M)
16	1263.6379	1262.6306	1262.6506	0	32	1.60E+02	NIELAINSFNK + Deamidated (NQ)
17	1277.6837	1276.6764	1276.7	0	33	1.30E+02	IDIHRPAQTR
18	1306.6764	1305.6691	1305.683	0	53	1.3	NGVQTFIVSWR
19	1306.6862	1305.6789	1305.683	0	47	5.20E+00	NGVQTFIVSWR
20	1329.61	1328.6027	1328.6758	0	34	68	ALAAMETSVPAWR + Oxidation (M)
21	1389.6544	1388.6471	1388.6646	0	64	0.086	R.FMTNPELPAEPK.A + Oxidation (M)
22	1405.6636	1404.6563	1404.7473	0	24	1.00E+03	LLAQINPHTQR + Deamidated (NQ)
23	1440.7407	1439.7334	1439.7521	0	60	2.20E-01	FHIDQVLALNDR
24	1464.6908	1463.6835	1463.6674	1	38	3.70E+01	KTAGQMNSATANPR + 2 Deamidated (NQ); Oxidation (M)
25	1528.7229	1527.7156	1527.7239	1	64	0.095	R.SYQSGVLEKDMAK.V + Oxidation (M)
26	1528.7593	1527.752	1527.798	1	30	2.50E+02	RHAEGALEFMLVR
27	1570.8456	1569.8383	1569.8555	0	123	1.10E-07	R.LPAALHGFEVLEFK.S
28	1586.829	1585.8217	1585.8174	0	41	2.00E+01	LPAALHGELVEMYK + Oxidation (M)
29	1586.8409	1585.8336	1585.8174	0	43	1.30E+01	LPAALHGELVEMYK + Oxidation (M)
30	1683.8477	1682.8404	1682.7426	1	23	1.30E+03	TVMNCNICVVKDGR + Deamidated (NQ); Oxidation (M)
31	1718.7946	1717.7873	1717.806	0	129	3.40E-08	K.TYPAGEAAPTGYVHER.-
32	2078.0981	2077.0908	2077.1167	0	126	7.70E-08	K.SNPLNRPGALEVSGTPIDLK.Q
33	2090.0444	2089.0371	2088.982	0	23	1.50E+03	SGHGMGVEIIANAMQTLQK + 2 Deamidated(NQ);Oxidation (M)
34	2148.9944	2147.9871	2148.0078	0	103	1.50E-05	K.HADSWWLHWQQLAER.S
35	2180.9885	2179.9812	2179.9864	0	24	1.20E+03	HADSWWLHWQQWITER + 2 Deamidated (NQ)
36	2422.1897	2421.1824	2421.2111	0	100	3.30E-05	K.CEFILSNSGHIQSILNPPGNPK.A + Carbamidomethyl (C)

a) The number of missed cleavage sites.

b) The score is the  $-\log_{10}(P)$  value, where P is the probability that the observed match is a random event. Individual ion scores of  $>56$  indicate identity or extensive homology ( $P \leq 0.05$ ).

c) Expected score based on BLAST search.

d) The sequence between the peptides was identified by MS. The amino acid before the period at the N terminal and that after the period at the C terminal indicate the cleavage sites.

**Supplementary Table 2.2. (Continued).**

<b>Band V</b>							
Peptide no.	$M_r$			Miss <sup>a)</sup>	Score <sup>b)</sup>	Expected <sup>c)</sup>	Peptide <sup>d)</sup>
	Observed	Exptl	Calculated				
1	803.4761	802.4688	802.4337	0	53	6.40E-01	SIAYPPR
2	817.3987	816.3915	816.3879	0	53	0.76	R.HSVGFDR.F
3	828.3979	827.3906	827.429	1	27	9.80E+01	KGAYAYR
4	828.4042	827.3969	827.3926	0	28	8.00E+01	GAQYAYR
5	891.3619	890.3546	890.3518	0	43	2.70E+00	HGDNEYR + Deamidated (NQ)
6	903.3601	902.3528	902.377	0	30	2.90E+01	YANDTYR + Deamidated (NQ)
7	924.4958	923.4885	923.4964	0	40	15	SSYVIEVK
8	939.4716	938.4643	938.428	0	29	1.80E+02	GLDGAMFGR + Oxidation (M)
9	951.488	950.4808	950.4743	0	33	9.40E+01	AITCTSNLK + Deamidated (NQ)
10	951.5015	950.4942	950.492	0	42	1.20E+01	SSTVSTELK
11	973.5695	972.5622	972.5577	2	43	1.10E+01	RITSGQRR
12	973.5701	972.5629	972.5716	1	37	4.50E+01	GVLTVSGGKR
13	983.5108	982.5035	982.4641	0	25	4.60E+02	INSTTTMSK + Deamidated (NQ)
14	1010.5897	1009.5824	1009.6535	1	36	2.20E+01	IIEAKVLPK
15	1119.5581	1118.5508	1118.5455	0	26	6.50E+02	INSINQSDVK + 2 Deamidated (NQ)
16	1163.6146	1162.6073	1162.6499	0	32	1.40E+02	GVFGSLPLFR
17	1193.6244	1192.6171	1192.6088	0	44	9.90E+00	AATNLFESALR + Deamidated (NQ)
18	1211.624	1210.6167	1210.5982	0	92	1.10E-04	R.FNDLFESALR.N
19	1222.6582	1221.6509	1221.6506	0	75	6.50E-03	M.SNAFSLAPLFR.H
20	1234.6425	1233.6352	1233.6466	0	41	21	VNAVFTAQTGR
21	1306.6952	1305.6879	1305.683	0	60	2.50E-01	NGVQTFIVSWR
22	1334.7163	1333.709	1333.7506	1	34	9.40E+01	KIWLALGLAYS
23	1409.7491	1408.7418	1408.7422	0	60	2.10E-01	R.IAINGORPALDNQ.-
24	1421.6964	1420.6891	1420.6834	0	39	34	LDVATGEAIDFDR
25	1421.6973	1420.69	1420.6834	0	41	2.10E+01	LNVATGEAIDFDR + Deamidated (NQ)
26	1539.8849	1538.8776	1538.878	0	151	1.20E-10	K.AASLANGLLNIDLVR.L
27	1551.8749	1550.8676	1550.9396	0	46	4.90E+00	VAGGIAAISGVGILAGLI
28	1568.7222	1567.7149	1567.7154	0	40	2.00E+01	NEAGSTYPPYNEVK
29	1580.7244	1579.7171	1579.7816	1	25	6.40E+02	GGGGTGGGGSTGPVPPGRR
30	1580.7321	1579.7248	1579.7729	0	26	5.90E+02	EELAYQSAGLLTR + Deamidated (NQ)
31	1683.8401	1682.8328	1682.8992	0	29	3.50E+02	VVQGTGNVGLFHVVVGAGK + 2 Deamidated (NQ)
32	1702.8475	1701.8402	1701.8434	0	120	2.60E-07	K.STDNVTVLHQGIAQR.A
33	1718.8398	1717.8325	1717.837	2	38	4.50E+01	SDKDAEQVIAEKQEK + Deamidated (NQ)
34	2009.9786	2008.9713	2008.9755	1	95	1.00E-04	R.HSVGFDRFNDLFESALR.N
35	2116.0906	2115.0833	2115.0848	0	182	1.90E-13	R.IVIAAGFQEEDLDLQVER.G
36	2132.0823	2131.075	2131.0909	1	35	96	GDVIALGFNQELDDLRSIR + Deamidated (NQ)

<b>Band VI</b>							
1	852.4163	851.409	851.3773	0	39	1.70E+01	EGEAYGAR
2	908.4755	907.4682	907.4433	0	39	2.30E+01	EASTMTR
3	918.4775	917.4703	917.4276	0	22	1.50E+03	MNEPSLAR + Deamidated (NQ)
4	950.4763	949.469	949.4691	0	24	8.50E+02	LDFVTCPR
5	973.4709	972.4636	972.4876	0	44	7.70E+00	ADEALGAAQK
6	979.588	978.5807	978.5862	0	48	1.30E+00	LHIINLEK
7	1018.5156	1017.5083	1017.5091	0	80	2.40E-03	R.LTATEDAAAR.A
7	1018.5156	1017.5083	1017.509	0	82	1.50E-03	LTATENAAAR + Deamidated (NQ)
8	1030.5343	1029.527	1029.5567	1	53	1.2	RASTPSAAAQK
9	1078.5746	1077.5673	1077.5818	0	42	13	GSFLSINAIR + Deamidated (NQ)
10	1101.589	1100.5817	1100.5826	1	69	0.033	R.KADEALGAAQK.A
11	1109.5554	1108.5481	1108.5526	0	69	2.50E-02	K.VGAHFHQTR.Y
12	1119.5812	1118.5739	1118.5203	0	42	1.70E+01	ANAQTAVSEAR + 2 Deamidated (NQ)
13	1149.6067	1148.5994	1148.6189	0	32	1.60E+02	IPPNDPNLLR + Deamidated (NQ)
14	1166.5988	1165.5915	1165.5914	0	31	1.50E+02	SLACGGNIYR
15	1221.7104	1220.7031	1220.6401	0	42	8.30E+00	ELLFSGGELTR
16	1232.5547	1231.5474	1231.5429	0	91	1.40E-04	K.AQQTADANER.A
17	1244.569	1243.5617	1243.568	0	34	5.80E+01	EPLTDAENAQR + Deamidated (NQ)
18	1306.6948	1305.6875	1305.683	0	75	8.20E-03	R.NGVQTFIVSWR.N
19	1323.6692	1322.6619	1322.65	1	25	7.10E+02	MSETKTEAAAIR + Oxidation (M)
20	1338.6755	1337.6682	1337.6874	2	31	2.00E+02	SRGNKGGFMVIR + Deamidated (NQ); Oxidation (M)
21	1409.7516	1408.7443	1408.7674	1	28	3.50E+02	LAQRVVLVSNGLT + 2 Deamidated (NQ)
22	1418.8083	1417.801	1417.7426	1	45	5.90E+00	RPVRRDASLSFR
23	1442.7574	1441.7501	1441.7024	0	26	5.50E+02	IPAAQFDGMHFVK + Deamidated (NQ)
24	1505.7699	1504.7626	1504.7674	0	54	1.20E+00	YLALLPYTDSHGR
25	1539.8627	1538.8554	1538.878	0	-70	1.80E-02	K.AASLANGLLNIDLVR.L
26	1539.8654	1538.8581	1538.878	0	71	1.50E-02	K.AASLANGLLNIDLVR.L
27	1586.8965	1585.8892	1585.9192	1	42	1.30E+01	ERVVPSIYLVNGIK
28	1586.9182	1585.9109	1585.9192	1	36	4.60E+01	ERVVPSIYLVNGIK
29	1619.8271	1618.8198	1618.7621	0	36	7.10E+01	LSGGGGGGLTVCLIEDER
30	1667.8622	1666.8549	1666.8389	0	40	2.90E+01	TLPMFNEALTFVER
31	1683.8398	1682.8325	1682.8338	0	83	1.20E-03	K.TLPMFNEALTFVER.L + Oxidation (M)
32	1699.8374	1698.8301	1698.8974	0	26	6.40E+02	VITGGIIGPATTMNER + Deamidated (NQ)
33	1806.891	1805.8837	1805.8907	2	119	4.10E-07	R.ADEAYRKADALGAAQK.A
34	2024.9935	2023.9862	2023.9792	0	108	4.70E-06	K.GYGFITPESGPDVVFHFR.A
35	2078.1113	2077.104	2077.1167	0	78	0.0039	K.SNPLNRPGALEVSGETPDLK.Q
36	2206.2007	2205.1934	2205.0293	0	21	2.00E+03	MPIMTETAVAEEASLPQAGR + Deamidated (NQ); 2 Oxidation (M)

a) The number of missed cleavage sites.

b) The score is the  $-\log_{10}(P)$  value, where P is the probability that the observed match is a random event. Individual ion scores of  $>56$  indicate identity or extensive homology ( $P \leq 0.05$ ).

c) Expected score based on BLAST search.

d) The sequence between the peptides was identified by MS. The amino acid before the period at the N terminal and that after the period at the C terminal indicate the cleavage sites.

**Supplementary Table 2.2. (Continued).**

<b>Band VII</b>							
Peptide no.	$M_r$			Miss <sup>a)</sup>	Score <sup>b)</sup>	Expected <sup>c)</sup>	Peptide <sup>d)</sup>
	Observed	Exptl	Calculated				
1	808.4423	807.435	807.4715	0	50	8.20E-01	KPLHSAR
2	929.554	928.5467	928.5342	0	38	3.30E+01	LLEAGATVR
3	945.5618	944.5545	944.5841	1	47	4.00E+00	MVLLKAVR + Oxidation (M)
4	960.5502	959.5429	959.4924	0	42	1.30E+01	QGDIIITANK + Deamidated (NQ)
5	1018.5213	1017.514	1017.509	0	62	1.50E-01	LTATENAAAAR + Deamidated (NQ)
6	1102.5682	1101.5609	1101.5414	0	54	1.00E+00	NIENVTAQGR + Deamidated (NQ)
7	1128.6777	1127.6704	1127.6523	2	45	4.60E+00	RSSPVALSRR
8	1180.6552	1179.6479	1179.64	0	69	2.30E-02	R.HVAHFSLLELK.N
9	1194.6394	1193.6321	1193.604	1	36	5.30E+01	GIGYLSKDDAR
10	1201.5947	1200.5874	1200.6536	1	37	4.40E+01	LDMKLNGLPGK + Oxidation (M)
11	1230.6115	1229.6042	1229.5968	0	56	5.30E-01	K.FYVFDLSPDK.S
12	1247.6042	1246.5969	1246.5805	0	36	6.40E+01	YMQTYLAWR + Oxidation (M)
13	1262.6844	1261.6771	1261.6666	0	55	8.10E-01	NDVLELIQYR
14	1277.6947	1276.6874	1276.6776	0	104	9.30E-06	K.NLATTEGAVVFR.N
15	1289.6853	1288.678	1288.7139	0	39	3.50E+01	NLALTEGAVVFR
16	1306.7017	1305.6944	1305.683	0	91	2.00E-04	R.NGVQTFIVSWR.N
17	1318.6924	1317.6851	1317.6131	0	33	1.20E+02	AGVMMIMGTTYK + Oxidation (M)
18	1318.6984	1317.6911	1317.6929	0	34	1.10E+02	ALEPTFADLSR
19	1338.6796	1337.6723	1337.6034	0	37	4.60E+01	NGVGFGLGEMSR
20	1389.6727	1388.6654	1388.6646	0	57	5.00E-01	R.FMTNPPELPAEPK.A + Oxidation (M)
21	1403.6923	1402.685	1402.6576	0	27	4.90E+02	STPSVNLQAQAAR + 4 Deamidated (NQ)
22	1442.7759	1441.7686	1441.7314	0	32	1.50E+02	ALPAHLADSTQYR
23	1552.7452	1551.7379	1551.7358	0	72	1.60E-02	R.FSDPAWSQNPLYK.R
24	1570.8711	1569.8638	1569.8555	0	125	6.50E-08	R.LPAALHGFEVLFK.S
25	1675.8722	1674.8649	1674.7598	1	48	5.00E+00	NGVNPKEFNDDVGR
26	1687.8667	1686.8594	1686.8577	0	28	4.80E+02	GVLDLFLVGNISGAPVAR + Deamidated (NQ)
27	1705.9324	1704.9251	1704.9159	0	35	7.40E+01	VENLTNPLGIGTPQPR
28	1722.962	1721.9547	1721.9424	0	120	2.10E-07	K.QAAENTLNLPVIGIR.G
29	2078.1313	2077.124	2077.1167	0	126	5.90E-08	K.SNPLNRPGALEVSGTPIDLK.Q
30	2107.0259	2106.0186	2106.013	0	132	2.00E-08	K.ELHSWISHSDLSPPQDISR.G
31	2149.0164	2148.0091	2148.0078	0	90	0.00032	K.HADSWWLHWQQLAER.S
32	2255.0002	2253.9929	2253.9882	0	116	5.80E-07	K.DLVNNGGMPSQVMDDAFEVKG.N + 2 Oxidation (M)
33	2311.1963	2310.189	2310.1492	1	36	8.30E+01	VIVQNAQRKPNVDVYTYSER + 3 Deamidated (NQ)
34	2618.3523	2617.345	2617.3421	0	167	7.00E-12	R.GQFVINLLTEAMSPNTNLSNPAAVK.R + Oxidation (M)
35	2774.4446	2773.4373	2773.4432	1	112	2.20E-06	R.GQFVINLLTEAMSPNTNLSNPAAVK.R + Oxidation (M)
36	3509.9614	3508.9541	3508.9406	0	89	2.40E-04	R.NDVLELIQYRPITESVHERPLLVPPQINK.F

<b>Band VIII</b>							
Peptide no.	$M_r$			Miss <sup>a)</sup>	Score <sup>b)</sup>	Expected <sup>c)</sup>	Peptide <sup>d)</sup>
	Observed	Exptl	Calculated				
1	808.4412	807.4339	807.4715	0	50	4.70E-01	KPLHSAR
2	828.4234	827.4161	827.4501	0	36	1.30E+01	DGALLPSR
3	929.564	928.5567	928.5892	1	50	1.30E+00	MVLLKAVR
4	945.5574	944.5502	944.5291	1	35	4.10E+01	LDSGQKAVK
5	960.5554	959.5481	959.54	1	65	4.00E-02	R.GKDLTTSAR.M
6	1123.6534	1122.6461	1122.6397	0	51	5.30E-01	SLLDGLGHLAK
7	1139.5364	1138.5291	1138.4682	0	20	5.70E+02	LCCCGNNISGR
8	1180.6503	1179.643	1179.64	0	65	2.60E-02	R.HVAHFSLLELK.N
9	1215.5934	1214.5861	1214.5601	0	24	3.90E+02	DMSSVSSYALR
10	1230.6095	1229.6022	1229.5968	0	59	1.20E-01	K.FYVFDLSPDK.S
11	1247.6006	1246.5933	1246.6703	0	33	4.20E+01	SLGCALGTISVAR
12	1262.6823	1261.675	1261.6666	0	69	1.30E-02	R.NDVLELIQYR.A
13	1277.6927	1276.6854	1276.6776	0	101	8.40E-06	K.NLATTEGAVVFR.N
14	1289.6714	1288.6641	1288.7074	1	27	2.40E+02	AASPRFVMIAR
15	1289.6874	1288.6801	1288.7139	0	38	1.80E+01	NLALTEGAVVFR
16	1306.7019	1305.6946	1305.683	0	99	1.40E-05	R.NGVQTFIVSWR.N
17	1322.691	1321.6837	1321.6415	1	29	1.20E+02	NGKVTFFYNHDK
18	1338.6855	1337.6782	1337.7052	0	31	75	NSSTVTLHVPQR
19	1375.6859	1374.6786	1374.6739	0	33	4.90E+01	QIDLSEVSSNQR
20	1552.7577	1551.7504	1551.7358	0	104	3.00E-06	R.FSDPAWSQNPLYK.R
21	1687.8848	1686.8775	1686.9152	2	32	6.00E+01	KATVENVVAEKSDGIK
22	1705.932	1704.9247	1704.9159	0	43	4.70E+00	VENLTNPLGIGTPQPR
23	1722.955	1721.9477	1721.9424	0	125	2.30E-08	K.QAAENTLNLPVIGIR.G
24	1755.9797	1754.9724	1754.9461	2	21	6.60E+02	ERLEEALVTVMRGR
25	1778.9189	1777.9116	1778.0163	1	25	2.90E+02	QLGPAALGRLTEAVAVR
26	1783.8943	1782.887	1782.886	0	68	1.40E-02	K.NVLLGQSELRPGDDDR.R
27	1939.9949	1938.9876	1938.9871	1	71	7.00E-03	K.NVLLGQSELRPGDDDR.F
28	2107.0254	2106.0181	2106.013	0	-139	8.70E-10	K.ELHSWISHSDLSPPQDISR.G
29	2107.0298	2106.0225	2106.013	0	141	5.20E-10	K.ELHSWISHSDLSPPQDISR.G
30	2254.9885	2253.9812	2254.0852	0	21	3.10E+02	VLQVDASTLLESIPDEEDPNA
31	2255.0098	2254.0025	2254.0938	2	22	2.90E+02	QAAGKATDDASLHAEGTAQERK
32	2311.219	2310.2117	2310.2444	1	31	5.40E+01	NQRALLDAAAQVAVSGVDAPVR
33	2596.3848	2595.3775	2595.322	2	21	4.60E+02	IDNLFKKVASFTEPEIQSEWSK
34	2618.3601	2617.3528	2617.3244	0	82	4.10E-04	R.GQFVINLLTEAMAPTNTLSNPAAVK.R
35	2774.4446	2773.4373	2773.4255	1	29	7.70E+01	GQFVINLLTEAMAPTNTLSNPAAVK.R
36	3509.9651	3508.9578	3508.9406	0	100	3.30E-06	R.NDVLELIQYRPITESVHERPLLVPPQINK.F

a) The number of missed cleavage sites.

b) The score is the  $-\log_{10}(P)$  value, where P is the probability that the observed match is a random event. Individual ion scores of  $>56$  indicate identity or extensive homology ( $P \leq 0.05$ ).

c) Expected score based on BLAST search.

d) The sequence between the peptides was identified by MS. The amino acid before the period at the N terminal and that after the period at the C terminal indicate the cleavage sites.

**Supplementary Table 2.2. (Continued).**

<b>Band IX</b>							
Peptide no.	$M_r$			Miss <sup>a)</sup>	Score <sup>b)</sup>	Expected <sup>c)</sup>	Peptide <sup>d)</sup>
	Observed	Exptl	Calculated				
1	808.4493	807.4421	807.4715	0	28	1.20E+02	KPLHSAR
2	929.5632	928.5559	928.509	1	33	9.60E+01	LDQGAKAAR
3	934.4607	933.4535	933.4953	1	35	7.30E+01	AAMLEKAGK + Oxidation (M)
4	945.5638	944.5565	944.5841	1	42	1.30E+01	MVLLKAVR + Oxidation (M)
5	960.5496	959.5423	959.5512	1	40	2.30E+01	RSGILTSAR
6	1067.5352	1066.5279	1066.5295	0	49	2.20E+00	SYQSGVLEGG
7	1067.5354	1066.5281	1066.5295	0	57	3.80E-01	R.SYQSGVLEGG.D
8	1180.6586	1179.6513	1179.64	0	61	1.40E-01	R.HVAHFSLLELK.N
9	1197.5535	1196.5462	1196.5972	1	25	4.80E+02	VNQTSTFKAMR + Oxidation (M)
10	1218.67	1217.6627	1217.6881	0	34	1.00E+02	GPVIGVHLVGD
11	1230.6108	1229.6035	1229.5968	0	52	1.40E+00	FYVFDLSPDK
12	1247.5995	1246.5922	1246.5805	0	38	3.30E+01	YMPTYLAWR + Oxidation (M)
13	1262.6755	1261.6682	1261.7142	1	42	1.70E+01	ITNNQLLKYR
14	1277.694	1276.6867	1276.6776	0	69	3.10E-02	K.NLATTEGAVVFR.N
15	1289.6842	1288.6769	1288.7139	0	58	4.60E-01	K.NLATTEGAVVFR.N
16	1306.691	1305.6837	1305.683	0	-62	1.40E-01	R.NGVQTFIVSWR.N
17	1306.6958	1305.6885	1305.683	0	66	5.50E-02	R.NGVQTFIVSWR.N
18	1389.6802	1388.6729	1388.6646	0	74	1.00E-02	R.FMTNPPELPAEPK.A + Oxidation (M)
19	1405.6807	1404.6734	1404.5762	0	27	5.60E+02	GEGAPQLCDACQR + Carbamidomethyl (C); Deamidated (NQ)
20	1528.7473	1527.74	1527.7239	1	68	3.90E-02	R.SYQSGVLEGG.DMAK.V + Oxidation (M)
21	1552.7577	1551.7504	1551.7358	0	47	4.70E+00	FSDPAWSQNPLYK
22	1570.8755	1569.8682	1569.8555	0	120	2.00E-07	R.LPAALHGEFVELFK.S
22	1570.8755	1569.8682	1569.8225	0	69	2.80E-02	R.LPAALHGEFVELFK.S + Oxidation (M)
23	1705.9291	1704.9218	1704.9159	0	33	1.20E+02	QASEHTLGLNPNVIGIR + Deamidated (NQ)
24	1722.9612	1721.9539	1721.9424	0	97	4.40E-05	K.QAAENTLNLNPNVIGIR.G
25	1734.9114	1733.9041	1733.8882	2	28	4.40E+02	DGKPKKALNNFMRSR
26	1783.8937	1782.8864	1782.886	0	48	4.50E+00	NVLLGQSELRPDGGDDDR
27	1939.9922	1938.9849	1938.9871	1	55	8.40E-01	K.NVLLGQSELRPDGGDDRR.F
28	2078.1379	2077.1306	2077.1167	0	132	1.60E-08	K.SNPLNRPGALEVSGTPIDLK.Q
29	2090.0972	2089.0899	2089.2371	2	21	2.20E+03	LPQREGPRIGLTLNPNVIGIR + Deamidated (NQ)
30	2107.019	2106.0117	2106.013	0	118	5.20E-07	K.ELHSWISHSDLSPPQDISR.G
31	2181.0098	2180.0025	2180.0183	0	25	8.60E+02	LDGMQLHFQGHVLSGCGFFK + Deamidated (NQ); Oxidation (M)
32	2181.0115	2180.0042	2180.0035	1	25	9.00E+02	RSWPDEAAWHEAAQGLAQR + 2 Deamidated (NQ)
33	2255.009	2254.0017	2253.9882	0	73	1.20E-02	K.DLVNNGGMPSQVMDMAFEVGGK.N + 2 Oxidation (M)
33	2255.009	2254.0017	2253.9882	0	73	1.20E-02	K.DLVNNGGMPSQVMDMAFEVGGK.N + Deamidated (NQ); 2 Oxidation (M)
34	2422.2246	2421.2173	2421.2111	0	120	3.00E-07	K.CEFILNSNGHISILNPPGNPK.A + Carbamidomethyl (C)
35	2618.3459	2617.3386	2617.3421	0	137	6.40E-09	R.GQFVINLLTEAMSPNTSLSNPAAVK.R + Oxidation (M)
36	3509.9541	3508.9468	3508.9406	0	108	3.40E-06	R.NDVLELIQYRIPITSVHERPLLVVPPQINK.F

<b>Band X</b>							
Peptide no.	$M_r$			Miss <sup>a)</sup>	Score <sup>b)</sup>	Expected <sup>c)</sup>	Peptide <sup>d)</sup>
	Observed	Exptl	Calculated				
1	808.4367	807.4294	807.4715	0	50	8.00E-01	KPLHSAR
2	828.4236	827.4164	827.4501	0	36	1.60E+01	ATALPAQR + Deamidated (NQ)
3	846.4392	845.4319	845.4759	0	35	7.20E+01	QFVSLPR
4	846.4459	845.4386	845.4429	0	45	7	SGMIVSPR
5	929.5566	928.5493	928.5892	1	44	8.10E+00	MVLLKAVR
6	945.5467	944.5394	944.5113	0	48	3.50E+00	VCGQLQAVK
7	960.5452	959.5379	959.54	1	58	3.70E-01	R.GKDLLTSAR.M
8	972.5431	971.5358	971.5036	0	36	5.70E+01	NTPGSELVR
9	1018.509	1017.5017	1017.509	0	73	1.10E-02	R.LTATENAAAR.A + Deamidated (NQ)
10	1102.5579	1101.5506	1101.5414	0	55	7.10E-01	EAAAAADSAGR
11	1123.6423	1122.635	1122.6397	0	47	3.00E+00	SLLDGLGHLAK
12	1123.6477	1122.6404	1122.6397	0	49	1.50E+00	SLLDGLGHLAK
13	1180.6394	1179.6321	1179.64	0	68	2.70E-02	R.HVAHFSLLELK.N
14	1192.6409	1191.6336	1191.6387	0	34	8.40E+01	DINTFVIELK + Deamidated (NQ)
15	1232.5486	1231.5413	1231.5429	0	75	4.80E-03	K.AQQTADANER.A
16	1247.5829	1246.5756	1246.5805	0	35	6.70E+01	YMPTYLAWR + Oxidation (M)
17	1263.5953	1262.588	1262.6401	1	36	5.80E+01	GRLQTMGSLR + Deamidated (NQ); Oxidation (M)
18	1306.6842	1305.6769	1305.683	0	80	2.30E-03	R.NGVQTFIVSWR.N
19	1318.6875	1317.6802	1317.6347	0	30	2.60E+02	LDAQGGDGIAMVR + Oxidation (M)
20	1389.6829	1388.6756	1388.7048	1	22	1.80E+03	FRDVSQDVLGPR + Deamidated (NQ)
21	1403.6975	1402.6902	1402.7106	1	35	9.20E+01	RHGFPTELYQR
22	1442.7704	1441.7631	1441.7215	0	30	2.50E+02	FIGAAPPEGHGPHR
23	1519.7671	1518.7598	1518.7817	0	36	6.50E+01	INLNNVYSLEIPK + 3 Deamidated (NQ)
24	1552.7448	1551.7375	1551.7358	0	94	9.60E-05	R.FSDPAWSQNPLYK.R
25	1570.8499	1569.8426	1569.8555	0	92	1.50E-04	R.LPAALHGEFVELFK.S
26	1606.8281	1605.8208	1605.825	0	41	2.40E+01	VLYEIEGVSEIAR
27	1675.8597	1674.8524	1674.8611	0	49	4.00E+00	AMQDITTALTVGAEVR
28	1705.9166	1704.9093	1704.9709	1	41	2.20E+01	MPAKNLAPVGGVPLVAR + Oxidation (M)
29	1705.9314	1704.9241	1704.9159	0	31	1.80E+02	QASEHTLGLNPNVIGIR + Deamidated (NQ)
30	1722.9398	1721.9325	1721.9424	0	120	2.30E-07	K.QAAENTLNLNPNVIGIR.G
31	1783.8936	1782.8863	1782.886	0	52	1.80E+00	NVLLGQSELRPDGGDDDR
32	1922.0448	1921.0375	1921.0493	2	35	7.60E+01	GVSSPVRQPSLLGPGSARR + Deamidated (NQ)
33	1939.9817	1938.9744	1938.9871	1	60	2.70E-01	K.NVLLGQSELRPDGGDDRR.F
34	2078.1196	2077.1123	2077.1167	0	82	1.60E-03	K.SNPLNRPGALEVSGTPIDLK.Q
35	2107.0159	2106.0086	2106.013	0	124	1.30E-07	K.ELHSWISHSDLSPPQDISR.G
36	2618.3279	2617.3206	2617.3421	0	135	1.00E-08	R.GQFVINLLTEAMSPNTSLSNPAAVK.R + Oxidation (M)

a) The number of missed cleavage sites.

b) The score is the  $-\log_{10}(P)$  value, where P is the probability that the observed match is a random event. Individual ion scores of  $>56$  indicate identity or extensive homology ( $P \leq 0.05$ ).

c) Expected score based on BLAST search.

d) The sequence between the peptides was identified by MS. The amino acid before the period at the N terminal and that after the period at the C terminal indicate the cleavage sites.

**Supplementary Table 2.2. (Continued).**

<b>Band XI</b>							
Peptide no.	$M_r$			Miss <sup>a)</sup>	Score <sup>b)</sup>	Expected <sup>c)</sup>	Peptide <sup>d)</sup>
	Observed	Exptl	Calculated				
1	808.4443	807.437	807.4715	0	32	4.90E+01	KPLHSAR
2	808.4446	807.4373	807.4715	0	38	1.20E+01	KPIHSAR
3	817.4036	816.3963	816.3878	0	34	5.90E+01	SHVGFNR + Deamidated (NQ)
4	828.4076	827.4004	827.4501	0	25	1.90E+02	ANPVSALR + Deamidated (NQ)
5	891.3716	890.3644	890.377	0	21	6.20E+02	NPPDEYR + Deamidated (NQ)
6	902.4819	901.4747	901.4505	0	38	4.20E+01	EGAQAE LGK
7	934.47	933.4628	933.4953	1	32	1.60E+02	AAMLEKAGK + Oxidation (M)
8	939.4736	938.4663	938.428	0	38	2.40E+01	GLDGAMFGR + Oxidation (M)
9	945.5576	944.5503	944.5365	0	37	4.00E+01	VEAALAIMK
10	1018.526	1017.5187	1017.509	0	59	3.00E-01	R.LTATENAAAR.A + Deamidated (NQ)
11	1102.561	1101.5537	1101.5526	1	56	6.10E-01	AERAATAAEGR
12	1180.6501	1179.6428	1179.64	0	60	1.60E-01	R.HVAHFSLELK.N
13	1197.5682	1196.5609	1196.5197	0	25	5.10E+02	TGAANYENVQK + 3 Deamidated (NQ)
14	1211.6045	1210.5972	1210.5982	0	78	2.80E-03	R.FNDLFESALR.N
15	1222.649	1221.6417	1221.6506	0	43	1.10E+01	SNAFSLAPLFR
16	1232.5614	1231.5541	1231.5429	0	61	1.50E-01	K.AAQTADAEANER.A
17	1247.5892	1246.5819	1246.6452	1	34	9.40E+01	MAAISRTL DNR
18	1262.6835	1261.6762	1261.6666	0	44	8.90E+00	NDVLELIQYR
19	1277.6857	1276.6784	1276.6776	0	86	6.20E-04	K.NLATTEGAVVFR.N
20	1306.6918	1305.6845	1305.683	0	89	3.30E-04	R.NGVQTFIVSWR.N
21	1389.6716	1388.6643	1388.6646	0	65	0.073	R.FMTNPPELPAEPK.A + Oxidation (M)
22	1409.7524	1408.7451	1408.829	0	37	4.30E+01	QPVDLSLAQVV LK
23	1539.8851	1538.8778	1538.878	0	114	6.70E-07	K.AASLANGLLNIDLVR.L
24	1552.777	1551.7697	1551.7358	0	41	2.20E+01	FSDPAWSQNPLYK
25	1570.8582	1569.8509	1569.8555	0	86	5.80E-04	R.LPAALHGEFVLELFK.S
26	1683.8495	1682.8422	1682.7426	1	34	1.10E+02	AKMLAGTDCTMESPR + Carbamidomethyl (C); Oxidation (M)
27	1702.8575	1701.8502	1701.8434	0	72	2.00E-02	K.STDNVTYLHQGIAQR.A
28	1722.9476	1721.9403	1721.9424	0	117	4.20E-07	K.QAAENTLNLNPNVIGIR.G
29	1794.8827	1793.8754	1793.8869	0	31	2.30E+02	FLETDPAMISAETTLR
30	1939.993	1938.9857	1938.9871	1	45	1.00E+01	NVLLGQSELRPGDDDRR
31	2078.1133	2077.106	2077.1167	0	124	1.00E-07	K.SNPLNRPGALEVSGTPI DLK.Q
32	2149.0337	2148.0264	2148.0078	0	105	1.10E-05	K.HADSWWLHWQQWLAER.S
33	2165.0425	2164.0352	2164.1561	1	31	2.70E+02	MANLIYLTLEGKQQGLISR + Deamidated (NQ); Oxidation (M)
34	2181.021	2180.0137	2180.1225	1	21	2.40E+03	DKAIEAWLTHSAAPSLDSIR
35	2181.0264	2180.0191	2179.9341	1	23	1.60E+03	HVSDDDSYNMSTRSWQPR
36	2206.2073	2205.2	2205.1277	2	30	2.40E+02	DNQQALNSYLAGKIDAKNLK + 2 Deamidated (NQ)

a) The number of missed cleavage sites.

b) The score is the  $-\log_{10}(P)$  value, where P is the probability that the observed match is a random event. Individual ion scores of  $>56$  indicate identity or extensive homology ( $P \leq 0.05$ ).

c) Expected score based on BLAST search.

d) The sequence between the peptides was identified by MS. The amino acid before the period at the N terminal and that after the period at the C terminal indicate the cleavage sites.

**Supplementary Table 2.3.** Amino acid alignment of peptides identified by MALDI-TOF MS in dominant HCPs with respective PHA synthase fusion protein and mapping of anti-PhaC1 antibody epitopes.

**Band I** (Amino acid coverage: 34%)

Reference sequence Ag-PhaC1<sub>pa</sub>

1	<i>MHLRRPGEEV</i>	<i>NLTTTTVDDR</i>	<i>RIATGKQAT</i>	<i>AEGRAINRRV</i>	<i>ENATAEGRAI</i>
51	<i>NRVENATAE</i>	<i>GRAINRRVES</i>	<i>SHSKETEARL</i>	<i>TATEDAAARA</i>	<i>QARADEAYRK</i>
101	<i>ADEALGAAQK</i>	<i>AQQTADEANE</i>	<i>RALRMLEKAS</i>	<i>RKPRGSGGGH</i>	<b>MSQKNNNELP</b>
151	<b>KQAAENTLNL</b>	<i>NPVIGIRGKD</i>	<i>LLTSARMVLL</i>	<i>QAVRQPLHSA</i>	<i>RHVAHFSLEL</i>
201	<b>KNVLLGQSEL</b>	<b>RPGDDRRFS</b>	<i>DPAWSQNPLY</i>	<i>KRYMQTYLAW</i>	<i>RKELHSWISH</i>
251	<i>SDLSPQDISR</i>	<i>GQFVINLLTE</i>	<i>AMSPTNSLSN</i>	<i>PAAVKRFFET</i>	<i>GGKSLLDGLG</i>
301	<i>HLAKDLVNNG</i>	<i>GMPSQVMDA</i>	<i>FEVGKNLATT</i>	<i>EGAVVFRNDV</i>	<i>LELIQYRPIT</i>
351	<i>ESVHERPLL</i>	<i>VPPQINKFYV</i>	<i>FDLSPDKSLA</i>	<i>RFCLRNGVQT</i>	<i>FIVSWRNPTK</i>
401	<i>SQREWGLTTY</i>	<i>IEALKEAIEV</i>	<i>VLSITGSKDL</i>	<i>NLLGACSGGI</i>	<i>TTATLVGHYV</i>
451	<i>ASGEKKNVAF</i>	<i>TQLVSVLDFE</i>	<i>LNTQVALFAD</i>	<i>EKTLEAAKRR</i>	<i>SYQSGVLEGG</i>
501	<i>DMAKVFAWMR</i>	<i>PNDLIWNYWV</i>	<i>NNYLLGNQPP</i>	<i>AFDILYWNND</i>	<i>TTRLPAALHG</i>
551	<i>EFVELFKSNP</i>	<i>LNRPGALEVS</i>	<i>GTPIDLKQVT</i>	<i>CDFYCVAGLN</i>	<i>DHITPWESCY</i>
601	<i>KSARLLGGKC</i>	<i>EFILSNSGHI</i>	<i>QSILNPPGNP</i>	<i>KARFMTNPPEL</i>	<i>PAEPKAWLEQ</i>
651	<i>AGKHADSWWL</i>	<b>HWQQWLAERS</b>	<b>GKTRKAPASL</b>	<b>GNKTYPAGEA</b>	<i>APGTYVHER</i>

**Band II** (Amino acid coverage: 24%)

Reference sequence Ag-PhaC1<sub>pa</sub>

1	<i>MHLRRPGEEV</i>	<i>NLTTTTVDDR</i>	<i>RIATGKQAT</i>	<i>AEGRAINRRV</i>	<i>ENATAEGRAI</i>
51	<i>NRVENATAE</i>	<i>GRAINRRVES</i>	<i>SHSKETEARL</i>	<i>TATEDAAARA</i>	<i>QARADEAYRK</i>
101	<i>ADEALGAAQK</i>	<i>AQQTADEANE</i>	<i>RALRMLEKAS</i>	<i>RKPRGSGGGH</i>	<b>MSQKNNNELP</b>
151	<b>KQAAENTLNL</b>	<i>NPVIGIRGKD</i>	<i>LLTSARMVLL</i>	<i>QAVRQPLHSA</i>	<i>RHVAHFSLEL</i>
201	<b>KNVLLGQSEL</b>	<b>RPGDDRRFS</b>	<i>DPAWSQNPLY</i>	<i>KRYMQTYLAW</i>	<i>RKELHSWISH</i>
251	<i>SDLSPQDISR</i>	<i>GQFVINLLTE</i>	<i>AMSPTNSLSN</i>	<i>PAAVKRFFET</i>	<i>GGKSLLDGLG</i>
301	<i>HLAKDLVNNG</i>	<i>GMPSQVMDA</i>	<i>FEVGKNLATT</i>	<i>EGAVVFRNDV</i>	<i>LELIQYRPIT</i>
351	<i>ESVHERPLL</i>	<i>VPPQINKFYV</i>	<i>FDLSPDKSLA</i>	<i>RFCLRNGVQT</i>	<i>FIVSWRNPTK</i>
401	<i>SQREWGLTTY</i>	<i>IEALKEAIEV</i>	<i>VLSITGSKDL</i>	<i>NLLGACSGGI</i>	<i>TTATLVGHYV</i>
451	<i>ASGEKKNVAF</i>	<i>TQLVSVLDFE</i>	<i>LNTQVALFAD</i>	<i>EKTLEAAKRR</i>	<i>SYQSGVLEGG</i>
501	<i>DMAKVFAWMR</i>	<i>PNDLIWNYWV</i>	<i>NNYLLGNQPP</i>	<i>AFDILYWNND</i>	<i>TTRLPAALHG</i>
551	<i>EFVELFKSNP</i>	<i>LNRPGALEVS</i>	<i>GTPIDLKQVT</i>	<i>CDFYCVAGLN</i>	<i>DHITPWESCY</i>
601	<i>KSARLLGGKC</i>	<i>EFILSNSGHI</i>	<i>QSILNPPGNP</i>	<i>KARFMTNPPEL</i>	<i>PAEPKAWLEQ</i>
651	<i>AGKHADSWWL</i>	<b>HWQQWLAERS</b>	<b>GKTRKAPASL</b>	<b>GNKTYPAGEA</b>	<i>APGTYVHER</i>

**Band III** (Amino acid coverage: 30%)

Reference sequence Ag-PhaC1<sub>pa</sub>

1	<i>MHLRRPGEEV</i>	<i>NLTTTTVDDR</i>	<i>RIATGKQAT</i>	<i>AEGRAINRRV</i>	<i>ENATAEGRAI</i>
51	<i>NRVENATAE</i>	<i>GRAINRRVES</i>	<i>SHSKETEARL</i>	<i>TATEDAAARA</i>	<i>QARADEAYRK</i>
101	<i>ADEALGAAQK</i>	<i>AQQTADEANE</i>	<i>RALRMLEKAS</i>	<i>RKPRGSGGGH</i>	<b>MSQKNNNELP</b>
151	<b>KQAAENTLNL</b>	<i>NPVIGIRGKD</i>	<i>LLTSARMVLL</i>	<i>QAVRQPLHSA</i>	<i>RHVAHFSLEL</i>
201	<b>KNVLLGQSEL</b>	<b>RPGDDRRFS</b>	<i>DPAWSQNPLY</i>	<i>KRYMQTYLAW</i>	<i>RKELHSWISH</i>
251	<i>SDLSPQDISR</i>	<i>GQFVINLLTE</i>	<i>AMSPTNSLSN</i>	<i>PAAVKRFFET</i>	<i>GGKSLLDGLG</i>
301	<i>HLAKDLVNNG</i>	<i>GMPSQVMDA</i>	<i>FEVGKNLATT</i>	<i>EGAVVFRNDV</i>	<i>LELIQYRPIT</i>
351	<i>ESVHERPLL</i>	<i>VPPQINKFYV</i>	<i>FDLSPDKSLA</i>	<i>RFCLRNGVQT</i>	<i>FIVSWRNPTK</i>
401	<i>SQREWGLTTY</i>	<i>IEALKEAIEV</i>	<i>VLSITGSKDL</i>	<i>NLLGACSGGI</i>	<i>TTATLVGHYV</i>
451	<i>ASGEKKNVAF</i>	<i>TQLVSVLDFE</i>	<i>LNTQVALFAD</i>	<i>EKTLEAAKRR</i>	<i>SYQSGVLEGG</i>
501	<i>DMAKVFAWMR</i>	<i>PNDLIWNYWV</i>	<i>NNYLLGNQPP</i>	<i>AFDILYWNND</i>	<i>TTRLPAALHG</i>
551	<i>EFVELFKSNP</i>	<i>LNRPGALEVS</i>	<i>GTPIDLKQVT</i>	<i>CDFYCVAGLN</i>	<i>DHITPWESCY</i>
601	<i>KSARLLGGKC</i>	<i>EFILSNSGHI</i>	<i>QSILNPPGNP</i>	<i>KARFMTNPPEL</i>	<i>PAEPKAWLEQ</i>
651	<i>AGKHADSWWL</i>	<b>HWQQWLAERS</b>	<b>GKTRKAPASL</b>	<b>GNKTYPAGEA</b>	<i>APGTYVHER</i>

Note:

Letters in 'Bold' represent peptides identified by MALDI-TOF MS

'Underlined' letters indicate linker

Letter in 'italics' indicate antigen fusion partner

'Highlighted' letters represent mapped anti-PhaC1 antibodies epitopes: Yellow, anti-PhaC1<sub>1</sub> (MSQKNNNELPKQAA); Green, anti-PhaC1<sub>67</sub> (QSELRPGDDRRFS); and Blue, anti-PhaC1<sub>529</sub> (RSGKTRKAPASLGN).

### Supplementary Table 2.3. (Continued).

#### Band IV (Amino acid coverage: 22%)

Reference sequence Ag-PhaC1<sub>Pa</sub>

1	<i>MHLRRPGEEV</i>	<i>NLTTTVD</i>	<i>RIATGKQ</i>	<i>AEGRAINRRV</i>	<i>ENATAEGRAI</i>
51	<i>NRRVENATAE</i>	<i>GRAINRRVES</i>	<i>SHSKETE</i>	<i>TATEDAAARA</i>	<i>QARADEAYRK</i>
101	<i>ADEALGAAQK</i>	<i>AQQTAD</i>	<i>RALRMLEK</i>	<i>RKPRGSGGGH</i>	<b>MSQKNNNELP</b>
151	<b>KQAA</b> ENTLNL	NPVIGIRGKD	LLTSARMVLL	QAVRQPLHSA	RHVAHFSLEL
201	KNVLLG <b>QSEL</b>	<b>RPGD</b> DRRFS	DPAWSQNPLY	KRYMQTYLAW	RKELHSWISH
251	SDLSPQDISR	GQFVINLLTE	AMSPTNSLSN	PAAVKRFFET	GGKSLLDGLG
301	HLAKDLVNNG	GMPSQVMDA	FEVGKNLATT	<b>EGAVVFR</b> NDV	LELIQYRPIT
351	ESVHERPLLV	VPPQINKFYV	FDLSPDKSLA	RFCLRNGVQT	<b>FIVSWRN</b> PTK
401	SQREWGLTTY	IEALKEAIEV	VLSITGSKDL	NLLGACSGGI	TTATLVGHYV
451	ASGEKKVNAF	TQLVSVLDFE	LNTQVALFAD	EKTLEAAKRR	<b>SYQSGV</b> LEGG
501	<b>DMAKVFA</b> WMR	PNDLIWNYWV	NNYLLGNQPP	AFDILYWNND	<b>TTRLPAAL</b> HG
551	<b>EFVELFK</b> SNP	<b>LNRPGA</b> LEVS	<b>GTPIDL</b> KQVT	CDFYCVAGLN	DHITPWESCY
601	KSARLLGGKC	<b>EFILSN</b> SGHI	<b>QSILNPP</b> GNP	<b>KARFMT</b> NPEL	<b>PAEPKAW</b> LEQ
651	AGKHADSWWL	<b>HWQQWLA</b> ERS	<b>GKTRKAP</b> ASL	<b>GNKTYPA</b> GEA	<b>APGTYV</b> HER

#### Band V (Amino acid coverage: 1.6%)

Reference sequence Ag-PhaC1<sub>Pa</sub>

1	<i>MHLRRPGEEV</i>	<i>NLTTTVD</i>	<i>RIATGKQ</i>	<i>AEGRAINRRV</i>	<i>ENATAEGRAI</i>
51	<i>NRRVENATAE</i>	<i>GRAINRRVES</i>	<i>SHSKETE</i>	<i>TATEDAAARA</i>	<i>QARADEAYRK</i>
101	<i>ADEALGAAQK</i>	<i>AQQTAD</i>	<i>RALRMLEK</i>	<i>RKPRGSGGGH</i>	<b>MSQKNNNELP</b>
151	<b>KQAA</b> ENTLNL	NPVIGIRGKD	LLTSARMVLL	QAVRQPLHSA	RHVAHFSLEL
201	KNVLLG <b>QSEL</b>	<b>RPGD</b> DRRFS	DPAWSQNPLY	KRYMQTYLAW	RKELHSWISH
251	SDLSPQDISR	GQFVINLLTE	AMSPTNSLSN	PAAVKRFFET	GGKSLLDGLG
301	HLAKDLVNNG	GMPSQVMDA	FEVGKNLATT	<b>EGAVVFR</b> NDV	LELIQYRPIT
351	ESVHERPLLV	VPPQINKFYV	FDLSPDKSLA	RFCLRNGVQT	<b>FIVSWRN</b> PTK
401	SQREWGLTTY	IEALKEAIEV	VLSITGSKDL	NLLGACSGGI	TTATLVGHYV
451	ASGEKKVNAF	TQLVSVLDFE	LNTQVALFAD	EKTLEAAKRR	<b>SYQSGV</b> LEGG
501	<b>DMAKVFA</b> WMR	PNDLIWNYWV	NNYLLGNQPP	AFDILYWNND	<b>TTRLPAAL</b> HG
551	<b>EFVELFK</b> SNP	<b>LNRPGA</b> LEVS	<b>GTPIDL</b> KQVT	CDFYCVAGLN	DHITPWESCY
601	KSARLLGGKC	<b>EFILSN</b> SGHI	<b>QSILNPP</b> GNP	<b>KARFMT</b> NPEL	<b>PAEPKAW</b> LEQ
651	AGKHADSWWL	<b>HWQQWLA</b> ERS	<b>GKTRKAP</b> ASL	<b>GNKTYPA</b> GEA	<b>APGTYV</b> HER

#### Band VI (Amino acid coverage: 9%)

Reference sequence Ag-PhaC1<sub>Pa</sub>

1	<i>MHLRRPGEEV</i>	<i>NLTTTVD</i>	<i>RIATGKQ</i>	<i>AEGRAINRRV</i>	<i>ENATAEGRAI</i>
51	<i>NRRVENATAE</i>	<i>GRAINRRVES</i>	<i>SHSKETE</i>	<i>TATEDAAARA</i>	<i>QARADEAYRK</i>
101	<i>ADEALGAAQK</i>	<i>AQQTAD</i>	<i>RALRMLEK</i>	<i>RKPRGSGGGH</i>	<b>MSQKNNNELP</b>
151	<b>KQAA</b> ENTLNL	NPVIGIRGKD	LLTSARMVLL	QAVRQPLHSA	RHVAHFSLEL
201	KNVLLG <b>QSEL</b>	<b>RPGD</b> DRRFS	DPAWSQNPLY	KRYMQTYLAW	RKELHSWISH
251	SDLSPQDISR	GQFVINLLTE	AMSPTNSLSN	PAAVKRFFET	GGKSLLDGLG
301	HLAKDLVNNG	GMPSQVMDA	FEVGKNLATT	<b>EGAVVFR</b> NDV	LELIQYRPIT
351	ESVHERPLLV	VPPQINKFYV	FDLSPDKSLA	RFCLRNGVQT	<b>FIVSWRN</b> PTK
401	SQREWGLTTY	IEALKEAIEV	VLSITGSKDL	NLLGACSGGI	TTATLVGHYV
451	ASGEKKVNAF	TQLVSVLDFE	LNTQVALFAD	EKTLEAAKRR	<b>SYQSGV</b> LEGG
501	<b>DMAKVFA</b> WMR	PNDLIWNYWV	NNYLLGNQPP	AFDILYWNND	<b>TTRLPAAL</b> HG
551	<b>EFVELFK</b> SNP	<b>LNRPGA</b> LEVS	<b>GTPIDL</b> KQVT	CDFYCVAGLN	DHITPWESCY
601	KSARLLGGKC	<b>EFILSN</b> SGHI	<b>QSILNPP</b> GNP	<b>KARFMT</b> NPEL	<b>PAEPKAW</b> LEQ
651	AGKHADSWWL	<b>HWQQWLA</b> ERS	<b>GKTRKAP</b> ASL	<b>GNKTYPA</b> GEA	<b>APGTYV</b> HER

#### Band VII (Amino acid coverage: 42%)

Reference sequence PhaC1<sub>Pa</sub>-Ag

1	<b>MSQKNNNELP</b>	<b>KQAA</b> ENTLNL	<b>NPVIGIR</b> KD	<b>LLTSARM</b> VLL	<b>QAVRQPL</b> HSA
51	<b>RHVAHF</b> SLEL	KNVLLG <b>QSEL</b>	<b>RPGD</b> DRRFS	<b>DPAWSQ</b> NPLY	<b>KRYMQTY</b> LAW
101	<b>RKELHS</b> WISH	<b>SDLSPQ</b> DISR	<b>GQFVIN</b> LLTE	<b>AMSPTNS</b> LSN	<b>PAAVKRFF</b> ET
151	<b>GGKSLL</b> DGLG	HLAKDLVNNG	<b>GMPSQV</b> MDA	<b>FEVGKNL</b> ATT	<b>EGAVVFR</b> NDV
201	<b>LELIQY</b> RPIT	<b>ESVHER</b> PLLV	<b>VPPQINK</b> FYV	<b>FDLSPDK</b> SLA	RFCLRNGVQT
251	<b>FIVSWRN</b> PTK	SQREWGLTTY	IEALKEAIEV	VLSITGSKDL	NLLGACSGGI
301	TTATLVGHYV	ASGEKKVNAF	TQLVSVLDFE	LNTQVALFAD	EKTLEAAKRR
351	<b>SYQSGV</b> LEGG	<b>DMAKVFA</b> WMR	PNDLIWNYWV	NNYLLGNQPP	AFDILYWNND
401	<b>TTRLPAAL</b> HG	<b>EFVELFK</b> SNP	<b>LNRPGA</b> LEVS	<b>GTPIDL</b> KQVT	CDFYCVAGLN
451	DHITPWESCY	KSARLLGGKC	<b>EFILSN</b> SGHI	<b>QSILNPP</b> GNP	<b>KARFMT</b> NPEL
501	<b>PAEPKAW</b> LEQ	<b>AGKHAD</b> SWWL	<b>HWQQWLA</b> ERS	<b>GKTRKAP</b> ASL	<b>GNKTYPA</b> GEA
551	<b>APGTYV</b> HERG	<b>DAAARA</b> QARA	<b>GGGGGG</b> ESGG	<b>GGGGGG</b> SGGG	<b>GGSPGS</b> SHSK
601	<i>ETE</i> ARLTATE	<i>TAE</i> GRAINRR	<i>DEA</i> YRKADEA	<i>LGAAQKA</i> QQT	<i>ADEANER</i> ALR
651	<i>MLEKAS</i> RKNA	<i>RIATGKQ</i> HRL	<i>VENAT</i> AEGRA	<i>INRRV</i> ENATA	<i>EGRAINRR</i> VE
701	<i>NLTTT</i> VDDR		<i>RP</i> GEEV		

Note:

Letters in 'Bold' represent peptides identified by MALDI-TOF MS

'Underlined' letters indicate linker

Letter in 'italics' indicate antigen fusion partner

'Highlighted' letters represent mapped anti-PhaC1 antibodies epitopes: Yellow, anti-PhaC1\_1 (MSQKNNNELPKQAA); Green, anti-PhaC1\_67 (QSELRPGDDDRRFS); and Blue, anti-PhaC1\_529 (RSGKTRKAPASLGN).

### Supplementary Table 2.3. (Continued).

#### Band VIII (Amino acid coverage: 32%)

Reference sequence PhaC1<sub>Pa</sub>-Ag

1	<b>MSQKNNNELP</b>	<b>KQAA</b> ENTLNL	NPVIGIRGKD	LLTSARMVLL	QAVRQPLHSA
51	RHVAHFSLEL	KNVLLG <b>QSEL</b>	<b>RP</b> GD <del>DDRR</del> FS	DPAWSQNPLY	KRYMQTYLAW
101	RKELHSWISH	SDLSPQDISR	GQFVINLLTE	AMSPTNLSLN	PAAVKRFFET
151	GGKSLLDGLG	HLAKDLVNNG	GMPQVDMDA	FEVGKNLATT	EGAVVFRNDV
201	LELIQYRPIT	ESVHERPLL	VPPQINKFYV	FDLSPDKSLA	RFCLRNGVQT
251	FIVSWRNPTK	SQREWGLTTY	IEALKEAIEV	VLSITGSKDL	NLLGACSGGI
301	TTATLVGHYV	ASGEKKVNAF	TQLVSVLDFE	LNTQVALFAD	EKTLEAAKRR
351	SYQSGVLEGG	DMAKVFAWMR	PNDLIWNYWV	NNYLLGNQPP	AFDILYWNND
401	TTRLPAALHG	EFVELFKSNP	LNRPGALEVS	GTPIDLKQVT	CDFYCVAGLN
451	DHITPWESCY	KSARLLGGKC	EFILSNSGHI	QSILNPPGNP	KARFMTNPEL
501	PAEPKAWLEQ	AGKHADSWWL	HWQQWLAERS	<b>GKTRKAPASL</b>	<b>GN</b> KTYPAGEA
551	APGTYVHERG	SVLAVAIDKR	GGGGGLES	GGSGGGGSGG	GGSPGSSHSK
601	<i>ETEARLTATE</i>	<i>DAAARAQARA</i>	<i>DEAYRKADEA</i>	<i>LGAAQKAQQT</i>	<i>ADEANERALLR</i>
651	<i>MLEKASRKNA</i>	<i>TAEGRAINRR</i>	<i>VENATAEGRA</i>	<i>INRRVENATA</i>	<i>EGRAINRRVE</i>
701	<i>NLTTTTVDDR</i>	<i>RIATGKQHLR</i>	<i>RPGEEV</i>		

#### Band IX (Amino acid coverage: 32%)

Reference sequence PhaC1<sub>Pa</sub>-Ag

1	<b>MSQKNNNELP</b>	<b>KQAA</b> ENTLNL	NPVIGIRGKD	LLTSARMVLL	QAVRQPLHSA
51	RHVAHFSLEL	KNVLLG <b>QSEL</b>	<b>RP</b> GD <del>DDRR</del> FS	DPAWSQNPLY	KRYMQTYLAW
101	RKELHSWISH	SDLSPQDISR	GQFVINLLTE	AMSPTNLSLN	PAAVKRFFET
151	GGKSLLDGLG	HLAKDLVNNG	GMPQVDMDA	FEVGKNLATT	EGAVVFRNDV
201	LELIQYRPIT	ESVHERPLL	VPPQINKFYV	FDLSPDKSLA	RFCLRNGVQT
251	FIVSWRNPTK	SQREWGLTTY	IEALKEAIEV	VLSITGSKDL	NLLGACSGGI
301	TTATLVGHYV	ASGEKKVNAF	TQLVSVLDFE	LNTQVALFAD	EKTLEAAKRR
351	SYQSGVLEGG	DMAKVFAWMR	PNDLIWNYWV	NNYLLGNQPP	AFDILYWNND
401	TTRLPAALHG	EFVELFKSNP	LNRPGALEVS	GTPIDLKQVT	CDFYCVAGLN
451	DHITPWESCY	KSARLLGGKC	EFILSNSGHI	QSILNPPGNP	KARFMTNPEL
501	PAEPKAWLEQ	AGKHADSWWL	HWQQWLAERS	<b>GKTRKAPASL</b>	<b>GN</b> KTYPAGEA
551	APGTYVHERG	SVLAVAIDKR	GGGGGLES	GGSGGGGSGG	GGSPGSSHSK
601	<i>ETEARLTATE</i>	<i>DAAARAQARA</i>	<i>DEAYRKADEA</i>	<i>LGAAQKAQQT</i>	<i>ADEANERALLR</i>
651	<i>MLEKASRKNA</i>	<i>TAEGRAINRR</i>	<i>VENATAEGRA</i>	<i>INRRVENATA</i>	<i>EGRAINRRVE</i>
701	<i>NLTTTTVDDR</i>	<i>RIATGKQHLR</i>	<i>RPGEEV</i>		

#### Band X (Amino acid coverage: 32%)

Reference sequence PhaC1<sub>Pa</sub>-Ag

1	<b>MSQKNNNELP</b>	<b>KQAA</b> ENTLNL	NPVIGIRGKD	LLTSARMVLL	QAVRQPLHSA
51	RHVAHFSLEL	KNVLLG <b>QSEL</b>	<b>RP</b> GD <del>DDRR</del> FS	DPAWSQNPLY	KRYMQTYLAW
101	RKELHSWISH	SDLSPQDISR	GQFVINLLTE	AMSPTNLSLN	PAAVKRFFET
151	GGKSLLDGLG	HLAKDLVNNG	GMPQVDMDA	FEVGKNLATT	EGAVVFRNDV
201	LELIQYRPIT	ESVHERPLL	VPPQINKFYV	FDLSPDKSLA	RFCLRNGVQT
251	FIVSWRNPTK	SQREWGLTTY	IEALKEAIEV	VLSITGSKDL	NLLGACSGGI
301	TTATLVGHYV	ASGEKKVNAF	TQLVSVLDFE	LNTQVALFAD	EKTLEAAKRR
351	SYQSGVLEGG	DMAKVFAWMR	PNDLIWNYWV	NNYLLGNQPP	AFDILYWNND
401	TTRLPAALHG	EFVELFKSNP	LNRPGALEVS	GTPIDLKQVT	CDFYCVAGLN
451	DHITPWESCY	KSARLLGGKC	EFILSNSGHI	QSILNPPGNP	KARFMTNPEL
501	PAEPKAWLEQ	AGKHADSWWL	HWQQWLAERS	<b>GKTRKAPASL</b>	<b>GN</b> KTYPAGEA
551	APGTYVHERG	SVLAVAIDKR	GGGGGLES	GGSGGGGSGG	GGSPGSSHSK
601	<i>ETEARLTATE</i>	<i>DAAARAQARA</i>	<i>DEAYRKADEA</i>	<i>LGAAQKAQQT</i>	<i>ADEANERALLR</i>
651	<i>MLEKASRKNA</i>	<i>TAEGRAINRR</i>	<i>VENATAEGRA</i>	<i>INRRVENATA</i>	<i>EGRAINRRVE</i>
701	<i>NLTTTTVDDR</i>	<i>RIATGKQHLR</i>	<i>RPGEEV</i>		

#### Band XI (Amino acid coverage: 26%)

Reference sequence PhaC1<sub>Pa</sub>-Ag

1	<b>MSQKNNNELP</b>	<b>KQAA</b> ENTLNL	NPVIGIRGKD	LLTSARMVLL	QAVRQPLHSA
51	RHVAHFSLEL	KNVLLG <b>QSEL</b>	<b>RP</b> GD <del>DDRR</del> FS	DPAWSQNPLY	KRYMQTYLAW
101	RKELHSWISH	SDLSPQDISR	GQFVINLLTE	AMSPTNLSLN	PAAVKRFFET
151	GGKSLLDGLG	HLAKDLVNNG	GMPQVDMDA	FEVGKNLATT	EGAVVFRNDV
201	LELIQYRPIT	ESVHERPLL	VPPQINKFYV	FDLSPDKSLA	RFCLRNGVQT
251	FIVSWRNPTK	SQREWGLTTY	IEALKEAIEV	VLSITGSKDL	NLLGACSGGI
301	TTATLVGHYV	ASGEKKVNAF	TQLVSVLDFE	LNTQVALFAD	EKTLEAAKRR
351	SYQSGVLEGG	DMAKVFAWMR	PNDLIWNYWV	NNYLLGNQPP	AFDILYWNND
401	TTRLPAALHG	EFVELFKSNP	LNRPGALEVS	GTPIDLKQVT	CDFYCVAGLN
451	DHITPWESCY	KSARLLGGKC	EFILSNSGHI	QSILNPPGNP	KARFMTNPEL
501	PAEPKAWLEQ	AGKHADSWWL	HWQQWLAERS	<b>GKTRKAPASL</b>	<b>GN</b> KTYPAGEA
551	APGTYVHERG	SVLAVAIDKR	GGGGGLES	GGSGGGGSGG	GGSPGSSHSK
601	<i>ETEARLTATE</i>	<i>DAAARAQARA</i>	<i>DEAYRKADEA</i>	<i>LGAAQKAQQT</i>	<i>ADEANERALLR</i>
651	<i>MLEKASRKNA</i>	<i>TAEGRAINRR</i>	<i>VENATAEGRA</i>	<i>INRRVENATA</i>	<i>EGRAINRRVE</i>
701	<i>NLTTTTVDDR</i>	<i>RIATGKQHLR</i>	<i>RPGEEV</i>		

Note:

Letters in 'Bold' represent peptides identified by MALDI-TOF MS

'Underlined' letters indicate linker

Letter in 'italics' indicate antigen fusion partner

'highlighted' letters represent mapped anti-PhaC1 antibodies epitopes: Yellow, anti-PhaC1\_1 (MSQKNNNELPKQAA); Green, anti-PhaC1\_67 (QSELRPGDDRRFS); and Blue, anti-PhaC1\_529 (RSGKTRKAPASLGN).

Supplementary Table 2.4. 33 known and putative PHA synthases from bacterial human pathogens.

Organism	Taxonomy ID (NCBI)	Protein/Gene	Amino acid sequence
1: <i>A. baumannii</i>	575584	HMPREF0010_00690	MKRLKSLVSEQSQIKHLSTRIFRPTLVLQSSTPEVIGEFNQTRVRYAATEKSFREPLVFAVLAAPLAINMAYDLYPYRSLIKYFQNAQFDVYLDVWGRGLGKDRHLNLFNFIEDIFPKAIELVIRTHSGSDQISLHGWSMAGIFVTLTYAHNHPNYVKNLVLGSDPDSYASGYGKLYRINNTIARINKLQERIVYGLPKRHLHTPGILNSLGFKILDKPQWDFDGHQHLKLNLDLQFQEHATLSSFLNNMIDYVGGINQDMFNWVWLCNLRQGGSLKDKKIELKIDCSLLVAGRSDDQVTAADAQSLTSSDQYFTLPGHGLGMSQAQAEWPKLATAWLSERSTKI
2: <i>A. calcoaceticus</i>	871585	BDGL_001038	MKRLKSLVSEQSQIKHLSTRIFRPTLVLQSSTPEVIGEFNQTRVRYAATEKSFREPLVFAVLAAPLAINMAYDLYPYRSLIKYFQNAQFDVYLDVWGRGLGKDRHLNLFNFIEDIFPKAIELVIRTHSGSDQISLHGWSMAGIFVTLTYAHNHPNYVKNLVLGSDPDSYASGYGKLYRINNTIARINKLQERIVYGLPKRHLHTPGILNSLGFKILDKPQWDFDGHQHLKLNLDLQFQEHATLSSFLNNMIDYVGGINQDMFNWVWLCNLRQGGSLKDKKIELKIDCSLLVAGRSDDQVTAADAQSLTSSDQYFTLPGHGLGMSQAQAEWPKLATAWLSERSTKI
3: <i>A. radioresistens</i>	575589	HMPREF0018_01802	MFTLKAIRIQQKTRFRHLSRVLNPSLVLQSSTPEVIGEFNQTRVRYAATEKSFREPLVFAVLAAPLAINMAYDLYPYRSLIKYFQNAQFDVYLDVWGRGLGKDRHLNLFNFIEDIFPKAIELVIRTHSGSDQISLHGWSMAGIFVTLTYAHNHPNYVKNLVLGSDPDSYASGYGKLYRINNTIARINKLQERIVYGLPKRHLHTPGILNSLGFKILDKPQWDFDGHQHLKLNLDLQFQEHATLSSFLNNMIDYVGGINQDMFNWVWLCNLRQGGSLKDKKIELKIDCSLLVAGRSDDQVTAADAQSLTSSDQYFTLPGHGLGMSQAQAEWPKLATAWLSERSTKI
4: <i>B. anthracis</i>	198094	PHAC	MTTFAFEWQKLELPEEYRKAIRVRAKSELILREPEQVGLTPKEVMTKTKLRYRIPKQEKTORVPIILYALINKPYIMDLTPGNSLVEYLDVDRGFVYMLDQWTFGLDSDHSLKFDFFDFDYIAKAVKKVMRTAKSDEISLGYCMGGTLLSYAALHPHPIRILFMTSPDFSEITGLYGPLDEKYNLDAKVDTFGMPPEMDFGNMMLKPTIMFGPYVALVDRSENERFVSWRVLQKRWVGDGPIPFVGESYRQWIRDFYGNKLVKGLVIRGQKRLANIKANVLSIKRDIHALPCQVEALLDHSIDSKQYVCLPTGHMSISYVGGTAVKQTYPTIGDMLDERSK
5: <i>B. pertussis</i>	257313	PHBC	MNHLSAAPVWVSPADLAELQADFSREWLRLCDEAKRGVLAGPADKRFAGAALWDDRRORLIMAHAYLLSARAWARLVEAAQVSEPMRNRIRFNSVQWVWDAMSPANFLAFNPDAQRAIVESAGRTLQEGMANLNDIQRISQTDTEFEIGRNVATTPGHVWFENSLQILQYAPQAKVGERPLVIVPNNIKHYLLDQPENSFVRYAQEQHTYFIISWRNPAAADTDGVDATWSEYLDVDAVLAALAVASDQSGQPQVNAAGFCVGTLYTAHNPVYKLNVLGSDPDSYASGYGKLYRINNTIARINKLQERIVYGLPKRHLHTPGILNSLGFKILDKPQWDFDGHQHLKLNLDLQFQEHATLSSFLNNMIDYVGGINQDMFNWVWLCNLRQGGSLKDKKIELKIDCSLLVAGRSDDQVTAADAQSLTSSDQYFTLPGHGLGMSQAQAEWPKLATAWLSERSTKI
6: <i>B. cenocepacia</i>	216591	PHBC	SGPLKVLGASGHVAGVNPAPKAKRSYVWNEGDLPESADDAEFAATEQPSWWTWVWELDAYVGGKRVAPPAQPSGAQFVIEPAPGRVYLQRD
7: <i>B. mallei</i>	243160	PHBC	MTASKNSSTSAAGTSAGNTGFGSAQPMQMFVAVLNWRFADPARAATASAVNPFATQFPTSPFQMPSPDFGAMASPFAGLTPVAIIPPERLOKLDQADYARDQVVALMQQAAAANKLESPELKDREFSGDAAWKASPAHFAAAWYLLNARYLQELADALETDPKTRERIRFVQQWTAAPAFNSFLALNPDQAKSILETQGESLROGMNMLLDLORQKISQDDESQFVYGNLGCCTEGSVAAYENDLIQIQTYPKTDKVFERPLVPPCINKFYLDLQENSLVAHVAHSGHQLVSWRNADASVAHKTWDDYDEGLAAIVVQVQVSGREINTLFCVGGTMTALATAVLAARGHEHPAASMTLLTAMLDFSDTGTGLDVFVD EAHVQMRQETGGKNGAOPGLMRGVFEANTFLRPNDLWVYVNDYKGRTPAPDFLLWNGDSTSLPGMYAVYLRNLYENKLRPEALTVCGEYVLSRIDVPTFIYGSREDHIVPWQTAAYASTSLSGPLKVLGASGHVAGVNPAPKAKRSYVWNEGDLPESADDAEFAATEQPSWWTWVWELDAYVGGKRVAPPAQPSGAQFVIEPAPGRVYLQRD
8: <i>B. mallei</i>	243160	PHAC	MDTRHAPESGAPDAPLPAHPPASAYEPEYRIFDIAKEASVAKLTSGLSPASLQALADWLHLAAVAGKRAELATLALRHAALLGQVYLLAATGRTPAAPAQSPGDRFRFRAGVQLEP YRFRWHQSFLAEQWWRARTRDVPVSPHEDVAFSARQMLDITFAPANTVATNPEIAQRALTGGANLQAGVWVNDVYVLRNLTQPPAGAEQFELGRNLATTPGRVFRNHLIELLQYSPPTPDYVAGVLPVPAWIMKYIYLDL SAHNSLIRYLVGEGHTVFCVSWRNVDASDRDLSDYDQENSLVAHVAHSGHQLVSWRNADASVAHKTWDDYDEGLAAIVVQVQVSGREINTLFCVGGTMTALATAVLAARGHEHPAASMTLLTAMLDFSDTGTGLDVFVD SFQLMSNDLWVSRVHDLGERTPMIDLMAWNAADSTRMPYRMHSEYLRHLFLDNLATNRYVDGQTVSVHNIRAPFFVGTGTEHDHIAFWRSYVYKHYLSGSDVTFVLTAGGHNAGVSEPHGAKRHRYRM KMTAAAAAPSISDFEVLGATDFEGSWWPAVHAWLARHSSPQRVAAPPLGKRGARTLGDAPGTYVFOK
9: <i>B. multivorans</i>	395019	BMUL_1483	MTASKNSSTSAAGTSAGNTGFGSAQPMQMFVAVLNWRFADPARAATASAVNPFATQFPTSPFQMPSPDFGAMASPFAGLTPVAIIPPERLOKLDQADYARDQVVALMQQAAAANKLESPELKDREFSGDAAWKASPAHFAAAWYLLNARYLQELADALETDPKTRERIRFVQQWTAAPAFNSFLALNPDQAKSILETQGESLROGMNMLLDLORQKISQDDESQFVYGNLGCCTEGSVAAYENDLIQIQTYPKTDKVFERPLVPPCINKFYLDLQENSLVAHVAHSGHQLVSWRNADASVAHKTWDDYDEGLAAIVVQVQVSGREINTLFCVGGTMTALATAVLAARGHEHPAASMTLLTAMLDFSDTGTGLDVFVD EAHVQMRQETGGKNGAOPGLMRGVFEANTFLRPNDLWVYVNDYKGRTPAPDFLLWNGDSTSLPGMYAVYLRNLYENKLRPEALTVCGEYVLSRIDVPTFIYGSREDHIVPWQTAAYASTSLSGPLKVLGASGHVAGVNPAPKAKRSYVWNEGDLPESADDAEFAATEQPSWWTWVWELDAYVGGKRVAPPAQPSGAQFVIEPAPGRVYLQRD
10: <i>B. multivorans</i>	395019	BMULJ_01759	MTASKNSSTSAAGTSAGNTGFGSAQPMQMFVAVLNWRFADPARAATASAVNPFATQFPTSPFQMPSPDFGAMASPFAGLTPVAIIPPERLOKLDQADYARDQVVALMQQAAAANKLESPELKDREFSGDAAWKASPAHFAAAWYLLNARYLQELADALETDPKTRERIRFVQQWTAAPAFNSFLALNPDQAKSILETQGESLROGMNMLLDLORQKISQDDESQFVYGNLGCCTEGSVAAYENDLIQIQTYPKTDKVFERPLVPPCINKFYLDLQENSLVAHVAHSGHQLVSWRNADASVAHKTWDDYDEGLAAIVVQVQVSGREINTLFCVGGTMTALATAVLAARGHEHPAASMTLLTAMLDFSDTGTGLDVFVD EAHVQMRQETGGKNGAOPGLMRGVFEANTFLRPNDLWVYVNDYKGRTPAPDFLLWNGDSTSLPGMYAVYLRNLYENKLRPEALTVCGEYVLSRIDVPTFIYGSREDHIVPWQTAAYASTSLSGPLKVLGASGHVAGVNPAPKAKRSYVWNEGDLPESADDAEFAATEQPSWWTWVWELDAYVGGKRVAPPAQPSGAQFVIEPAPGRVYLQRD
11: <i>B. pseudomallei</i>	272560	PHBC	MQQLFVLSGASGHVAGVNPAPKAKRSYVWNEGDLPESADDAEFAATEQPSWWTWVWELDAYVGGKRVAPPAQPSGAQFVIEPAPGRVYLQRD
12: <i>B. pseudomallei</i>	272560	BPSS1954	LNARYLQELADALETDPKTRERIRFVQQWTAAPAFNSFLALNPDQAKSILETQGESLROGMNMLLDLORQKISQDDESQFVYGNLGCCTEGSVAAYENDLIQIQTYPKTDKVFERPLVPPCINKFYLDLQENSLVAHVAHSGHQLVSWRNADASVAHKTWDDYDEGLAAIVVQVQVSGREINTLFCVGGTMTALATAVLAARGHEHPAASMTLLTAMLDFSDTGTGLDVFVD EAHVQMRQETGGKNGAOPGLMRGVFEANTFLRPNDLWVYVNDYKGRTPAPDFLLWNGDSTSLPGMYAVYLRNLYENKLRPEALTVCGEYVLSRIDVPTFIYGSREDHIVPWQTAAYASTSLSGPLKVLGASGHVAGVNPAPKAKRSYVWNEGDLPESADDAEFAATEQPSWWTWVWELDAYVGGKRVAPPAQPSGAQFVIEPAPGRVYLQRD





**Supplementary Table 2.5. Percent Identity Matrix from multiple sequence alignment of 33 known and putative PHA synthases from bacterial human pathogens.**

1: <i>A. baumannii</i> (HMPREF0010_00690)	100.00	94.18	60.00	29.23	21.30	20.69	21.84	19.23	20.98	20.98	22.06	19.23	18.71	20.06	19.29	18.28	18.43	18.82	21.56	18.67	20.23	18.75	18.07	21.02	19.29	18.93	20.62	18.58	18.88	20.38	20.87	18.71	16.37	
2: <i>A. calcoceticus</i> (BDGL_001038)	94.18	100.00	60.56	27.69	22.19	21.26	22.41	19.82	21.55	21.55	22.65	19.82	18.71	20.65	19.88	21.57	18.09	17.42	21.56	18.99	20.53	19.06	18.38	21.07	19.29	19.53	20.62	19.47	20.06	21.00	20.56	18.13	16.08	
3: <i>A. radiorisens</i> (HMPREF0018_01802)	60.00	60.56	100.00	27.30	21.05	18.98	20.68	18.77	19.55	19.55	20.93	18.77	18.79	21.35	19.71	21.90	17.45	16.84	21.30	20.00	20.09	18.77	23.49	19.65	19.01	20.91	17.78	18.37	21.05	20.19	16.14	15.56		
4: <i>B. anthracis</i> (PHAC)	29.23	27.69	27.30	100.00	24.78	25.36	25.36	23.68	25.65	25.65	25.37	23.68	23.70	24.56	24.12	24.57	19.93	20.21	21.81	20.45	22.97	21.81	20.19	23.53	17.89	19.30	20.43	24.13	25.00	22.50	31.92	26.72	23.70	
5: <i>B. pertussis</i> (PHBC)	21.30	22.19	21.05	24.78	100.00	56.55	57.54	35.71	57.30	57.30	57.79	35.90	41.24	32.64	31.62	29.41	16.76	17.52	17.86	17.15	35.89	18.48	18.16	19.20	37.38	38.46	17.65	35.42	35.80	23.67	38.58	37.08		
6: <i>B. cereospacia</i> (PHBC)	20.69	21.26	18.98	25.36	56.55	100.00	83.23	33.63	93.40	93.40	83.78	33.63	38.47	37.76	30.37	28.28	20.22	21.37	17.55	17.87	34.13	17.89	17.59	16.67	36.92	36.55	14.90	35.90	36.08	16.84	24.12	38.96	39.48	
7: <i>B. malii</i> (PHBC)	21.84	22.41	20.68	25.36	57.54	83.23	100.00	34.55	84.35	84.35	99.00	34.55	38.93	32.47	30.28	28.09	18.89	19.43	18.04	18.73	35.05	18.84	18.32	17.88	38.10	36.80	14.86	34.97	35.66	16.84	23.24	39.76	38.89	
8: <i>B. malii</i> (PHAC)	19.23	19.82	18.77	23.68	35.71	33.63	34.55	100.00	34.33	34.74	99.83	37.48	49.57	48.19	50.09	20.06	20.90	19.51	21.11	30.92	21.18	20.05	19.81	29.93	32.06	19.26	31.83	32.19	19.95	21.36	33.75	33.57		
9: <i>B. multivorans</i> (BMUL_1483)	20.98	21.55	19.55	25.65	57.30	93.40	84.35	34.33	100.00	100.00	85.14	34.33	39.51	33.28	30.72	28.79	19.11	20.23	18.09	18.73	34.68	18.68	18.37	16.97	37.48	36.73	15.86	36.08	36.43	17.38	23.82	39.83	39.83	
10: <i>B. multivorans</i> (BMUL_L_01759)	20.98	21.55	19.55	25.65	57.30	93.40	84.35	34.33	100.00	100.00	85.14	34.33	39.51	33.28	30.72	28.79	19.11	20.23	18.09	18.73	34.68	18.68	18.37	16.97	37.48	36.73	15.86	36.08	36.43	17.38	23.82	39.83	39.83	
11: <i>B. pseudomallei</i> (PHBC)	22.06	22.65	20.93	25.37	57.79	83.78	99.00	34.74	85.14	85.14	100.00	34.74	39.68	32.46	30.42	28.95	18.29	19.83	17.60	18.73	35.01	18.47	18.42	17.99	38.79	37.48	14.81	35.71	36.43	16.94	23.35	40.60	39.89	
12: <i>B. pseudomallei</i> (BPS1954)	19.23	19.82	18.77	23.68	35.90	33.63	34.55	99.83	34.33	34.74	100.00	37.48	49.57	48.19	50.09	20.06	20.90	19.51	21.11	30.92	21.18	20.05	19.81	29.93	32.06	19.26	31.83	32.19	19.95	21.36	33.75	33.57		
13: <i>L. pneumophila</i> (pg0599)	18.71	18.71	18.79	23.70	41.24	38.47	38.93	37.48	39.51	39.51	39.68	37.48	100.00	35.00	34.65	34.33	19.77	20.00	15.95	15.59	15.78	15.78	16.27	17.59	32.65	33.77	14.62	39.93	40.45	16.62	19.76	40.00	39.83	
14: <i>L. pneumophila</i> (pg1058)	20.06	20.65	21.35	24.56	32.64	32.76	32.47	49.57	33.28	33.28	32.46	49.57	35.00	100.00	83.36	63.59	17.51	17.43	17.98	18.05	30.15	17.79	15.86	18.52	29.13	29.07	17.88	31.16	32.07	15.11	20.77	32.50	30.70	
15: <i>L. pneumophila</i> (pg1097)	19.29	19.88	19.71	24.12	31.62	30.37	30.28	48.19	30.72	30.72	30.42	48.19	34.65	83.36	100.00	63.18	17.61	17.43	16.39	16.86	28.65	15.95	15.09	16.98	29.18	29.18	16.49	30.60	31.15	14.33	20.00	31.77	31.23	
16: <i>L. pneumophila</i> (pg2260)	21.28	21.57	21.90	24.57	29.41	28.28	28.09	50.09	28.79	28.79	28.95	50.09	34.33	63.59	63.18	100.00	16.71	17.43	18.31	17.16	29.07	17.84	16.71	18.52	27.44	28.36	16.88	30.65	31.36	15.15	20.94	31.73	30.84	
17: <i>L. borgpetersenii</i> (LBL_2592)	18.43	18.09	17.45	19.93	16.76	20.22	18.89	20.06	19.11	19.11	18.29	20.06	19.77	17.51	17.61	16.71	100.00	88.13	17.43	19.72	16.24	16.24	19.02	18.95	16.38	19.25	15.47	16.19	19.36	20.23	19.80	15.46	16.81	15.67
18: <i>L. interrogans</i> (LA_2034)	18.82	17.42	16.84	20.21	16.72	21.37	19.43	20.90	20.23	20.23	19.83	20.90	20.00	17.43	17.43	88.13	100.00	19.93	20.76	16.18	19.54	19.47	15.38	20.35	16.52	16.34	18.99	19.58	21.67	14.29	18.37	17.49		
19: <i>M. abscessus</i> (MAB_2348)	21.56	21.56	21.30	21.81	17.86	17.55	18.04	19.51	18.09	18.09	17.60	19.51	15.95	17.98	16.39	18.31	17.43	19.93	100.00	66.14	17.34	63.36	64.98	22.70	15.19	19.28	57.68	15.26	16.35	50.92	24.29	17.16	17.43	
20: <i>M. avium</i> (MAP1389)	18.67	18.99	20.00	20.45	17.15	17.87	18.73	21.11	18.73	18.73	18.73	21.11	15.59	18.05	16.86	17.16	19.72	20.76	66.14	100.00	17.30	82.11	84.02	23.64	17.11	17.06	58.53	16.86	17.75	51.31	25.33	16.28	15.99	
21: <i>M. kansasii</i> (MKANNA1_010100013815)	20.23	20.53	20.00	22.87	35.89	34.13	35.05	30.92	34.68	34.68	35.01	30.92	30.95	30.15	28.65	29.07	16.24	16.18	17.34	17.30	100.00	17.69	17.11	18.27	40.75	39.43	15.97	29.54	29.36	16.94	23.01	33.70	33.52	
22: <i>M. leprae</i> (ML1346)	18.75	19.06	20.99	21.81	18.48	17.89	18.64	21.18	18.68	18.68	18.47	21.18	15.78	17.79	15.95	17.84	19.02	19.54	63.36	82.11	17.69	100.00	85.67	24.86	16.94	18.80	55.77	15.90	16.71	51.28	25.87	18.04	17.24	
23: <i>M. tuberculosis</i> (MT1723)	18.07	18.38	18.77	20.19	18.16	17.59	18.32	20.05	18.37	18.37	18.42	20.05	16.27	15.86	16.71	18.95	19.47	64.98	84.02	17.11	85.67	100.00	22.25	17.17	18.48	57.79	15.86	16.67	51.73	24.84	17.72	17.46		
24: <i>N. farcinica</i> (NFA_45720)	21.02	21.97	23.49	23.53	19.20	16.67	17.88	18.81	16.97	16.97	17.99	19.81	17.59	18.52	16.98	18.52	16.38	15.38	22.70	23.64	18.27	24.86	22.25	100.00	21.25	19.31	24.29	14.91	14.29	22.99	22.88	16.26	15.95	
25: <i>P. aeruginosa</i> (PhaC1)	19.29	19.29	19.65	17.89	37.38	36.92	38.10	29.93	37.48	37.48	38.79	29.93	32.65	29.13	29.18	27.44	19.25	20.35	15.19	17.11	40.75	16.94	17.17	21.25	100.00	58.78	15.24	32.16	32.16	16.39	19.64	33.64	33.83	
26: <i>P. aeruginosa</i> (PhaC2)	18.93	19.53	19.01	19.30	38.46	36.55	36.80	32.06	36.73	36.73	37.48	32.06	36.73	29.07	29.18	28.36	16.47	16.52	19.28	17.06	39.43	18.80	18.48	19.31	58.78	100.00	16.53	34.20	33.09	19.67	21.66	33.77	34.14	
27: <i>R. typhi</i> (PHBC)	20.62	20.62	20.91	20.43	17.65	14.90	14.86	19.26	15.66	15.66	14.81	19.26	13.62	16.68	16.49	16.88	16.19	16.34	57.68	58.53	15.87	55.77	57.79	24.29	15.24	16.53	100.00	15.76	15.50	50.87	25.16	15.90	15.13	
28: <i>P. prinzweileri</i> (E:RP820)	18.58	19.47	17.78	24.13	35.42	35.90	34.97	31.83	36.08	36.08	35.71	31.83	39.93	31.16	30.60	30.65	19.36	18.99	15.26	16.86	29.54	15.90	15.86	14.91	32.16	34.20	15.76	100.00	95.72	15.93	18.99	37.80	37.80	
29: <i>R. prowazekii</i> (E:RP820)	18.88	20.06	18.37	25.00	35.80	36.08	35.66	32.19	36.43	36.43	36.43	36.43	36.43	40.45	32.07	31.15	31.36	20.23	19.58	16.35	17.75	29.36	16.71	16.67	14.29	32.16	33.09	15.50	95.72	100.00	16.48	18.99	37.80	38.33
30: <i>S. rugosus</i> (HMPREF0336_01483)	20.38	21.00	21.05	22.50	19.06	16.84	16.84	19.95	17.38	17.38	16.94	19.95	16.62	15.11	14.33	15.15	19.80	21.67	50.92	51.31	16.94	51.28	51.73	22.89	16.39	19.67	50.87	15.93	16.48	100.00	26.90	17.30	27.57	
31: <i>S. maltophilia</i> (SMAL_2415)	20.87	20.56	20.19	31.92	23.67	24.12	23.24	21.36	23.82	23.82	23.35	21.36	19.76	20.77	20.00	20.94	14.29	24.29	25.33	25.87	24.84	23.81	23.87	24.84	22.89	19.64	21.66	25.16	18.99	18.99	26.90	100.00	22.87	22.29

**Supplementary Table 2.6.** Strains, plasmids, and oligonucleotides used in this study.

Strain or plasmid or oligo	Description	Reference
<b><i>E. coli</i></b>		
XL1-Blue	<i>recA1 endA1 gyrA96 thi-1 hsdR17 supE44 relA1 lac</i> [F' <i>proAB lacI<sup>f</sup> lacZ ΔM15 Tn10 (Tet<sup>r</sup>)</i> ]	Stratagene
ClearColi BL21(DE3)	F– <i>ompT hsdSB (rB- mB-) gal dcm lon λ</i> (DE3 [ <i>lacI lacUV5-T7 gene 1 ind1 sam7 nin5</i> ]) <i>msbA148 ΔgutQΔkdsD ΔlpxLΔlpxMΔpagPΔlpxPΔeptA</i>	Lucigen
<b><i>P. aeruginosa</i></b>		
<i>P. aeruginosa</i> PAO1	Prototroph, nonmucoid	ATCC 15692
PAO1 <i>ΔphaC1ZC2</i>	PHA-negative mutant of PAO1 lacking functional <i>phaC1<sub>Pa</sub></i> and <i>phaZ</i>	[1]
PAO1 <i>ΔphaC1ZC2 Δalg8</i>	PAO1 <i>ΔphaC1ZC2</i> derivative with markerless, isogenic <i>alg8</i> deletion, double mutant	This study
PAO1 <i>ΔphaC1ZC2 Δalg8 ΔpelF</i>	PAO1 <i>ΔphaC1ZC2 Δalg8</i> derivative with markerless, isogenic <i>pelF</i> deletion, triple mutant	This study
<b>Plasmids</b>		
pEX100T:: <i>ΔpelF</i> ΩGm	Amp <sup>r</sup> Cb <sup>r</sup> Gm <sup>r</sup> , vector pEX100T with <i>Sma</i> I-inserted <i>pelF</i> deletion construct	[2]
pEX100T:: <i>Δalg8</i> ΩGm	Amp <sup>r</sup> Cb <sup>r</sup> Gm <sup>r</sup> ; vector pEX100T with <i>Sma</i> I-inserted <i>alg8</i> deletion construct	[3]
pFLP2	Amp <sup>r</sup> Cb <sup>r</sup> ; broad-host-range vector encoding Flp recombinase	[4]
pGEM-T easy	Cloning vector, f1 origin, Amp <sup>r</sup>	Promega
pUC57	Cloning vector, ColE1 origin, Amp <sup>r</sup>	Fermentas
pUC57_Ag	pUC57 derivative containing <i>E. coli</i> codon optimized OprI/F-AlgE fusion antigen fragment (OprI-OprF(x3)-L6-L5) flanked by <i>Nde</i> I/ <i>Bam</i> HI sites	This study
pET16b	Amp <sup>r</sup> , T7 promoter, His <sub>10</sub> -tag	Novagen
pET16b-HisAg	pET16b derivative containing His <sub>10</sub> -tagged <i>E. coli</i> codon optimized OprI/F-AlgE fusion antigen fragment (OprI-OprF(x3)-L6-L5) in <i>Nde</i> I/ <i>Bam</i> HI sites of pET16b	This study
pBHR71	pBluescript SK- derivative; Amp <sup>r</sup> ; P <sub>lac</sub> ; containing <i>phaC1</i> gene coding for PHA <sub>MCL</sub> synthase of <i>P. aeruginosa</i> PAO1	[5]
pBBR1MCS-5	Gm <sup>r</sup> ; broad-host-range vector; P <sub>lac</sub>	[6]
pBBR1JO-5	Gm <sup>r</sup> , P <sub>lac</sub> , pBBR1MCS-5 with MCS from pBluescript SK-	[7]
pBBR1JO-5_C1	pBBR1JO-5 derivative containing Shine-Dalgarno- <i>phaC1</i> fragment from pBHR71 in <i>Xba</i> I/ <i>Bam</i> HI sites of pBBR1JO-5	This study
pGEM-T_C1(-)	PHA <sub>MCL</sub> synthase gene fragment amplified from pBHR71 with stop codon removed flanked by <i>Xba</i> I/ <i>Bam</i> HI	This study
pBBR1JO-5_C1(-)	pBBR1JO-5 derivative containing <i>Xba</i> I/ <i>Bam</i> HI inserted PHA <sub>MCL</sub> synthase gene fragment from pGEM-T_C1(-)	This study
pET-14b PhaC-linker-SG-linker-GFP	pET-14b PhaC-linker-GFP derivative containing the SG linker sequence upstream of <i>gfp</i>	[8]
pGEM-T_LSGLgfp	LSGLgfp fragment with flanking <i>Bgl</i> III/ <i>Bam</i> HI sites amplified from pET-14b PhaC-linker-SG-linker-GFP	This study

pBBR1JO-5_C1gfp	BglIII/BamHI LSGLgfp fragment from pGEM-T_LSGLgfp inserted into BamHI site of pBBR1JO-5_C1(-) downstream of 3' end of <i>phaC1<sub>Pa</sub></i>	This study
pHERD20T	Amp <sup>r</sup> Cb <sup>r</sup> , pUCP20T P <sub>lac</sub> replaced with fragment of <i>araC</i> -P <sub>BAD</sub> cassette	[9]
pHERD20T-2	pHERD20T derivative were a 13 bp fragment of 5' end of LacZα is removed	This study
pHERD20T-2_C1	Shine-Dalgarno- <i>phaC1<sub>Pa</sub></i> fragment from pBBR1JO-5_C1 inserted in to XbaI/HindIII site of pHERD20T-2	This study
pUC57_Ag(N)	pUC57 derivative containing <i>P. aeruginosa</i> codon optimized OprI/F-AlgE fusion antigen fragment (L5-L6-OprF(x3)-OprI-Linker (GSGGG) flanked by XbaI/NdeI sites	This study
pHERD20T-2_AgC1	Codon optimized Ag fragment from pUC57_Ag(N) inserted in to XbaI/NdeI sites of pHERD20T-2_C1 upstream of <i>phaC1<sub>Pa</sub></i>	This study
pUC57_Ag(C)	pUC57 derivative containing <i>P. aeruginosa</i> codon optimized OprI/F-AlgE fusion antigen fragment (OprI-OprF(x3)-L6-L5) flanked by SmaI/EcoRI sites	This study
pBBR1JO-5_C1Ag	Condon optimized OprI/F-AlgE fusion antigen fragment from pUC57_Ag(C) inserted in to SmaI/EcoRI site of pBBR1JO-5_C1gfp replacing GFP	This study
pHERD20T-2_C1Ag	<i>phaC1<sub>Pa</sub></i> -LSGL-Ag fragment from pBBR1JO-5_C1Ag inserted in to XbaI/HindIII sites of pHERD20T-2	This study

#### Oligonucleotides

Alg8_XUP	5' GCGTCGAGGCCAAGGTCCC	[2]
Alg8_XDN	5' CCTGGCGTTGTCCGTAGTCG	[2]
PeIF_XUP	5' ACATGCTGCAACGGCCGCCCT	[2]
PeIF_XDN	5' TAGGCGCGCAGGGTCGCCGTA	[2]
F_phaC1	5' AAATCTAGAAATAAGGAGATATACATATGAGTCAGAAGAACAAT AACGAG	This study
R_phaC1_(-) stop_BamHI	5' ATTGGATCCTCGTTCATGCACGTAGGTTCCG	This study
F_BglIII_LSGLgfp	5' AATAGATCTGTGCTGGCGGTGGCGATTGATAAACGCGG	This study
R_LSGLgfp_BamHI	5' GCCGGATCCTCATTGTATAGTTCATCCATGCCATGTG	This study

1. Pham, T.H., J.S. Webb, and B.H.A. Rehm, *The role of polyhydroxyalkanoate biosynthesis by Pseudomonas aeruginosa in rhamnolipid and alginate production as well as stress tolerance and biofilm formation*. Microbiology, 2004. **150**(10): p. 3405-3413.
2. Ghafoor, A., I.D. Hay, and B.H.A. Rehm, *Role of exopolysaccharides in Pseudomonas aeruginosa biofilm formation and architecture*. Applied and Environmental Microbiology, 2011. **77**(15): p. 5238-5246.
3. Remminghorst, U. and B.H.A. Rehm, *In vitro alginate polymerization and the functional role of Alg8 in alginate production by Pseudomonas aeruginosa*. Applied and Environmental Microbiology, 2006. **72**(1): p. 298-305.
4. Hoang, T.T., et al., *A broad-host-range Flp-FRT recombination system for site-specific excision of chromosomally-located DNA sequences: application for isolation of unmarked Pseudomonas aeruginosa mutants*. Gene, 1998. **212**(1): p. 77-86.
5. Langenbach, S., B.H.A. Rehm, and A. Steinbuchel, *Functional expression of the PHA synthase gene PhaC1 from Pseudomonas aeruginosa in Escherichia coli results in poly(3-hydroxyalkanoate) synthesis*. Fems Microbiology Letters, 1997. **150**(2): p. 303-309.
6. Kovach, M.E., et al., *Four new derivatives of the broad-host-range cloning vector pBBR1MCS, carrying different antibiotic-resistance cassettes*. Gene, 1995. **166**(1): p. 175-176.

7. Peters, V. and B.H.A. Rehm, *In vivo monitoring of PHA granule formation using GFP-labeled PHA synthases*. FEMS Microbiology Letters, 2005. **248**(1): p. 93-100.
8. Jahns, A.C. and B.H.A. Rehm, *Tolerance of the Ralstonia eutropha class I polyhydroxyalkanoate synthase for translational fusions to its C terminus reveals a new mode of functional display*. Applied and Environmental Microbiology, 2009. **75**(17): p. 5461-5466.
9. Qiu, D., et al., *PBAD-based shuttle vectors for functional analysis of toxic and highly regulated genes in Pseudomonas and Burkholderia spp. and other bacteria*. Applied and Environmental Microbiology, 2008. **74**(23): p. 7422-7426.

## Link to next chapter

In chapter 2, the production of vaccine PHA beads in an opportunistic pathogen *P. aeruginosa* was successfully demonstrate, this resulted in vaccine beads carrying copurifying HCPs that represented as a large antigenic repertoire and was able to induce a dominant Th1 type response required for the control of *P. aeruginosa* infection.

This study demonstrated the feasibility of utilizing the PHA production system of the disease causing opportunistic pathogen to produce particulate subunit vaccines that were immunogenic. This represents a novel approach to subunit vaccine development, which is applicable to a range of infectious diseases.

Therefore, to further exemplify this concept, in chapter 3 we describe the development of an antigen-displaying PHA bead based prophylactic vaccine for the prevention of the disease tuberculosis caused by the pathogen *M. tuberculosis*.

In this chapter a slightly different approach was described, where the use of nonpathogenic *M. smegmatis* as a model organism for pathogen *M. tuberculosis* was investigated. This involved the engineering, production, and validation (immunological and challenge) of Ag85A-ESAT-6 displayed on PHA beads produced in *M. smegmatis*. This example would give support to the concept of using a model organism for the production of vaccine PHA bead that can protect against disease.

## Chapter 3: Engineering mycobacteria for the production of self-assembling biopolyesters displaying mycobacterial antigens for use as tuberculosis vaccine

Jason W. Lee,<sup>1</sup> Natalie A. Parlane,<sup>2</sup> Bernd H. A. Rehm,<sup>1,3</sup> Bryce M. Buddle,<sup>2</sup> and Axel Heiser<sup>2\*</sup>

*Institute of Fundamental Sciences, Massey University, Palmerston North, New Zealand<sup>1</sup>; AgResearch, Hopkirk Research Institute, Palmerston North, New Zealand<sup>2</sup>; and PolyBatics, Palmerston North, New Zealand<sup>3</sup>*

\*Corresponding author: Axel Heiser, e-mail: axel.heiser@agresearch.co.nz,  
phone: +64 6 351 8691

### Abstract

Tuberculosis (TB) is a disease caused by *Mycobacterium tuberculosis* or *Mycobacterium bovis* and still remains one of the world's biggest global health burdens. Recently, engineered polyhydroxyalkanoate (PHA) biobeads produced in both *E. coli* and *Lactococcus lactis* displaying mycobacterial antigens were found to induce significant cell mediated immune responses in mice. We observed that such PHA beads contained host cell proteins as impurities, which we hypothesized to have the potential to induce immunity. In this study we aimed to develop PHA beads produced in mycobacteria (mycobacterial PHA biobeads, MBB) and test their potential as TB vaccine in a mouse model. As a model organism, nonpathogenic *Mycobacterium smegmatis* was engineered to produce MBB or MBB with immobilized mycobacterial antigens Ag85A and ESAT-6 on their surface (A:E-MBB). Three key enzymes involved in the poly(3-hydroxybutyric acid) pathway, namely  $\beta$ -ketothiolase (PhaA), acetoacetyl-CoA reductase (PhaB), and PHA synthase (PhaC), were engineered into *E. coli*-mycobacteria shuttle plasmids and expressed in trans. Immobilization of specific antigens to the surface of the MBB was achieved by creating a fusion with the PHA synthase which remains covalently attached to the polyester core, resulting in PHA biobeads displaying covalently immobilized antigens. MBB, A:E-MBB and a mycobacterial vector control (MVC) were used in a mouse immunology trial, with comparison to PBS vaccinated and BCG vaccinated groups. We successfully produced MBB and A:E-MBB and used them as vaccines to induce a cellular immune response to mycobacterial antigens.

### 3.1 Introduction

Tuberculosis (TB) is a major cause of morbidity and mortality worldwide. The latest World Health Organization (WHO) global tuberculosis report estimates 10.4 million new TB cases worldwide and approximately 1.4 million TB deaths in 2015 [1]. Current TB control strategies employ a partially effective live attenuated vaccine called Bacillus Calmette–Guérin (BCG) [2] for the prevention of severe cases of TB in children and use of multiple anti-tuberculosis drugs for the treatment of TB. These strategies have been successful in reducing both the incidence and prevalence of TB globally.

However, the emergence of multidrug-resistant TB (MDR-TB) and extensively drug-resistant TB (XDR-TB) strains of *M. tuberculosis* has complicated TB control [3, 4]. Furthermore, the burden of HIV-associated TB (HIV-TB) remains problematic and accounts for a large proportion (25%) of all TB related deaths [1].

BCG vaccine is a live attenuated strain of *M. bovis* that was developed in the early 20th century for the prevention of TB globally, and to date BCG still remains the only available TB vaccine on the market. BCG however is seen only to protect against severe forms of childhood TB (tuberculous meningitis and miliary TB) and confers variable protection in adolescents and adults against pulmonary TB [2, 5, 6]. Although regarded as safe, complications from BCG vaccination in immunocompetent individuals can occur. Adverse events linked to BCG vaccination range from mild, localized complications to more serious, systemic or disseminated BCG disease in which *M. bovis* BCG is confirmed in one or more anatomical sites far from both the site of injection and regional lymph nodes. Furthermore, immunocompromised individuals such as those suffering from HIV are at a significantly higher risk of developing BCG-related diseases [6, 7].

Consequently, there is great interest in new and novel vaccines that can offer better protection than the current BCG vaccine and which can also confer protection from TB in HIV-infected individuals. Currently, significant efforts are being made to developing new and improved vaccines against TB, with 13 candidate vaccines in clinical trials and a number in early development [1, 2, 5, 6]. However, a limited understanding of the immunity to *M. tuberculosis* is significantly hindering vaccine development [8].

Particulate vaccine delivery systems offer an advantageous approach to vaccine development. These systems are useful as they mimic various properties of pathogens, with size being the most important factor [9, 10]. Further advantages of particulate delivery systems include the potential to target antigen-presenting cells (APC), the potential for controlled antigen release, displaying multiple antigens and inclusion of immunomodulatory molecules [11-13]. Furthermore, particulate vaccine delivery systems can enhance the immune response as they demonstrate adjuvating properties [10, 14] by promoting the uptake and trafficking of antigens to the local lymph nodes, which is a key step in the generation of potent immune responses. A range of factors such as size, shape, and surface charge can influence immune response and antigen uptake by APCs, and solubility of the particulate delivery system used [9, 10]. Studies have shown that protective cellular immune responses are preferentially induced when antigens are displayed on small particulates such as virus-like particles (VLPs) [15], liposomes [16], immune stimulating complexes (ISCOMs) [17], chitosan [18], polylactide co-glycolide (PLG) microparticles [13] and polyhydroxyalkanoate (PHA) biobeads [12, 19-21].

PHA biobeads are of particular interest and offer an exciting and new avenue for vaccine design. In comparison to other particulate systems PHA biobeads offers two distinct advantages: (1) vaccine antigens are covalently bound in uniform direction to the surface and (2) these antigen-displaying beads can be produced in a one-step process [22].

The most commonly found PHA is polyhydroxybutyrate (PHB) and requires three key enzymes,  $\beta$ -ketothiolase, acetoacetyl-CoA reductase, and PHA synthase (encoded by *phaA*, *phaB*, and *phaC*, respectively) for PHA biobead formation [22, 23].

Recently, our group demonstrated the use of PHA biobeads with surface immobilized antigens produced in *E. coli* as safe and efficient vaccine delivery agents [20]. These PHA biobeads were engineered to display *M. tuberculosis* vaccine candidate antigen 85A (Ag85A) and early secreted antigenic target 6-kDa protein (ESAT-6) by creating a gene fusion with the PHA synthase and expressing in an *E. coli* production hosts.

As an alternative to *E. coli* a number of other bacteria, such as Gram-positive *L. lactis*, have been exploited as possible production hosts [19, 24]. PHA biobeads produced from both *E. coli* and *L. lactis* and displaying mycobacterial proteins Ag85A and ESAT-6 were tested as vaccine in mice and were found to induce a significant protection mediated by Th1 and interleukin IL-17A-biased T cell responses [12].

During these experiments we found that bacterial host cell proteins were attached to the surface of the partially purified PHA biobeads and we hypothesize that they too could function as antigens. If produced in mycobacteria instead of *E. coli* or *L. lactis* such PHA biobeads should carry mycobacterial antigens on their surface, including not only known antigens but also many yet undiscovered antigens that have the potential to induce protective immunity [21].

The aim of this study was to investigate the hypothesis that PHA biobeads can be produced in mycobacteria and function as vaccines protecting against mycobacterial infection. Therefore, we engineered *M. smegmatis* as a model organism for the production of antigen-displaying PHA biobeads presenting the fusion protein Ag85A-ESAT-6 [12, 20]. These PHA biobeads were expected to include host cell proteins derived from *M. smegmatis* that might serve as additional antigens enhancing the induction of protective immunity and/or contribute adjuvanting properties. Mouse vaccinations were performed to assess efficacy of these PHA biobeads.

Mycobacterial PHA biobeads potentially provide a new vaccination platform combining a large antigenic repertoire (comparable to that of live vaccines) with high safety (noninfectious vaccine and absence of any genetic material) and ease and cost efficiency of production.

## 3.2 Methods

### Bacterial strains, and cultivation conditions

Bacterial strains used in this study are listed in **Table 3.1**. *E. coli* strains were cultivated in Luria broth (Difco, Detroit, MI). For LB agar 1.5% (w/v) agar was added to liquid. *M. smegmatis* was cultivated on BBL Middlebrook 7H9 broth or 7H10 agar (BD, Franklin Lakes, NJ, USA) supplemented with 0.2% glycerol (v/v) and 10% (v/v) OADC (BD). Additionally to 7H9 broth was supplemented with 0.05% Tween-80 (v/v).

If required, antibiotics were added to medium at the following concentrations: ampicillin, 100 µg/mL (*E. coli*); kanamycin, 30 µg/mL (*E. coli* and *M. smegmatis*); and hygromycin, 200 µg/mL (*E. coli*) or 90 µg/mL (*M. smegmatis*). Unless stated otherwise, *E. coli* strains and *M. smegmatis* mc<sup>2</sup>155 were cultivated at 37°C with aeration at 200 × rpm. When required for protein induction, tetracycline or isovaleronitrile was added at a final concentration of 30 ng/mL or 50 µM/mL, respectively.

### Construction of plasmids for the production of PHB

All plasmids and oligonucleotides used can be found in **Table 3.1**. All synthesized genes have been codon usage optimized for *M. tuberculosis*. DNA sequencing was used to confirm all amplified and final plasmids. Several different plasmids were generated for the expression of PHA synthase alone (*phaC*) or as a fusion protein with antigens Ag85A-ESAT-6 utilizing either the nitrile (pMycVec1 and pMV261 derivatives) or tetracycline (pMIND derivatives) inducible promoter. A single plasmid was generated for the expression of PHB precursor genes (*phaAB*) regulated under a weak constitutive *M. smegmatis* promoter (Pwmyc).

A one-plasmid system was also created which encoded all three genes, with *phaC* regulated under the nitrile promoter (pNit) and genes *phaA* and *phaB* under Pwmyc utilizing the pMV261 vector [25] for comparison with the two-plasmid system for protein and PHB production.

**Table 3.1.** Bacterial strains and plasmids used in this study

Strain and plasmid	Description	Reference or source
<b><i>E. coli</i></b>		
XL1-Blue	<i>recA1 endA1 gyrA96 thi-1 hsdR17 supE44 relA1 lac</i> [F' <i>proAB lacI</i> <sup>fl</sup> <i>lacZ</i> ΔM15 Tn10 (Tet <sup>r</sup> )]	Stratagene
BL21(DE3)	<i>E. coli</i> B F <sup>-</sup> <i>dcm ompT hsdS</i> (r <sub>B</sub> <sup>-</sup> m <sub>B</sub> <sup>-</sup> ) <i>gal</i> λ(DE3)	Stratagene
<b><i>Mycobacterium smegmatis</i></b>		
mc <sup>2</sup> 155	Ept <sup>-</sup> , Kan <sup>S</sup>	[26]
<b>Plasmids</b>		
pMycVec1	<i>E. coli</i> -mycobacteria vector, pAL5000 origin, ColE1 origin (pBR322); Kan <sup>R</sup>	[27]
pMycVec1_pNit- <i>gfp</i>	pNit promoter and ext- <i>gfp</i> from pNit-1:: <i>gfp</i>	This study
pMycVec1_pNit- <i>phaC</i>	pNit promoter and <i>phaC</i> from pET-16b_pNit- <i>phaC</i>	This study
pMycVec2	pMS2 cloning vector for mycobacteria, pJAZ38 origin, ColE1 origin (pUC19); Hyg <sup>R</sup>	This study
pMycVec2_Pwmyc- <i>phaAB</i>	Amplified <i>phaAB</i> regulated under constitutive promoter Pwmyc	This study
pMIND	<i>E. coli</i> -mycobacteria vector, pAL5000 origin, ColE1 origin; pTetRO; Kan <sup>R</sup> ; Hyg <sup>R</sup>	[28]
pMIND_pTet- <i>phaC</i>	<i>M. tuberculosis</i> codon usage optimized <i>phaC</i> regulated under <i>tetRO</i> operator	This study
pMV261_pNit	<i>E. coli</i> -mycobacteria vector with pNit promoter. pAL5000 origin, pUC origin; Kan <sup>R</sup>	This study
pNit-1:: <i>gfp</i>	pMV261 containing ext- <i>gfp</i> reporter gene regulated under pNit promoter	[25]
pMV261_pNit- <i>phaC</i>	<i>phaC</i> from pUC57_ <i>phaC</i> regulated under pNit	This study
pMV261_pNit-A:E- <i>phaC</i>	Ag85A-ESAT-6 hybrid gene upstream of <i>phaC</i> regulated under pNit	This study
pMV261_pNit- <i>phaC</i> -Pwmyc- <i>phaAB</i>	pMV261_pNit- <i>phaC</i> derivative containing genes fragment <i>phaCAB</i> from pUC57_pTet- <i>phaC</i> -Pwmyc- <i>phaAB</i> _PacI	
pET-16b	Ap <sup>R</sup> , T7 promoter	Novagen
pET-16b_pNit- <i>gfp</i>	pET-16b derivative containing <i>gfp</i> regulated under pNit promoter	This study
pET-16b_pNit- <i>phaC</i>	<i>phaC</i> derived from pUC57_ <i>phaC</i>	This study
pMCS69	pBBR1MCS derivative containing <i>phaAB</i> genes from <i>Cupriavidus necator</i>	[29]
pHAS-Ag85A-ESAT-6	pHAS containing Ag85A-ESAT-6 hybrid gene upstream of <i>phaC</i>	[20]
pGEM-T_Pwmyc	Encoding a synthesized weak constitutive promoter (Pwmyc) from <i>M. smegmatis</i>	This study
pUC57_ <i>phaC</i>	Synthesized <i>phaC</i> from <i>Cupriavidus necator</i> codon usage optimized for expression in <i>M. tuberculosis</i>	This study
pUC57- <i>phaC</i> -Pwmyc- <i>phaAB</i>	Synthesized <i>phaC</i> regulated under <i>tetRO</i> operator and genes <i>phaAB</i> regulated under weak constitutive <i>M. smegmatis</i> promoter Pwmyc. All genes codon usage optimized for expression in <i>M. tuberculosis</i> .	This study
pUC57- <i>phaC</i> -Pwmyc- <i>phaAB</i> _PacI	Same as pUC57_ <i>phaC</i> -Pwmyc- <i>phaAB</i> but with the introduction of PacI restriction site downstream of <i>phaB</i>	This study
pUC57_3' <i>phaB</i> _PacI	Encoding synthesized gene fragment for the introduction of PacI site to 3' end of <i>phaB</i>	This study
<b>Oligonucleotides</b>		
5' – 3'		
fwd_BamHI_pNit	ATAGGATCCAGGACCCTTGTCATTCACGTCGAATTC	This study
rev_pNit_XbaI	TGT CGT CAT ATC TAG ACT ACG AAA CCT CCG TCG G	This study
fwd_NheI_ <i>phaAB</i>	AAAGCTAGCAAGGAGTACACAATGACTGACGTTGTCATCG	This study
rev_ <i>phaAB</i> _PacI	TATTTAATTAATCAGCCCATATGCAGGCCGCGTTGAG	This study
fwd_A:E	ACATATGTTTTCCCGGCCGGGCTTG	This study
rev_A:E	TCATATGACTAGTTGCGAACATCCCAGTGACG	This study

Plasmid pMycVec1\_pNit-*phaC* (**Supplementary Fig. 3.1**). This plasmid encodes the gene for the class I PHA synthase (*phaC*) regulated under a strong nitrile inducible promoter pNit (pNit-1::*gfp* was kindly provided by Chris Sasseti, University of Massachusetts, Worcester). Firstly, the nitrile promoter and ext-*gfp* encoding fragment was amplified from plasmid pNit-1::*gfp* [25] using primers fwd\_BamHI\_pNit and rev\_pNit\_XbaI. Resultant fragment was ligated into intermediate cloning vector pGEM-T Easy (Promega, Madison, WI, USA). Following confirmation, pNit-*gfp* fragment was excised using BamHI and XbaI and successively ligated at complementary sites with intermediate cloning vector pET-16b or vector pMycVec1 for constructing final plasmid pMycVec1\_pNit-*gfp*. NdeI and SwaI were used to replace ext-*gfp* encoding fragment in pET-16b\_pNit-*gfp* with *M. tuberculosis* codon-optimized gene *phaC* with complementary sites isolated from pUC57-*phaC*. DNA fragment encoding pNit-*phaC* from plasmid pET-16b\_pNit-*phaC* was then excised using BamHI and XbaI and subsequently ligated with *E. coli*–Mycobacterium shuttle plasmid pMycVec1

Plasmid pMycVec2\_Pwmyc-*phaAB* (**Supplementary Fig. 3.2**). The *E. coli* codon usage optimized genes *phaA* and *phaB* required for precursor synthesis in the two-plasmid system were amplified from plasmid pMCS69 [26] using primers fwd\_NheI-*phaAB* and rev-*phaAB*\_PacI and subsequently ligated into pGEM-T easy. The amplified fragment containing *phaA* and *phaB* was excised using NheI and PacI following confirmation by DNA sequencing. A synthesized DNA fragment containing the weak constitutive promoter Pwmyc from *M. smegmatis* was excised from pGEM-T\_Pwmyc using EcoRV and NheI. DNA fragments encoding for precursor genes (*phaA* and *phaB*) and Pwmyc were used in a single ligation reaction with *E. coli*–Mycobacterium shuttle plasmid pMycVec2 linearized with EcoRV and PacI.

Plasmid pMIND\_pTet-*phaC* (**Supplementary Fig. 3.3**). The DNA fragment encoding codon-optimized gene *phaC* was excised from plasmid pUC57-*phaCAB* using BamHI and HindIII. Fragment was subsequently ligated in to the corresponding sites of plasmid pMIND [27] downstream of the inducible tetracycline promoter (pTet). pMIND was a gift from Brian Robertson (Addgene plasmid #24730).

Plasmid pMV261\_pNit-*phaC* (**Supplementary Fig. 3.4**). Plasmid pNit-1::*gfp* was hydrolyzed with NdeI and HindIII excising reporter ext-*gfp* to allow the ligation of codon-optimized gene *phaC* from plasmid pUC57\_ *phaC* into the corresponding sites.

Plasmid pMV261\_pNit-A:E-*phaC* (**Supplementary Fig. 3.5**) DNA fragment encoding fusion antigens Ag85A-ESAT-6 was amplified from existing plasmid pHAS-Ag85A-ESAT-6 [20] using primers fwd\_A:E and rev\_A:E. Resultant fragment was then ligated into vector pGEM-T. Subsequently, DNA fragment encoding for Ag85A-ESAT-6 was excised using NdeI and ligated into the corresponding sites in plasmid pMV261\_pNit-*phaC* located downstream of pNit promoter and upstream of codon-optimized *phaC*.

Plasmid pMV261\_pNit-*phaC*-Pwmyc-*phaAB* (**Supplementary Fig. 3.6**). A single vector system utilizing vector pMV261. Firstly, PacI site was introduced downstream of *phaB* in plasmid pUC57\_ *phaCAB* using a small synthesized DNA fragment from plasmid pUC57\_3'*phaB*\_PacI encoding short segment of the 3' end of *phaB* and PacI site. This allowed the subcloning of the entire DNA fragment encoding codon-optimized *phaC*, and precursor genes (*phaA* and *phaB*) regulated under a weak constitutive mycobacterial promoter Pwmyc. Fragment was excised from plasmid pUC57\_3'*phaB*\_PacI using XhoI and SpeI and inserted into the corresponding sites of plasmid pUC57\_ *phaC*-Pwmyc-*phaAB*. Consequently, DNA fragment encoding PHA synthase and precursor genes was excised from pUC57\_ *phaC*-Pwmyc-*phaAB*\_PacI using NdeI and PacI and ligated into the corresponding sites in vector pMV261\_pNit-*phaC* downstream of pNit promoter, resulting in the replacement of the existing *phaC* gene.

### **PHB accumulating growth conditions**

To assess the ability of *M. smegmatis* to accumulate PHB *in vivo*, strains were cultivated under PHB accumulating conditions. 10 mL of 7H9 broth supplemented 1% glucose (v/v) as carbon source and antibiotics was inoculated with frozen glycerol stock cultures and cultivated for 20 hours. 50 mL of fresh supplemented 7H9 broth with antibiotics was then added to the preculture and cultivated for another 20 hours. Large 1 L cultures of supplemented 7H9 broth with antibiotics was inoculated with 3% (v/v) preculture and cultivated until OD<sub>600</sub> of 0.3 – 0.4. Once OD<sub>600</sub> was reached, protein

expression was induced by the addition of isovaleronitrile at a final concentration of 50  $\mu\text{M}$  and then further cultivated for 72 hours.

### **Isolation of mycobacterial PHA biobeads (MBB)**

Forty-eight hour post-induction cultures were harvested by centrifugation at  $9000 \times g$  for 20 min. Sediment was washed once and then suspended as a 25% slurry (w/v) with 1x PBS (pH 7.4). 1 mL of the 25% slurry was aliquoted into 2 mL screw cap tubes containing 1/3 volume or 500  $\mu\text{L}$  (v/v) acid washed 0.1 mm glass beads and chilled on ice for 10 min prior to cell lysis. Lysis was achieved by using a Hybaid RiboLyser (FP120HY-230) using the following procedure: 6 m/s for 3 times 1 min intervals with 2 min cooling steps in between each interval. Lysates was separated from glass beads by centrifuging briefly at  $3000 \times g$  for 10 sec. 1 mL of the 25% lysate was then loaded on to a glycerol gradient consisting of a 44%/66%/90% (v/v) glycerol layers made in 1x PBS (pH 7.4). Separation was achieved by centrifugation at  $100,000 \times g$  for 1.5 h and MBB were recovered from the 66% and 90% glycerol interface. Isolated MBB were washed two times using 1x PBS (pH 7.4) with centrifugation at  $9500 \times g$  for 30 min and then formulated in 1x PBS (pH 7.4) as a 20% (w/v) slurry. To ensure sterile preparations, washed MBB were heat treated in sterile 2 mL screw cap tubes at  $80^\circ\text{C}$  for 30 min. Sterility was confirmed by cell culture on antibiotic free supplemented BBL Middlebrook 7H10 agar (BD).

### **PHB analysis by Gas chromatography-mass spectrometry (GC/MS)**

40 – 60 mg of lyophilized material was suspended in 2 mL of chloroform and subjected to methanolysis in 2 mL methanol in the presence of 15% (v/v) sulfuric acid. Methanolysis was performed in a heated oil bath for 5 hour at  $100^\circ\text{C}$ . After methanolysis, tubes were cooled to room temperature, 2 mL of distilled water added, and briefly vortex. Samples were then left at room temperature for phase separation. The bottom phase containing methyl esters of the corresponding fatty acid constituents was recovered and analyzed by GC/MS for 3- hydroxyalkanoate methyl esters.

### **TEM**

Transmission electron microscopy (TEM) analysis was used to assess isolated PHA biobead material produced in *M. smegmatis*. Samples were processed for analysis as described previously [28].

### **Protein analysis**

Proteins were separated using sodium dodecyl sulfate-polyacrylamide gel electrophoresis (SDS-PAGE) and visualized by staining with Coomassie Brilliant Blue. Immunoblot was used to confirm PhaC or Ag85A-ESAT-6-PhaC fusion protein on MBB or the production of GFP. Protein bands separated by SDS-PAGE were transferred to nitrocellulose membrane using i-BLOT system (Invitrogen, Carlsbad, CA). Membrane was blocked with 1% skim milk in PBST for 1 h. Following washing with PBST, primary antibodies were diluted in 1% BSA and used accordingly: for detection of PhaC, 1:20,000 rabbit polyclonal (GenScript, NJ); ESAT-6, 0.1 µg/mL rabbit polyclonal (Abcam, Cambridge, United Kingdom); and GFP, 0.75 µg/mL rabbit polyclonal (A01388, GenScript, NJ). Following incubation for 1 h, the membrane was washed three times using PBST for 5 min. Secondary antibody anti-Rabbit HRP at 1:25,000 (Ab6721, Abcam, UK) was diluted in 1% BSA, added and incubated for 1 h. Following three PBST washes, development was carried out using SuperSignal West Pico chemiluminescent substrate (Thermofisher, Waltham, MA).

BCA protein assay kit (23227, Thermo Scientific, IL) was used according to manufacturer's instructions to quantify the total protein in the isolated MBB material.

### **Mouse immunization trial**

To evaluate the efficacy of MBB as a vaccine for tuberculosis a mouse immunology trial was performed. All animal experiments were approved by the Grasslands Animal Ethics committee (approval # 13100; Palmerston North, New Zealand).

*Animals.* C57BL/6 female mice, aged 6 to 8 weeks, at the start of the experiment were obtained from the AgResearch Ruakura Small Animal Unit (Hamilton, New Zealand). The animals were assigned to one of five vaccination groups (12 animals per group) and housed at AgResearch's PC2 Ulyatt-Reid Small Animal Facility (Palmerston North, New Zealand). The animals were kept in a separate room of this PC2 facility but not under specific pathogen free conditions.

*Vaccination.* All vaccine groups except BCG group received a total of three vaccinations, with one vaccination given every two weeks by subcutaneous injection. Control group were vaccinated with either phosphate buffered saline (PBS) or a *M.*

*smegmatis* vector control lysate (MVC) group, which did not contain any MBB. Two further groups were vaccinated with either MBB or MBB displaying Ag85A-ESAT-6 (A:E-MBB). BCG control group received a single dose of  $10^6$  CFU of BCG Pasteur strain 1173P2 (kindly provided by the Malaghan Institute of Medical Research, Wellington, New Zealand).

*Cell mediated immune response.* Seven weeks after the first immunization seven mice from each group were euthanized and splenocytes prepared for further analysis. Splenocytes were stimulated in vitro using various antigen preparations at a final concentration of 5  $\mu\text{g}/\text{mL}$ : (a) PBS (as unstimulated negative control), (b) Concanavalin A (ConA; C-0412, Sigma-Aldrich; a mitogen, used as positive control, (data not shown), (c) purified protein derivative from *M. bovis* (PPD-B; Prionics AG, Switzerland), (d) MBB, (e) peptides from Ag85A (aa99–118, aa145–152) and ESAT-6 (aa1–16, aa9–24, aa17–32, aa57–72, aa80–95), or (f) PhaC peptides (aa110–118 and aa118–126). Supernatants from these cultures were harvested and the amount of secreted IFN- $\gamma$  and IL-17 determined by ELISA.

*Tuberculosis challenge.* Fifteen weeks after the first vaccination, all remaining mice ( $n = 5$  per group) were challenged with *M. bovis* by the aerosol route [29]. *M. bovis* was grown from a low-passage seed lot in Tween albumin broth to early mid-log phase and aliquots of cultures were frozen at  $-70^\circ\text{C}$ , until required. To infect mice by low-dose aerosol exposure, diluted thawed stock were administered using a Madison chamber aerosol generation device calibrated to deliver approximately 50 bacteria into the lungs. Aerosol infections, maintenance and manipulation of infected mice performed under strict isolation conditions in a biohazard facility (PC3 Ulyatt-Reid Animal Facility).

*Postmortem examinations.* Five weeks after challenge with *M. bovis*, all mice were euthanized, and spleens and lungs were removed. Spleen and lung samples were mechanically homogenized and plated in tenfold dilutions on selective Middlebrook 7H11 agar with OADC supplement. Plates were incubated at  $37^\circ\text{C}$  in humidified air for three weeks before counting colonies. Numbers of CFU/organ were converted to  $\log_{10}$  CFU values.

*Statistical analysis.* For the analysis of cytokine measurements from culture supernatants of stimulated splenocytes One-way ANOVA was carried out with 5 treatments (vaccine levels) separately for each of IL-17 & IFN- $\gamma$  and separately for in vitro stimulation with "PPDB", MBB" and peptide subsets. The 'ANOVA assumptions' (normality, homogeneity of variances etc.) were examined using model residuals and fitted values via diagnostic graphs and for normality and Levene's test for homogeneity of variances. Transformations were required & the log (natural) transformations gave reasonably satisfactory ANOVA assumptions. All analyses were carried out using the R software version 3.3.1 [30].

For statistical analysis of bacterial counts of the lung and spleen of vaccinated mice, raw data was analyzed with One-way ANOVA with pairwise comparison between groups using Tukey's post-hoc test. Significance of pairwise comparisons between groups is indicated by 'letter-based' representation ( $p < 0.05$ ). 'ANOVA assumptions' of Normality and homogeneity of variance were examined using Shapiro-Wilk test for normality and Levene's test for homogeneity of variances.

'Letter-based' representation of significance is interpreted as follows; groups that share a common letter are not statistically significant to each other, while groups that don't share a common letters are statistically significant to each other ( $p < 0.05$ ). Alphabetical order donates significance, with a higher letter being more significant to a lower letter i.e.  $a < b < c$ .

### 3.3 Results

#### 3.3.1 Production of MBB

The initial strategy to establish the PHB pathway (genes *phaCAB*) in *M. smegmatis* was to apply a two-plasmid system utilizing compatible *E. coli*–*Mycobacterium* shuttle plasmids pMycVec1 and pMycVec2 [31]. PhaC was designed to be expressed on the higher copy number plasmid pMycVec1 utilizing a strong nitrile-inducible promoter (pNit) [25] to promote high expression, while *phaAB* genes [26] required for the production of precursor (*R*)-3-hydroxybutyrate-CoA were selected to be expressed under a weak constitutive mycobacterial promoter (*P<sub>wmyc</sub>*) [31] on the low copy number plasmid pMycVec2, as the precursor is required in catalytic amounts. Mycobacterium codon-optimized gene and nonoptimized *phaAB* genes were used and all amplified DNA fragments and final plasmids were confirmed by sequencing. Unfortunately, expression of this two-plasmid system consisting of pMycVec1\_pNit-*phaC* and pMycVec2\_*P<sub>wmyc</sub>*-*phaAB* in *M. smegmatis* under PHB accumulating conditions did not result in PHB production. Results from SDS-PAGE and immunoblot with anti-PhaC antibodies suggest PhaC protein was not being produced. Similarly, GFP reporter was not detectable by SDS-PAGE and immunoblot with GFP specific polyclonal antibodies using the same pMycVec1 expression system with *gfp* gene regulated under the pNit promoter. This suggests a possible problem with the pMycVec1 expression system utilizing promoter pNit.

An alternative cloning strategy was designed based on the pMIND plasmid [25, 27] utilizing a weaker tetracycline inducible promoter (pTet) for the expression of the same codon-optimized *phaC* in *M. smegmatis*. Expression of pMIND\_*phaC* in *M. smegmatis* as a two-plasmid system with pMycVec2\_*P<sub>wmyc</sub>*-*phaAB* also failed to produce detectable PhaC protein or PHB. However, coexpression of pMIND\_*phaC* in *E. coli* BL21(DE3) and pMCS69 plasmid encoding *phaAB*, showed accumulation of 1.2% PHB per (w/w) cellular dry weight (CDW) in whole-cell samples analyzed by GC/MS (**Supplementary Fig. 3.7**), indicating pMIND\_*phaC* was functional. As to why pMIND\_*phaC* was not functional in *M. smegmatis* is unknown.

Subsequently, functionality of the pNit promoter was shown by transforming *M. smegmatis* with the plasmid pNit-1::*gfp* [25] coding an ext-GFP reporter. Induction

resulted in intense fluorescence (**Supplementary Fig. 3.8a**) and the presence of GFP was confirmed by SDS-PAGE and immunoblot (**Supplementary Fig. 3.8b,c**). Therefore, plasmid pMV261 was engineered for the production of PhaC regulated under pNit.

MBB vaccine was produced in *M. smegmatis* cotransformed with pMycVec2\_Pwmyc-*phaAB* and pMV261\_pNit-*phaC* (**Fig. 3.1a,b**) under PHB accumulating conditions. Production of PHB was confirmed by GC/MS (**Table 3.2** and **Supplementary Fig. 3.9**). Cells were disrupted by bead mill and subsequently MBB were enriched on a glycerol gradient as described in the Materials and Methods. This vaccine preparation was called MBB. PhaC protein was visualized on SDS-PAGE in whole-cell and in isolated PHA biobead material and was subsequently confirmed by immunoblotting (**Fig. 3.2**). Using the same protocol, a vector control was produced based on *M. smegmatis* transformed with pMycVec2\_Pwmyc-*phaAB* and an empty pMV261\_pNit. This preparation was called MVC (*M. smegmatis* vector control) and contains no PHB and hence no PHA biobeads.

Additional to the two-plasmid system, a one-plasmid system (pMV261\_pNit-*phaC*-Pwmyc-*phaAB*) (**Fig. 3.1c**) containing codon-optimized genes *phaCAB* utilizing the backbone of vector pMV261 was created as a comparison. Resulting yields of 1.2% PHB (w/w) per CDW as shown by GC/MS (**Table 3.2** and **Supplementary Fig. 3.9**).

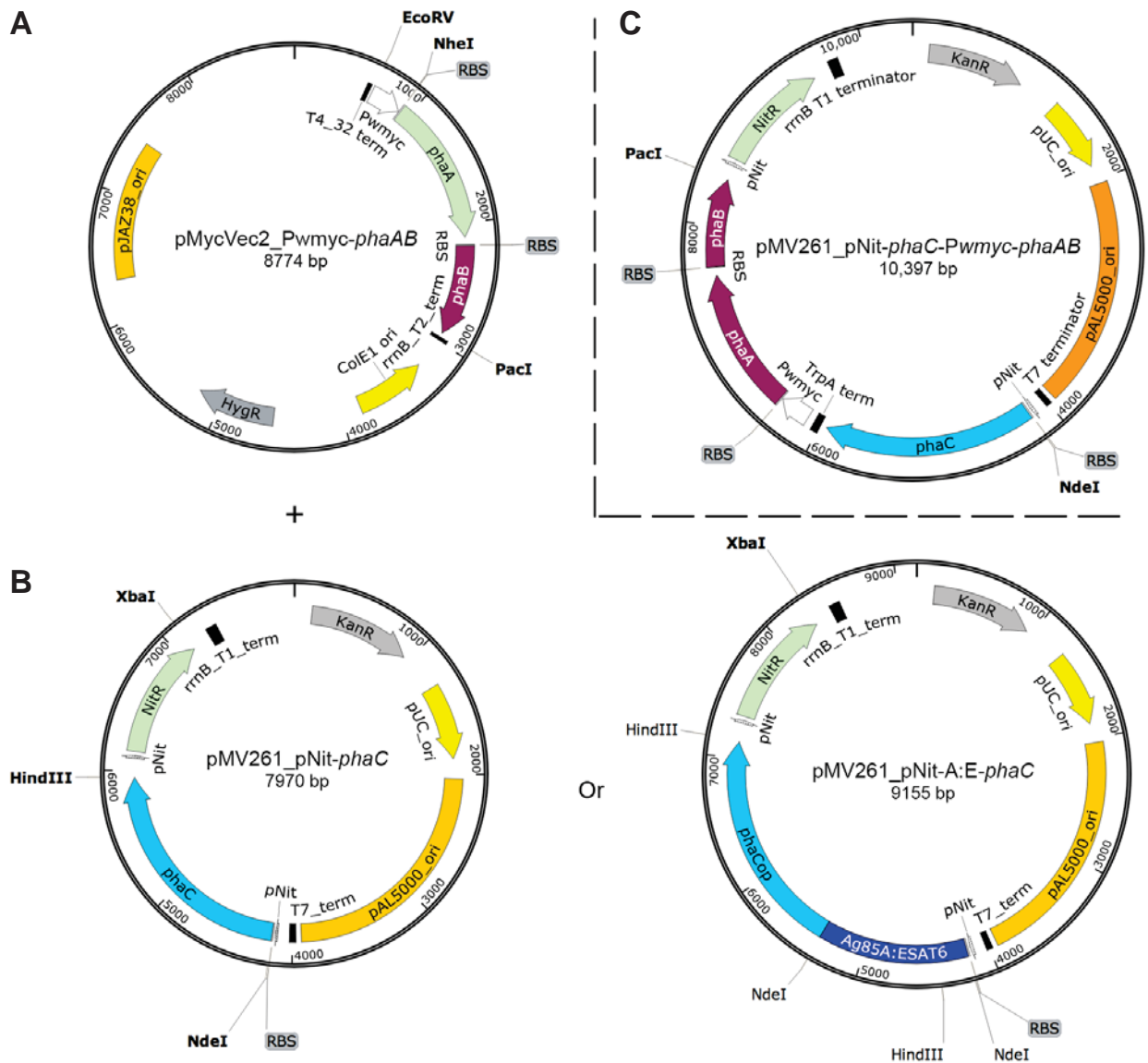


**Figure 3.1. Two-plasmid and one-plasmid system for PHB expression in mycobacteria.** Two-plasmid system requires coexpression of (a) plasmid pMycVec2\_Pwmyc-phaAB (encoding for genes *phaAB* regulated under a weak constitutive mycobacterial promoter for synthesis of PHB precursor) and (b) plasmid pMV261\_pNit-phaC (encoding PHA synthase) or pMV261\_pNit-A:E-phaC (encoding fusion protein with Ag85A-ESAT-6) are regulated under an inducible nitrile promoter pNit. (c) The one-plasmid system encodes *phaC* regulated under pNit and genes *phaAB* under Pwmyc. All depicted restriction sites are singular. Kan<sup>R</sup> and Hyg<sup>R</sup> confer resistance to kanamycin and hygromycin, respectively. Origins of replication in *E. coli* and mycobacterium are labeled. Transcription terminators are indicated by black bars.

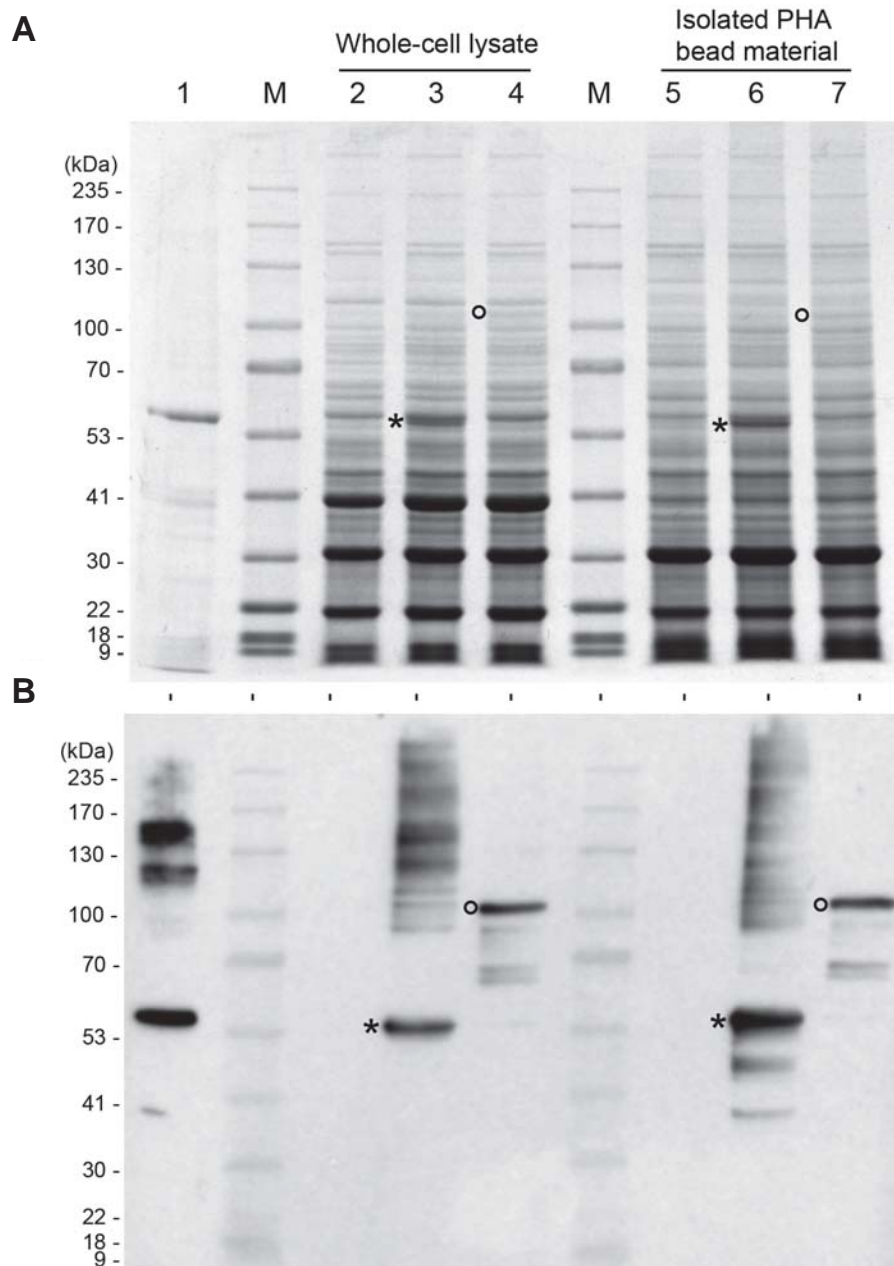


**Figure 3.2. SDS-PAGE and immunoblot analysis of proteins from whole-cell lysate and isolated mycobacterial PHA biobeads material.** (a) SDS-PAGE with Coomassie Blue staining and (b) immunoblot with anti-PhaC polyclonal antibodies. *M. smegmatis* whole-cell lysates: lane 1, positive control *E. coli* BL21 derived PhaC PHA biobeads; lane M, molecular weight standard; lane 2, pMycVec2\_Pwmyc-*phaAB* (MVC) negative control; lane 3, pMycVec2\_Pwmyc-*phaAB* and pMV261\_*phaC* (MBB); lane 4, pMycVec2\_Pwmyc-*phaAB* and pMV261\_A:E-*phaC* (A:E-MBB) and isolated mycobacterial PHA biobeads material from *M. smegmatis*: lane 5, MVC; lane 6, MBB; lane 7, A:E-MBB. (Asterisk), PhaC protein; and (Circle), A:E-PhaC protein.

### 3.3.2 Production of MBB displaying Ag85A and ESAT-6 (A:E-MBB)

Once stable expression of MBB was achieved, genes for a fusion protein consisting of the *M. tuberculosis* antigens Ag85A and ESAT-6 were engineered for display on the MBB surface (**Fig. 3.1b**). A previously developed gene fusion product of Ag85A-ESAT-6 [20] was attached to the 5' end of *phaC* resulting in plasmid pMV261\_pNit-A:E-*phaC*. Expression of pMV261\_pNit-A:E-*phaC* and pMycVec2\_Pwmyc-*phaAB* as a two-plasmid system (**Fig. 3.1a,b**) in *M. smegmatis* resulted in formation of A:E-MBB in these cells. The resulting yield of less than 1% PHB (w/w) per CDW as indicated by GC/MS (**Table 3.2** and **Supplementary Fig. 3.9**) was lower than for the MBB. The presence of the fusion protein in these preparations was confirmed by immunoblot with an ESAT-6 specific antibody (**Supplementary Fig. 3.10**). MBB were produced according to the same protocol as the MBB and MVC and this third vaccine preparation was called A:E-MBB (mycobacterial PHA biobeads displaying Ag85A-ESAT-6).

**Table 3.2.** PHB biosynthesis of *M. smegmatis* harboring various plasmids

Plasmid <sup>a</sup>	PHB (% w/w) <sup>b</sup>
No plasmid <sup>c</sup>	ND
pMV261_pNit- <i>phaC</i> <sup>d</sup>	<1
pMV261_pNit- <i>phaC</i> + pMycVec2_Pwmyc- <i>phaAB</i> <sup>c</sup>	5.2
pMV261_pNit- <i>phaC</i> -Pwmyc- <i>phaAB</i> <sup>e</sup>	1.2
pMV261_pNit-A:E- <i>phaC</i> + pMycVec2_Pwmyc- <i>phaAB</i> <sup>d</sup>	<1

<sup>a</sup> *M. smegmatis* mc<sup>2</sup>155 strain harboring various plasmids (one-plasmid or two-plasmid systems) grown under PHB accumulating conditions as described in the Materials and Methods.

<sup>b</sup> PHB yield is expressed as percentage PHB per mg dry weight of whole-cells calculated from known PHB standards.

<sup>c</sup> Experiments were conducted in triplicate, and the mean values are shown. The standard deviation was < 0.9.

<sup>d</sup> Value shown from a single measurement.

<sup>e</sup> Experiment was conducted in duplicate, and the mean value is shown. The standard deviation was 0.05.

### 3.3.4 TEM analysis

Isolated MBB materials MBB and A:E-MBB and vector control material MVC were analyzed by TEM (**Fig. 3.3**). Abundant small circular inclusions typical of PHA biobeads could be seen in MBB and A:E-MBB preparations. Interestingly, these inclusions tend to be clustered around electron dense staining material. Seemingly more of these inclusions could be observed in the MBB preparation compared to A:E-MBB. Some circular inclusions could be seen in the MVC preparation (**Fig. 3.3a**) and this may suggest possible isolation of lipophilic inclusions typically produced in mycobacterium [32] in MBB and A:E-MBB preparations (**Fig. 3.3b,c**). In addition to possible lipophilic inclusions, large amount of cellular debris can be seen in all preparations.

### 3.3.5 MBB vaccination and Challenge with *M. bovis*

Spleen cells from mice vaccinated with MBB showed strong IFN- $\gamma$  responses when stimulated in vitro with MBB. These were significantly higher than all other responses ( $p < 0.057$  for MVC,  $p < 0.001$  for PBS, A:E-MBB and BCG; **Fig. 3.4**) and approximately 33 times higher than the response from BCG vaccinated animals against PPD-B (*M. bovis* purified proteins). IFN- $\gamma$  responses from the group vaccinated with A:E-MBB however showed much lower responses but still approximately three times higher than the response of BCG vaccinated animals against PPD-B. IFN- $\gamma$  release in the MVC group to MBB was also very high. Animals vaccinated with vaccines generated in *M. smegmatis*, including the MVC control, showed very strong IL-17 responses when stimulated with MBB. These were significantly higher than responses from the PBS and BCG groups ( $p < 0.001$ ) (**Fig. 3.4**) and approximately 90 to 160 times higher than the response from BCG vaccinated animals against PPD-B. For IL-17 the A:E-MBB vaccinated group showed significantly increased amounts of IL-17 compared to PBS, MBB and BCG ( $p < 0.001$ ) but not the MVC control.

Spleen cells stimulated with peptides showed higher IFN- $\gamma$  secretion (**Fig. 3.4**) when stimulated with MVC, MBB or A:E-MBB ( $p < 0.005$ ) when compared to PBS and BCG. Also, increased IL-17 secretion from the A:E-MBB vaccinated group when stimulated with Ag85A and ESAT-6 peptides compared to the other vaccinated groups ( $p < 0.022$ ) indicating a strong peptide specific response.

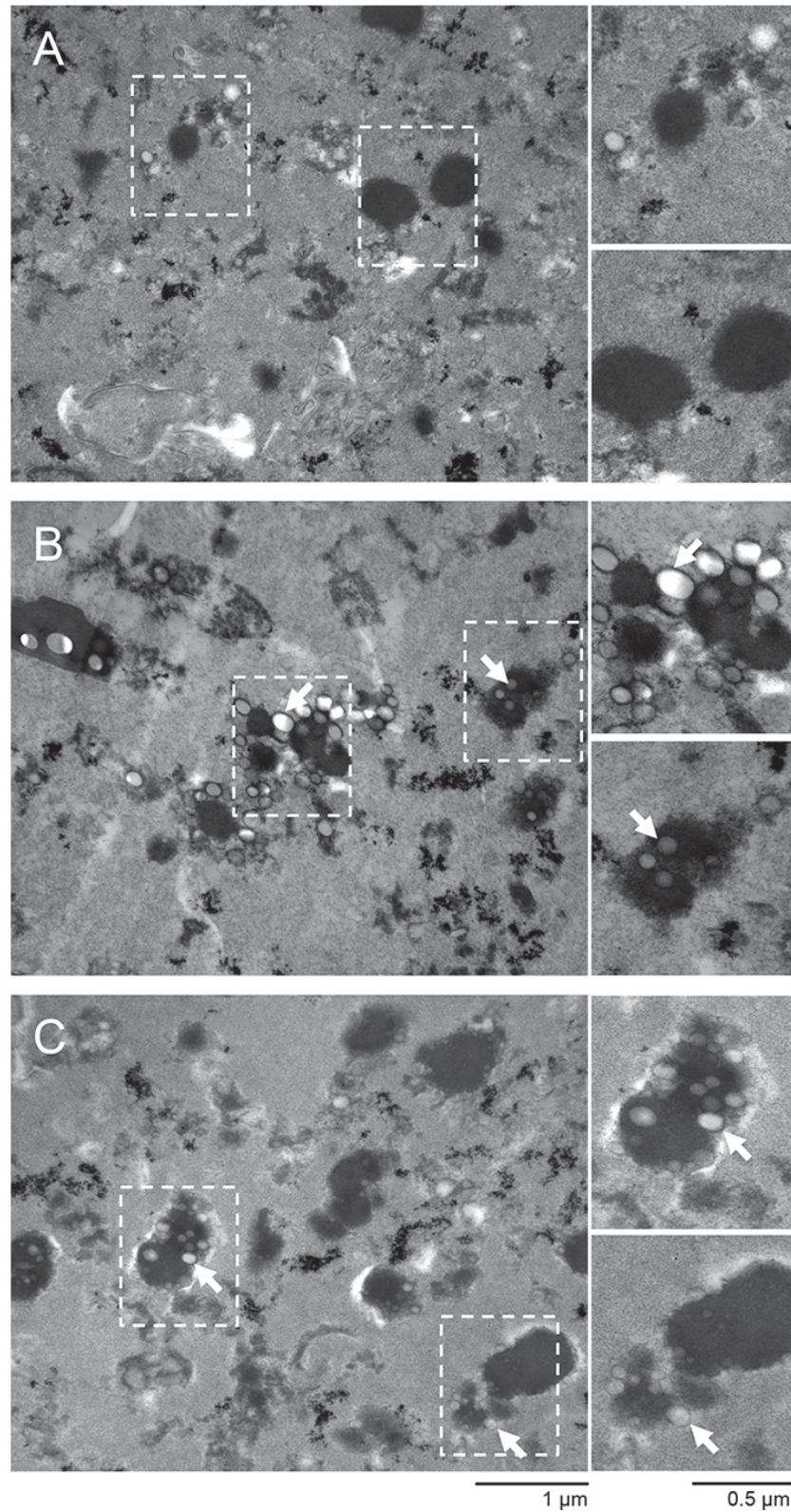


**Figure 3.3. TEM analysis of isolated mycobacterial PHA biobeads material by density gradient.** Biobeads recovered from the 66%/90% interface of a glycerol gradient were subjected to TEM analysis. (a), MVC; (b), MBB; and (c), A:E-MBB. All samples contain cellular debris and possible lipophilic inclusions. Mycobacterial PHA biobeads isolated material contains a large number of spherical inclusions of variable size, which is often localized with an unknown electron dense staining material. White arrow indicates mycobacterial PHA biobeads.

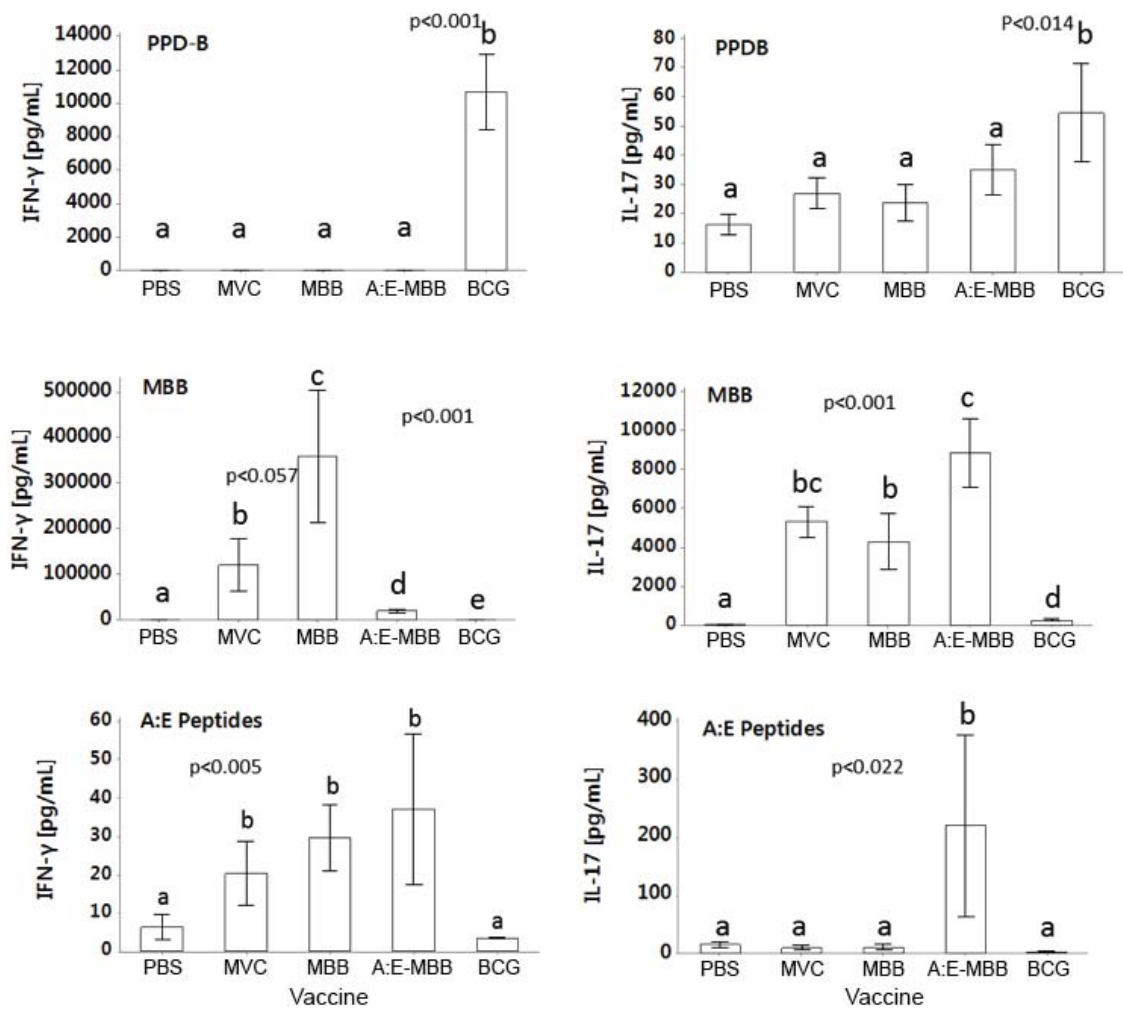


**Figure 3.4 Cytokine responses from vaccinated mice.** Vaccines were produced as described. Mice were vaccinated with either PBS, MVC, MBB, A:E-MBB (MBB\_AE), or BCG. Seven weeks after the first immunization, mice were euthanized and splenocytes stimulated *in vitro* with PPD-B, MBB, or Ag85A-ESAT-6 (A:E) peptides. The amount of secreted IFN- $\gamma$  (left) and IL-17 (right) were determined by ELISA (n=7 per vaccine group; mean  $\pm$  s.e.m). Means with the same letter are not significantly different from each other based on analysis by One-way ANOVA. The 'ANOVA assumptions' (normality, homogeneity of variances etc.) were examined using model residuals and fitted values via diagnostic graphs and Shapiro's test for normality and Levene's test for homogeneity of variances.

After challenge with *M. bovis*, mean lung and spleen counts indicated protection in four out of five BCG vaccinated animals compared to the PBS vaccinated control group (Fig. 3.5). Two out of five animals in the A:E-MBB vaccinated group also showed low count. No differences were seen between the lung and spleen counts for animals receiving MVC and MBB compared to group receiving PBS.

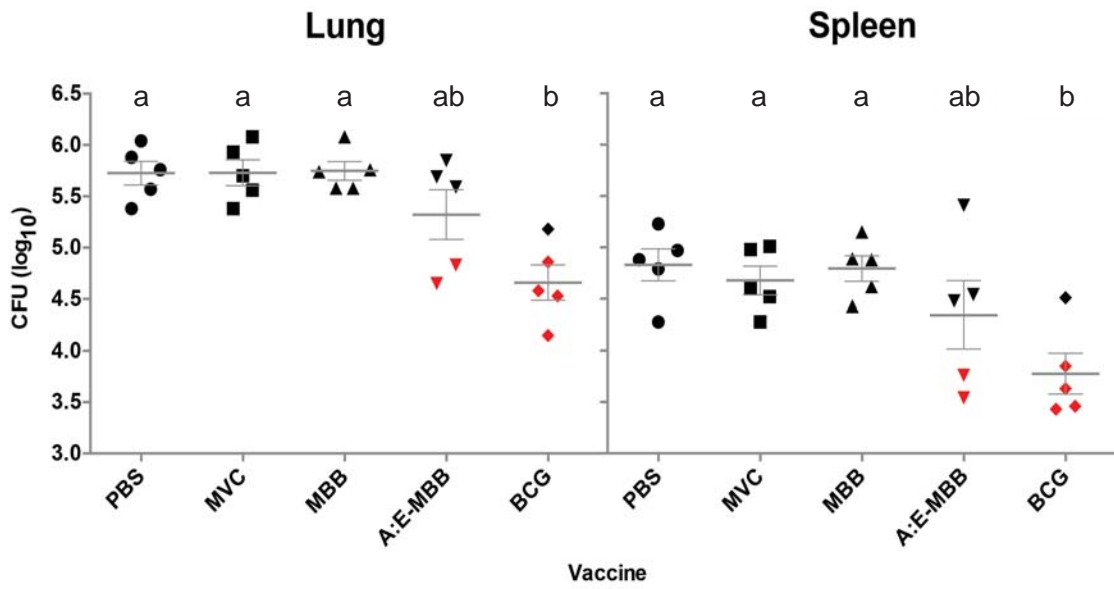


**Figure 3.5 Bacterial counts in lungs and spleens of vaccinated mice.** Lung (left) and spleen (right) culture results following vaccination of mice with PBS, MVC, MBB, A:E-MBB, or BCG. Mice were vaccinated three times at biweekly intervals or once in the case of BCG and then challenged with *M. bovis* 15 weeks later, followed by postmortem after a further 5 weeks. Data of graphs are reported as means  $\pm$  s.e.m and individual mice are reported (5 per group) as individual data points. Data points indicating protection defined as a reduction of bacterial load by at least 1 log are indicated in red. Statistical significance ( $p < 0.05$ ) is indicated by 'letter-based' representation of pairwise comparisons between groups.

### 3.4 Discussion

The use of PHA biobeads produced in bacteria as particulate vaccine-delivery system engineered to display vaccine candidates against diseases such as tuberculosis has been previously shown [12, 19, 20, 33]. The production of these PHA biobeads utilizes engineered heterologous hosts such as *E. coli* and *L. lactis* for the production by establishing the pathway for PHB production. Despite subsequent enrichment by glycerol gradient such PHA biobeads can carry and display host cell proteins. These impurities can induce immune responses [19, 34]. Mycobacterial cell wall (e.g. peptidoglycan, glycolipids, and mycolic acids) and intracellular (e.g. heat shock proteins and CpG) components are known to be responsible for the immunoadjuvant effect of Freund's complete adjuvant [35]. FCS is a water-in-oil emulsion containing inactivated *M. tuberculosis* and is a well-known potent stimulator of cell-mediated immunity [35].

In this study we engineer *M. smegmatis* as a model organism for *M. tuberculosis* aimed at the production of mycobacterial PHA biobeads (MBB) and of MBB displaying Ag85A-ESAT-6 (A:E-MBB). By producing PHA biobeads in a related rather than a nonrelated host, the copurified host compounds resemble that of the disease causative pathogen. These compounds provide pathogen specific adjuvant effects as well as a large antigenic repertoire that could be utilized as potential inducers of protective immunity.

Here the PHB biosynthesis pathway (genes *phaCAB*) was successfully established in the host *M. smegmatis*. Members belonging to the *Mycobacteriaceae* do not naturally produce PHA, though putative synthases have been identified e.g. MT1723 from *M. tuberculosis*. Establishment of the PHB biosynthesis pathway was difficult and several strategies had to be explored to accomplish it.

The initial two-plasmid system strategy involved expressing *phaC* under a strong nitrile inducible promoter (pNit) [25] and *phaAB* under a weak constitutive mycobacterial promoter (P<sub>wmyc</sub>) in compatible pMycVec1 and pMycVec2 vectors, respectively. However, expression and cultivation under PHB accumulating conditions failed to produce detectible PHB due to the absence of recombinant PhaC protein being

produced after induction. Similar results were obtained when GFP was being expressed under the same expression system in vector pMycVec1. Therefore, it was thought the lack of recombinant protein production was due to a dysfunctional pNit promoter. Consequently, an alternative pMIND plasmid utilizing a tetracycline inducible promoter (pTet) [27] was utilized for the expression of *phaC*. However, similarly no PhaC protein could be detected under inducing and PHB accumulating conditions in *M. smegmatis*. Subsequent analysis was able to confirm that the pTet promoter was functional but only when expressed in trans in *E. coli* BL21 (**Supplementary Fig. 3.7**). This implies pTet was not functional in *M. smegmatis* for unknown reasons.

Functionality of the pNit promoter was later confirmed after further analysis utilizing GFP reporter protein in *M. smegmatis* only when expressed on the vector pMV261 (**Supplementary Fig. 3.8**). Comparison of the dysfunctional vector pMycVec1 with pMV261 suggested the absence of PhaC protein with pMycVec1 plasmid was due to certain inherent property of the noncoding regions of the pMycVec1. There is little difference in the coding regions between the two plasmids as they share the same origin of replication, selectable marker, and promoter. Therefore, *phaC* was designed to be expressed on pMV261 under the pNit promoter and used as a two-plasmid system with plasmid pMycVec2\_Pwmyc-*phaAB* that harbors the *phaAB* genes regulated under the Pwmyc promoter. For the hypothetical advantage of having a simpler production system a single plasmid system version was also developed on the pMV261 backbone.

GC/MS analysis (**Table 3.2**) of recombinant *M. smegmatis* harboring PHB genes demonstrated compared to that for the one-plasmid system that the two-plasmid system was better and could accumulated 4.3 times more PHB in vivo. The two-plasmid system was subsequently used for the production of MBB and A:E-MBB.

Recombinant *M. smegmatis* producing MBB was able to accumulate 5.2% (w/w) CDW (**Table 3.2**) which is comparable to recombinant PHB production in *L. lactis* [24], but less than what can be achieved with recombinant *E. coli* (up to 80% (w/w) CDW) [24, 36]. The production of A:E-MBB however resulted in substantially less PHB (< 1 % (w/w) CDW). Both the PHA synthase (PhaC) and fusion protein variant (A:E-PhaC) was not found to be overproduced in *M. smegmatis* using the current pNit gene expression system (**Fig. 3.2**).

Furthermore, it was found that translational fusion of Ag85A-ESAT-6 to the N terminus of PhaC seems to impact negatively on recombinant protein production compared to PhaC alone. Other studies have shown translational fusions to PhaC impacted on PHA accumulation in vivo and this variation seems to be strongly dependent on the PHA synthase fusion partner [36-38]. Further improvements to protein production and PHB yield needs to be explored.

The ability to isolate PHA biobeads from nonbiobead associated host cell debris was a limiting factor in this study. Complete lysis and isolation of mycobacterial PHA biobeads proved challenging due to the properties of mycobacteria's thick and waxy cell wall [39]. SDS-PAGE analysis (**Fig. 3.2a**) of the whole-cell and isolated material showed minor difference its protein profile, suggesting substantial amount of host cell impurities in the isolated PHA biobead material of which is reflected with TEM (**Fig. 3.3b,c**). These impurities could include cell wall debris, mesosomes [40], and possibly nonPHA intracellular lipophilic inclusions [32, 40]. The PHA biobeads were often colocalized with electron dense staining bodies of unknown origin and function. In the future further improvements to the isolation protocol need to be explored to improve recovery of MBB and removal of nonbiobead associated impurities.

To gain a preliminary understanding of the immunogenicity of MBB and A:E-MBB and also to evaluate the hypothesis that copurified mycobacterial antigens contribute to the immune response these biobeads were used in a mouse vaccination study. Cytokine secretion by in vitro stimulated splenocytes from vaccinated animals and disease progression were analyzed.

The cytokine IFN- $\gamma$  has long been known to play a major role in the protection against tuberculosis. More recently IL-17 has been identified as a further key cytokine for control of tuberculosis [41, 42]. Hence, supernatants after in vitro restimulation were analyzed for secretion of IFN- $\gamma$  and IL-17 using ELISA.

All mice vaccinated with mycobacterial derived PHA biobeads, including the MVC control, showed strong IFN- $\gamma$  and IL-17 responses when stimulated with MBB (**Fig. 3.4**). These responses were stronger than the response from BCG vaccinated animals against PPD-B (**Fig. 3.4**). Mice vaccinated with MBB showed the strongest IFN- $\gamma$  response when stimulated with MBB, which was higher than all other responses. Compared to MBB vaccinates, IFN- $\gamma$  responses from the group vaccinated with A:E-MBB were much lower. This lower response is likely due to the low concentration of PHA biobeads in these preparations or replacement or masking of epitopes on the PHA biobeads surface by the displayed Ag85A-ESAT-6.

A strong adjuvant effect of *M. smegmatis* derived material “contaminating” the vaccine is a probable cause for the high IFN- $\gamma$  release shown by the MVC vaccinated control group. This supports our hypothesis that contaminating material originating from the pathogen can stimulate an immune response. Future work will have to investigate what amount of contaminating material leads to an optimal pathogen specific immune response.

IL-17 has been proposed as being important for protection by mediating the recruitment of neutrophils and promoting the entry of Th1 cells to the site of granuloma formation [43]. The A:E-MBB vaccinated group showed a significantly increased secretion of IL-17 compared to the other groups when stimulated with MBB (**Fig. 3.4**). As mice vaccinated with MVC also showed a strong IL-17 response it is likely the IL-17 response was due to the host cell impurities in the MBB and A:E-MBB preparations.

After challenge with *M. bovis*, mean lung and spleen counts indicated protection in four out of five BCG vaccinated animals compared to the PBS vaccinated control group (**Fig. 3.5**). Two out of five animals in the A:E-MBB vaccinated group also showed low count. No differences were seen between the lung and spleen counts for animals receiving MVC and MBB compared to group receiving PBS.

The strong IFN- $\gamma$  and IL-17 responses seen with MBB and A:E-MBB did not correlate with lower bacterial counts in the lung and spleen of individual mice challenged with *M. bovis* (**Fig. 3.5**). However, 2 out of 5 animals in the A:E-MBB vaccinated group showed CFU counts suggesting protection. This suggests antigens Ag85A-ESAT-6 displayed on

the A:E-MBB can be protective [12, 33]. Mice vaccinated with A:E-MBB demonstrated a strong peptide specific secretion of IL-17 to Ag85A-ESAT-6 peptides indicating that a specific immune response was developed to Ag85A and/or ESAT-6 displayed on the surface of A:E-MBB (**Fig. 3.4**). The variable protection seen with A:E-MBB vaccine could be a result of sub-optimal concentration of biobeads.

This study used MBB produced in *M. smegmatis*, which was chosen over *M. tuberculosis* and *M. bovis* for its faster growth in culture leading to faster production of MBB. However, *M. smegmatis* and *M. tuberculosis* and *M. bovis* differ significantly genetically [44, 45]. *M. smegmatis* lacks a large proportion of proteins found in the pathogenic strains [46]. Hence, the immune response to impurities of *M. smegmatis* is likely be less effective in conferring protection against pathogenic strains such as *M. bovis*. The strategy of engineering *M. bovis* or *M. tuberculosis* for the production of MBB or A:E-MBB may consequently offer better vaccine efficacy utilizing this approach.

The use of TB antigen-displaying biobeads produced in *E. coli* in a heterologous prime-boost strategy has been previously investigated [33]. Biobead vaccines can contain a large repertoire of compounds that have the potential to increase the effect of the boost vaccine [47]. However, future studies will have to investigate the adjuvant effects of copurified host compounds by comparison with highly purified vaccine preparations. We propose that mycobacterial derived biobeads may be advantageous for use in a heterologous prime-boost strategy as a prime and/or boost. Studies have shown that a heterologous prime-boost strategy is more protective than a homologous prime-boost strategy [48-50].

### **3.5 Conclusions**

This study proves the feasibility of the production of PHA biobeads in mycobacteria and also provides preliminary insights into their efficacy as vaccines against tuberculosis. Future studies should include improvements of the mycobacterial PHA biobeads production process, production of PHA biobeads in *M. bovis* and/or *M. tuberculosis*, and inclusion of additional or alternative mycobacterial antigens. More detailed immunological and challenge trials would be undertaken on these new preparations.

In summary, we have introduced a promising new vaccination platform combining a large antigenic repertoire (comparable to that of live vaccines) with high safety (noninfectious vaccine and absence of any genetic material) and ease and cost efficiency of production.

### 3.6 Acknowledgements

The authors wish to acknowledge Dr. Siva Ganesh (AgR Ltd) for performing the statistical analyses for this study and Dr. Chris Sasseti (University of Massachusetts Medical School) for kindly providing the plasmid pNit-1::gfp. We would also like to acknowledge the Manawatu Microscopy and Imaging Centre for preparation of electron microscopy sections and use of their facilities. This research was funded by Bill & Melinda Gates Foundation's Grand Challenges Explorer Grant (number OPP1070028) and further supported by Massey University and AgResearch Ltd.

### 3.7 References

1. WHO, *World Health Organisation. Global tuberculosis report 2016*. 2016.
2. Evans, T.G., L. Schrager, and J. Thole, *Status of vaccine research and development of vaccines for tuberculosis*. *Vaccine*, 2016. **34**(26): p. 2911-2914.
3. Da Silva, P.E.A. and J.C. Palomino, *Molecular basis and mechanisms of drug resistance in Mycobacterium tuberculosis: classical and new drugs*. *Journal of Antimicrobial Chemotherapy*, 2011. **66**(7): p. 1417-1430.
4. Gandhi, N.R., et al., *Multidrug-resistant and extensively drug-resistant tuberculosis: a threat to global control of tuberculosis*. *The Lancet*, 2010. **375**(9728): p. 1830-1843.
5. Nossal, G.J.V., *Vaccines of the future*. *Vaccine*, 2011. **29**: p. D111-D115.
6. Tang, J., W.-C. Yam, and Z. Chen, *Mycobacterium tuberculosis infection and vaccine development*. *Tuberculosis*, 2016. **98**: p. 30-41.
7. Shahmohammadi, S., M.J. Saffar, and M.S. Rezaei, *BCG-osis after BCG vaccination in immunocompromised children: Case series and review*. *Journal of Pediatrics Review*, 2014. **2**(1): p. 62-74.
8. Ernst, J.D., *The immunological life cycle of tuberculosis*. *Nature Reviews Immunology*, 2012. **12**(8): p. 581-591.
9. Bachmann, M.F. and G.T. Jennings, *Vaccine delivery: a matter of size, geometry, kinetics and molecular patterns*. *Nature Reviews Immunology*, 2010. **10**(11): p. 787-796.
10. Zhao, L., et al., *Nanoparticle vaccines*. *Vaccine*, 2014. **32**(3): p. 327-337.
11. Bramwell, V.W. and Y. Perrie, *Particulate delivery systems for vaccines: what can we expect?* *Journal of Pharmacy and Pharmacology*, 2006. **58**(6): p. 717-728.
12. Parlane, N.A., et al., *Vaccines displaying mycobacterial proteins on biopolyester beads stimulate cellular immunity and induce protection against tuberculosis*. *Clinical and Vaccine Immunology*, 2012. **19**(1): p. 37-44.
13. Silva, A.L., et al., *Poly-(lactic-co-glycolic-acid)-based particulate vaccines: Particle uptake by dendritic cells is a key parameter for immune activation*. *Vaccine*, 2015. **33**(7): p. 847-854.
14. Singh, M., et al., *Poly(lactide-co-glycolide) microparticles with surface adsorbed antigens as vaccine delivery systems*. *Current Drug Delivery*, 2006. **3**(1): p. 115-20.
15. Frieze, K.M., D.S. Peabody, and B. Chackerian, *Engineering virus-like particles as vaccine platforms*. *Current Opinion in Virology*, 2016. **18**: p. 44-49.
16. Schwendener, R.A., *Liposomes as vaccine delivery systems: a review of the recent advances*. *Therapeutic Advances in Vaccines*, 2014. **2**(6): p. 159-182.
17. Sun, H.-X., Y. Xie, and Y.-P. Ye, *ISCOMs and ISCOMATRIX™*. *Vaccine*, 2009. **27**(33): p. 4388-4401.
18. Koppolu, B. and D.A. Zaharoff, *The effect of antigen encapsulation in chitosan particles on uptake, activation and presentation by antigen presenting cells*. *Biomaterials*, 2012.
19. Parlane, N.A., et al., *Production of a particulate hepatitis C vaccine candidate by an engineered Lactococcus lactis strain*. *Applied and Environmental Microbiology*, 2011. **77**(24): p. 8516-8522.
20. Parlane, N.A., et al., *Bacterial polyester inclusions engineered to display vaccine candidate antigens for use as a novel class of safe and efficient vaccine delivery agents*. *Applied and Environmental Microbiology*, 2009. **75**(24): p. 7739-7744.

21. Martínez-Donato, G., et al., *Protective T cell and antibody immune response against Hepatitis C Virus using the biopolyester beads based vaccine delivery system*. *Clinical and Vaccine Immunology*, 2016: p. 370-378.
22. Draper, J., et al., eds. *Polyhydroxyalkanoate inclusions: polymer synthesis, self-assembly and display technology*. *Bionanotechnology: biological self assembly and its applications*, ed. B.H.A. Rehm. 2013, Caister Academic Press: Norfolk 8045-8053.
23. Rehm, B.H.A., *Biogenesis of microbial polyhydroxyalkanoate granules: a platform technology for the production of tailor-made bioparticles*. *Current Issues in Molecular Biology*, 2007. **9**(1): p. 41-62.
24. Mifune, J., K. Grage, and B.H.A. Rehm, *Production of functionalized biopolyester granules by recombinant Lactococcus lactis*. *Applied and Environmental Microbiology*, 2009. **75**(14): p. 4668-4675.
25. Pandey, A.K., et al., *Nitrile-inducible gene expression in mycobacteria*. *Tuberculosis*, 2009. **89**(1): p. 12-16.
26. Amara, A. and B. Rehm, *Replacement of the catalytic nucleophile cysteine-296 by serine in class II polyhydroxyalkanoate synthase from Pseudomonas aeruginosa-mediated synthesis of a new polyester: identification of catalytic residues*. *Biochemical Journal*, 2003. **374**: p. 413-421.
27. Blokpoel, M.C., et al., *Tetracycline-inducible gene regulation in mycobacteria*. *Nucleic Acids Research*, 2005. **33**(2).
28. Grage, K. and B.H.A. Rehm, *In vivo production of scFv-displaying biopolymer beads using a self-assembly-promoting fusion partner*. *Bioconjugate Chemistry*, 2007. **19**(1): p. 254-262.
29. Bianchi, M.E., *DAMPs, PAMPs and alarmins: all we need to know about danger*. *Journal of Leukocyte Biology*, 2007. **81**(1): p. 1-5.
30. R\_Core\_Team, *R: A language and environment for statistical computing*. 2016, R Foundation for Statistical Computing.
31. Kaps, I., et al., *Energy transfer between fluorescent proteins using a co-expression system in Mycobacterium smegmatis*. *Gene*, 2001. **278**(1-2): p. 115-124.
32. Garton, N.J., et al., *Intracellular lipophilic inclusions of mycobacteria in vitro and in sputum*. *Microbiology*, 2002. **148**(10): p. 2951-2958.
33. Parlane, N.A., et al., *Novel particulate vaccines utilizing polyester nanoparticles (bio-beads) for protection against Mycobacterium bovis infection—A review*. *Veterinary Immunology and Immunopathology*, 2014. **158**(1): p. 8-13.
34. Dagouassat, N., et al., *Development of a quantitative assay for residual host cell proteins in a recombinant subunit vaccine against human respiratory syncytial virus*. *Journal of Immunological Methods*, 2001. **251**(1): p. 151-159.
35. Billiau, A. and P. Matthys, *Modes of action of Freund's adjuvants in experimental models of autoimmune diseases*. *Journal of Leukocyte Biology*, 2001. **70**(6): p. 849-860.
36. Chen, S., et al., *New skin test for detection of bovine tuberculosis on the basis of antigen-displaying polyester inclusions produced by recombinant Escherichia coli*. *Applied and Environmental Microbiology*, 2014. **80**(8): p. 2526-2535.
37. Jahns, A.C. and B.H.A. Rehm, *Tolerance of the Ralstonia eutropha Class I Polyhydroxyalkanoate Synthase for Translational Fusions to Its C Terminus Reveals a New Mode of Functional Display*. *Applied and Environmental Microbiology*, 2009. **75**(17): p. 5461-5466.
38. Hooks, D.O., P.A. Blatchford, and B.H.A. Rehm, *Bioengineering of bacterial polymer inclusions catalyzing the synthesis of N-acetylneuraminic acid*. *Applied and environmental microbiology*, 2013. **79**(9): p. 3116-3121.
39. Zuber, B., et al., *Direct visualization of the outer membrane of mycobacteria and corynebacteria in their native state*. *Journal of Bacteriology*, 2008. **190**(16): p. 5672-5680.
40. Bleck, C.K.E., et al., *Comparison of different methods for thin section EM analysis of Mycobacterium smegmatis*. *Journal of Microscopy*, 2010. **237**(1): p. 23-38.
41. Khader, S.A., et al., *IL-23 and IL-17 in the establishment of protective pulmonary CD4+ T cell responses after vaccination and during Mycobacterium tuberculosis challenge*. *Nature Immunology*, 2007. **8**(4): p. 369-377.
42. Monin, L., et al., *Immune requirements for protective Th17 recall responses to Mycobacterium tuberculosis challenge*. *Mucosal immunology*, 2015. **8**(5): p. 1099-1109.
43. Kaufmann, S.H.E. *Tuberculosis vaccines: time to think about the next generation*. in *Seminars in Immunology*. 2013. Elsevier.
44. Smith, S.E., et al., *Comparative genomic and phylogenetic approaches to characterize the role of genetic recombination in mycobacterial evolution*. *PLoS One*, 2012. **7**(11).

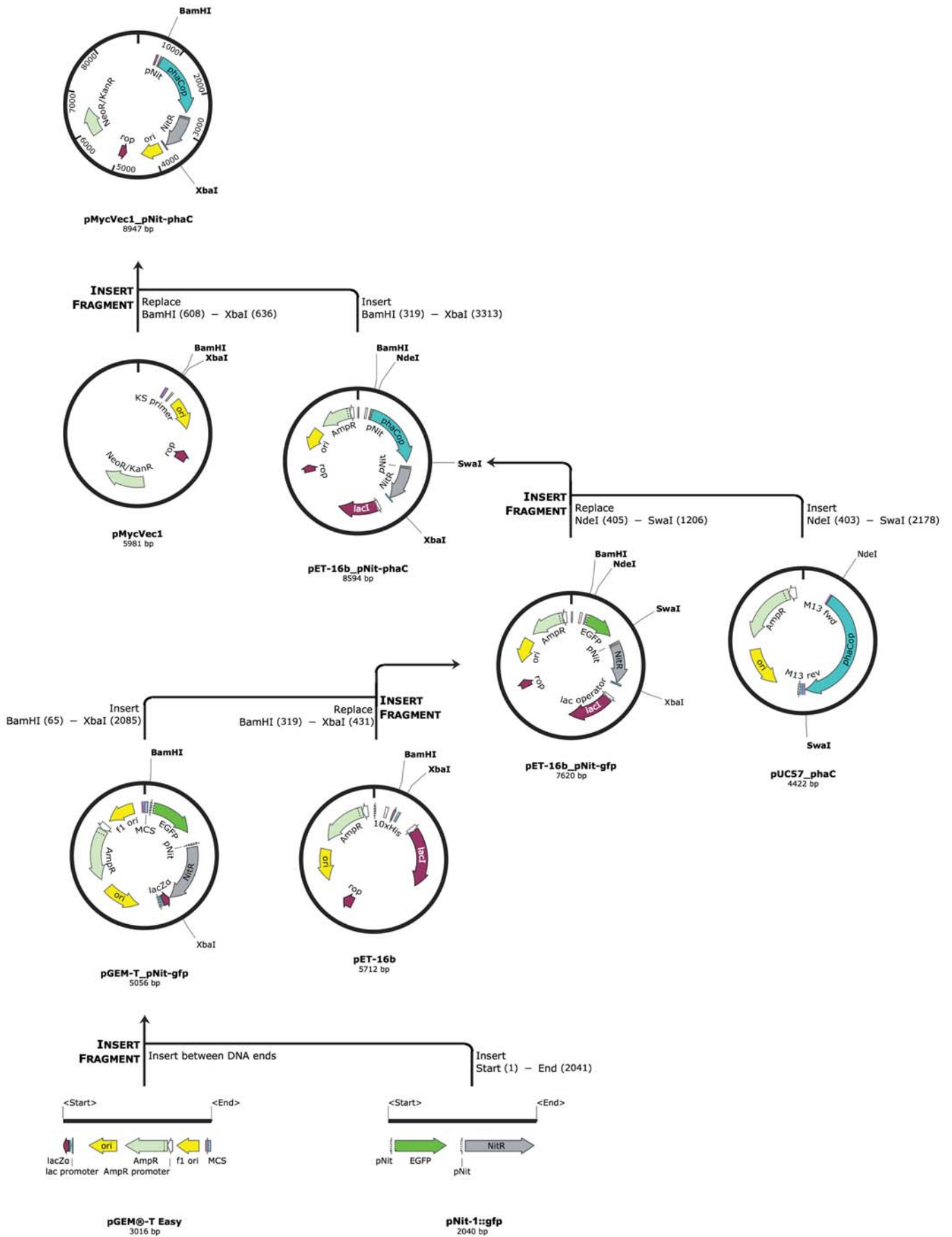
45. Devulder, G., M.P. De Montclos, and J.P. Flandrois, *A multigene approach to phylogenetic analysis using the genus Mycobacterium as a model*. International Journal of Systematic and Evolutionary Microbiology, 2005. **55**(1): p. 293-302.
46. Altaf, M., et al., *Evaluation of the Mycobacterium smegmatis and BCG models for the discovery of Mycobacterium tuberculosis inhibitors*. Tuberculosis, 2010. **90**(6): p. 333-337.
47. Woodland, D.L., *Jump-starting the immune system: prime-boosting comes of age*. Trends in Immunology, 2004. **25**(2): p. 98-104.
48. Lu, S., *Heterologous prime-boost vaccination*. Current Opinion in Immunology, 2009. **21**(3): p. 346-351.
49. McShane, H. and A. Hill, *Prime-boost immunisation strategies for tuberculosis*. Microbes and Infection, 2005. **7**(5): p. 962-967.
50. Nolz, J.C. and J.T. Harty, *Strategies and implications for prime-boost vaccination to generate memory CD8 T cells*, in *Crossroads between Innate and Adaptive Immunity III*. 2011, Springer. p. 69-83.

# **Supplementary material for: Engineering mycobacteria for the production of self-assembling biopolyesters displaying mycobacterial antigens for use as tuberculosis vaccine**

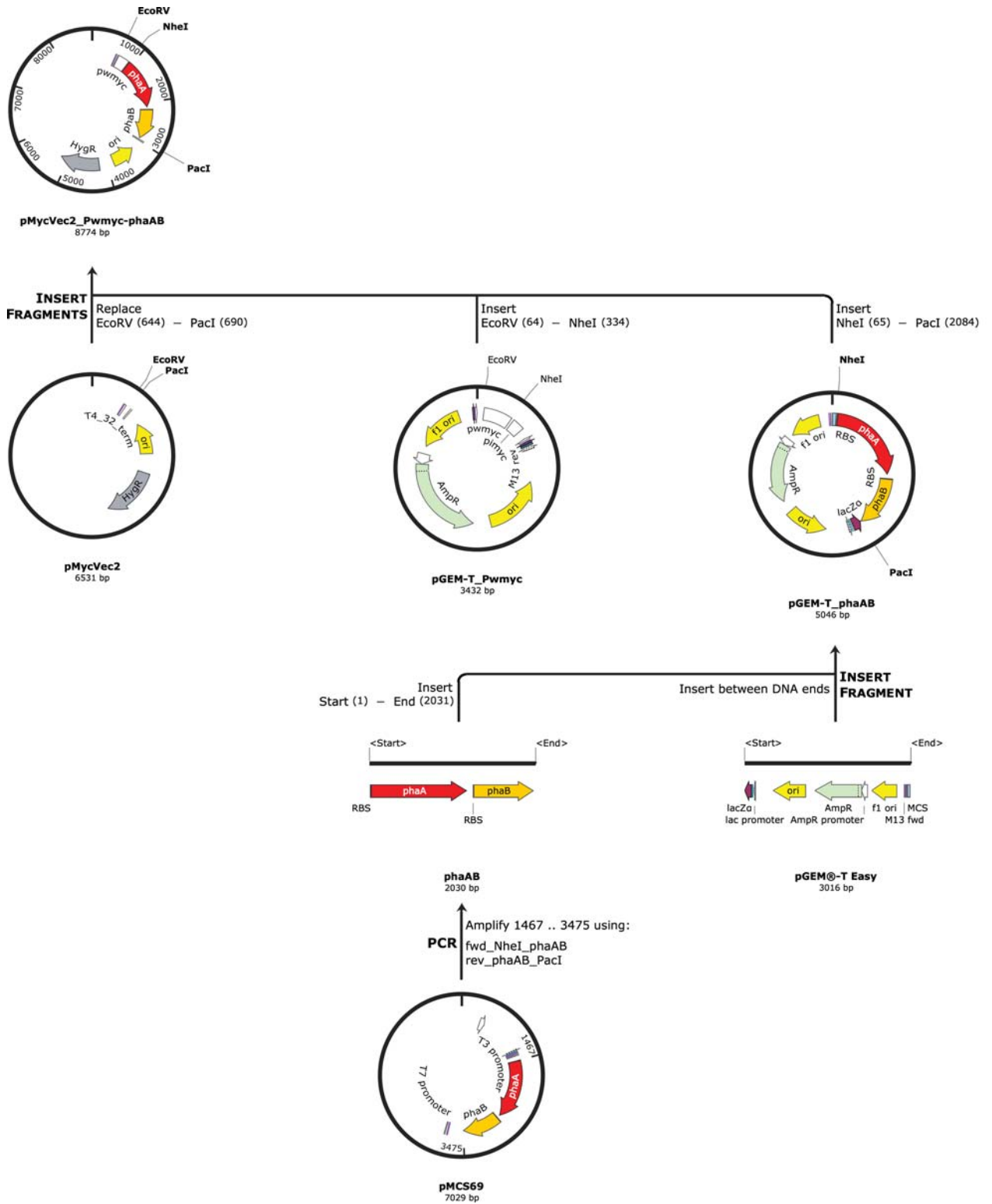
Jason W. Lee,<sup>1</sup> Natalie A. Parlane,<sup>2</sup> Bernd H. A. Rehm,<sup>1,3</sup> Bryce M. Buddle,<sup>2</sup> and Axel Heiser<sup>2\*</sup>

*Institute of Fundamental Sciences, Massey University, Palmerston North, New Zealand<sup>1</sup>; AgResearch, Hopkirk Research Institute, Palmerston North, New Zealand<sup>2</sup>; and PolyBatics, Palmerston North, New Zealand<sup>3</sup>*

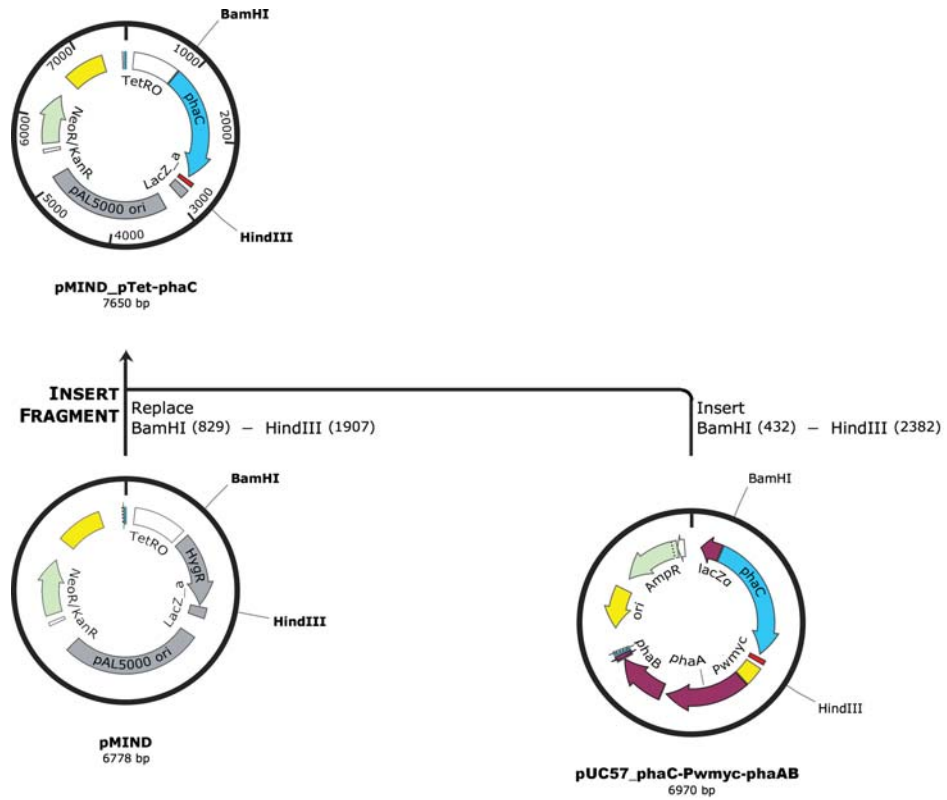
\*Corresponding author: Axel Heiser, e-mail: [axel.heiser@agresearch.co.nz](mailto:axel.heiser@agresearch.co.nz),  
phone: +64 6 351 8691



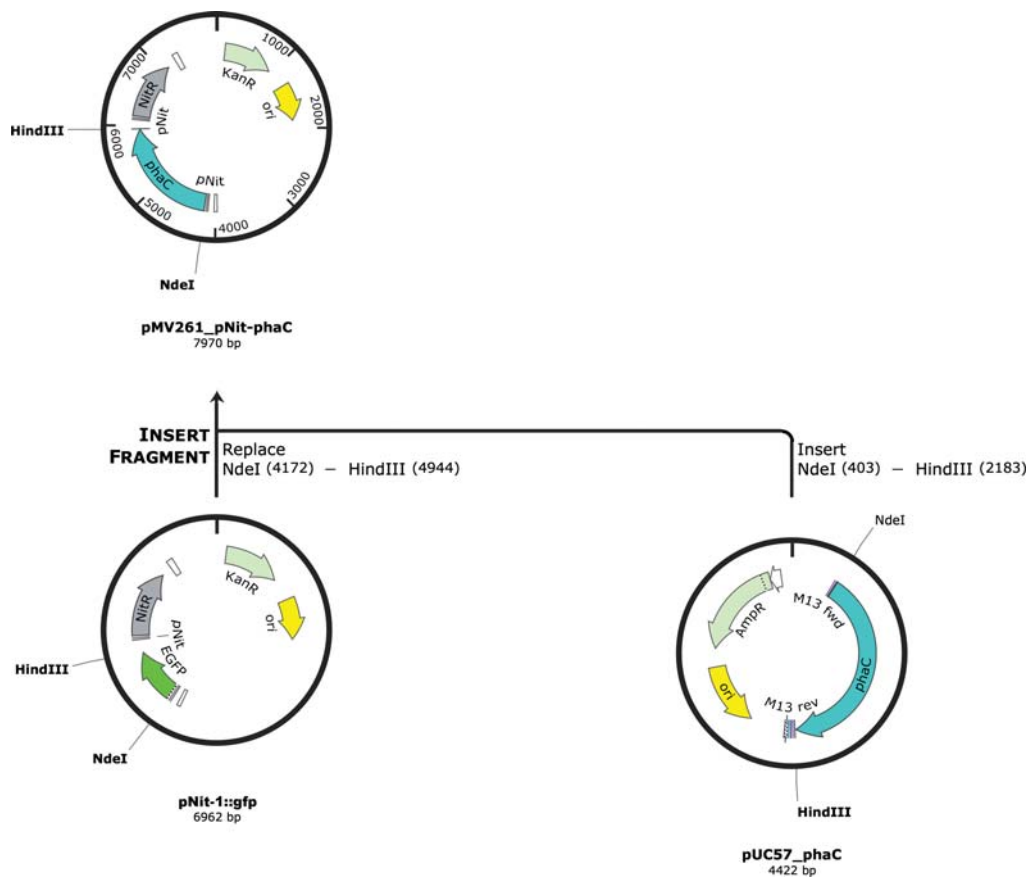
Supplementary Figure 3.1. Construction of plasmid pMycVec1\_pNit-phaC.



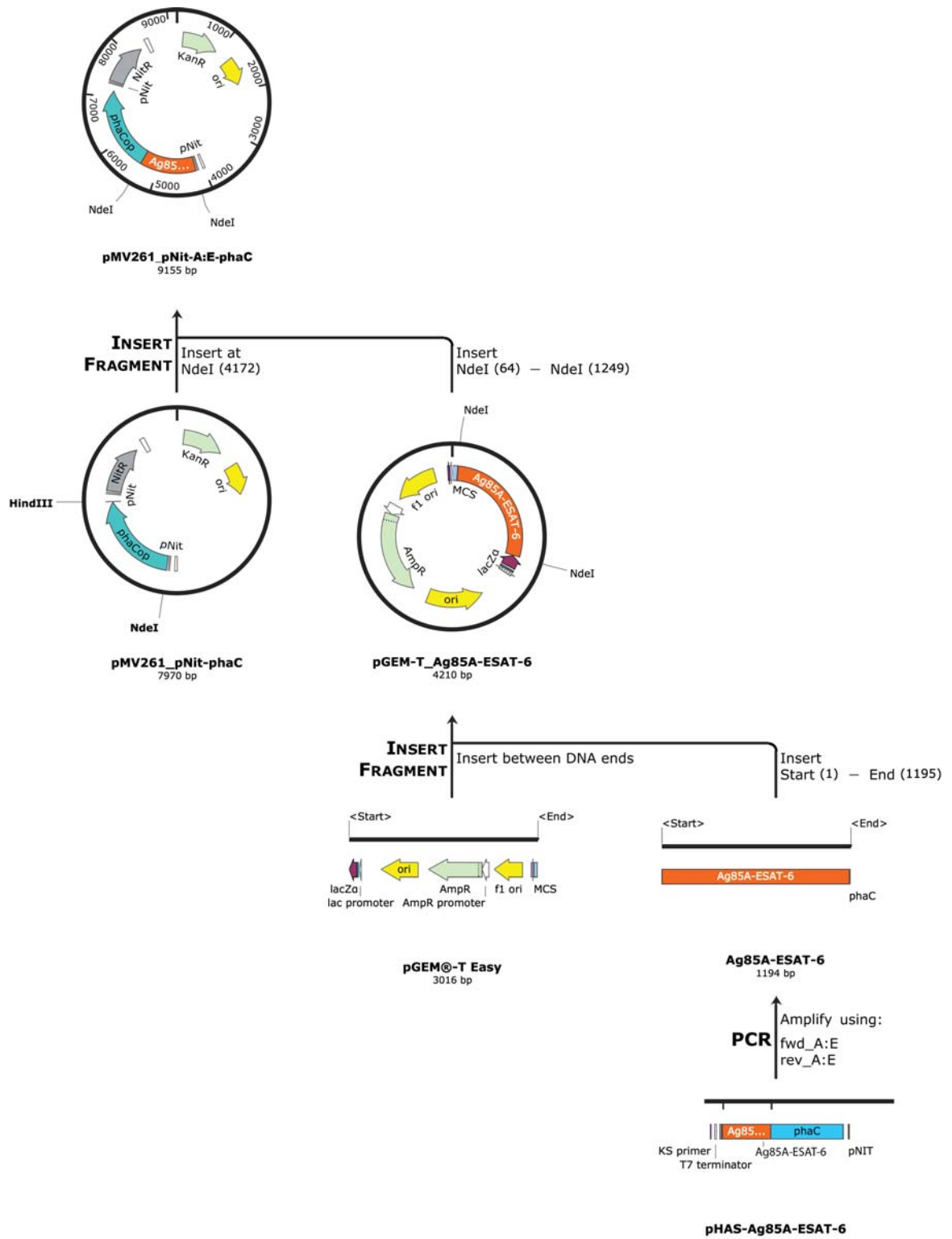
Supplementary Figure 3.2. Construction of plasmid pMycVec2\_Pwmyc-phaAB.



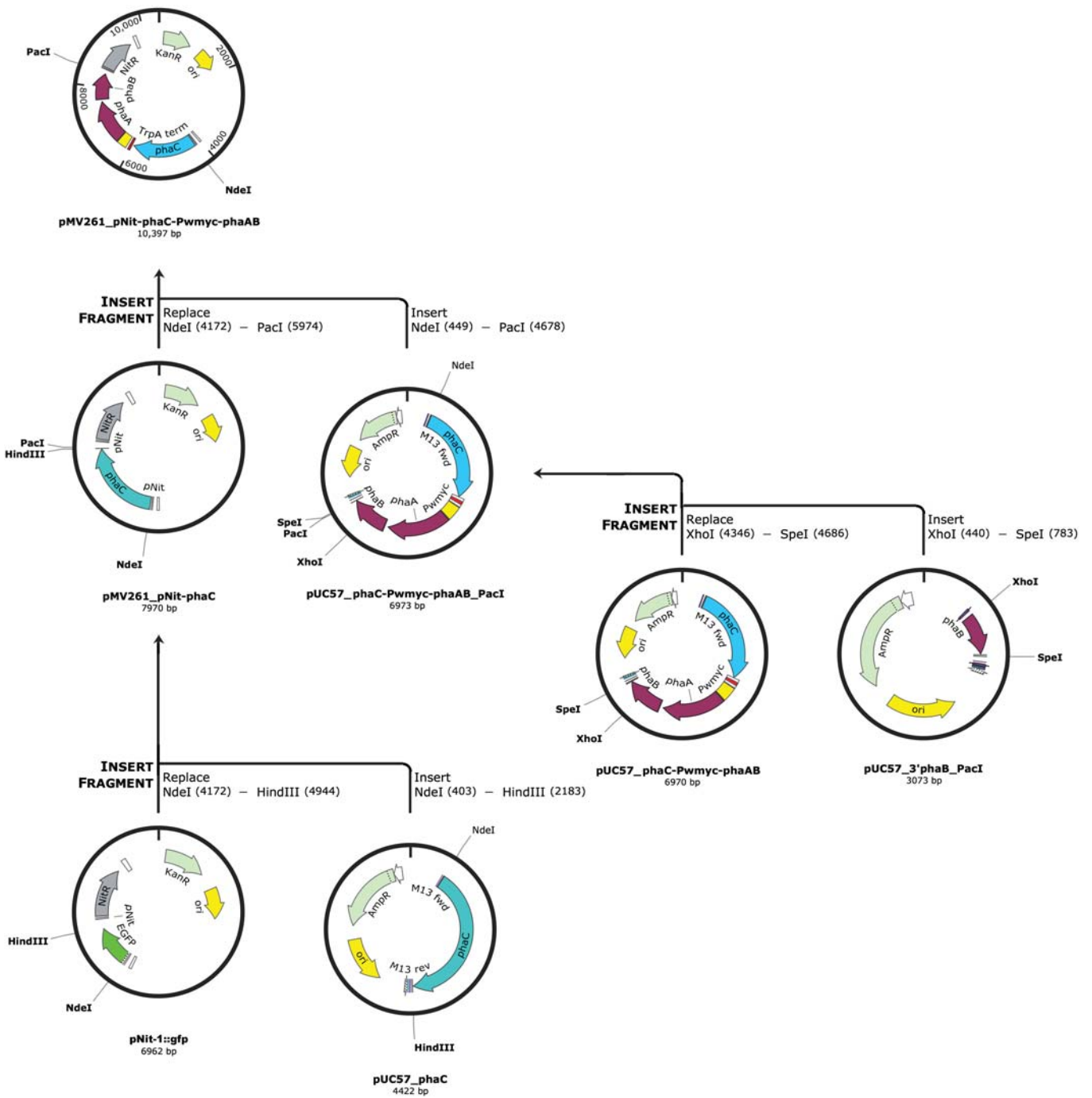
Supplementary Figure 3.3. Construction of plasmid pMIND\_pTet-phaC



Supplementary Figure 3.4. Construction of plasmid pMV261\_pNit-phaC.

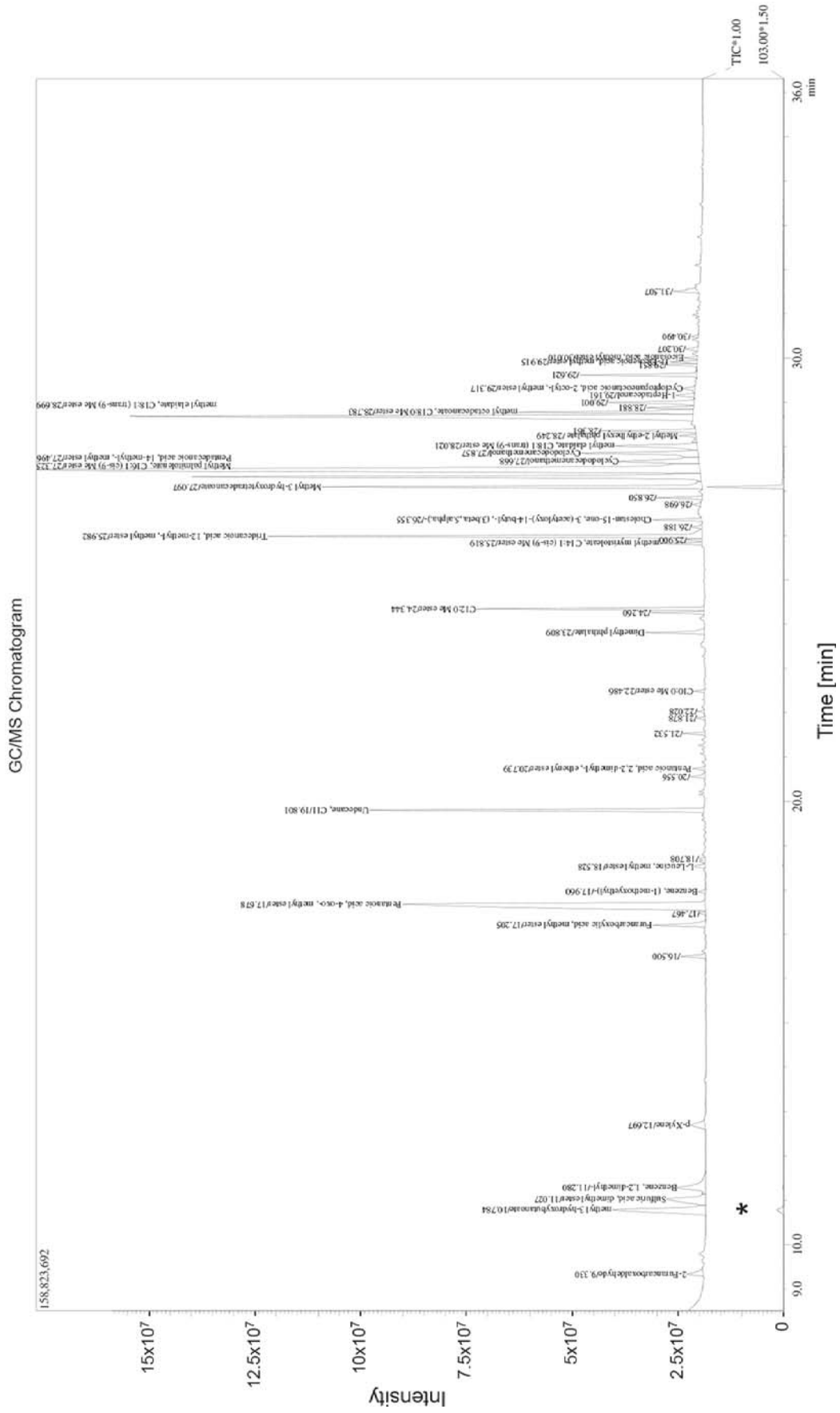


Supplementary Figure 3.5. Construction of plasmid pMV261\_pNit-A:E-phaC.



Supplementary Figure 3.6. Construction of plasmid pMV261\_pNit-phaC-Pwmyc-phaAB.

Sample Name : *E. coli* BL21 (pMCS69) + pMIND\_pTet-phaC  
 Injection Volume : 1.00



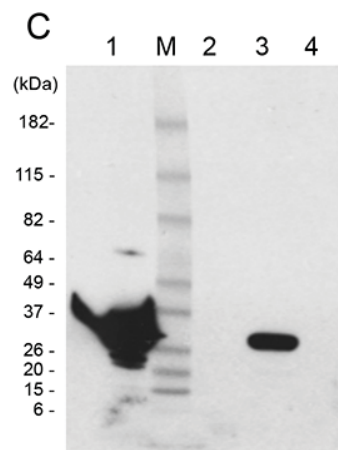
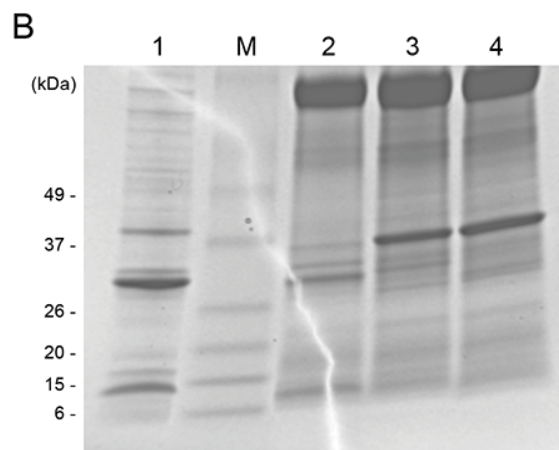
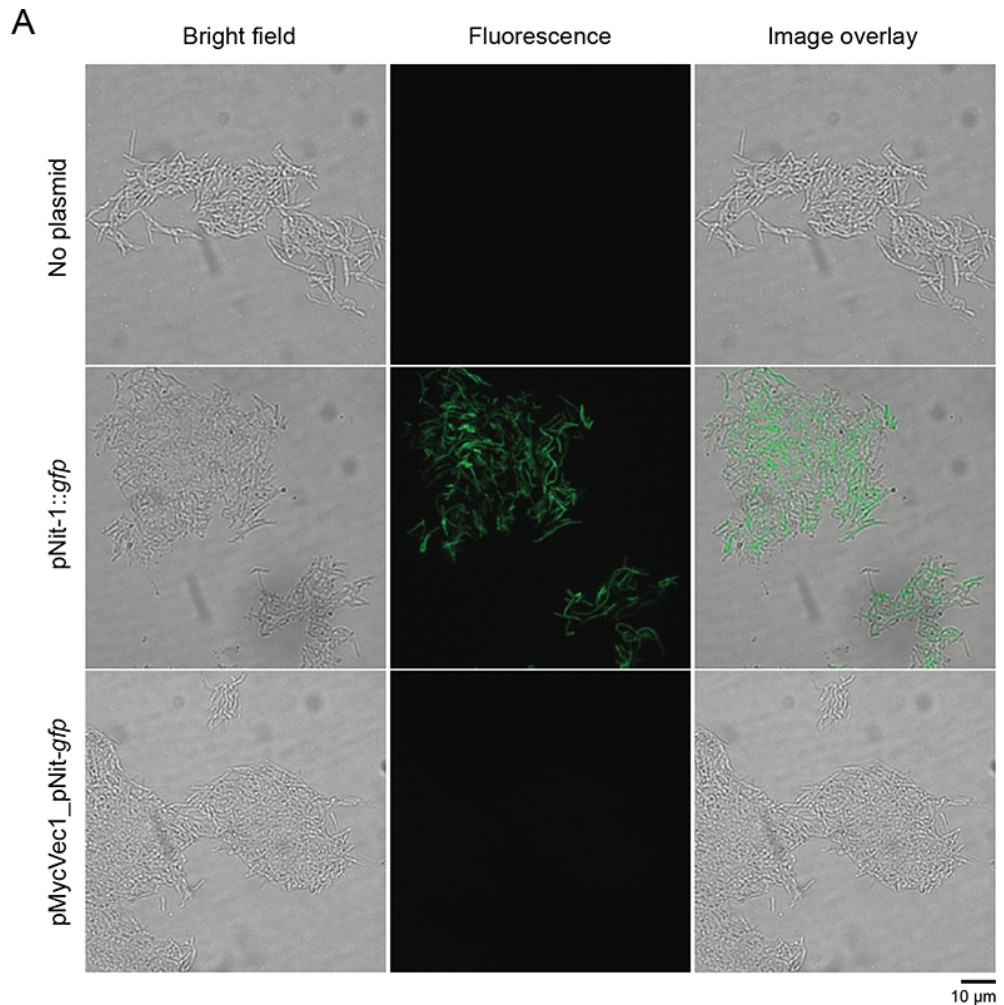
**Supplementary Figure 3.7. Analysis of PHB in whole-cell by GC/MS.** *E. coli* BL21 harboring plasmids pMCS69 and pMIND\_pTet-phaC were cultivated under PHB accumulating conditions. Whole-cell samples were prepared and subjected to GC/MS analysis as described in the Methods. (Asterisk), Methyl ester of PHB (methyl 3-hydroxybutanoate).

Sample Name : *E. coli* BL21 (pMCS69) + pMIND\_pTet-*phaC*  
 Injection Volume : 1.00

GC/MS Peak Report TIC

Peak#	Rt/Time	Area%	Name
1	9.330	0.41	
2	10.784	3.23	2-Furancarboxaldehyde
3	69.129741	1.58	methyl 3-hydroxybutanoate
4	11.280	1.24	Sulfuric acid, dimethyl ester
5	54579662	0.50	Benzene, 1,2-dimethyl-
6	21930778	0.41	p-Xylene
7	18041122	1.01	
8	44269514	0.10	Furancarboxylic acid, methyl ester
9	17.678	11.02	
10	483386702	0.11	Pentanoic acid, 4-oxo-, methyl ester
11	4886808	0.21	Benzene, (1-methoxyethyl)-
12	9203406	0.17	L-Leucine, methyl ester
13	7594987	4.98	
14	218217837	0.24	Undecane, C11
15	10587835	0.18	
16	8017009	0.29	Pentanoic acid, 2,2-dimethyl-, etheryl ester
17	12750456	0.10	
18	4439990	0.09	
19	4096429	0.13	C10:0 Me ester
20	5554627	0.81	Dimethyl phthalate
21	35613445	0.65	
22	28515207	2.90	C12:0 Me ester
23	24.344	0.50	methyl myristoleate, C14:1 (cis-9) Me ester
24	127257642	0.22	
25	22075866	6.55	Tridecanoic acid, 12-methyl-, methyl ester
26	9627947	0.15	
27	287107573	0.61	Cholestan-15-one, 3-(acetyloxy)-14-butyl-, (3.beta.,5.alpha.)
28	6496418	0.12	
29	26.355	0.55	
30	5231724	5.52	Methyl 3-hydroxytetradecanoate
31	23992020	8.53	Methyl palmitoleate, C16:1 (cis-9) Me ester
32	242222700	19.05	Pentadecanoic acid, 14-methyl-, methyl ester
33	373885099	2.07	Cyclododecanemethanol
34	835402100	1.86	Cyclododecanemethanol
35	90868584	0.32	methyl elaidate, C18:1 (trans-9) Me ester
36	101056175	1.32	Methyl 2-ethylhexyl phthalate
37	81495977	11.36	methyl elaidate, C18:1 (trans-9) Me ester
38	13943365	2.61	methyl octadecanoate, C18:0 Me ester
39	58026807	0.67	
40	497960844	1.42	
41	114311012	0.33	
42	29346647	0.24	Cyclopropenecarboxylic acid, 2-octyl-, methyl ester
43	62460134	0.40	
44	14385251	0.33	
45	10511719	0.16	
46	73045028	0.21	
47	29.621	0.09	
48	29.851	0.49	
49	17748660	0.09	
50	14411642	100.00	11-Eicosenoic acid, methyl ester
	7005998		Eicosanoic acid, methyl ester
	9440735		
	3811359		
	21285235		
	43885254416		

Supplementary Figure 3.7. (Continued).



**Supplementary Figure 3.8. Confirmation of pNit promoter activity.** *M. smegmatis* harboring various plasmid systems encoding *gfp* regulated under nitrile inducible promoter (pNit) were grown under protein inducive conditions. (a) Fluorescent microscopy analysis of *M. smegmatis* without plasmid and with plasmid pNit-1::gfp for detection of GFP. Protein analysis was performed by (b) SDS-PAGE and (c) immunoblot analysis. Samples were arranged accordingly: lane 1, GFP positive control; lane M, molecular weight standard; lane 2, *M. smegmatis* with no plasmid; lane 3, pNit-1::gfp; and lane 4, pMycVec1\_pNit-gfp.



Sample Name : *M. smegmatis mc<sup>2</sup>155*  
 Injection Volume : 1.00

GC/MS Peak Report TIC

Peak#	R.Time	Area	Name	Area%
1	9.175	42433880	2-Furancarboxaldehyde	0.84
2	10.762	6901020	Ethylbenzene	0.14
3	11.243	32060657	Benzene, 1,2-dimethyl-	0.63
4	12.700	11532733	Benzene, 1,2-dimethyl-	0.23
5	16.497	13247578		0.26
6	16.641	5273001		0.10
7	17.641	244522219	Pentanoic acid, 4-oxo-, methyl ester	4.82
8	18.588	10751966	1-Hexanol, 2-ethyl-	0.21
9	18.676	56721540	Butanedioic acid, dimethyl ester	1.12
10	19.623	12399055		0.24
11	19.844	196172219	Decane, 2-nUndecane, C11ethyl-	3.87
12	20.198	4169067	Octanoic acid, methyl ester	0.08
13	20.626	5790970		0.11
14	20.789	8091122		0.16
15	21.582	27852754		0.55
16	21.927	21337654		0.42
17	22.078	23983693		0.47
18	22.281	23697288	Methyl 2,3,4-tri-O-methyl-6-deoxy- $\alpha$ -D-mannopyranoside	0.47
19	22.344	33698118		0.66
20	22.541	8563933	Decanoic acid, methyl ester	0.17
21	23.859	44577015	Dimethyl phthalate	0.88
22	24.263	5504149	9-Octadecenoic acid (Z)-, methyl ester	0.11
23	24.388	35344782	Dodecanoic acid, methyl ester	0.70
24	24.822	6439249	Dodecanoic acid, 4-methyl-, methyl ester	0.13
25	25.832	29065029	Eicosenoic acid, methyl ester	0.57
26	25.897	33876641	methyl myristolate, C14:1 (cis-9) Me ester	0.67
27	26.026	254500211	Tridecanoic acid, 12-methyl-, methyl ester	5.02
28	26.239	5840412		0.12
29	26.348	24487564	Nonadecanoic acid, methyl ester	0.48
30	26.767	21543867	methyl pentadecanoate, C15:0 Me ester	0.42
31	27.025	5906772		0.12
32	27.416	673280705	Methyl palmitolenate, C16:1 (cis-9) Me ester	13.27
33	27.567	865089404	Pentadecanoic acid, 14-methyl-, methyl ester	17.06
34	27.789	247607764	Heptadecanoic acid, 10-methyl-, methyl ester	4.88
35	27.908	20612683		0.41
36	28.041	34116704	Cyclopropanecarboxylic acid, 2-hexyl-, methyl ester	0.67
37	28.180	32507892	Heptadecanoic acid, methyl ester	0.64
38	28.308	5579473		0.11
39	28.430	83852937		1.65
40	28.746	706768607	7-Octadecenoic acid, methyl ester	13.93
41	28.866	369671884	Heptadecanoic acid, 14-methyl-, methyl ester, (+/-)-	7.29
42	29.000	20587645		0.41
43	29.116	393934547	Octadecanoic acid, 10-methyl-, methyl ester	7.77
44	29.201	23939056	8-Heptadecene, 9-octyl-	0.47
45	29.666	103717879		2.04
46	29.933	4835622	11-Eicosenoic acid, methyl ester	0.10
47	30.072	87914539	methyl arachidate, C20:0 Me ester	1.73
48	30.142	5614221		0.11
49	31.213	44835265	Docosanoic acid, methyl ester	0.88
50	32.386	91191433	methyl lignocerate, C24:0 Me ester	1.80
		5071944418		100.00

Supplementary Figure 3.9. (Continued).



Sample Name  
Injection Volume

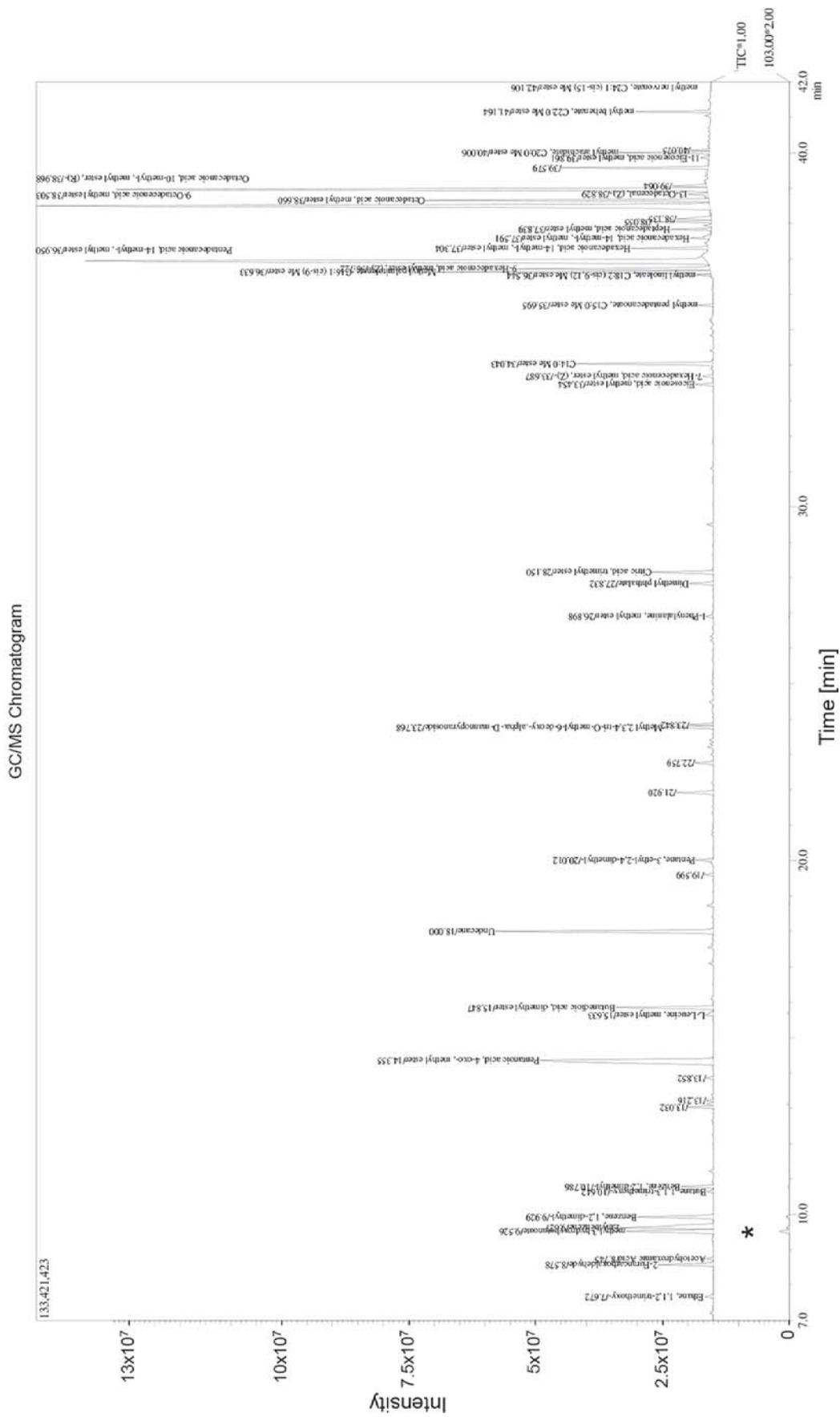
: *M. smegmatis mc<sup>2</sup>155* (pMycVec2\_Pwmyc\_phaAB) + pMV261\_phaC  
: 1.00

GC/MS Peak Report TIC

Peak#	R.Time	Area	Name	Area%
1	9.178	38418036	2-Furancarboxaldehyde	0.80
2	10.814	708934395	methyl 3-hydroxybutanoate	14.75
3	11.248	33850792	Benzene, 1,2-dimethyl-	0.70
4	12.551	46522870	Butane, 1,1,3-trimethoxy-	0.97
5	12.688	13598686	Benzene, 1,2-dimethyl-	0.28
6	16.524	32550167	methyl 3-hydroxyoctanoate	0.68
7	16.633	6807288		0.14
8	17.635	233511530	Pentanoic acid, 4-oxo-, methyl ester	4.86
9	18.479	3647766	Hexanoic acid, 5-oxo-, methyl ester	0.08
10	18.584	9915279	1-Hexanol, 2-ethyl-	0.21
11	18.669	48132432	Butanedioic acid, dimethyl ester	1.00
12	19.619	6530655		0.14
13	19.839	200087099	Undecane, C11	4.16
14	20.191	4622523	Octanoic acid, methyl ester	0.10
15	20.620	6116816		0.13
16	20.782	8753277		0.18
17	21.116	11329132		0.24
18	21.577	29522286		0.61
19	21.924	20139395		0.42
20	22.074	60292183		1.25
21	22.278	29104957	Methyl 2,3,4-tri-O-methyl-6-deoxy-alpha-D-mannopyranoside	0.61
22	22.342	31668125	Methyl 2-O-acetyl-3,4-di-O-methyl-6-deoxy-alpha-D-mannopyranoside	0.66
23	22.534	11287773		0.23
24	23.131	4514535		0.09
25	23.234	4474010		0.09
26	23.911	115051862	Citric acid, trimethyl ester	2.39
27	24.387	16624556	Dodecanoic acid, methyl ester	0.35
28	25.833	25825525	Eicosenoic acid, methyl ester	0.54
29	25.900	20068668	methyl myristoleate, C14:1 (cis-9) Me ester	0.42
30	26.024	179221908	Tridecanoic acid, 12-methyl-, methyl ester	3.73
31	26.240	7283103		0.15
32	26.349	5586254	Heptadecanoic acid, methyl ester	0.12
33	26.770	21157027	methyl pentadecanoate, C15:0 Me ester	0.44
34	27.399	447883091	Methyl palmitoleate, C16:1 (cis-9) Me ester	9.32
35	27.546	678667701	Pentadecanoic acid, 14-methyl-, methyl ester	14.12
36	27.784	114506381	Hexadecanoic acid, 14-methyl-, methyl ester	2.58
37	27.908	12594137	Cyclopropanecarboxylic acid, 2-hexyl-, methyl ester	0.26
38	28.045	23265343	Heptadecanoic acid, methyl ester	0.48
39	28.179	26837580	Heptadecanoic acid, methyl ester	0.56
40	28.307	4361956		0.09
41	28.433	58650185		1.22
42	28.741	574299558	7-Octadecenoic acid, methyl ester	11.95
43	28.848	275166774	Heptadecanoic acid, 15-methyl-, methyl ester	5.72
44	28.998	15177734		0.32
45	29.100	329042471	Octadecanoic acid, 10-methyl-, methyl ester, (R)-	6.85
46	29.198	17236494	8-Heptadecene, 9-octyl-	0.36
47	29.663	65392644		1.56
48	30.069	55866234	Eicosanoic acid, methyl ester	1.16
49	31.209	31257141	Docosanoic acid, methyl ester	0.65
50	32.375	81616650	methyl lignocerate, C24:0 Me ester	1.70
		4806972984		100.00

Supplementary Figure 3.9. (Continued).

Sample Name : *M. smegmatis mc<sup>2</sup>155* (pMycVec2\_Pwmyc\_phaAB) + pMV261\_A:E-phaC  
 Injection Volume : 1.00



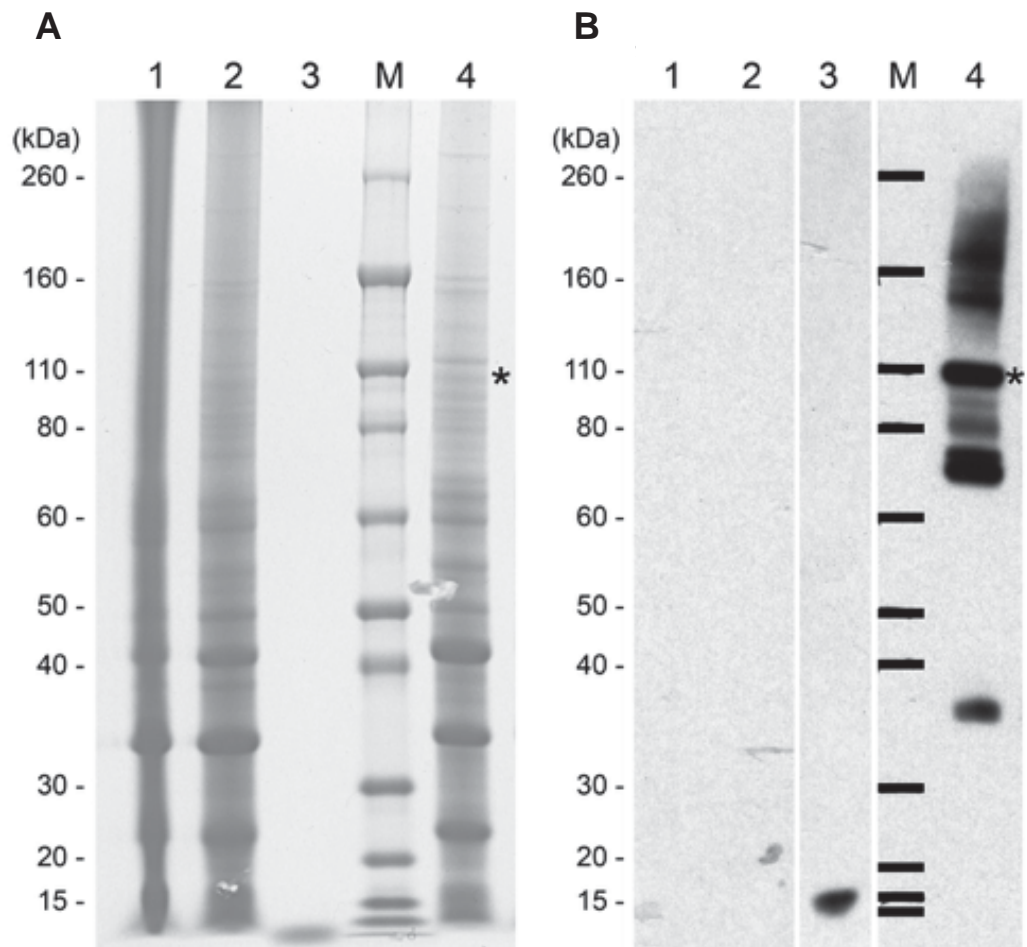
Supplementary Figure 3.9. (Continued).

Sample Name : *M. smegmatis mc<sup>2</sup>-155 (pMycVec2\_pwmyc\_phaAB) + pMV261\_A:E-phaC*  
 Injection Volume : 1.00

GC/MS Peak Report TIC

Peak#	R.Time	Area	Name	Area%
1	4.199	3935885		0.12
2	5.260031	5266031	Ethane, 1,1,2-trimethoxy-	0.15
3	6.772	33648244	2-Furanicarboxaldehyde	0.99
4	8.745	4252881	Acetohydroxamic Acid	0.12
5	9.526	71507176	methyl 3-hydroxybutanoate	2.10
6	9.627	88003097	Ethylbenzene	2.58
7	9.929	54604866	Benzene, 1,2-dimethyl-	1.60
8	10.642	4236918	Butane, 1,1,3-trimethoxy-	0.12
9	10.786	19821349	Benzene, 1,2-dimethyl-	0.58
10	13.032	14607048		0.43
11	13.216	4278135		0.13
12	13.852	4733977		0.14
13	14.355	218115592	Pentanoic acid, 4-oxo-, methyl ester	6.40
14	15.633	7596528	L-Leucine, methyl ester	0.22
15	15.847	64863201	Butanedioic acid, dimethyl ester	1.90
16	18.000	157701476	Undecane	4.63
17	19.599	5243040		0.15
18	20.012	9543702	Pentane, 3-ethyl-2,4-dimethyl-	0.28
19	21.920	25361132		0.74
20	22.759	11275262		0.33
21	23.768	29718255		0.33
22	23.842	12942496		0.87
23	26.898	4628358		0.38
24	27.832	14915984	Methyl 2,3,4-tri-O-methyl-6-deoxy-alpha-D-nannopyranoside	0.14
25	28.150	40174392		0.44
26	33.454	11140472		1.18
27	33.687	7020500		0.33
28	34.043	86534504		0.21
29	35.695	7440526		2.54
30	36.544	7075596		0.22
31	36.633	151999448		0.21
32	36.722	113611806		4.46
33	36.930	593128248		3.33
34	37.304	40246214		17.41
35	37.591	12569515		1.18
36	37.839	18709285		0.37
37	38.055	28178130		0.55
38	38.135	24801999		0.83
39	38.503	593781453		0.73
40	38.660	142049873		17.43
41	38.829	13382966		4.17
42	38.968	400657246		0.39
43	39.064	20162647		11.76
44	39.579	69190080		0.59
45	39.861	5137947		2.03
46	40.006	42542562		0.15
47	40.075	7834610		1.25
48	41.164	35132887		0.23
49	42.106	6741763		1.03
50	42.215	56997562		0.20
		3407045864		1.67
				100.00

Supplementary Figure 3.9. (Continued).



**Supplementary Figure 3.10. Confirmation of ESAT-6.** *M. smegmatis* harboring various plasmid systems regulated under nitrile inducible promoter (pNit) were grown under protein inducive conditions. (a) SDS-PAGE and (b) immunoblot with anti-ESAT-6 polyclonal Ab. Samples were arranged accordingly: lane 1, pMycVec2\_Pwmyc-*phaAB* and pMV261\_*phaC* (MBB), lane 2, pMycVec2\_Pwmyc-*phaAB* (MVC) negative control; lane 3, ESAT-6 positive control; lane M, molecular weight standard; lane 4, pMycVec2\_Pwmyc-*phaAB* and pMV261\_A:E-*phaC* (A:E-MBB). Asterisk indicates A:E-PhaC protein.

## Chapter 4: Discussion and outlook

### 4.1 Discussion

Chapters 2 and 3 are written in a format for peer-reviewed journals and therefore, each chapter contains its own relevant discussion and conclusions. A summary of the findings and subsequent outlook will be discussed in the section.

This thesis is focused on expanding the application of PHA beads as an effective vaccine delivery system. Subunit vaccines tend to be poorly immunogenic and require the need for adjuvants/delivery system and/or booster vaccinations [1]. A number of vaccine delivery systems are available such VLPs, chitosan, and liposomes, however, PHA beads offers two advantages over the other systems: 1) a one step production process and 2) the display of vaccine candidates which are covalently attached to the beads surface in a uniform orientation [2]. The use of PHA beads as a novel delivery system that enables the efficient display of vaccine candidate antigens relevant to the disease tuberculosis or hepatitis C has been recently investigated [3-7]. These antigen-displaying (vaccine) PHA beads were produced in engineered heterologous bacterial production hosts such as *E. coli* or *L. lactis*. The PHA bead delivery system was shown to greatly improve immunogenicity of the displayed vaccine candidate antigens [3-5]. However, a limitation of the current vaccine PHA bead approach like other subunit vaccines is that they only provide a limited repertoire of antigens of the disease pathogen as compared to live attenuated, killed inactivated, and OMV vaccines.

Therefore, the concept of directly utilizing the disease causative pathogen or model organism for the production of vaccine PHA beads with a large antigenic repertoire was investigated. This approach was based on observations during the production and isolation of vaccine PHA beads in heterologous bacterial hosts, which resulted in the beads having a degree of protein and other impurities derived from the production host. These impurities from the disease causative pathogen or model organism were hypothesized to have the potential to induce greater protective immunity compared to expression of the same vaccine PHA bead in a heterologous bacterial production host. Additionally, this approach of producing vaccine beads would reduce the need for extensive downstream processing, saving both time and money.

To exemplify this concept, two different infectious diseases in humans were chosen, namely disease caused by the opportunistic pathogen *P. aeruginosa* (chapter 2) and tuberculosis caused by the pathogen *M. tuberculosis* (chapter 3). These two bacteria cause high levels of mortality and morbidity worldwide. Currently, there is no commercially available vaccine against *P. aeruginosa* and the only licensed vaccine available for the prevention of TB caused by *M. tuberculosis* demonstrates little to no protection in adults against pulmonary TB. For the disease caused by *P. aeruginosa* we described the engineering of the bacterium to promote the production of PHA and vaccine candidate exopolysaccharide (EPS) Psl production; a new mode of functional display using the class II PHA synthase (C terminus); and the engineering, production, and immunological validation of OprI/F-AlgE fusion antigen-displayed on PHA beads. While for the disease tuberculosis we took a slightly different approach by investigating the use of nonpathogenic *M. smegmatis* as a model organism for pathogen *M. tuberculosis*. We described the engineering, production, and validation (immunological and challenge) of Ag85A-ESAT-6 displayed on PHA beads. This example would give support to the concept of using a model organism for the production of vaccine PHA bead that can protect against disease. This was because the production of vaccine PHA beads in a pathogenic host could potentially face similar regulatory and safety concerns as those associated with whole killed/inactivated vaccines e.g. live pathogen contamination and reactivity [1, 8].

In chapter 2, *P. aeruginosa* was successfully engineered to promote both the production of PHA and vaccine candidate EPS Psl by disruption of genes encoding key enzymes Alg8 (glycosyltransferase) and PelF (glycosyltransferase) involved in competing biosynthesis pathways towards the production of alginate and the glucose-rich Pel polysaccharide, respectively, were targeted (**Fig. 2.2a,b** and **Supplementary Fig. 2.1**) [9, 10]. By increasing the PHA yield we can make the product commercially cost effective. EPS Psl is seen as a major virulence factor of *P. aeruginosa* that has the potential to purify with the vaccine PHA beads during isolation and hence providing additional antigenic material. However, this triple knockout mutant production strain still needs to be fully characterized.

Another aspect to chapter 2 was to investigate the tolerance of the class II PHA synthase to C terminal translational fusions as a new mode of functional display. Only recently has the class I PHA synthase has been shown to tolerate translational fusions to its C terminus [11]. The mode of protein/antigen-display on the beads has been shown to impact both PHA bead formation *in vivo* and fusion protein levels [12, 13]. More importantly, the mode of antigen-display on the surface of the PHA beads may affect antigen recognition and uptake of the beads by professional APCs. In this chapter it was shown that the class II PHA synthase from *P. aeruginosa* can indeed tolerate translationally fused proteins/antigen (GFP or OprI/F-AlgE fusion antigen) at its C terminus by employing a similar designer linker used in the class I PHA synthase to allow both the PHA synthase and fusion partner to remain functionally active (**Fig. 2.3**). Translational fusions to the C terminus of the class II PHA synthase was found to negatively impact PHA accumulation *in vivo*, while protein production varied depending on the fusion partner. Similar effects of the fusion protein on PHA synthase activity and protein production can be seen with the class I PHA synthase and this variation seems to be strongly dependent on the PHA synthase fusion partner [11, 12, 14].

Both *P. aeruginosa* (chapter 2) and *M. smegmatis* (chapter 3) were successfully engineered to produce fusion antigen-displaying PHA beads either by harnessing the native PHA production system or by establishing the PHA producing machinery (PHB pathway), respectively. These vaccine PHA beads were isolated from either host with varying degrees of success due to the different cell wall properties of the two bacteria. Vaccine PHA beads from *P. aeruginosa* were isolated to approximately 90% purity as assessed by GC/MS (**Fig. 3.5c**), while large amounts of host cell impurities were seen to be isolated with *M. smegmatis* vaccine PHA beads (**Figs. 3.2 and 3.3**). The isolated PHA beads in addition to the fusion antigen was found to contain a large number of copurifying HCP impurities from the host. Importantly some were identified as vaccine candidate antigens i.e. OprI and OprF from *P. aeruginosa* PHA beads (**Fig. 2.6d**). These copurifying HCP impurities are hypothesized to provide a large antigenic repertoire comparable to whole killed or OMV vaccines, which can potentially act as an adjuvant and/or induce protective immunity [15, 16]. Novel vaccines that incorporate multiple antigen/epitopes capable of signaling through multiple TLRs [17, 18] are

thought to lead to stronger, longer lasting, and more specific immune responses than a single antigen/epitope alone [19, 20].

Vaccinations with vaccine PHA beads with copurifying impurities were found to generate antigen specific immune responses to the fusion antigens and HCP impurities. Mice vaccinated with *P. aeruginosa* vaccine PHA beads displaying OprI/F-AlgE fusion antigen formulated in the absence of additional adjuvant (i.e. alum) elicited an antigen specific immune responses with a Th1 type pattern. The response was characterized by IgG2c isotype (**Fig. 2.8a**) and increased cytokine IFN- $\gamma$  (**Fig. 2.10**). This Th1 type immune response is seen to be important for protection against infection from *P. aeruginosa* [21-24]. Furthermore, cytokines IL-6, IL-10, and low but significant levels of IL-17a and IL-2 were also measured (**Fig. 2.10**). Here cytokines IL-6 and IL-10 was proposed to limit damage in the lungs of cystic fibrosis (CF) patients caused by hyper inflammation associated with exacerbated recruitment of neutrophils. The generation of antigen specific IgG2c serum antibodies may play a critical role in clearance of acute infection with *P. aeruginosa* [25]. These results are in agreement with other studies whereby proteins immobilized to PHA beads as delivery system and used as a vaccine are capable of generating a cell-mediated immune response [3, 4].

The HCP impurities copurified with the PHA beads from *P. aeruginosa* were found to illicit a strong immune response. Vaccination with *P. aeruginosa* PHA beads in the absence of OprI/F-AlgE fusion antigen was capable of inducing antigen specific antibodies to the OprI/F-AlgE fusion antigen (**Fig. 2.8a**). This suggests an immune response was made to HCP impurities of which contained antigens OprI and/or OprF and/or AlgE. This is not surprising as these proteins are normally found in the outer membrane of this bacterium [26, 27]. Furthermore, serum antibodies were also generated to a wide range of epitopes of the HCPs copurified with PHA beads (**Fig. 2.8b**). The generation of an immune reaction to various proteins including conserved vaccine candidates OprI and/or OprF and/or AlgE would be expected to provide some cross-protection between different strains. This is exemplified in **Fig. 2.8c,d** where functional antibodies generated from vaccination with vaccine beads produced in *P. aeruginosa* PAO1 was able to react and mediate killing of *P. aeruginosa* FRD1, PD300, and PA14 strains.

The immune response to *P. aeruginosa* vaccine PHA beads could also be further enhanced by formulation with alum adjuvant (**Supplementary Fig. 2.9**) and this suggests enhancement for a stronger immune response could be achieved by formulation with an appropriate adjuvant.

Vaccination of mice with *M. smegmatis* vaccine PHA beads displaying Ag85A-ESAT-6 fusion antigen formulated with alum generated significant levels of cytokine IFN- $\gamma$  and IL-17a when restimulated with *M. smegmatis* PHA beads in the absence of Ag85A-ESAT-6 fusion antigen (**Fig. 3.4**). Cytokines IFN- $\gamma$  and TNF have been found to be critical in the control of *M. tuberculosis* [28]. A strong adjuvating effect of the contaminating material from the host was also shown in the *M. smegmatis* vector control group. This suggests immune responses were made to the copurified impurities. Mycobacterial cell wall (e.g. peptidoglycan, glycolipids, and mycolic acids) and intracellular (e.g. heat shock proteins and CpG) components that maybe found on the vaccine beads are known to be responsible for the immunoadjuvant effect of Freund's complete adjuvant, a well-known potent stimulator of cell-mediated immunity [29].

However the strong IFN- $\gamma$  and IL-17a results seen with *M. smegmatis* vaccine PHA beads did not correlate with increased protection against *M. bovis* challenge in a mouse model (**Fig. 3.5**). Only PHA beads displaying Ag85A-ESAT-6 fusion antigen demonstrated partial protection (**Fig. 3.5**). This indicates Ag85A-ESAT-6 fusion antigen was protective.

In contrast to the *P. aeruginosa* example, only the *M. smegmatis* vaccine PHA beads displaying Ag85A-ESAT-6 fusion antigen was able to elicit an antigen specific response to Ag85A-ESAT-6 (**Fig. 3.4**). This is not surprising as *M. tuberculosis* vaccine candidate antigens Ag85A and ESAT-6 are absent in nonpathogenic strain *M. smegmatis* and consequently from the HCP impurities. Moreover it has been shown that *M. smegmatis* lacks a large proportion of proteins from the pathogenic strains such as *M. tuberculosis* and *M. bovis* [30]. Hence the lack of significant protein homology between the *M. smegmatis* and *M. bovis* might have resulted in the reduced efficacy of the *M. smegmatis* vaccine PHA beads to protect against challenge with *M. bovis*. The genetic relatedness between the model organism and disease causative pathogen is a

factor that needs to be considered for when producing vaccine PHA beads in the model organism. This highlights a limitation of using a model organism as the production host.

In conclusion, the results in this thesis support: 1) the feasibility of harnessing the native capacity of the opportunistic pathogen *P. aeruginosa* or establishing the PHB pathway in nonpathogenic model organism *M. smegmatis* to produce PHA beads as reserve materials for the design and production of vaccine PHA beads displaying candidate antigens with a large antigenic repertoire, and 2) the ability of these vaccine PHA beads to generate a protective immune response.

## 4.2 Outlook

This section describes different aspects of improving vaccine bead design, production, isolation, and purification and also further experiments for both pseudomonas and mycobacterial vaccine PHA beads.

### 4.2.1 Optimization of PHA production and antigen-display

**Linker optimization.** As mentioned in the discussion in chapter 2, optimization of the designer linker on the C terminus of the class II PHA synthase may be required to obtain optimum display of the OprI/F-AlgE fusion antigen on the surface of the vaccine PHA beads. This is due to the inherent fixed orientation of the PHA synthase on the bead surface and requires the specific properties of the designer linker to enable the surface exposure of the fusion partner [11]. The designer linker adapted for use here was originally designed for the class I PHA synthase, and therefore optimization for use with the class II PHA synthase needed to be investigated. Both the length and hydrophobicity of the linker needs to be considered. Accessibility of the antigen on the beads surface is critical for antigen processing by APCs and consequently the immune response developed [31].

**Antigen-display through use of multiple repeating epitopes.** The immune response to vaccine candidates can be enhanced by the generation of fusion antigens that contained tandemly repeated sequences of antigenic epitopes to increase immunogenicity [32, 33]. This can be achieved through improved antigen presentation and processing by APCs. For example, Jin et al [33] was able to demonstrate that immunization of mice with 6 copies of the Th2 peptide P277 as a fusion protein produced a higher Th2 type response than with a single copy of P277. Furthermore, this study showed that increasing certain Th1 or Th2 epitopes could be used to alter the Th1/Th2 balance. Thus, by increasing the number of Th1 epitopes such as OprI in the OprI/F-AlgE fusion antigen (**Fig. 2.5a**), a stronger Th1 immune response with the *P. aeruginosa* vaccine PHA beads could be generated.

**Epitope arrangement.** Optimizing antigen-display can also involve the rearrangement of antigenic epitopes of the antigen fusion or position on the terminus of the PHA synthase. The effect of this is presumably to allow better access and presentation of

certain antigenic epitopes to APCs. For instance, epitope OprI in the OprI/F-AlgE fusion antigen could be rearranged to the end of the fusion antigen furthest from the PHA synthase i.e. OprI-5-6-(OprF)<sub>x3</sub>-PhaC1<sub>Pa</sub> (**Fig. 4.1a**) instead of the current arrangement 5-6-(OprF)<sub>x3</sub>-OprI-PhaC1<sub>Pa</sub>. As a result, OprI would be more accessible and consequently could better modulate immune response towards a Th1 type response.

Furthermore, instead of arranging epitopes within a single fusion protein to be fused to a single terminus, epitopes could be separated so they can be displayed on different terminus of the PHA synthase. For example, OprI which is the larger antigen could be arranged on its own and fused to the C terminus of PHA synthase while epitopes of OprF and AlgE could be arranged as a single fusion antigen to be translationally fused to the N terminus of the PHA synthase i.e. 5-6-(OprF)<sub>x3</sub>-PhaC1<sub>Pa</sub>-OprI (**Fig. 4.1b**). Another way would be translationally fusing the OprI/F-AlgE fusion antigen to both terminus of the PHA synthase and thereby doubling the number of epitopes for displayed i.e. 5-6-(OprF)<sub>x3</sub>-PhaC1<sub>Pa</sub>-OprI-(OprF)<sub>x3</sub>-6-5 (**Fig. 4.1c**).

The rearrangement of antigenic epitopes or increasing copy number by utilizing both terminus of the PHA synthase could have an added affect of enhancing *in vivo* PHA accumulation as observed in Chen et al [12].

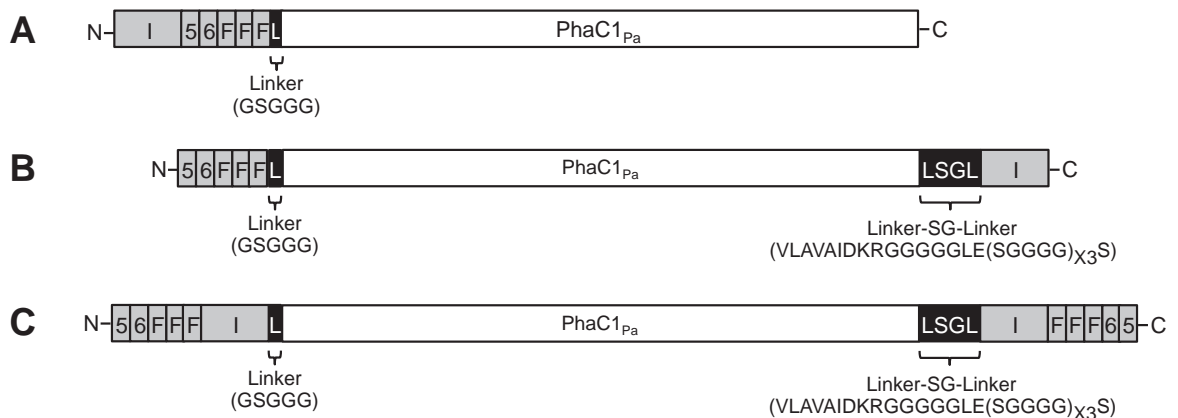


**Figure 4.1. Epitope arrangement.** Optimizing antigen-display by rearranging antigenic epitopes (a) to allow better antigen presentation of certain epitopes and (b) by splitting antigens to be displayed on both terminus of PhaC<sub>Pa</sub> or (c) fusing antigen fusion to both terminus of PhaC<sub>Pa</sub>.

**Culture and induction conditions.** Bioreactors offer the ability to significantly increase biomass and in turn *in vivo* PHA accumulation compared to culturing by Erlenmeyer flasks. Bioreactors allow the user to control a range of growth factors that include oxygen and pH to maintain optimal growth and induction. Sartorius BIOSTAT® Bplus and Qplus bioreactors are examples of small-scale bioreactors which could be utilized.

**Genes and Promoters.** Optimization of the promoters regulating genes involved in PHA biosynthesis can further enhance PHA accumulation *in vivo* and consequently the display of fusion protein on the beads surface.

*Pseudomonas PHA beads.* *In trans* expression of the PHA synthase can be enhanced by looking at other possible expression systems in *P. aeruginosa*. However, the array of strong inducible gene expression systems for pseudomonas is currently limited.

*Mycobacterial PHA beads.* In chapter 3, several strong gene expression systems were explored for the expression of the PHA synthase in *M. smegmatis*, namely nitrile-inducible [34] and tetracycline-efflux system [35]. Two alternative strong mycobacterial gene expression systems are described below.

Riboswitch-based system [36]. This riboswitch-based gene expression system encompasses a mycobacterial promoter (variant of Phsp60) and a synthetic RNA aptamer that binds to theophylline. Briefly, in the absence of theophylline, the riboswitch mRNA transcript adopts a specific confirmation that binds the ribosome binding site and prevents transcription. When theophylline is present, the aptamer binds the theophylline and therefore releasing RBS. This system is a titratable system and shown to be comparable to that of the nitrile-inducible and Tet systems. The added advantage of this system is that no exogenous regulator proteins are required and induction is reversible.

Pristinamycin-inducible system [37]. This system is comprised of the *Streptomyces coelicolor* Pip repressor, the *Streptomyces pristinaespiralis ptr* promoter, and inducer streptogramin pristinamycin I. This system work similarly to the *lac* Operon and allows for efficient gene expression in both *M. smegmatis* and *M. tuberculosis*. An increase in

promoter activity of 50-fold and 400-fold in *M. smegmatis* and *M. tuberculosis*, respectively, can be achieved after induction and the system can be fully repressed in the absence of inducer.

Other possible aspects to consider include improving the promoter regulating expression of *phaAB* for precursor synthesis. It is possible that expression of *phaAB* may be a limiting factor in mycobacterial PHA production, although only catalytic amounts are required. Alternative weak constitutive mycobacterium promoters such as *Pimyc* and *Psmyc* with higher promoter activity than the currently used *Pwmyc* could be considered for the expression of *phaAB* [38].

#### **4.2.2 Bead isolation**

Optimization of PHA beads isolation for both *P. aeruginosa* (chapter 2) and *M. smegmatis* (chapter 3) is required to improve PHA yield, uniformity, and removal of nonbead associated materials.

**Mechanical methods.** Alternative methods of mechanical disruption include the use of microfluidizers and homogenizers. These methods of cell disruption produce significantly higher shear forces that can offer substantial improvements to cell disruption compared to bead mill, sonication, and French press technologies used in this thesis.

The use of the microfluidizer is of particular interest as it offers the highest shear forces and combined with high impact forces it can efficiently lyse tough cells such as *M. smegmatis* compared to other methods. Efficient lysis is important to release the maximum number of PHA beads from cells and to reduce the number of viable organisms and in turn minimize downstream processing. This type of mechanical disruption also allows for efficient particle dispersion. Importantly this method allows for repeatability and scalability.

Furthermore, mechanical methods offer efficient lysis without the need for additional lytic enzymes (e.g. lysozyme), which is favored in the vaccine context.

However the main drawback of mechanical disruption methods is the generation of biological aerosols, which in the context of working with pathogens is a safety concern and will need to be considered.

**Non-mechanical methods.** Non-mechanical disruption methods use chemicals and/or enzymes such as antibiotics, surfactants, chaotropic agents, chelates, and organic solvents to permeabilize cells. An advantage of this type of method of disruption is that they don't generate biological aerosols. Chemical and/or enzyme methods of disruption tend to be more specific and delicate compared to mechanical disruption. This is particularly important for maintaining the natural structure of proteins/antigens that can possibly be denatured by mechanical disruption methods as a result of heat and high shear forces.

Chemical/enzyme methods however can be affected by a range of environmental conditions (e.g. temperature) making reproducibility and scalability difficult. Cost is a major factor that needs to be considered, as specific chemical/enzymes may be required depending on organism and scale up would be costly.

**Chemical and mechanical disruption.** A combination of both chemical and mechanical disruption offers the best solution to cell disruption. Chemicals which increase cell permeabilization can permit lower shear forces to be used and therefore, reducing the amount of biological aerosol generated and minimizing protein denaturation.

#### **4.2.3 Bead purification**

Nonbead associated materials can be removed by an efficient and scalable method such as crossflow filtration. The concept of PHA bead purification by crossflow filtration for the removal of nonbead-associated contaminants has been demonstrated in our lab. This method of purification was shown to be more efficient than gradient-based separation methods and resulted in significantly cleaner PHA bead material.

#### 4.2.4 Alternative antigens

The PHA bead delivery system allows for the incorporation and surface display of various antigenic epitopes. Identification of appropriate protective epitopes suitable use as a prophylactic vaccine is critical of epitope-based vaccines [39]. In thesis a number of immune dominant vaccine candidates were used. Alternative vaccine candidates are available and have been used successfully by other research groups. These alternative candidates can be used in place or in addition to the currently used antigens.

*Pseudomonas PHA beads.* *P. aeruginosa* is an organism which shows enormous phenotypic variability and adaptive differences, which makes the selection of antigens critical. Of particular interest is EPS Psl, which is seen as a promising vaccine candidate that was initially considered for use with *P. aeruginosa* vaccine PHA beads. Psl is an extracellular matrix polysaccharide that is serotype-independent and is found expressed on the surface of both nonmucoid and mucoid clinical isolates. Psl functions as a virulence factor in preventing opsonization and for surface attachment. It has been demonstrated that antibodies directed against Psl were able to mediate effective opsonophagocytic killing *in vitro*, inhibiting attachment to lung epithelial cells, and provided prophylactic protection in animal models [40].

In chapter 2 we promoted the production of Psl by engineering *P. aeruginosa*. Here Psl is thought to copurify with the PHA beads. However, this method of attachment is difficult to control and/or is inefficient. A more controlled method of Psl codelivered with PHA beads could be achieved by either mixing purified Psl material with PHA beads during formulation or by attaching purified Psl onto PHA beads.

To achieve attachment of Psl to PHA beads surface, a naturally occurring Psl adhesion protein (CdrA) from *P. aeruginosa* could be utilized. This protein shows similarities to extracellular adhesions that belong to two-partner secretion systems. The mature CdrA protein is 150 kDa and is exported out of the cell by CdrB. Evidence has been provided which demonstrates that CdrA binds directly to Psl, functioning as a Psl cross-linker and/or possibly acts in tethering Psl to the cell surface [40, 41].

*Mycobacterial PHA beads.* Promising alternative vaccine candidates for Mycobacterium include: Ag85B (Ag85 complex protein) [42-44], TB10·4 (antigen belonging to *esat-6* subfamily) [42, 45], Mtb32 (secreted serine protease) [46-48], and Mtb39 [46, 47, 49]. All antigens have demonstrated protective immunity in animals and/or humans.

#### **4.2.5 Adjuvants**

Addition of adjuvants have the potential to induce protective immune response and long-lasting immunity [50]. Adjuvant can have a major effect on the polarization of the immune response. Subunit vaccines tend to be poor inducer of immunity and typically require adjuvants [51].

In the absence of formulating with adjuvant, vaccine PHA beads derived from opportunistic pathogen *P. aeruginosa* was associated with HCPs and capable of inducing a strong immune response (**Figs. 2.8a** and **2.10**). However, the addition of adjuvant alum enhanced the immune response (**Fig. 2.9**). Therefore, by exploring the use of different adjuvants we could enhance the immune response to vaccine PHA beads. The range of approved adjuvants for human use is currently very limited [51, 52]. Examples of approved adjuvants include MF59, AS03 (squalene-in-water emulsions), and AS04 (MPL plus alum) [53]. A large number of other adjuvants are being used experimentally or in clinical development.

#### **4.2.6 Alternative mycobacterial production host**

Although we were able to show an antigen specific immune response to Ag85A-ESAT-6 surface displaying PHA beads produced in a nonpathogenic model organism, *M. smegmatis* (**Fig. 3.4**), production in this bacterium may not be as beneficial as bead production in pathogenic mycobacterium strains such as *M. bovis* or *M. tuberculosis*. *M. smegmatis* lack a large proportion of proteins found in pathogenic strains which includes a large range of vaccine candidates [30, 54, 55]. Consequently, the immune response to copurifying impurities of *M. smegmatis* is likely to be less effective in conferring protection against pathogenic strains. Therefore, production in these pathogenic strains may produce vaccine PHA beads that can offer better vaccine efficacy.

#### 4.2.7 Characterization of *P. aeruginosa* mutant $\Delta\text{CA8}\Delta\text{F}$

The *P. aeruginosa* triple mutant PAO1  $\Delta\text{phaC1ZC2}$   $\Delta\text{alg8}$   $\Delta\text{pelF}$  generated in this study (**Fig. 2.2**) was not characterized as this was beyond the scope of the current project. The scope of the project focused on the generation of antigen-displaying PHA beads with copurifying impurities in a pathogenic host and when used as a vaccine could induce an immune reaction. Optimized PHA production in the production host was not the main objective. However, a subsequent study looking at improving PHA production in *P. aeruginosa* would require characterizing this mutant strain.

#### 4.2.8 Challenge trial – *Pseudomonas* vaccine beads

In chapter 2 we were able to successfully demonstrate that vaccination with *P. aeruginosa* vaccine PHA beads was able to produce a significant Th1 type immune response compared to controls (**Figs. 2.8a** and **2.10**). However, vaccine efficacy has yet to be assessed in a relevant animal model. Here we will focus mainly on the use of mouse models. Mouse models to study CF pathology are widely used and seen as being cost effective, easy to maintain, and have a range of available reagents. However, like for other diseases animal models such as the mouse model show limitations due to physiological differences between mice and humans [56, 57].

A range of factors needs to be considered for an appropriate mouse model to show vaccine efficacy of the *P. aeruginosa* vaccine PHA beads. These factors include the mouse strain, *P. aeruginosa* strain, dose, and route of administration.

A large number of CF mice have been described elsewhere [56-59]. Severity of the CF disease and phenotype in these cystic fibrosis transmembrane conductance regulator (Cftr) KO mouse can vary and is dependent on the genetic background of the mouse strain [58]. The major phenotypic traits of CF mice have been extensively reviewed [58-60]. Selection of an appropriate mouse model is important as not all Cftr KO mice display CF lung phenotype relevant to pulmonary infection. Of particular interest are the *Scnn1a*-, *Scnn1b*- and *Scnn1c*-transgenic mice [61]. These transgenic mice show similar characteristic lung pathology to human CF such as reduced mucus clearance, neutrophilic inflammation, and pro-inflammatory cytokines.

Infection of CF individuals typically involves the nonmucoid form of the organism that subsequently reverts to the chronic mucoid form over time. The nonmucoid form can be eliminated easily relative to the mucoid form that can form protective biofilms [59, 61-64]. It is therefore important to validate vaccine efficacy in both model types. A range of methods has been described to establishment acute or chronic pulmonary *P. aeruginosa* infections in mice.

Acute infection mouse models generally describe the use of planktonic cultures of nonmucoid strains of *P. aeruginosa* of which can be delivered intratracheally, intranasally, or by aerosol [60, 62-64]. Chronic infection mouse models typically involve encapsulation of mucoid alginate overproducing *P. aeruginosa* phenotype in agar or agarose beads to mimic biofilm formation. These beads tend to be delivered intratracheally or intranasally. Encapsulation helps retain bacteria in the airways mimicking a biofilm. Several chronic infection models have also been described in literature [60, 65, 66]. It is important to note that these chronic infection models only partially mimic chronic infection in humans.

#### **4.2.9 Route of administration - Mucosal immunity**

Recent studies have indicated that mucosal immunization tends to be more effective than systemic vaccination for mucosal pathogens [60, 65-69]. The primary route of infection from *P. aeruginosa* and *M. tuberculosis* is by the respiratory tract. Vaccines that can closely mimic mucosal pathogen can efficiently stimulate innate responses and consequently adaptive response to the targeted pathogen. Therefore, inducing mucosal immunity may lead to greater pulmonary protection against these bacterium and of which should be investigated.

Mucosal vaccination elicits the secretion of IgA that is part of the adaptive immune response [67]. Secreted IgA promotes entrapment of antigens and microbes in the mucus, prevent epithelial attachment, and antibody-dependent cell-mediated cytotoxicity.

Furthermore, certain proteins can enhance mucosal immunity such as OprI of *P. aeruginosa*. OprI has been shown to promote adherence to mucosal surfaces and suggested to promote mucosal immunity by enhancing delivery to APC [70].

#### **4.2.10 Heterologous prime-boost strategy**

The use of a heterologous prime-boost vaccination strategy is increasing gaining traction. Heterologous prime-boost is defined by multiple immunizations using different vaccination methods with the same antigens, and appears to be a promising strategy to improve immunogenicity and/or protection [70, 71]. Heterologous prime-boost strategy aims to elicit both humoral and cell-mediated immune responses [71].

The use of TB antigen-displaying PHA beads produced in heterologous host as a homologous prime-boost strategy has been previously investigated [6]. The study involved subcutaneous vaccination with BCG prime and boosting with Ag85A-ESAT-6 displaying PHA beads. Disappointingly, no significant difference was seen relative to the groups immunized with BCG or Ag85A-ESAT-6 beads alone.

The lack of significant difference might be due to the prime and boost using the same vaccination route and/or specific boosting with antigens Ag85A-ESAT-6 on PHA beads was not effective at improving T cell responses to the target antigens. Studies have shown that a heterologous prime-boost strategy is more protective than homologous prime-boost strategies were antigens are delivered using the same route [71-73]. While another study has suggested specific priming rather than specific boosting gave an enhanced immune response [74].

The usefulness of PHA beads in a prime-boost strategy as a prime and/or boost is something that should be further explored. We propose that our PHA beads generated in pathogenic host may have more advantages for use as in a heterologous prime-boost strategy than PHA beads produced in a heterologous host. PHA beads produced in this study contain a large repertoire of antigens that could elicit a stronger boost than just with the target antigens alone. Costimulation with HCPs may be essential for optimal response with target antigens [74]. For example, heterologous prime-boost strategy against TB could involve mucosal priming with BCG or mycobacterial PHA beads and subsequent systemic boost using mycobacterial PHA beads. A similar strategy could be applied to pseudomonas PHA beads but with mucosal prime with beads and systemic boost with beads. A prime-boost strategy involving mucosal prime and systemic boost has been shown to be more effective than using a mucosal vaccination regime alone [75].

### 4.3 References

1. Moyle, P.M. and I. Toth, *Modern subunit vaccines: development, components, and research opportunities*. ChemMedChem, 2013. **8**(3): p. 360-376.
2. Grage, K., et al., *Bacterial polyhydroxyalkanoate granules: biogenesis, structure, and potential use as nano-/micro-beads in biotechnological and biomedical applications*. Biomacromolecules, 2009. **10**(4): p. 660-669.
3. Parlane, N.A., et al., *Production of a particulate hepatitis C vaccine candidate by an engineered Lactococcus lactis strain*. Applied and Environmental Microbiology, 2011. **77**(24): p. 8516-8522.
4. Parlane, N.A., et al., *Vaccines displaying mycobacterial proteins on biopolyester beads stimulate cellular immunity and induce protection against tuberculosis*. Clinical and Vaccine Immunology, 2012. **19**(1): p. 37-44.
5. Parlane, N.A., et al., *Bacterial polyester inclusions engineered to display vaccine candidate antigens for use as a novel class of safe and efficient vaccine delivery agents*. Applied and Environmental Microbiology, 2009. **75**(24): p. 7739-7744.
6. Parlane, N.A., et al., *Novel particulate vaccines utilizing polyester nanoparticles (bio-beads) for protection against Mycobacterium bovis infection—A review*. Veterinary Immunology and Immunopathology, 2014. **158**(1): p. 8-13.
7. Martínez-Donato, G., et al., *Protective T cell and antibody immune response against Hepatitis C Virus using the biopolyester beads based vaccine delivery system*. Clinical and Vaccine Immunology, 2016: p. 370-378.
8. Zepp, F., *Principles of vaccine design-Lessons from nature*. Vaccine, 2010. **28**: p. C14-C24.
9. Ghafoor, A., I.D. Hay, and B.H.A. Rehm, *Role of exopolysaccharides in Pseudomonas aeruginosa biofilm formation and architecture*. Applied and Environmental Microbiology, 2011. **77**(15): p. 5238-5246.
10. Pham, T.H., J.S. Webb, and B.H.A. Rehm, *The role of polyhydroxyalkanoate biosynthesis by Pseudomonas aeruginosa in rhamnolipid and alginate production as well as stress tolerance and biofilm formation*. Microbiology, 2004. **150**(10): p. 3405-3413.
11. Jahns, A.C. and B.H.A. Rehm, *Tolerance of the Ralstonia eutropha Class I Polyhydroxyalkanoate Synthase for Translational Fusions to Its C Terminus Reveals a New Mode of Functional Display*. Applied and Environmental Microbiology, 2009. **75**(17): p. 5461-5466.
12. Chen, S., et al., *New skin test for detection of bovine tuberculosis on the basis of antigen-displaying polyester inclusions produced by recombinant Escherichia coli*. Applied and Environmental Microbiology, 2014. **80**(8): p. 2526-2535.
13. Hooks, D.O., P.A. Blatchford, and B.H.A. Rehm, *Bioengineering of bacterial polymer inclusions catalyzing the synthesis of N-acetylneuraminic acid*. Applied and Environmental Microbiology, 2013. **79**(9): p. 3116-3121.
14. Blatchford, P.A., et al., *Immobilization of organophosphohydrolase OpdA from Agrobacterium radiobacter by overproduction at the surface of polyester inclusions inside engineered Escherichia coli*. Biotechnology and Bioengineering, 2012. **109**(5): p. 1101-1108.
15. van der Pol, L., M. Stork, and P. van der Ley, *Outer membrane vesicles as platform vaccine technology*. Biotechnology Journal, 2015. **10**(11): p. 1689-1706.
16. Pathirana, R.D. and M. Kaparakis - Liaskos, *Bacterial membrane vesicles: Biogenesis, immune regulation and pathogenesis*. Cellular Microbiology, 2016. **18**(11): p. 1518-1524.
17. Dadley-Moore, D., *Learning from our successes*. Nature Reviews Immunology, 2006. **6**(4): p. 256-257.
18. Querec, T., et al., *Yellow fever vaccine YF-17D activates multiple dendritic cell subsets via TLR2, 7, 8, and 9 to stimulate polyvalent immunity*. Journal of Experimental Medicine, 2006. **203**(2): p. 413-424.
19. Tarcha, E.J., et al., *Multivalent recombinant protein vaccine against coccidioidomycosis*. Infection and immunity, 2006. **74**(10): p. 5802-5813.
20. Shirliff, M., J. Harro, and J. Leid, *Multivalent vaccine protection from staphylococcus aureus infection*. 2013, Google Patents.
21. Hartl, D., et al., *Pulmonary TH2 response in Pseudomonas aeruginosa-infected patients with cystic fibrosis*. Journal of allergy and clinical immunology, 2006. **117**(1): p. 204-211.
22. Moser, C., et al., *Improved outcome of chronic Pseudomonas aeruginosa lung infection is associated with induction of a Th1 - dominated cytokine response*. Clinical & Experimental Immunology, 2002. **127**(2): p. 206-213.

23. Moser, C., et al., *The immune response to chronic Pseudomonas aeruginosa lung infection in cystic fibrosis patients is predominantly of the Th2 type*. *Apmis*, 2000. **108**(5): p. 329-335.
24. Johansen, H.K., et al., *Interferon - gamma (IFN -  $\gamma$ ) treatment decreases the inflammatory response in chronic Pseudomonas aeruginosa pneumonia in rats*. *Clinical & Experimental Immunology*, 1996. **103**(2): p. 212-218.
25. Brennan, F.R., et al., *Pseudomonas aeruginosa outer-membrane protein F epitopes are highly immunogenic in mice when expressed on a plant virus*. *Microbiology*, 1999. **145**(1): p. 211-220.
26. Mizuno, T. and M. Kageyama, *Separation and characterization of the outer membrane of Pseudomonas aeruginosa*. *Journal of Biochemistry*, 1978. **84**(1): p. 179-191.
27. Rehm, B.H.A., et al., *Overexpression of algE in Escherichia coli: subcellular-localization, purification, and ion-channel properties*. *Journal of Bacteriology*, 1994. **176**(18): p. 5639-5647.
28. Quesniaux, V.F.J., et al., *TNF in host resistance to tuberculosis infection*. 2010.
29. Billiau, A. and P. Matthys, *Modes of action of Freund's adjuvants in experimental models of autoimmune diseases*. *Journal of Leukocyte Biology*, 2001. **70**(6): p. 849-860.
30. Altaf, M., et al., *Evaluation of the Mycobacterium smegmatis and BCG models for the discovery of Mycobacterium tuberculosis inhibitors*. *Tuberculosis*, 2010. **90**(6): p. 333-337.
31. Vyas, J.M., A.G. Van der Veen, and H.L. Ploegh, *The known unknowns of antigen processing and presentation*. *Nature Reviews Immunology*, 2008. **8**(8): p. 607-618.
32. Lo - Man, R., et al., *Induction of T cell responses by chimeric bacterial proteins expressing several copies of a viral T cell epitope*. *European Journal of Immunology*, 1993. **23**(11): p. 2998-3002.
33. Jin, L., et al., *A Th1-recognized peptide P277, when tandemly repeated, enhances a Th2 immune response toward effective vaccines against autoimmune diabetes in nonobese diabetic mice*. *The Journal of Immunology*, 2008. **180**(1): p. 58-63.
34. Pandey, A.K., et al., *Nitrile-inducible gene expression in mycobacteria*. *Tuberculosis*, 2009. **89**(1): p. 12-16.
35. Blokpoel, M.C., et al., *Tetracycline-inducible gene regulation in mycobacteria*. *Nucleic Acids Research*, 2005. **33**(2).
36. Seeliger, J.C., et al., *A riboswitch-based inducible gene expression system for mycobacteria*. *PLoS one*, 2012. **7**(1).
37. Forti, F., A. Crosta, and D. Ghisotti, *Pristinamycin-inducible gene regulation in mycobacteria*. *Journal of Biotechnology*, 2009. **140**(3-4): p. 270-277.
38. Kaps, I., et al., *Energy transfer between fluorescent proteins using a co-expression system in Mycobacterium smegmatis*. *Gene*, 2001. **278**(1-2): p. 115-124.
39. Sette, A. and J. Fikes, *Epitope-based vaccines: an update on epitope identification, vaccine design and delivery*. *Current Opinion in Immunology*, 2003. **15**(4): p. 461-470.
40. DiGiandomenico, A., et al., *Identification of broadly protective human antibodies to Pseudomonas aeruginosa exopolysaccharide Psl by phenotypic screening*. *The Journal of Experimental Medicine*, 2012. **209**(7): p. 1273-1287.
41. Borlee, B.R., et al., *Pseudomonas aeruginosa uses a cyclic-di-GMP-regulated adhesin to reinforce the biofilm extracellular matrix*. *Molecular Microbiology*, 2010. **75**(4): p. 827-842.
42. Abel, B., et al., *The novel tuberculosis vaccine, AERAS-402, induces robust and polyfunctional CD4+ and CD8+ T cells in adults*. *American Journal of Respiratory and Critical Care medicine*, 2010. **181**(12): p. 1407-1417.
43. Dietrich, J., et al., *Mucosal administration of Ag85B-ESAT-6 protects against infection with Mycobacterium tuberculosis and boosts prior bacillus Calmette-Guerin immunity*. *The Journal of Immunology*, 2006. **177**(9): p. 6353-6360.
44. Agger, E.M., et al., *Protective immunity to tuberculosis with Ag85B-ESAT-6 in a synthetic cationic adjuvant system IC31*. *Vaccine*, 2006. **24**(26): p. 5452-5460.
45. Dietrich, J., et al., *Exchanging ESAT6 with TB10. 4 in an Ag85B fusion molecule-based tuberculosis subunit vaccine: efficient protection and ESAT6-based sensitive monitoring of vaccine efficacy*. *The Journal of Immunology*, 2005. **174**(10): p. 6332-6339.
46. Reed, S.G., et al., *Defined tuberculosis vaccine, Mtb72F/AS02A, evidence of protection in cynomolgus monkeys*. *Proceedings of the National Academy of Sciences*, 2009. **106**(7): p. 2301-2306.
47. Von Eschen, K., et al., *The candidate tuberculosis vaccine Mtb72F/AS02A: tolerability and immunogenicity in humans*. *Human Vaccines*, 2009. **5**(7): p. 475-482.
48. Skeiky, Y.A.W., et al., *Cloning, expression, and immunological evaluation of two putative secreted serine protease antigens of Mycobacterium tuberculosis*. *Infection and Immunity*, 1999. **67**(8): p. 3998-4007.

49. Dillon, D.C., et al., *Molecular characterization and human T-Cell responses to a member of a novel Mycobacterium tuberculosis mtb39Gene family*. Infection and Immunity, 1999. **67**(6): p. 2941-2950.
50. Ryan, E.J., L.M. Daly, and K.H.G. Mills, *Immunomodulators and delivery systems for vaccination by mucosal routes*. TRENDS in Biotechnology, 2001. **19**(8): p. 293-304.
51. Aguilar, J. and E. Rodriguez, *Vaccine adjuvants revisited*. Vaccine, 2007. **25**(19): p. 3752-3762.
52. Rappuoli, R., et al., *Vaccines for the twenty-first century society*. Nature Reviews Immunology, 2012. **12**(3): p. 225-225.
53. Coffman, R.L., A. Sher, and R.A. Seder, *Vaccine adjuvants: putting innate immunity to work*. Immunity, 2010. **33**(4): p. 492-503.
54. Smith, S.E., et al., *Comparative genomic and phylogenetic approaches to characterize the role of genetic recombination in mycobacterial evolution*. PloS One, 2012. **7**(11).
55. Devulder, G., M.P. De Montclos, and J.P. Flandrois, *A multigene approach to phylogenetic analysis using the genus Mycobacterium as a model*. International Journal of Systematic and Evolutionary Microbiology, 2005. **55**(1): p. 293-302.
56. Acosta, A., et al., *The importance of animal models in tuberculosis vaccine development*. 2013.
57. Dharmadhikari, A.S. and E.A. Nardell, *What animal models teach humans about tuberculosis*. American Journal of Respiratory Cell and Molecular Biology, 2008. **39**(5): p. 503-508.
58. Guilbault, C., et al., *Cystic fibrosis mouse models*. American Journal of Respiratory Cell and Molecular Biology, 2007. **36**(1): p. 1-7.
59. Wilke, M., et al., *Mouse models of cystic fibrosis: phenotypic analysis and research applications*. Journal of Cystic Fibrosis, 2011. **10**: p. S152-S171.
60. Kukavica-Ibrulj, I. and R.C. Levesque, *Animal models of chronic lung infection with Pseudomonas aeruginosa: useful tools for cystic fibrosis studies*. Laboratory Animals, 2008. **42**(4): p. 389-412.
61. Mall, M., et al., *Increased airway epithelial Na<sup>+</sup> absorption produces cystic fibrosis-like lung disease in mice*. Nature Medicine, 2004. **10**(5): p. 487-493.
62. Flemming, H.-C. and J. Wingender, *The biofilm matrix*. Nature Reviews Microbiology, 2010. **8**(9): p. 623-633.
63. Høiby, N., B. Frederiksen, and T. Pressler, *Eradication of early Pseudomonas aeruginosa infection*. Journal of Cystic Fibrosis, 2005. **4**: p. 49-54.
64. Jensen, P.Ø., et al., *The immune system vs. Pseudomonas aeruginosa biofilms*. FEMS Immunology & Medical Microbiology, 2010. **59**(3): p. 292-305.
65. Guilbault, C., et al., *Cystic fibrosis lung disease following infection with Pseudomonas aeruginosa in Cfr knockout mice using novel non-invasive direct pulmonary infection technique*. Laboratory Animals, 2005. **39**(3): p. 336-352.
66. Hoffmann, N., et al., *Novel mouse model of chronic Pseudomonas aeruginosa lung infection mimicking cystic fibrosis*. Infection and Immunity, 2005. **73**(4): p. 2504-2514.
67. Neutra, M.R. and P.A. Kozlowski, *Mucosal vaccines: the promise and the challenge*. Nature Reviews Immunology, 2006. **6**(2): p. 148-158.
68. Sorichter, S., et al., *Immune responses in the airways by nasal vaccination with systemic boosting against Pseudomonas aeruginosa in chronic lung disease*. Vaccine, 2009. **27**(21): p. 2755-2759.
69. Bolton, D.L., et al., *Comparison of systemic and mucosal vaccination: impact on intravenous and rectal SIV challenge*. Mucosal Immunology, 2012. **5**(1): p. 41-52.
70. Loots, K., H. Revets, and B.M. Goddeeris, *Attachment of the outer membrane lipoprotein (OprI) of Pseudomonas aeruginosa to the mucosal surfaces of the respiratory and digestive tract of chickens*. Vaccine, 2008. **26**(4): p. 546-551.
71. Lu, S., *Heterologous prime-boost vaccination*. Current Opinion in Immunology, 2009. **21**(3): p. 346-351.
72. McShane, H. and A. Hill, *Prime-boost immunisation strategies for tuberculosis*. Microbes and Infection, 2005. **7**(5): p. 962-967.
73. Nolz, J.C. and J.T. Harty, *Strategies and implications for prime-boost vaccination to generate memory CD8 T cells*, in *Crossroads between Innate and Adaptive Immunity III*. 2011, Springer. p. 69-83.
74. Luijckx, T., et al., *Heterologous prime-boost strategy to overcome weak immunogenicity of two serosubtypes in hexavalent Neisseria meningitidis outer membrane vesicle vaccine*. Vaccine, 2006. **24**(10): p. 1569-1577.

75. Göcke, K., et al., *Mucosal vaccination with a recombinant OprF-I vaccine of Pseudomonas aeruginosa in healthy volunteers: comparison of a systemic vs. a mucosal booster schedule.* FEMS Immunology & Medical Microbiology, 2003. **37**(2-3): p. 167-171.

## Appendix



**MASSEY UNIVERSITY**  
GRADUATE RESEARCH SCHOOL

**STATEMENT OF CONTRIBUTION  
TO DOCTORAL THESIS CONTAINING PUBLICATIONS**

(To appear at the end of each thesis chapter/section/appendix submitted as an article/paper or collected as an appendix at the end of the thesis)

We, the candidate and the candidate's Principal Supervisor, certify that all co-authors have consented to their work being included in the thesis and they have accepted the candidate's contribution as indicated below in the *Statement of Originality*.

**Name of Candidate:** Jason Wong Lee

**Name/Title of Principal Supervisor:** Prof. Bernd H. A. Rehm

**Name of Published Research Output and full reference:**

Lee, J. W., Parlane, N. A., Wedlock, D. N., & Rehm, B. H. A. (2017). Bioengineering a bacterial pathogen to assemble its own particulate vaccine capable of inducing cellular immunity. *Scientific Reports*, 7.

**In which Chapter is the Published Work:** Chapter 2

Please indicate either:

- The percentage of the Published Work that was contributed by the candidate: 80%  
and / or
- Describe the contribution that the candidate has made to the Published Work:

  
\_\_\_\_\_  
Candidate's Signature

22 MAR 2017  
Date

  
\_\_\_\_\_  
Principal Supervisor's signature

22/3/2017  
Date



**MASSEY UNIVERSITY**  
GRADUATE RESEARCH SCHOOL

**STATEMENT OF CONTRIBUTION  
TO DOCTORAL THESIS CONTAINING PUBLICATIONS**

(To appear at the end of each thesis chapter/section/appendix submitted as an article/paper or collected as an appendix at the end of the thesis)

We, the candidate and the candidate's Principal Supervisor, certify that all co-authors have consented to their work being included in the thesis and they have accepted the candidate's contribution as indicated below in the *Statement of Originality*.

**Name of Candidate:** Jason Wong Lee

**Name/Title of Principal Supervisor:** Prof. Bernd H. A. Rehm

**Name of Published Research Output and full reference:**

Lee, J. W., Parlane, N. A., Rehm, B. H. A., Buddle, B. M., & Heiser, A. (2017).  
Engineering mycobacteria for the production of self-assembling biopolyesters displaying mycobacterial antigens for use as a tuberculosis vaccine. *Applied and environmental microbiology*, 85(4), 2289-2289.

**In which Chapter is the Published Work:** Chapter 3

Please indicate either:

- The percentage of the Published Work that was contributed by the candidate: 60%  
and / or
- Describe the contribution that the candidate has made to the Published Work:

  
\_\_\_\_\_  
Candidate's Signature

22 MAR 2017  
\_\_\_\_\_  
Date

  
\_\_\_\_\_  
Principal Supervisor's signature

22/3/2017  
\_\_\_\_\_  
Date

# COPYRIGHT FORM AND DECLARATION CONFIRMING CONTENT OF DIGITAL VERSION OF THESIS

Student ID number: 

0	2	1	2	5	9	6	5
---	---	---	---	---	---	---	---

Student's name:

Jason Lee

Thesis title:

Novel particulate vaccine candidates  
recombinantly produced by pathogenic and  
nonpathogenic bacterial hosts

## Complete this section only if you opted to self-print your thesis

I confirm that the content of the digital version of this thesis is the final amended version following the examination process, and is identical to the bound paper copy.

Signed on: 

Day	Month	Year

Student's signature: \_\_\_\_\_

In signing this form I understand that...

- This material will be freely available on the internet
- I am still the copyright owner
- The digital copy will only be used for private research or study and may not be reproduced elsewhere without my permission as per the Copyright and Access information

### AND [tick one]

I confirm that my thesis **DOES NOT** contain **ANY** material of which copyright belongs to third parties, (**or**) that all such material falls within the limits permitted by the Copyright Act 1994.

**OR**

I confirm that my thesis **DOES** contain material of which copyright belongs to third parties and which **I HAVE** obtained written permission, and attach copies of all permissions, for all material of which copyright belongs to third parties and which does not fall within the limits permitted by the Copyright Act 1994.

**OR**

I confirm that my thesis **DOES** contain material of which copyright belongs to third parties and which **I HAVE NOT** obtained written permission. I have identified all such material in the digital copy of my thesis, and attach documentation fully referencing the material and where possible providing links to electronic sources of the material. I understand that this content will be removed before my thesis is made available in the institutional repository, Massey Research Online.

Signed on: 

Day	Month	Year
2 2	0 3	2 0 1 7

Student's signature:





**Title:** Bioengineering a bacterial pathogen to assemble its own particulate vaccine capable of inducing cellular immunity

**Author:** Jason W. Lee, Natalie A. Parlane, D. Neil Wedlock, Bernd H. A. Rehm

**Publication:** Scientific Reports  
**Publisher:** Nature Publishing Group  
**Date:** Feb 2, 2017

Copyright © 2017, Rights Managed by Nature Publishing Group

[LOGIN](#)

If you're a [copyright.com user](#), you can login to RightsLink using your copyright.com credentials. Already a [RightsLink user](#) or want to [learn more?](#)

### Creative Commons

The article for which you have requested permission has been distributed under a Creative Commons CC-BY license (please see the article itself for the license version number). You may reuse this material without obtaining permission from Nature Publishing Group, providing that the author and the original source of publication are fully acknowledged, as per the terms of the license.

For license terms, please see <http://creativecommons.org/>

[CLOSE WINDOW](#)

Are you the [author](#) of this NPG article?

To order reprints of this content, please contact the Nature Publishing Group reprint office by e-mail: [reprints@nature.com](mailto:reprints@nature.com).

Copyright © 2017 [Copyright Clearance Center, Inc.](#) All Rights Reserved. [Privacy statement](#). [Terms and Conditions](#).  
Comments? We would like to hear from you. E-mail us at [customercare@copyright.com](mailto:customercare@copyright.com)

AMERICAN  
SOCIETY FOR  
MICROBIOLOGY**Title:** Engineering Mycobacteria for the  
Production of Self-Assembling  
Biopolyesters Displaying  
Mycobacterial Antigens for Use  
as a Tuberculosis Vaccine**Author:** Jason W. Lee, Natalie A. Parlane,  
Bernd H. A. Rehm et al.**Publication:** Applied and Environmental  
Microbiology**Publisher:** American Society for  
Microbiology**Date:** Mar 1, 2017

Copyright © 2017, American Society for Microbiology

LOGIN

If you're a **copyright.com**  
**user**, you can login to  
RightsLink using your  
copyright.com credentials.  
Already a **RightsLink user** or  
want to [learn more?](#)

### Permissions Request

This article published by ASM does not require requestors to obtain permission for this type of reuse, provided the original work is properly cited.

BACK

CLOSE WINDOW